SOIL-BASED ANALYSIS METHODS TO AID THE DETECTION OF CROPMARKS OVER BURIED FEATURES

By

LLEYTON JAMES PRING

A thesis submitted to

The University of Birmingham

For the degree of

DOCTOR OF PHILOSOPHY

School of Civil Engineering

College of Engineering and Physical Sciences

University of Birmingham

May 2016

Abstract

Without contention, aerial surveying has been one of the most fundamental and effective tools in archaeological research. The mapping of marks using aerial surveys, which appear in the crops over buried features, has revealed tens of thousands of new archaeological sites in Britain in the last few years. These cropmarks appear over features, such as infilled ditches, hidden below the ground surface, where the soils have been anthropogenically altered, and differ from those nearby. The crops rooted in, or near to, these features have a different pattern of growth than those surrounding it, and sometimes this difference manifests visually as a cropmark.

It is a combination of soil type, crop type and weather factors which influence the timing of cropmark appearance. Cropmarks have most commonly been found at times when the weather is dry and in areas where soils are coarse-grained and drain quickly, causing crops to come under stress due to a lack of water. This knowledge informs aerial archaeologists in the planning of surveys. However, targeting these areas in dry conditions is increasingly rerecording known sites and the rate of new discoveries is slowing. There is also bias in the dataset as areas where soils are clay-dominated and retain water for longer do not as readily show cropmarks over buried features and are not surveyed as often. It is recognised that there is a need for change in the methods of aerial survey to address the gaps in the geographical dataset and perpetuate the usefulness of aerial survey in archaeological research.

This research assessed the underlying geotechnical characteristics to increase the understanding of why these cropmarks form and the conditions in which they appear. Data have been obtained from a desk study, site investigations, geotechnical characterisation and long-term monitoring of water content at four research sites (case studies) in the UK. This

information has been used to compare suctions in the soils within a buried feature with those adjacent to it, and the results were analysed in conjunction with the appearance of the cropmark above. The importance of cost effective methods in cultural heritage research has also been considered. Site investigations, geotechnical characterisation and long-term monitoring are all costly and intrusive. An existing hydrogeological model with database inputs has been tested against data from long-term monitoring to assess whether the results of analyses can be reproduced using only desk study sources.

Three methods have been proposed which use existing data from sources such as the archaeological record and the British Geological Survey. The three methods use the same data inputs to assess cropmark appearance for a particular area, but each method has a different approach. The three methods have been tested for the areas around the research sites. The results do not always agree with the current knowledge of the likely conditions in which cropmarks form. For example, in the tested areas, cropmarks formed in areas of clay-dominated soils in wet conditions, and cropmarks were recorded across a much wider range of soil water conditions than was expected from current knowledge.

The combined results of the cases tested in this research show that further information on cropmark appearance can be derived from both intrusive investigations and existing data sources using the methods presented in this research. This increased knowledge of why, and in what conditions, cropmarks form, has the potential to aid aerial archaeologists in the planning of surveys in areas where cropmarks are less often recorded.

This work is dedicated to my family.

Acknowledgements

The author acknowledges the support and contributions of many people, without whom, it would not have been possible. A special thanks go to the author's supervisors, Dr Nicole Metje and Prof David Chapman for their guidance throughout. The consultants from the DART Project Consortium, Dr Bob Evans and Dr Keith Wilkinson, and particular thanks to Dan Boddice for data contributions, and the other PhD students, Rob Fry and David Stott. The landowners at the research locations, particularly Tony Norris and Tom Overbury. Thanks go to the staff at the University of Birmingham, particularly Dr Giulio Curioni, Seb Ballard and Helen Booth, and to students who worked alongside the project, Laura Thring and Andrew Howell. The author gratefully acknowledges the financial support provided by the Engineering and Physical Sciences Research Council (EPSRC). Special thanks are also owed to my friends and family, in particular to Rosie Wiltshire, for their continual support in so many ways throughout.

Contents

List of Figures

List of Tables

Notation

This section defines the literal and mathematical notations used in this thesis.

Definitions

AHRC	Arts and Humanities Research Council
AS	Adjacent Section
AWC	Available Water Capacity
BD	Bulk Disturbed sample
BGS	British Geological Survey
CCC	Cirencester Cherry Copse
Clay	The soil fraction with a particle diameter <2μm.
CQF	Cirencester Quarry Field
DART	Detection of Archaeological residues using Remote sensing Techniques
DCF	Diddington Clay Field
DPF	Diddington Pasture Field
DS	Ditch Section
EA	Environment Agency
EAW	Easily Available Water
ESPRC	Engineering and Physical Sciences Research Council
FC	Field Capacity
GIS	Geographical Information System
GWC	Gravimetric Water Content
HE	Historic England
HEA	Historic England Archive
LandIS	Land Information System

LD	Laser Diffraction
LiDAR	Light Detection and Radar
LL	Liquid Limit
mbgl	metres below ground level
MORECS	Met Office Rainfall and Evaporation Calculation System
NGPPD	National Geotechnical Physical Properties Database
NMP	National Mapping Project
OS	Ordnance Survey
PMM	Parent Material Map
PSD	Particle Size Distribution
RAU	Royal Agricultural University
RAW	Restricted Available Water
RCAHMS	Royal Commission on the Ancient and Historical Monuments of Scotland
Research Locations	The two study areas around Cirencester and Diddington
Research Sites	The four monitoring sites, CQF, CCC, DCF and DPF
SH	Sedimentation by Hydrometer method
SPAW model	Soil Plant Air Water model
Sv	Sieve method
SWCC	Soil Water Characteristic Curve
TDR	Time Domain Reflectometry
TOM	Total Organic Matter
UD	Undisturbed sample
VWC	Volumetric Water Content

Mathematical Terms

Volumetric Water Content Terms, θ, expressed as a decimal percentage

θ_r	Residual water content
θ_s	Saturated water content, equal to porosity
θ_{SAT}	Degree of saturation
θ_{33}	VWC at suction 33 kPa, field capacity
θ_{1500}	VWC at suction 1500 kPa, permanent wilting point
θ_j	Average VWC of soils within rooting depth at time *j*
$\theta_{j(l)}$	VWC of soil layer *l* at time *j*
$\theta_{33(l)}$	VWC at suction 33 kPa, field capacity of soil layer *l*

Matric Suction Terms, Ψ, kPa

Ψ_e	The matric suction at air entry
Ψ_{33}	Matric suction at 33kPa, field capacity
Ψ_{1500}	Matric suction at 1500kPa, permanent wilting point

Empirical Methods

FX	Fredlund and Xing
SR	Saxton and Rawls
PA	Perrera
ZA	Zapatta

FX Method Terms

Ψ_r	FX fitting parameter relating to the suction at residual water content
a	FX fitting parameter related to the air entry value of the soil
b	FX fitting parameter related to the rate of water extraction once the air entry value has been exceeded
c	FX fitting parameter relating to the residual water content

SR Method Terms

A	SR coefficient
B	SR coefficient
C	SR proportion of clay (expressed as a decimal percentage)
S	SR proportion of sand (expressed as a decimal percentage)
R	SR proportion of gravel (expressed as a decimal percentage)
OM	SR percentage of organic matter (%)
ρ_m	Dry density of matric soil (sand, silt and clay fraction) (Mg/m^3)
ρ_R	Dry density of gravel (assumed to be 2.65 Mg/m^3)

Plasticity and PSD Terms

PI	Plasticity Index (%)
PL	Plastic Limit (%)
LL	Liquid Limit (%)
wPI	Weighted Plasticity Index (see below)
GI	Group Index (see below)
$D_{(x)}$	Diameter such that *x*% is finer (mm)

Water Flow Terms

K_s	Saturated hydraulic conductivity
K_θ	Unsaturated hydraulic conductivity at VWC θ
q	Estimated water flow per time step across layer boundaries (cm)
$K_\theta(\theta)$	Mean unsaturated hydraulic conductivity of the two layers being considered as a function of their respective VWC (cm/hour)
$h(\theta)$	Matric potential head difference between the two layers being considered as a function of their respective VWC (cm)
D	Distance between the layer midpoints (cm)
t	Time (hours)

Soil Moisture Deficit Terms, δ

δ_j	Average SMD of soils within rooting depth at time j (mm)
$\delta_{j(l)}$	SMD of soil layer l at time j (mm)
δ_{min}	Simulated minimum SMD (mm)
Z_r	Rooting Depth (mm)

Post-Processing Terms

T_l	Thickness of soil layer l (mm)
n	Number of soil layers
θ_j	Average VWC of soils within rooting depth at time j (expressed as a decimal percentage)
$\theta_{j(l)}$	VWC of soil layer l at time j (expressed as a decimal percentage)
$\theta_{33(l)}$	VWC at suction 33 kPa of soil layer l (expressed as a decimal percentage)

Weighted Plasticity Index

A weighted plasticity index, *wPI*, is used in the determination of the California Bearing Ratio (CBR). It is calculated from the percentage finer than 0.075mm, P_{200}, expressed as a decimal, and the *PI* using the definition

$$wPI = P_{200} \times PI$$

Group Index

The Group Index of a soil is a parameter used in pavement design from the AASHTO (American Association of State Highway and Transportation Officials). The Group Index of the soil, *GI*, is related to the plasticity of the soil and P_{200} by the definition

$$GI = (P_{200} - 35)\big(0.2 + 0.005(LL - 40)\big) + 0.01(P_{200} - 15)(PI - 10)$$

The *GI* cannot be negative, therefore if $GI < 0$ it is classed as $GI = 0$.

CHAPTER 1. INTRODUCTION

1.1 OVERVIEW

The UK has a rich and diverse cultural heritage. It is also finite and diminishing under the threat of a fast developing society. Prospection for new, and the investigation of known, archaeological sites is crucial to the protection of that heritage.

Without contention, aerial surveying has been one of the most fundamental and productive tools in archaeological research. Between 2011 and 2014, the mapping of features appearing on aerial images alone led to the discovery of 14000 new sites in England alone (Historic England, 2015a). One of the most common of these features is cropmarks which appear above soils which have been anthropogenically altered, such as infilled ditches, hidden below the ground surface.

The appearance of these cropmarks is dependent on a combination of factors relating to the soils, the weather and the crop. The temporal window for imaging these cropmarks can be short, with visual differences between the crops rooted in or near to buried features, compared to those in the surrounding area, sometimes only being apparent for a few days. They have most commonly been found at times when the weather is dry in areas where soils are coarse-grained and drain quickly, causing crops to come under stress from lack of water. However, the soil and soil water related mechanisms which cause cropmarks to appear are poorly understood.

Although aerial surveying has been fundamental in the discovery of buried archaeological features, recent reports suggest that the future of aerial surveys may be limited. The need of surveyors to have high returns results in the repeated surveying of areas which are known to commonly produce cropmarks. Areas of clay-dominated soils, where cropmarks have less

commonly been recorded, are less often surveyed, introducing bias into the dataset. As a result, the usefulness of aerial surveys in the discovery of new sites is reducing, and what was once a fundamental tool in archaeology is in need of review. Improved knowledge of the conditions in which cropmarks appear would further inform surveyors in maximising the results of surveys.

This study approaches the problem from an engineering viewpoint, combining statistical analysis and a geotechnical understanding of soils with knowledge of the geographical and temporal appearance of cropmarks. Four buried ditch features in two locations in the UK have been investigated by way of a desk study, site investigation, geotechnical characterisation and long-term monitoring of soil water content and weather. The results have been used to test an existing hydrogeological model for application in simulating the soil water characteristics of soils, both to improve understanding of the geographical and temporal appearance of cropmarks and to establish three methods that maximise the use of existing datasets with little or no need for costly data collection. These methods can be applied to increase knowledge of why, and in what conditions, cropmarks become apparent, providing information for aerial archaeologists that can be used to address bias in survey results.

1.2 THE DART PROJECT

1.2.1 Project Background

This study has been undertaken in association with the DART Project (Detection of Archaeological residues using Remote sensing Techniques), led by the University of Leeds. The DART project was a science and heritage programme funded jointly by the Engineering and Physical Sciences Research Council (EPSRC) and the Arts and Humanities Research

Council (AHRC), which ran from October 2010 to September 2013. The project website can be accessed via <dartproject.info>.

The project has been run across many disciplines, and included consultants from research, cultural heritage and industrial bodies in the fields of aerial archaeology, geoarchaeology, soil science, geotechnics, geophysics and plant biology. Three PhD students were directly funded by the project with specialisms in archaeological geophysics (Dan Boddice, University of Birmingham and Rob Fry, University of Bradford), and archaeology and geographic information science (David Stott, University of Leeds).

1.2.2 Project Ethos

The DART Project has a foothold in the open science movement. It has been run as an open science project, and all the raw data from all the research conducted can be openly accessed via the DART CKAN Portal (DART, 2013). Two reasons are given for this different approach to research in Beck and Neylon (2012); to maximize the research impact by placing the project data and the processing algorithms into the public domain as soon as was practicable; and to build a community of researchers and other end-users around the data so that collaboration, and by extension, research value, can be enhanced.

1.2.3 Project Aim and Objectives

Aerial and geophysical techniques of detection are known to be typically unresponsive in areas of certain soil types, mainly clay-dominated soils, often termed “difficult” by archaeologists. An enhanced knowledge of the contrast factors affecting remote sensing techniques would lead to a greater understanding of the response of these detection techniques in these “difficult” soils. The aim of the DART Project was to increase the understanding of the contrast factors of buried archaeological features and the surrounding

geological and sedimentary formations. This would improve the way remote sensing surveys are planned in terms of the most appropriate sensor(s) in the most appropriate conditions, increasing either the likelihood of a positive result or confidence in a negative result.

Listed below are the overarching practical objectives for the DART Project as a whole. Further information relating to specific aspects of the project, outside the scope of this study, can be found in the relevant referenced theses.

1. To excavate, log and sample four buried ditch features in the UK, each cut into differing soil types.
2. To characterise the soils, sampled both within and adjacent to the ditch features, using both geoarchaeological and geotechnical techniques.
3. To monitor the water content and temperature of the soils within and adjacent to the ditch features for a period of at least 1 year (Boddice, 2014).
4. To carry out monthly geophysical surveys (Fry, 2014) and spectroradiometry surveys (Stott, 2014) over the features over the monitoring period.

1.2.4 Involvement of this Study

The DART Project collected archaeological, geophysical and aerial data from four research sites in the UK. Each site comprised a buried ditch feature and was intensively studied over a period of at least one year. The techniques used include archaeological excavation, geoarchaeological laboratory testing, aerial imagery, spectroscopy and geophysical surveying. This study complements the range of information collected by the DART Project with analysis of the buried ditch features through geotechnical characterisation.

Assistance was provided by the author in the background research regarding weather data acquisition, in the design, construction and installation of bespoke mountings for the monitoring stations, and in site investigations.

1.3 AIM AND OBJECTIVES

1.3.1 Aim

The aim of the research is to propose cost effective, soil based methods of analysis that can be applied to improve the understanding of cropmark appearance and optimise the use of aerial surveys for the detection of buried archaeological features.

1.3.2 Objectives

There are nine objectives relating to the present research in order to fulfil the stated aim:

1. To determine the gaps in the current knowledge by carrying out a critical review of the literature, focussing on cropmark appearance and aerial survey.

2. To complete a desk study and site investigation of two locations in the UK, hereon termed “research locations”, to assess the level of information currently available, and to log and sample four buried ditch features (two at each research location) in different background geologies.

3. To carry out a geotechnical characterisation of soils, both inside and adjacent to buried ditch features, at four sites in the UK, hereon termed “research sites”, in order to determine the differences and significance in cropmark appearance.

4. To assess the differences between the soil water characteristics of vertical sections through, and adjacent to, buried ditch features, comparing the results with the appearance of cropmarks to determine the mechanisms of differential growth.

5. To determine the background Soil Moisture Deficit (SMD) at the four research sites, and compare the results with the appearance of cropmarks within the same soil unit, to determine the conditions in which differential growth over buried features becomes apparent as a cropmark.

6. To determine whether an existing hydrogeological model, the SPAW (Soil Plant Air Water) model, with measured soil, crop and weather inputs, can accurately simulate the water content and SMD to aid future predictions of optimal survey periods.

7. To assess the sensitivity of the SPAW model to soil input parameters, in the context of using existing soil database records in the place of measured inputs to assess the difference in results depending on the level of detail in the input information.

8. To derive, and test, simple and inexpensive methodologies to analyse existing data to improve understanding of the conditions in which cropmarks appear, aiding the planning of aerial reconnaissance.

9. To use the results of the tests of the proposed methods to determine if they would aid archaeologists, both in the planning of aerial surveys by improving understanding of bias in the existing dataset.

1.4 THESIS STRUCTURE

The thesis comprises nine chapters. Chapter 2 presents a critical review of the relevant literature. It provides a background to archaeology, the current knowledge of the geographical and temporal appearance of cropmarks over buried features, and how aerial archaeologists use this information in survey. It concludes with a number of knowledge gaps which have shaped the study.

Chapter 3 presents the outline methodology for the study, explaining how the objectives have been addressed.

Chapter 4, Data Acquisition, presents the data collected though a desk study, the methods and results of site investigation, and the methods used for long-term monitoring of four buried ditch features.

Chapter 5 presents the results of a geotechnical characterisation of the soils at the locations of the buried ditch features, comparing the properties of vertical sections through and adjacent to the features.

Chapter 6, Hydrogeological Modelling, firstly determines whether knowledge of the soil water characteristics, from direct soil water measurements, of the buried ditch features and the adjacent soils can indicate the mechanisms which cause cropmarks to appear, and the background conditions at the time they appear. Secondly, it determines whether a hydrogeological model can simulate the results of direct measurements, using both measured or known soil, crop and weather data, and information from database sources alone.

Chapter 7, Methods of Cropmark Analysis, proposes three methods which utilise predominantly existing data acquired during the desk study, which can be applied to increase knowledge of the conditions in which cropmarks appear.

Chapter 8 is a broad discussion of how the models and methods presented in this study can aid aerial survey in continuing to be a valuable resource in the detection of buried archaeological features.

Chapter 9 presents the conclusions of the study and provides recommendations for future work.

CHAPTER 2. LITERATURE REVIEW

2.1 INTRODUCTION

This chapter presents a review of the literature relating to aerial survey in archaeology. It begins by providing a general background on archaeology as a discipline and the emergence of aerial survey as a fundamental tool in archaeological reconnaissance (Section 2.2).

Aerial archaeology relies on the appearance of marks on the ground surface, where there is a visual difference in the soils or crops above buried features, revealing their geometry. Section 2.3 explains the types of features which can be identified by aerial survey, and the classification of marks and the known mechanisms by which they form.

The current practice in aerial survey is summarised in Section 2.4. It explains the understanding of the distribution of marks by soil type, as discovered by reconnaissance and mapping programmes. It also presents the models and methods used in aerial survey and bias inherent in the data.

The chapter concludes with a list of knowledge gaps identified from the literature review which underpin this study.

2.2 A BACKGROUND TO ARCHAEOLOGY

2.2.1 What is 'Archaeology'?

The field of archaeology and the processes it involves are explained in many texts, though there are many definitions of the term. Opinions are not only varied, but have changed through time as the discipline has grown into one of serious scientific study.

Archaeology attempts to recreate past events through accumulation of evidence and interpretation (Coles, 1972). Piggott (1959) states that "material objects of human origin, whether they be art, architecture or broken pots are of interest to the archaeologist as a student of material evidence, the tangible and visible products and achievements of extinct communities". The umbrella of 'tangible' products which Piggott describes has grown since his writing, to include some which are not necessarily visible. Further evidence can be found preserved in the landscape as an archaeological residue, such as a biological, chemical or physical change to the soils (Beck, 2011).

The factual evidence is subject to interpretation to recreate the past, allowing for inaccuracies. It is often uncertain and inadequate for this purpose, but is the best available (McBurney, 1963). The development of archaeology as a field of study has been hampered by these uncertainties and inadequacies. At times, archaeologists were thought to be eccentrics and the subject of ridicule (Pallottino, 1968), but it has grown as a subject as new investigation processes and interpretative methods are applied to ancient puzzles.

The public awareness and acceptance of archaeology improved greatly as archaeology took some giant strides forward in the years following the First World War. There is little doubt that the development of archaeological aerial photography played a fundamental part in the onset of modern scientific archaeology. Pallottino (1968) states that this is "an incalculably valuable and almost miraculous means of reconnaissance". An analogy commonly used to explain the value of aerial photography is a fly on the surface of a rug cannot see the full pattern woven in the rug, but once it is in the air it can see the whole picture. The picture comprise visible differences in the colour of soils (soil marks) or crops (cropmarks) over the locations of buried features, or slight topographical differences which change the appearance of the ground (shadow marks).

Aerial survey is one of many techniques which form the ever increasing archaeological "toolkit" for collection of evidence. It forms the basis of historic landscape characterisation and mapping, and has grown from pictures taken out the windows of aeroplanes, to imaging sensors mounted on planes and satellites that can measure reflectance outside the visible spectrum. Geophysical techniques, such as resistivity, magnetometry, electro-magnetometry and ground penetrating radar, have been adapted for non-intrusive archaeological ground-based surveys. Where evidence can be retrieved from intrusive investigations, there is a wide range of laboratory analyses such as dating and chemical composition. The subject of geoarchaeology stems from soil science and uses laboratory methods, such as determination of particle size distribution, to characterise archaeological soils, with the aim of understanding site formation processes.

Most of the techniques used in archaeological detection have been derived from other disciplines. Methodologies have been borrowed from physics, chemistry, geology, biology, economics, political science, sociology, climatology, botany and other natural sciences (Daniel, 1967). Pallottino (1968) writes "practically the whole conception of environmental and stratigraphical excavation, all the laboratory analysis, much of the sociological, technological, and economic observations concerning ancient civilisations, are the direct result of the collaboration between the natural sciences and archaeology". These techniques have now grown into a separate discipline with its own specialities (Scollar et al., 1990).

Archaeology, then, could be considered to include the application of a set of scientific techniques to detect or investigate an archaeological site. The results of these techniques are scientific evidence upon which an archaeological interpretation can be based.

2.2.2 A Brief History of Aerial Archaeology

Major Elsdale of the British Army took the first known archaeological aerial photographs from a free balloon during the 1880's. During the First World War, the military used photography from aeroplanes for mapping, the new discipline of photogrammetry. The value of aerial photography for archaeology was compounded when, whist mapping Mesopotamia, Lieutenant-Colonel Beazeley (1870 - 1961) saw the remains of an ancient city complete with ornamental gardens along the River Tigris to the north of Bagdad in present day Iraq. He states "detail was unrecognisable on the ground, but was well shown up in the photographs, as the slight difference in the colour of the soil came out with marked effect" (Beazeley, 1919).

There was a rapid growth of aerial photography for military use, improving the quality of the photographs (Reeves, 1936). In 1920, Osbert Crawford (1886 - 1957) persuaded the Royal Air Force to photograph British archaeological sites, resulting in his appointment as the first Archaeology Officer to the Ordnance Survey. Crawford published the results of an aerial survey with Alexander Keiller (1889 - 1955) in *'Wessex from the Air'* in 1928. The work of Crawford and Keiller, led to the recognition of aerial photography as a tool for locating and recording archaeological sites (Parrington, 1983).

More recent developments in archaeological aerial survey include laser scanning using Light Detection and Radar (LiDAR), and hyper- and multi-spectral imaging outside the visible light spectrum.

2.3 THE HIDDEN PAST

2.3.1 Surface Indication of Archaeological Features

Archaeological evidence comes in all shapes and sizes, from large upstanding sites like Stonehenge to tiny objects buried in the ground. However, tangible artefacts like these

are not the only evidence that is available for archaeological interpretation. There are hidden features buried below the ground surface where anthropogenic changes have been made to the underlying soils, such as the remains of buildings and roads, or infilled defensive ditches. These features can affect the growth of crops or the overlying surface soils, when compared to the surrounding area. Where the contrast between the crops or soil above a buried feature and the surrounding area is detectable, the geometry of the hidden feature is revealed. Figure 2.1, taken near Eynsham, Oxfordshire in June 1995, shows Bronze Age burial sites and other buried features in detail, illustrating how striking these marks can be.

This section presents information relating to the composition of these features and the known mechanisms behind their appearance at the ground surface in terms of the anthropogenic changes to the soils.

Figure 2.1 Cropmarks near Eynsham, June 1995. Photograph from <heritage-explorer.co.uk>

2.3.2 Commonly Detected Features

The archaeological features that are most often recorded through the appearance of marks at the surface can be divided into two categories; those features which have cut away the soil or rock and have been subsequently infilled, such as ditches, pits, post-holes, cellars,

wells, graves and quarries; and features which have added material to the ground, such as the remains of roads and tracks, building foundations, floors and walls (Wilson, 2000). The most commonly recorded features are those which fall into the first of these categories (Rapp and Hill, 1998).

Where soil or rock has been removed, a range of processes may have occurred at the relict surface of the cut. The subsequent infilling replaces the removed material with different deposits. Features may have been artificially filled with anthropogenic material relatively soon after the cut was made, such as rubbish pits or holes dug for posts. Where cuts remained open for a period of time, weathering processes may have occurred, such as ditches cut for irrigation, or growth of vegetation on the open surface. Wind-blown material such as leaves, or sediment transported by water, may have been deposited in the cut. Should a feature have been abandoned, equalisation of the ground surface will occur over time, where surrounding surface soils slump into the feature.

Where there are features such as building foundations, walls and floors and additional material has been added to the ground. Roads and tracks may have added larger particles such as gravel to reinforce the ground surface. The additional loading in these areas also may have compacted the ground, altering the naturally formed soils beneath.

All these cases will cause alteration to the soil or rock from the natural state, and the properties of the soils forming the features will differ from those in the surrounding area. This difference in the soil properties can sometimes cause markings by proxy at the ground surface, such as a difference in the colour of bare soils or a difference in the way a crop has grown above the feature. These marks reveal their geometry, such as the circle of an Iron Age ring ditch, or the rectilinear outline of a Roman villa.

2.3.3 Classification of Marks

The marks which reveal buried archaeological features appear in a number of forms. The aerial archaeology pioneer O. G. S. Crawford categorised different types of marks as either shadow marks, soil marks or cropmarks, a classification still used today.

Shadow Marks

Where there are micro-topographical differences in the ground surface, shadows can be cast in low light revealing the geometry of the topography. This shadowing affect can also cause differential melting of frost and snow on the faces of upstanding earthworks hidden from the sun. Shadow marks are less common since the "massive ploughing up" of lowland Britain in the 1950's and 1960's, but can produce striking images (Drewett, 2012).

Soil Marks

The difference in the appearance, colour or reflectance of bare surface soils above a buried archaeological feature is known as a soil mark.

Cropmarks

Cropmarks appear when an archaeological feature causes differential crop growth, resulting in a detectable difference in the crops above the feature compared to that of the surrounding area. Parchmarks are a subcategory of cropmarks, which appear in permanent pasture (such as grass). They appear as plants wilt and discolour in dry conditions.

Shadow marks, by definition, are caused by topographical differences in the ground surface. Their appearance is governed by climatic (e.g. frost and snow cover) and imaging (e.g. low sun angle) factors. The properties of the soils have little effect on the

timing of their appearance, with the exception of possible differences in thermal properties. Therefore, they are outside the scope of this study. By far the most common type of mark recorded in the UK are cropmarks (e.g. Riley, 1982; St Joseph, 1977). Cowley (2012) reported that around 99% of markings recorded in survey in Scotland occurred in crop or grass, and only 1% as soil marks, although Grady (2014) felt this was an overestimation for survey in England. This study therefore focuses on those factors which govern the appearance of cropmarks, though there is some cross-over between these factors and those which cause soil marks, and any relevant discussion has been included.

2.3.4 Differential Crop Growth

Crop growth is dependent on the water available in the soil to transfer nutrients to the plants. Three conditions must be met to allow for this transfer: an adequate nutrient supply in the soil, water to transfer nutrients from the soil to the roots and allow plant uptake and translocation within the plant, and a rooting system reaching the water to transfer the nutrients to the plant (Jones and Evans, 1975).

As crops advance through the phases of growth, changes occur in the appearance of the plant. An example for wheat plants is given in Figure 2.2. Differential growth occurs where a different growth pattern is experienced by plants rooted in or near to a buried archaeological feature compared with those in the surrounding area. Though these differences can be present throughout the life of a crop from germination to maturity, they may not always be apparent to an observer. For a cropmark to become apparent, this difference in growth must be detectable, usually as a difference in colour.

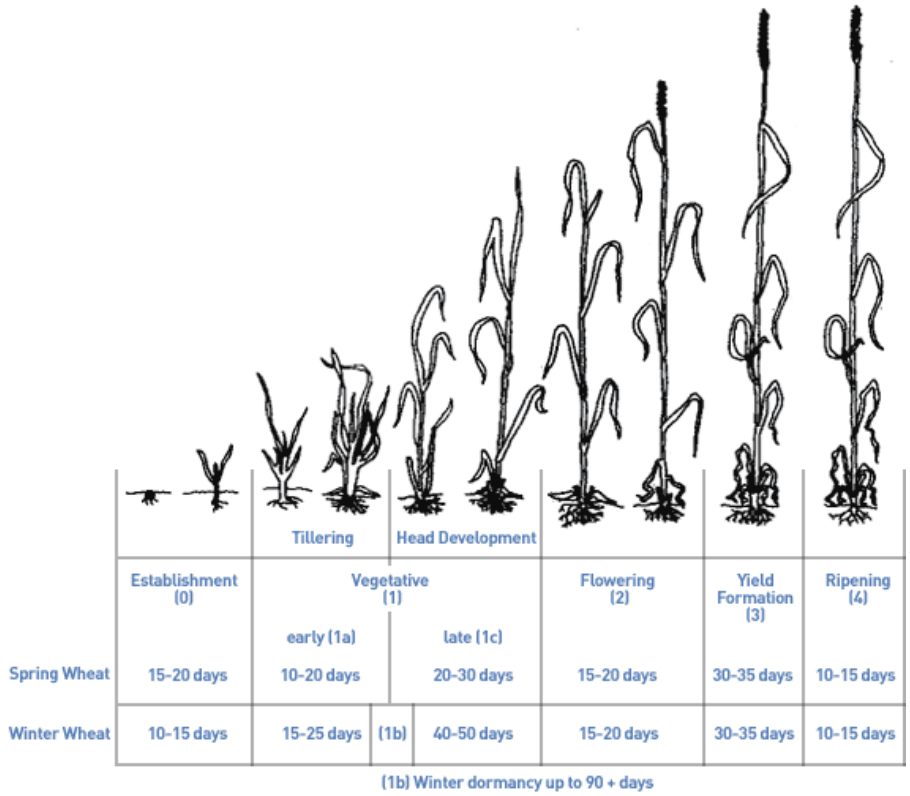

Figure 2.2 Stages of crop growth in wheat (Large, 1954).

Differential crop growth can be caused by a difference in the germination rates of seeds or a difference in the stage of growth. For crops where the growth rate is enhanced, differences can be apparent at stages throughout the life of the crop. At the emergence and tillering phases, increased greenness can be detected due to a higher leaf area index (the area of leaf surface). Once stem elongation has begun, the increased height of the crop can cause shadowing due to a change in relief. As heads or flowers appear or during the ripening of plants, there is a difference in colour. The reverse is true for crops where growth is inhibited.

It is not only a difference in the growth rate of a crop, causing it to enter new growth stages at different times, which can cause cropmarks to occur. Both crop height and the overall length of the growth cycle can be affected by the provision of water to a crop (Featherstone and Bewley, 2000). Inhibited growth may mean the plant never reaches

the same leaf area index or height as those that are uninhibited. At times when crops become under stress, differential wilting and discolouration can occur where crops have differential access to soil water (Jones and Evans, 1975). This is the case where parchmarks form in pasture.

The enhancement or inhibition of crop growth occurs due to differences in the properties of feature soils and those of the soils surrounding it, however the type of crop is also a fundamental factor as different plants respond differently to the soil conditions. Where the growth of crops above an archaeological feature is enhanced compared to those in the surrounding area, the mark is classed as positive. Where growth is inhibited above an archaeological feature, the mark is classed as negative.

2.3.5 Mechanisms of Cropmark Appearance

There are numerous mechanisms which can cause marks to appear. Those most common are given below.

Where buried features increase the water retention capacity in areas of coarse grained soils, cropmarks may occur in dry conditions as the surrounding crops become stressed, discolouring and wilting due to a lack of water supply. This mechanism can occur even if the feature is below rooting depth as the rate of redistribution of soil water perched above a feature is slowed (Worssam and Taylor, 1969) (see Figure 2.3(a)). Soil water content is also an important factor in soil colour variation (Jones and Evans, 1975; Scollar et al., 1990).

It follows that the reverse case, where a coarse grained feature is present in an area with fine grained soils, should also produce crop marks due to differences in the soil water characteristics. However, Evans and Jones (1977) mention that in areas with soils of high permeability, dry conditions have a much more significant effect on crop growth

than in areas where water is retained in the near surface soils for longer periods without recharge, and cropmarks in fine grained background soils are uncommon. This may be due to water being retained in the coarse grained feature perched over less permeable fine grained soils.

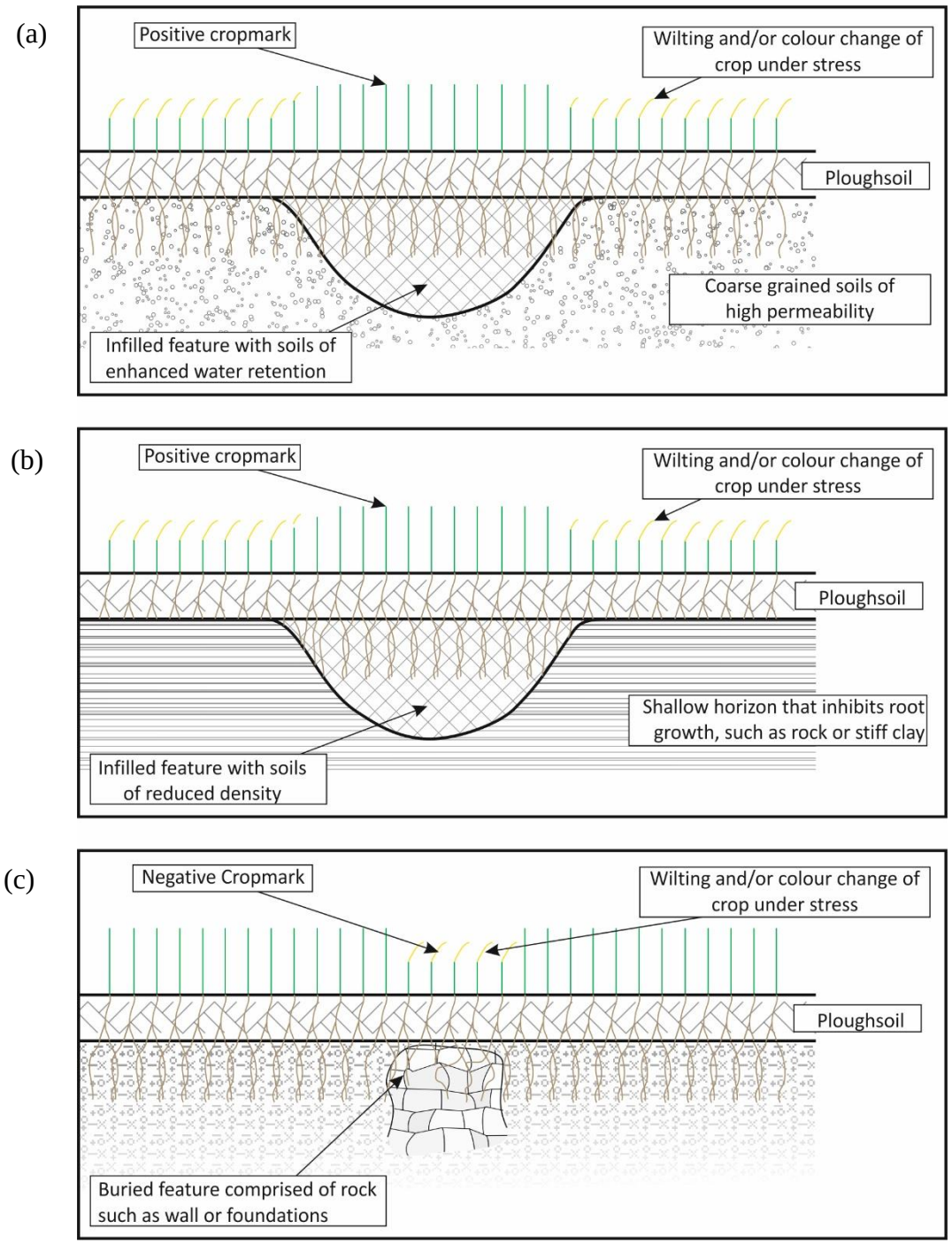

Figure 2.3 Mechanisms of cropmark appearance.

(a) Positive cropmark over coarse grained soils. (b) Positive cropmark over shallow soils. (c) Negative cropmark over a feature comprising rock.

Many cropmarks occur where soils are shallow over a horizon from which plants cannot easily draw water, such as shallow rock or stiff clays (Jones and Evans, 1975; Evans and Jones, 1977; Evans and Catt, 1987). Where features have been cut into these horizons and filled with soil of lower density, root development, and therefore crop growth is enhanced (Figure 2.3(b)). Cropmarks are common on soils <0.3m deep, though in drier conditions, marks appear in soils <0.50cm deep (Evans and Catt, 1987; Evans, 1990).

The reverse case of this would be where a feature comprises rock or compacted material, such as walls, foundations or roads. This could reduce the water holding capacity or inhibit root development (Figure 2.3(c)).

Another mechanism over shallow rock is where gravel is incorporated into the topsoil, either through ploughing or frost action. When approximately <30% of the ground surface is covered in gravel or larger sized particles, drilling, germination and growth of the crop is poorer (Evans, 1990). Where rock or gravel has been used for foundations, walls or roads, the reverse case can occur, where particles which formed part of the feature can be brought to the surface.

Seeds planted in smeared (from ploughing or drilling) clay soils above the plastic limit germinate slower than on less clayey or friable soils (Evans, 1990; Evans and Catt, 1987). Evans and Catt (1987) suggested that crop patterns occurring over natural geological formations had been caused by smearing of clayey soils during the drilling of seeds, inhibiting germination. The patterns were apparent in a crop when seeds were drilled while the clay soils were above the plastic limit, but did not appear when the seeds were drilled during a drier period when the clay soils were below the plastic limit. At the time of their writing, they did not attribute this mechanism to the formation of cropmarks over archaeological features. However, it follows that cropmarks could be attributed to this

mechanism should a buried feature comprise soils of differing plasticity. Plasticity is affected by the presence of organic matter. Those features with increased organic material such as ditches which have been open long enough for vegetation to grow, for wind-blown organic matter to gather, or for natural infilling by slumping of organic surface soils to occur, theoretically could produce cropmarks.

The soil mechanisms of cropmark formation listed above can be attributed to those factors which inhibit the physical development of the crop, such as inhibited germination in smeared clay soils or factors which affect the soil water characteristics, such as the water retentive capacity of the soils. These factors are not mutually exclusive, for example in shallow rock where root growth is inhibited there may also be reduced soil water reserves. Therefore, both the depths of soil horizons and the soil geotechnical properties such as porosity, density and particle size distribution are significant to the formation of crop and soil marks. Jones and Evans (1975) and Evans and Catt (1987) conclude that that it is the indirect, combined effects of geology and climate on soil water availability that is more significant in the formation of cropmarks, rather than the physical nature of the soils alone.

2.4 AERIAL SURVEY

2.4.1 Aerial Survey in Archaeology

Aerial survey is undoubtedly one of the most useful tools for archaeological research. It is a cost effective method of both discovering and recording archaeological sites, and in some areas has revolutionised the understanding of human settlement in certain periods, producing spectacular results (Cowley and Brophy, 2001; Cowley, 2002). No other survey technique has done more over the last 80 years to change the perception of the distribution of archaeological remains in Britain (MacLeod, 2011).

Aerial survey is still revealing new archaeological information in areas which have been intensively studied for many years, with new discoveries often making the news (Owen, 2009). Stonehenge has been studied at ground level for centuries. Lieutenant P. H. Sharpe is generally credited with taking the first aerial image in 1906 (Barber, 2005). Since then thousands of images of the area have been taken from the air in varying conditions. Prior to 2001, the archaeological record contained 2062 records within a study area around Stonehenge. Since the onset of a national mapping programme in excess of 500 new records have been added (Historic England, 2015d). In 2013, dry ground conditions within the site itself, caused by not having a long enough hosepipe to water the whole area, gave rise to cropmarks that provided evidence that the lintelled circle may have once been complete (BBC, 2014).

Bewley (2001) states that there is a "growing realisation within the profession that understanding the nature, extent and significance of the aerial evidence is a fundamental requirement for the conservation and management of archaeological sites".

2.4.2 Distribution of Cropmarks in the UK

In the UK, the largest number of cropmarks have been located on river terraces, though they are also frequently recorded soils with parent materials of chalk, limestone, sandstone. They are also often seen in areas of shallow rock (Jones and Evans, 1975; Evans, 1990). Evans (2007) found that, of those UK soils where cropmarks are recorded frequently and extensively (an area covering 25% of England and Wales), 95% were in areas where soils are shallow to hard rock, sands or gravels.

It is accepted without opposition that deep soils of predominantly clay-sized particles less commonly show cropmarks than those with a higher permeability. The non-productive nature of clay-dominated soils in terms of archaeological prospection has led

to these areas being largely ignored, under the assumption that they were either not settled and no features were present, or they simply never produced marks and were not worth investigating. Mills and Palmer (2007) tackles these assumptions head on, stating that their volume could be seen as a "call to arms" for more research-led investigations to be held in these soils which archaeologists term "difficult". Evans (2007) defines these "difficult" soils as those which are deep and hold large soil water reserves.

Though this "difficulty" is well documented from the extensive experience of aerial surveyors, there is little literature relating to why this is the case. In a study relating to the soil associations in England and Wales and the appearance of cropmarks Evans (2007) reports that this is because the soils can hold the water required for growth during dry spells, and for cropmarks to occur a feature must be deep and release soil water more readily than the adjacent consolidated soils. It follows that there must be differences in the soil suction, changing the plants' ability to access water held in the soil.

No literature could be found relating the appearance of cropmarks to geotechnical aspects of clays, although Grady (2014) commented that low plasticity clays are more productive than those of high plasticity. Cropmarks have been found on the Fenlands of Lincolnshire and Cambridgeshire with the humose infill considered to be the cause (Riley, 1982, 1996). In these cases, it may be the difference in the plasticity of the fenland clays that causes differential growth.

The type of crop also plays a fundamental part, since cropmarks appear more readily in some plants than others. The different water requirements and rooting systems of crops means that different plants react differently to changing soil water conditions.

2.4.3 Soil Moisture Deficit as an Indicator of Cropmark Appearance

Cropmarks are known to appear in certain soil, crop and weather conditions. To assess the combined effect of these a single parameter of Soil Moisture Deficit (SMD) is used, expressed in mm. It is defined as the amount of water required to bring the soil water content to Field Capacity (FC), and is represented by Equation 2.1. FC is loosely defined as the amount of water a soil can hold against gravity, commonly represented by the water content at suctions of 33 kPa.

$$SMD = [FC - \theta]Z_r \qquad [\ 2.1\ ]$$

Where θ is the soil water content (decimal percentage)
and Z_r is the rooting depth (mm)

Equation 2.1 is far from definitive. The term $FC - \theta$ results is a dimensionless water content which is not crop-dependent. The Z_r term adds dimension to the result so it can be compared with weather data, for example, rainfall and evapotranspiration that are measured in mm. The equation has a high dependence on rooting depth such that the SMD calculated using the rooting depth for sugar beet, with a maximum of 1400mm (Hough and Jones, 1997) would be double that calculated for potatoes with a maximum rooting depth of 700mm (Hough and Jones, 1997). The rooting depth is not only dependent on the type of crop, both the availability of soil water and the soil horizon depth can affect root development. Where near surface soils do not contain the required water for growth, roots penetrate deeper, and roots reaching a horizon which is difficult to penetrate may preferentially develop laterally.

When SMD occurs, plants will use the available water stored in the ground. Once the finite available soil water reserves are spent, plants will come under stress, wilting or losing their greenness due to a lack of nutrients transferred by soil water.

SMD is modelled as a potential SMD, calculated on a number of parameters, including potential evapotranspiration (an estimate of the loss of water from the soil due to evaporation from the surface and transpiration by plants) and rainfall, which may be inaccurate at a local scale. For example, collective monthly rainfall is calculated over a wide area and may be temporally or spatially inaccurate. Therefore, the actual SMD may vary from the potential SMD. It follows that the accuracy of potential SMD may vary from place to place dependent on the availability of accurate data to apply to the model. Throughout this study the term SMD is used to represent potential SMD.

A study of cropmarks and naturally formed crop patterns at 45 localities found that 14% produced cropmarks at a SMD of less than 40mm, 32% developed cropmarks when the SMD was between 50-100mm, 41% between 100-150mm and 20% from 150-200mm (Jones and Evans, 1975). It was concluded that the search for sites from the air could be made more efficient by concentrating photography into periods where SMD exceeds 50mm. Further study on this topic in Evans (1990) suggests that, in areas with clay-dominated soils, SMD must be >150mm by the end of June, indicated by values of >100mm by the end of May. These values are used to inform planning of aerial surveys for prospection archaeology in the UK.

2.4.4 The Met Office Rainfall and Evaporation Calculation System

Both RCAHMS (Royal Commission on the Ancient and Historical Monuments of Scotland) and HE use SMD data obtained using the Met Office Rainfall and Evaporation Calculation System (MORECS). This model uses a number of crop, soil and weather inputs for the calculation of SMD over 40km grid squares across the UK, such that the value relates to a specific crop type.

The calculations for MORECS are presented in detail in (Hough and Jones, 1997); a summary is given here. The potential evapotranspiration for a grid square is calculated using a modified version of the Penman-Monteith Equation (Monteith and Unsworth, 1990), with meteorological input parameters. The results are used to estimate actual evapotranspiration using an additional parameter of Available Water Capacity (AWC), based on the soil and crop type. The SMD is calculated as daily iterations of a water balance, where the difference between the rainfall and actual evapotranspiration are added to the SMD of the previous day, with account taken for loss due to interception of rainfall by plants.

The meteorological parameters are determined from a network of weather stations across the country. Crop inputs (e.g. leaf area index and surface resistance) are defined for 11 crop types, including grass, and winter wheat and barley, though also include ground cover such as bare soil and water.

The AWC component is divided into two categories; the Easily Available Water (EAW), held at suctions of between 5kPa (for fine soils) or 10kPa (for coarse soils) and 200kPa; and the Restricted Available Water (RAW), held at suctions of 200kPa to 1500kPa. This lower limit of 5-10kPa approximates FC and the upper limit of 1500kPa approximates the permanent wilting point, with 200kPa being used as the division between water which is easily accessible to plants and water which is more difficult to take up. Each of the crop types defines depths for EAW and RAW. EAW is available to a maximum rooting depth, whereas the additional water reserve of RAW is available where there is a shallower, denser rooting structure. The soil data used for modelling are taken from the Land Information System, LandIS, a spatial geodatabase of UK soils operated by Cranfield University.

Aerial surveyors use weekly values of SMD calculated using MORECS (40km grid squares) for grass, and values are monitored from April throughout the spring and summer seasons to select areas for survey.

2.4.5 Aerial Archaeology in Practice

Prospection for marks on the ground is not the only requirement of aerial survey. Over a flying season, a number of known protected sites, including upstanding sites, are selected for monitoring from the air, though buildings can be targeted at other times of year, leaving times of high SMD, where marks from buried features are considered most likely to occur, for prospecting.

In search of cropmarks, aerial surveyors follow the results of work in Jones and Evans (1975), Evans and Jones (1977), Evans and Catt (1987) and Evans (1990) to relate the likely appearance of cropmarks to SMD and soils, and is the basis of the predictive model use for planning of aerial survey.

In areas where values reach above 50mm SMD indicated by MORECS, and shallow or coarse grained soils are present, cropmarks should start to appear and when these figures reach over 100mm, marks should become distinctive. Cropmarks are only expected on clays when SMD is over 150mm, and even then they may only appear "with luck" (Grady, 2007). Using a combination of soil maps and MORECS data, areas can be selected for survey.

2.4.6 Bias in Aerial Data

2.4.6.1 Distribution Bias in Soils

There is an inherent bias in distribution of buried features identified as surface marks. Where there has been a lack of understanding or assessment of this bias, survey results are often misused during archaeological synthesis (Cowley, 2002). The accepted

"difficulty" in surveying in areas of deep or clay-dominated soils has resulted in a lower density of identified features, compared with those areas of shallow or coarse grained soils. This has misled some archaeologists into thinking that areas where there is a low density of known features were not as commonly settled as those where greater numbers have been identified (Mills and Palmer, 2007), the assumption is that if cropmarks are more commonly recorded on shallow or coarse grained soils, there was more settlement in these areas. However, this does not take into account that an absence of evidence is not evidence of absence.

Although it is known from the considerable experience of aerial surveyors that cropmarks occur more readily on well drained or shallow soils, this is not the only cause of distribution bias. There are factors in the distribution of land use; for example, less permeable soils are more likely to be used for pasture than arable crops (Featherstone and Bewley, 2000), and since grass does not respond to differences in available water as readily as other crops, it is less likely to experience differential growth.

This bias in distribution is apparent where recorded cropmarks have been mapped against soils. This is illustrated in Figure 2.4, reproduced from Cowley (2007), where a high density of cropmarks are evident on sand and gravel ridges surrounding the estuarine clay, which is almost devoid of cropmarks. Cowley (2007) adds that with the exception of a single cropmark recorded on the clay, all others were actually on gravel ridges that were not recorded on the geological map.

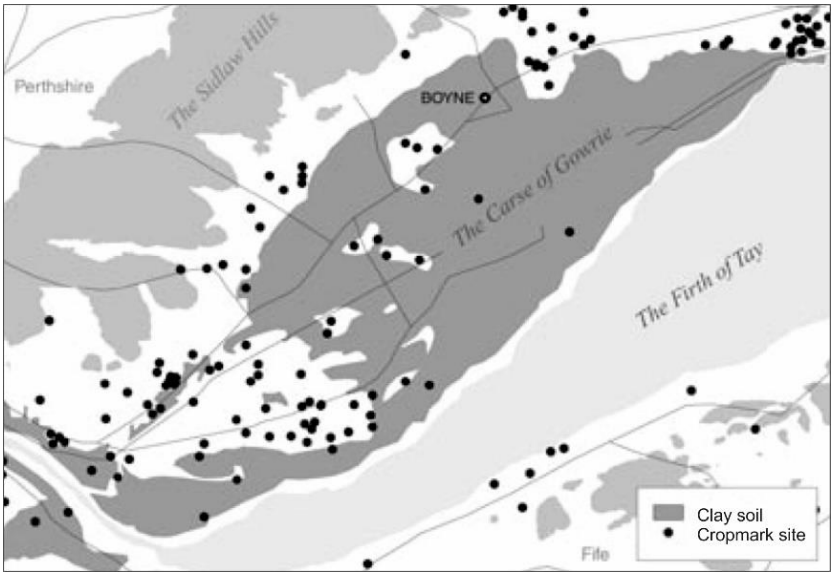

Figure 2.4 Distribution of cropmarks in the Carse of Gowrie shown against the generalised extent of clay-dominated soils. Crown copyright RCHAMS. (Cowley, 2007).

2.4.6.2 Methodological Bias

The data presented in Figure 2.4 clearly point to a conclusion that the clay is less likely to reveal cropmarks. However, Cowley (2007) goes on to reveal that the survey methods used have been conditioned by an emphasis on high returns from survey, targeting the more productive areas or "honey-pots". The result is that areas of clay-dominated soils have not been subject to such intensive examination, and ignored at times of high SMD when the predictive model indicates that cropmarks may be present in these areas, in favour of high returns and repeat photography of known sites in coarse grained or shallow soils.

In the early years of aerial survey, there was an explosion in the discovery of previously unrecorded sites, and repeated surveying of honey-pots guaranteed high returns, and understandably these areas were intensively targeted. Following the predictive model has allowed aerial archaeologists to successfully record and map these areas, ensuring flights are made in the optimum conditions for a high return. However, new discoveries

in these honey-pots are less common (Cowley, 2007), and increasingly survey results are the re-recording of known sites. Assessing the aerial survey programme though a measure of performance causes an inevitable focus on those areas with a reasonably predictable return, taking the focus away from the discovery of new sites in less responsive soils (Cowley, 2002, 2007).

The predictive model used for planning of surveys has been directly based on the data arising from survey results, comparing the extensiveness and frequency of cropmark appearance on mapped soil units. Therefore, if bias in survey methods is accepted, then there must also be a bias in the data upon which the model is based.

2.4.6.3 Addressing the Bias

The approach of aerial surveyors is changing, and gaps in the dataset where less productive soils are present are being targeted to address this bias. Presenting this, Grady (2007) found the response of archaeologists to this view to be varied, with some believing that clay-dominated soils remain unproductive, and others insisting that they should be a priority. However, there was a consensus that clay-dominated soils should be targeted in exceptional drought years.

Contrary to this consensus, SMD below those in the predictive model have been shown to reveal cropmarks on clay soils. Cowley (2007) describes a sortie planned for the monitoring of buildings, as there was little expectation for recording cropmarks due to a SMD of 60-70mm. Shortly after take-off, by chance, a cropmark was noted in clay soils. Though the cropmark was not spectacular, it is proof that values of SMD below those given in the predictive model do not preclude the appearance of cropmarks, even in "difficult" soils.

Aerial surveyors have accepted the predictive model, so it can be assumed that in their experience they have found the model useful in the prediction of cropmark appearance. Their achievements in research are revolutionary, therefore the reliance of survey planning on the model has certainly had merit. However, there is a view that areas which have been intensively studied (such as the honey-pots) are reaching or have reached "saturation", that is, all that can be found using aerial imagery within the visible spectrum has already been found (Beck, 2011). New methods of survey are being called upon to help address this bias.

2.4.7 Recent Aerial Methods

Although imaging from light aircraft is the most common method used in aerial survey, more recent developments in imaging technology are being assessed for their application to archaeological research. Some of these methods are outlined below.

Micro-topographic changes in the both the elevation of the ground surface and the surface of ground cover, such as vegetation, can be revealed using LiDAR sensors. Satellite imagery from Google Earth and Bing Maps is available to a wide audience, however the resolution of the data is lower than aerial imagery. The most detailed views are still added to these tools using images from aerial survey. There are however a number of satellites in operation which provide the higher resolution required for archaeological research, such as IKONOS, Quickbird, WorldView and GeoEye (Historic England, 2015c). Multi- and hyper-spectral remote sensing widens the imaging spectrum to outside the visible range. The applications in archaeology of imagery outside the visible range is discussed at length in Beck (2011). As with traditional aerial survey, each of these methods has both great potential and drawbacks in archaeological research.

2.5 IN SUMMARY

Buried archaeological features, such as ditches, post-holes, foundations and roads, alter the properties of the ground. The location and geometry of the features can become apparent on the ground surface as markings. Most markings are due to differential growth of crops, though rarely they can also appear as difference in soil colour.

Cropmarks occur due to the response of crops to the different subsurface soil conditions of features such as infilled cuts and buried walls or foundations. The crops rooted in these features respond and develop differently to those in the surrounding area. At times when the differential growth manifests as a detectable difference in the appearance of the crop, either due to the inhibition or enhancement of growth above a feature, cropmarks develop. The mechanisms which govern the appearance of these cropmarks are a combination of physical factors affecting development, such as inhibition of root development in shallow rock, and the ability of the crop to access soil water, particularly at times where available water is below that of the crop requirement for optimum growth. The access of crops to soil water is a fundamental factor in the development of cropmarks and is a complex interaction of weather and soil properties.

Cropmarks are most obvious from an aerial viewpoint. Programmes of aerial reconnaissance and mapping are run across the UK to monitor known sites and prospect for new, previously unrecorded sites. A model predicting the likely appearance of cropmarks has been based on the available survey data, cross referenced with SMD models and soil maps. It has been used in practice by aerial surveyors to plan surveys of areas of different soil conditions at times when soil water conditions are optimum, achieving a high return of cropmarks.

From the experience of surveyors, it is known that cropmarks are common in areas of coarse grained or shallow soils, and are rare in deep clay dominant soils. The reasons for this have not been researched in practice, though it is proposed that the ability of clay soils to retain water and release it during dry spells reduces the likelihood of plants coming under water stress.

Studies on the distribution of settlement in the landscape are hampered by gaps in the data in areas of clay-dominated soils, where it is not known if the absence of evidence truly represents an absence of settlement. Though surveyors know from experience that bias in the dataset exists due to the non-productive nature of areas with clay soils, this is not the only cause. There is now a view that survey methods have skewed results. The requirement to fulfil targets has meant that surveys have been aimed at high returns, re-visiting honey-pots where the density of cropmarks is high. In the early days of aerial survey, this was understandable, as new sites were being recorded. Though these areas still give high returns in the right conditions allowing for the re-recording of sites, new discoveries are less common. Since areas which have been frequently surveyed may be approaching saturation, the focus of surveyors is changing from the re-recording of known sites, to discovering new.

Aerial surveyors use a model that predicts the likelihood of cropmark appearance using SMD, relating the data to soil types. With the information provided by the model, surveyors are able to make judgements when planning surveys, depending on the conditions. They can choose whether to target areas for high returns, or to tackle areas where there are gaps in the data, usually when extreme dry conditions prevail. However, the model has been based on the results of previous surveys, which have been shown to contain bias. Using the model, may then perpetuate the bias. New sites have been

discovered by chance in conditions where they would be assumed to be unlikely from current research and the predictive model.

A lack of understanding of why clay soils are less likely to show cropmarks has led to a view that traditional aerial surveying is approaching its limit in the discovery of new archaeological sites. Archaeologists are turning to developments in imaging technology to fill the gaps left by traditional aerial survey methods.

2.6 THE MISSING LINK

The focus of aerial surveying is changing from the want for large returns, towards the need to address inherent bias and fill gaps in the dataset to perpetuate its usefulness in archaeological research. It has been shown that the bias in data stems from two main sources: the distribution bias due to the properties of the background soil or rock; and the methodological bias from survey practice. Further knowledge of these biases would not only lead to increased productivity in survey and aid discovery of new sites in areas considered to be less productive, but also lead to a better understanding of the true distribution of settlement.

The two causes of bias represent problems at two scales. At a small scale, analysing the differences between soils forming a feature and those adjacent to it, to determine the mechanism causing cropmark appearance, would aid understanding of bias due to the properties of the background soil or rock. At a larger scale, over an area such as a geological or soil unit, only the properties of the background soils are considered. Increased knowledge of the required background conditions for the appearance of cropmarks over soil or rock units would aid methodical survey in areas where cropmarks rarely appear.

At the small scale, the basic mechanisms which cause differential crop growth resulting in cropmarks received much attention in research in the latter part of the 20th century. Differences in the availability of soil water for plant uptake is understood to be the controlling factor in differential crop growth over archaeological features, though the physical structure of the subsurface is also important. This information has not been built on in recent years, with research leaning towards study at the large scale using new technologies and data analysis methods.

Remote sensing surveys are carried out to find areas of interest by looking for anomalies, that is, to find where there is something that differs from the area around it. It is understandable that once an archaeologist has found an anomaly, such as a cropmark, the focus is to determine the cause in an archaeological context. Interpretation of the cropmark may be based only on the geometry of the feature, though if subsequent excavation is carried out analysis is focused on gaining further evidence for archaeological interpretation. This may include geoarchaeological laboratory analysis of the properties of the feature soils (such as water content, particle size distribution and organic content as loss on ignition), using methods derived from soil science. However, comparison with the soils adjacent to the feature, to determine the mechanism by which the anomaly appeared, is outside the scope of geoarchaeological investigation.

If this comparison of the properties of the feature and the properties of the surrounding soils were assessed, they could reveal a quantitative set of conditions in which the anomaly is apparent. However, information gained through geoarchaeological excavation receives little comparison with the results of aerial survey. Jordan (2013) states that geoarchaeology is "marginal to the business of aerial archaeology" and that there are very few remote sensing (both aerial and geophysical) surveys which involve

any observation of soil profiles as a means of direct calibration and control. There may be a view that to collect soil data which are comparable with remote sensing surveys, sampling must be done at the same time as the aerial survey, which is considered to be a difficult prospect (Jordan, 2013). However, although crop and weather, and therefore soil water conditions, are in constant flux, the soil properties remain relatively stable, and sampling does not need to be contemporary to provide data on the soil water characteristics. With information on soil properties from subsequent investigation and historical weather data, the hydrogeology could be modelled to understand soil water conditions at the point of the aerial survey.

At the large scale, it has been shown that traditional aerial surveys, imaging within the visible spectrum, have been fundamental to archaeological reconnaissance, with the discovery of a wealth of archaeological features that are hidden beneath the ground surface. However, the rate of discovery of new sites is slowing, as areas which have been repeatedly overflown because of their productive nature, are approaching saturation. The less productive areas, where there are clay-dominated soils, are only expected to show cropmarks in extreme dry conditions, where the SMD is over 150mm. However, some aerial surveyors are now targeting these areas when the SMD is over 100mm in the hope that there may be exceptions to the model, as was discovered by Cowley (2007).

Archaeologists are looking for ways to address the methodological bias in their survey. There is hope that developments in imaging technology and data analysis may fill these gaps in the data and there is a noticeable focus in recent research towards these methods (Jordan, 2013). Developments in these areas will undoubtedly improve surveys, and may go some way to filling the gaps in the dataset left by traditional surveys. However, whether the survey method uses traditional or new technologies, the understanding as to

why features are or are not apparent in certain conditions is still lacking. Aerial archaeology requires integration with other forms of survey, and should not be considered a separate "specialism" (Bewley and Rączkowski, 2002).

Since the work of an aerial archaeologist is to provide evidence for interpretation, there is a focus on positive results. The use of the predictive model in planning of surveys means that most surveys are carried out in conditions considered optimal or near optimal for high returns. This methodology has been shown to be productive in the re-recording of previously known sites, but does not necessarily aid identification of new sites, that may appear as a cropmark in differing conditions.

A further difficulty for analysis of the data is that a surveyor with the remit of taking aerial images of archaeological features does not image the ground where no features are present. The result is a lack of proven negative data. The positive data (an image with a cropmark) has an image date, which can be compared with other historical data. The negative information goes unrecorded and remains within the experience of the surveyor.

The missing link is the gap between the analysis at the small scale, the mechanisms of cropmark appearance, and the comparison of these data with the results of large scale aerial surveys. It is hypothesised that to perpetuate the usefulness of traditional aerial surveys, there is a need to calibrate the results of aerial surveys against ground conditions, to improve the understanding of the conditions in which they appear. Factors relating to soil, weather and crop, and their combined influence on the soil water, need to be assessed, not only at times when a cropmark is evident, but also when a known feature cannot be detected remotely. In the context of this study, the need for comparison of the results from ground investigations and traditional aerial surveys has been identified. However, the knowledge of the differences between the properties of features and the

surrounding soils would allow calibration of all remote sensing surveys, whether they are geophysical, and aerial or satellite imaging both inside and outside the visible range.

2.7 KNOWLEDGE GAPS

A number of gaps in knowledge have been identified from a critical review of the literature. These gaps are outlined below.

1. Aerial surveying for the detection of archaeological features hidden below the ground surface mainly relies on cropmarks becoming apparent on the ground surface. These cropmarks are caused by the differential growth of plants rooted in or near to the feature soils compared with those rooted in the adjacent soil or rock as they respond differently to the change in ground conditions. A number of mechanisms of cropmark appearance, relating to the differences in soil properties and the availability of soil water have been identified. However, no studies could be found which quantify the differences in the geotechnical properties between archaeological features and the adjacent soils.
2. The significance of the relationship between soil, weather and crops and their combined influence on soil water and the timing of cropmark appearance has been identified. However, there are no studies on the differences in the soil water characteristics of archaeological features and the adjacent soils in the context of cropmark appearance.
3. Aerial surveys are planned using a simple predictive model to assess the likelihood of cropmark appearance over two soil types, using SMD as an indicator. Although this model has been used in practice for many years, there are no studies of validation or refinement, perhaps because, until now, it has been successful in producing high returns.

4. There is a distributional bias in the results of aerial surveys which has been related to the soil type. Clay-dominant soils are considered less likely to produce cropmarks than coarse grained soils. This fact is well documented from the experience of surveyors, although little study has been carried out as to why this is the case.
5. Historically aerial surveyors have used a predictive model to carry out surveys in optimum conditions for high returns. This has resulted in a methodological bias in the dataset. This bias is now recognised and surveyors wish to address it by increasing surveys in less productive areas. Although the model indicates that extreme prolonged dry periods are needed for cropmarks to appear in clay-dominant soils, cropmarks have been discovered by chance in moderately dry conditions. This suggests that there are situations that the simple model does not allow for, although the model may also be flawed due to its basis on biased data.
6. Aerial surveys are not routinely calibrated with data from ground investigations.

The following chapter presents the methodology derived to address these knowledge gaps.

CHAPTER 3. METHODOLOGY

3.1 INTRODUCTION

It is hypothesised that to perpetuate the usefulness of traditional aerial survey, there is a need to calibrate the results against ground conditions, to improve understanding of the conditions in which they appear. The aim of this study is to propose cost effective soil-based methods that can be applied to improve understanding of cropmark appearance to optimise the use of aerial survey for detection buried archaeological features.

The literature review shows that understanding the likely appearance of cropmarks requires analyses on two scales. At the small scale, the causes of differential crop growth and mechanisms of cropmark appearance require a comparison of the soils forming a feature and those adjacent to it. At the larger scale, for aerial surveying, the composition of features is unknown, and indication of cropmark appearance is based on knowledge of background conditions alone.

The first two knowledge gaps relate to the mechanisms of cropmark appearance and the differences between feature and adjacent soils. Although a number of basic mechanisms of cropmark appearance have been identified, there is a lack of understanding of the differences in the soil and soil water characteristics between feature and background soils which cause differential crop growth, particularly where clay-dominated soils are present. This study presents the results of a comparison of both the geotechnical properties and the soil water characteristics of soils forming buried features and the soils adjacent to them.

The remaining knowledge gaps relate to methods in aerial survey. A simple model predicting the likelihood of cropmark appearance has, until now, aided aerial

archaeologists in achieving high returns from survey over coarse grained or shallow soils. However, recording of cropmarks in areas of clay-dominated soils is less common. This may be due to a combination of factors; cropmarks are less likely to appear in these areas; and these areas are less commonly surveyed. This has resulted in both a distributional and methodological bias, leaving gaps in the dataset. This study proposes and tests a number of cost effective analysis methods which can be used to validate and refine the simple predictive model by calibrating aerial data with information relating to the ground conditions. Applying these methods to a wide area over a range of soil types would increase understanding of the appearance of cropmarks in different soil types, refining the predictive model for use in aerial survey, and hence addressing the methodological bias. Improving the methods of aerial survey to increase the recording of cropmarks in areas of clay dominant soils would address the distributional bias.

This chapter presents the outline methodology used to derive conceptual models which can be used to improve understanding of cropmark appearance at both large and small scale. Comprehensive methodologies are given in the relevant chapters.

3.2 DATA ACQUISITION

Initially, data were required for analysis. The DART Project selected four research sites at two locations for analysis and monitoring, each for a period of at least a year. Each of the research sites comprised a buried ditch feature in different background geological conditions. The locations of the four ditch features, from hereon known as the "research sites", were within two farms: Harnhill Farm near Cirencester, Gloucestershire; and Lodge Farm, in Diddington, Cambridgeshire; from hereon these are referred to as the research locations. Two of the ditch features were located in areas of clay-dominated soils (one in the Cirencester research location and one in the Diddington research

location), one in shallow limestone (at the Cirencester research location) and one in sands and gravels (at the Diddington research location).

This research begins with a desk study of the two research locations, assessing the geographical, hydrological, topographical, geological, geotechnical, hydrogeological, historical and archaeological settings. This gives an indication of the level of information which can be accessed through desk research and provides information for the subsequent analyses.

Site investigations of the four research sites were carried out in conjunction with the DART Project, with geotechnical aspects of the investigation being carried out by the author. Investigations were designed to fulfil the requirements of both the project and this associated study. The buried ditch features were selected and located by the DART Project using a combination of geophysical and borehole surveys. Using archaeological methods, a trench was excavated perpendicular to each of the features, revealing the ditch in cross section. Using both archaeological and geotechnical methods, the sections were logged and samples were taken from vertical profiles both through the features and the adjacent soils for laboratory analysis. Prior to backfilling of the trenches, bespoke monitoring stations were constructed at each of the research sites, comprising buried soil water and temperature probes in vertical profiles both through the feature and adjacent to it (extensively described in Boddice, 2014) and a weather station. Monitoring of each of the research sites continued for a period of at least a year. Throughout the monitoring period, the DART Project commissioned aerial surveys, providing images of the locations.

The information and the results of the desk study, the site investigation methods and the long-term monitoring techniques are presented in Chapter 4.

3.3 GEOTECHNICAL CHARACTERISATION

To determine the geotechnical differences between the feature soils and adjacent soils at each of the research sites, a geotechnical characterisation was performed.

Samples retrieved during the site investigations were subject to a suite of geotechnical laboratory testing. The samples selected for testing were taken from vertical profiles through each of the four ditch features, from ground level to the soil or rock horizon below, and through the naturally formed soil profile between 1-3m laterally from the centre line of the ditch, to the same approximate depth. For all subsequent analyses, the soil profiles were considered as these two vertical sections, one through the ditch feature, the Ditch Section (DS), and one adjacent to it, the Adjacent Section (AS).

The geotechnical characterisation comprised determination of Particle Size Distribution (PSD), density and plasticity. In addition, external commercial geochemical testing for Total Organic Matter (TOM) was carried out on samples retrieved from nearby boreholes (<5m from the sampled sections).

The results of the geotechnical characterisation and a comparison of properties of the feature and adjacent sections are presented in Chapter 5.

3.4 MODELLING SOIL WATER CHARACTERISTICS

3.4.1 Introduction

The literature review showed that a number of the known mechanisms of cropmark appearance were due to differences in the availability of soil water to plants rooted in or near to buried features and those in the adjacent soils. The SMD model used by aerial surveyors to indicate likely cropmark appearance is also directly dependent on soil water.

This part of the study aims to use models of soil water to improve understanding of both the mechanisms of cropmark appearance, by comparing the differences between the AS and DS, and background SMD, represented by the AS, relating them to the appearance of cropmarks.

For analysis, it has been necessary to derive a grading system for the appearance of cropmarks. All locations where a cropmark is known to have been present on any single image was reviewed on all images and given one of three grades; not visible; indicative; or mappable (these are explained and defined in Section 6.2).

Initially these two analyses are carried out using measured data from the long-term monitoring, site investigation and the geotechnical characterisation, with the minimum use of empirical calculation.

The measured data is progressively replaced with models and database inputs to determine if the results of the two analyses can be reproduced without the need for costly monitoring and intrusive investigation.

3.4.2 Analysis Using Measured Data

3.4.2.1 Section Comparisons

The long-term monitoring stations recorded hourly permittivity (using TDR) and temperature at probe locations in approximately vertical sections through the AS and DS. The results were converted to Volumetric Water Content (VWC) using empirical equations, and daily averages determined for each of the soil horizons. This process was carried out by D. Boddice of the DART Project and the methods of data collection and conversion to VWC are extensively covered in Boddice (2014).

The ability of a plant to take up water is not dependent on VWC alone, but is governed by suctions in the soil. The permanent wilting point of plants is generally accepted to be at a suction of 1500 kPa. When suctions exceed this plants wilt and do not fully recover when suctions reduce, although this is likely to be species dependent (Nyambayo and Potts, 2010). Therefore, the parameter of suction was used to compare the soil water between sections.

The Soil Water Characteristic Curve (SWCC) plays a fundamental role in understanding the hydromechanical behaviour of unsaturated soils (Pham and Fredlund, 2008; Malaya and Sreedeep, 2012; Zhai and Rahardjo, 2012; Pedroso and Williams, 2010). It is defined as the relationship between the soil water content and the soil suction (also known as negative pore water pressure or water potential). It was necessary to determine the SWCCs for the site soils, to convert the measured VWC to suctions. A number of empirical models for determination of SWCCs were compared. The method presented by (Saxton and Rawls, 2006) was found to give reasonable results.

The Saxton and Rawls (SR) method requires inputs of clay, sand, gravel and organic matter content, and matric density. The results of the geotechnical characterisation were used as inputs into the equation for each soil horizon. Using this method, the daily TDR VWC was converted to daily suctions. The relationship between suction and VWC is Log (suction) – Normal (VWC), so the logarithm base 10 of daily suction values were used for comparison of the sections.

Where possible, by taking weighted averages of the soil horizons in each level, the suctions of the AS and DS have been compared at three levels: above the ditch; from the top to the base of the ditch; and below the ditch. The results have been compared with

the appearance of the cropmark above the feature at each of the research sites. This process gives information on the possible mechanisms of cropmark appearance.

3.4.2.2 Background SMD

The data from the AS at each of the research sites reflected the results of the geological and geotechnical setting described in the desk study (see Section 4.3). The soil in the AS was considered to be representative of the background soil conditions in each case. The daily SMD was calculated from the FC (determined from the SWCC) and daily suction using Equation 2.1. These results were compared with the appearance of cropmarks in the area, where possible. The results give the conditions in which cropmarks are not only apparent, but also where there is no cropmark visible.

3.4.3 Analysis Using Modelled Data

To this point, hydrogeological modelling has used measured inputs wherever possible, with empirical methods being used only where necessary. This part of the study determines whether the VWC values calculated from TDR measurements, can be replaced with modelled VWC, and provide robust data for the two analyses (section comparisons and background SMD). Using modelled VWC for analysis requires only site investigation and geotechnical characterisation data, without the need for long-term monitoring of the VWC and installation of monitoring stations.

An existing hydrogeological model, the Soil Plant Air Water (SPAW) model, estimates daily soil water budgets in vertical soil sections using the SR method for determination of the SWCC, and was considered most appropriate for modelling the water in the soil sections.

Three categories of data are required for input - soil, weather and crop - which were derived from the geotechnical characterisation, the on-site weather stations, and crop data

provided by the landowner where available. Using the model outputs of daily VWC and FC, the daily Log suction and daily SMD were derived using post-processing.

To ensure the robustness of the model for application to this analysis, a selection of data was first tested against measured VWC data and the SMD calculated from the measured VWC. An inconsistency in the model output (refer to Section 6.6.1 for further information) was investigated using a sensitivity analysis. Although the causes of the inconsistency were identified, they could not be resolved. In the tested case, it was found that the model could simulate measured data with the addition of a correction factor to compensate for the model inconsistency.

3.4.4 Analysis Using Database Inputs

An assessment of the model output using database soil inputs into the SPAW model was tested against the model output using soil data from the site investigation and geotechnical characterisation. The geological and geotechnical information from the desk study was used to create soil profiles for input. The results were assessed in conjunction with the sensitivity analysis to determine if using database information could give SMD output comparable with using the measured data.

The same analysis was applied replacing known crop data with example data from files within the SPAW model, and replacing weather data from the on-site monitoring stations with freely available data from nearby weather stations.

Using the SPAW model with database soil crop and weather inputs to model background SMD does not require site investigation, long-term monitoring or geotechnical characterisation. Only desk study information is needed, reducing the cost of obtaining SMD data.

3.5 METHODS OF CROPMARK ANALYSIS

Current practice in aerial archaeology uses a simple predictive model for the likelihood of cropmark appearance using SMD as an indicator. Advice to aerial surveyors is that SMD of >50mm increases the likelihood of cropmarks in shallow or coarse grained soils, and SMD of >150mm increases the likelihood of cropmarks in clay-dominated soils.

Chapter 7 proposes three methods which can be used to validate and refine the predictive model. All the models can be applied with input data from desk study alone, without the need for site investigation or monitoring.

The data acquisition phase includes a desk study which provides information relating to the geology and recorded archaeological sites at the two research locations. The source data in the archaeological record was searched to determine the dates of images in which buried sites were recorded as cropmarks. Historical SMD data was sought for these dates.

The three methods use these data as inputs, but each have a different approach. The first, the cropmark approach, determines the SMD at times when sites appeared as cropmarks. The second, the flight productivity approach, addresses bias in the data by making assumptions about survey methods, determining a value of the productivity of flights made at known SMD. The third, the ground conditions approach, gives a percentage area of a particular geological ground condition which shows cropmarks at known SMD.

Each of the methods is tested using the data derived from the desk study and the outputs compared with the current knowledge on cropmark appearance.

3.6 CHAPTER SUMMARY

The initial processes of the study were to acquire data for the four research sites through desk study, site investigation and monitoring (Objective 2), and to perform a geotechnical

characterisation of the soils from vertical profiles through and adjacent to the buried ditch features (Objective 3). The results of the geotechnical characterisation determined the differences between the properties of the soils in the AS and DS.

The suctions of the AS and DS have been determined from both measured and modelled data. The differences have been compared at times when images show cropmarks above the feature (Objective 4). Using the results of the AS to represent background SMD, the results have been compared with the appearance of cropmarks in the same soil unit (Objective 5). The differences between the results using measured and modelled inputs has been assessed (Objective 6).

The measured soil data was replaced with soil profiles constructed using information from the desk study. Using the results of this analysis in conjunction with the results of the sensitivity analysis, the use of database inputs in place of measured inputs has been evaluated (Objective 7).

The proposed conceptual models of cropmark appearance can be used to provide additional data relating to the appearance of cropmarks with respect to the SMD and the background geological ground conditions. Use of these models over a wider area would aid in refining the current knowledge and informing aerial surveyors (Objective 8).

The results of all these analyses are discussed in Chapter 8, which determines how the proposed models would aid archaeologists, both in the planning of aerial surveys, and improve understanding of bias in the existing dataset (Objective 9)

CHAPTER 4. DATA ACQUISITION

4.1 INTRODUCTION

This chapter presents the results of desk studies, the methods and results of site investigations, and methods of long-term monitoring of buried ditch features. The site investigation and monitoring was carried out in association with the DART Project, which selected four linear buried features at two research locations in the UK for analysis. Soil samples were retrieved from each of the features and the surrounding soils for subsequent geotechnical characterisation.

This chapter gives an outline of the collaborative investigations and monitoring of the research sites selected by the DART Project. This is followed by a comprehensive desk study of the two research locations. The practical work carried out to investigate the features at each of the four research sites, both as part of this study and by the DART Project, is described along with the long-term monitoring of the features by the DART Project.

4.2 SITE SELECTION

The process of site selection was governed by the DART Project Consortium, with the requirements of all researchers involved needing to be met, as well as the need to arrange access to private land. The overarching requirements for site selection was that a suitable buried ditch feature had to be present that allowed the investigation of the feature and the nearby area, using a variety of techniques (e.g. archaeological, spectral and geophysical investigation), and that monitoring could continue for a period of at least 1 year.

Initially it was decided that two UK research locations were required to allow for monitoring in different weather patterns: one in the east of the country, which typically

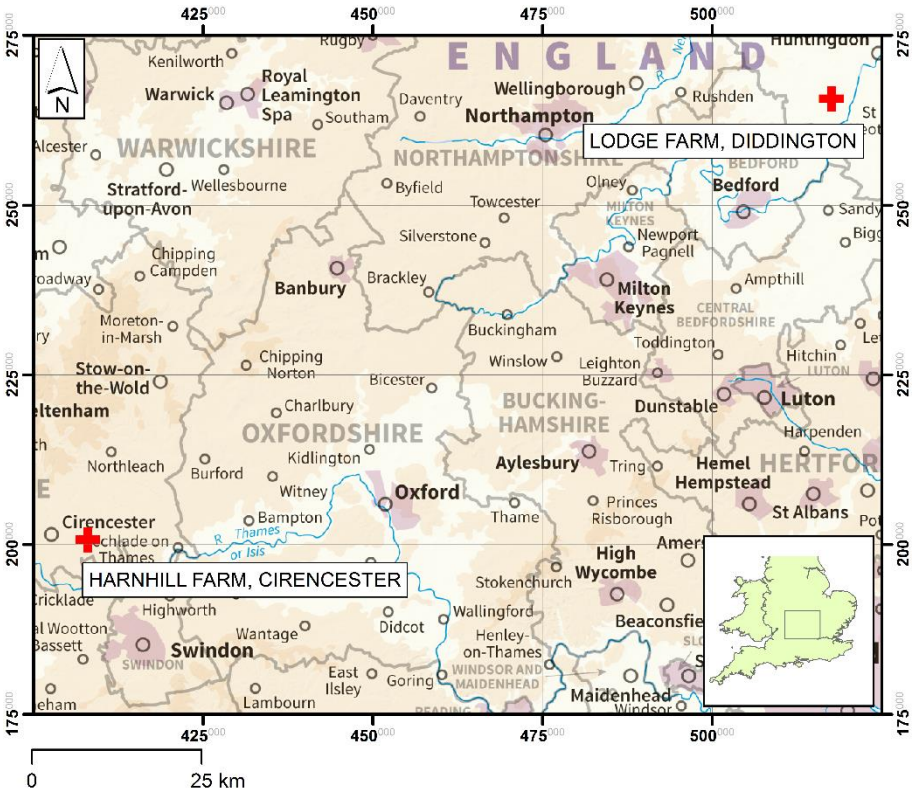

Figure 4.1 The research locations at Diddington and Cirencester. Mapping (Ordnance Survey, 2005, 2014).

receives lower total rainfall and one in the west, where the total rainfall is typically higher. Access for the installation of monitoring equipment was granted by two landowners; The Royal Agricultural University (RAU), owners of Harnhill Farm near Cirencester, Gloucestershire; and Thornhill Estates Ltd., owners of Lodge Farm in Diddington, Cambridgeshire. Figure 4.1 shows the locations research locations.

To allow for data collection in different ground conditions, each research location comprised two research sites, where the underlying soil or rock as determined by geological mapping differed. Since current remote sensing archaeological detection and investigation techniques are less successful at determining subsurface conditions in clay-dominated soils, two of the research sites were located where background soils were clay-dominated, one at each research location. For comparison, the second research site at

Cirencester was located on shallow limestone bedrock, and the second research site at Diddington was located on river terrace deposits.

The DART Project identified a buried linear ditch feature at each of the research sites, using a combination of magnetometry and borehole surveys. Suitable locations for the excavation and long-term monitoring of the features were planned in conjunction with the landowners.

The next section presents the results of desk studies conducted for the two research locations.

4.3 DESK STUDY

4.3.1 Introduction

A desk study provides the background data available for a site prior to any on site investigations. In the case of this research, it covers the geographical, hydrological and topographical, geological and geotechnical, hydrogeological, and historical and archaeological information for the Cirencester and Diddington research locations. It brings together information from a number of sources including: Ordnance Survey (OS) mapping; Memoirs of the Geological Survey; British Geological Survey (BGS) geological mapping; soil mapping (Cranfield Soil and Agrifood Institute, Soilscapes); BGS borehole and trial pit records; the BGS National Geotechnical Physical Properties Database (NGPPD); historical aerial imagery held by the Historic England Archive (HEA); and archaeological records held by Historic England (HE).

The purpose of the desk study was to provide contextual information for the site investigation and geotechnical characterisation phases. It also provides a background of historical and archaeological information for assessment in subsequent analyses.

4.3.2 Research Location at Cirencester

4.3.2.1 Geographical Setting

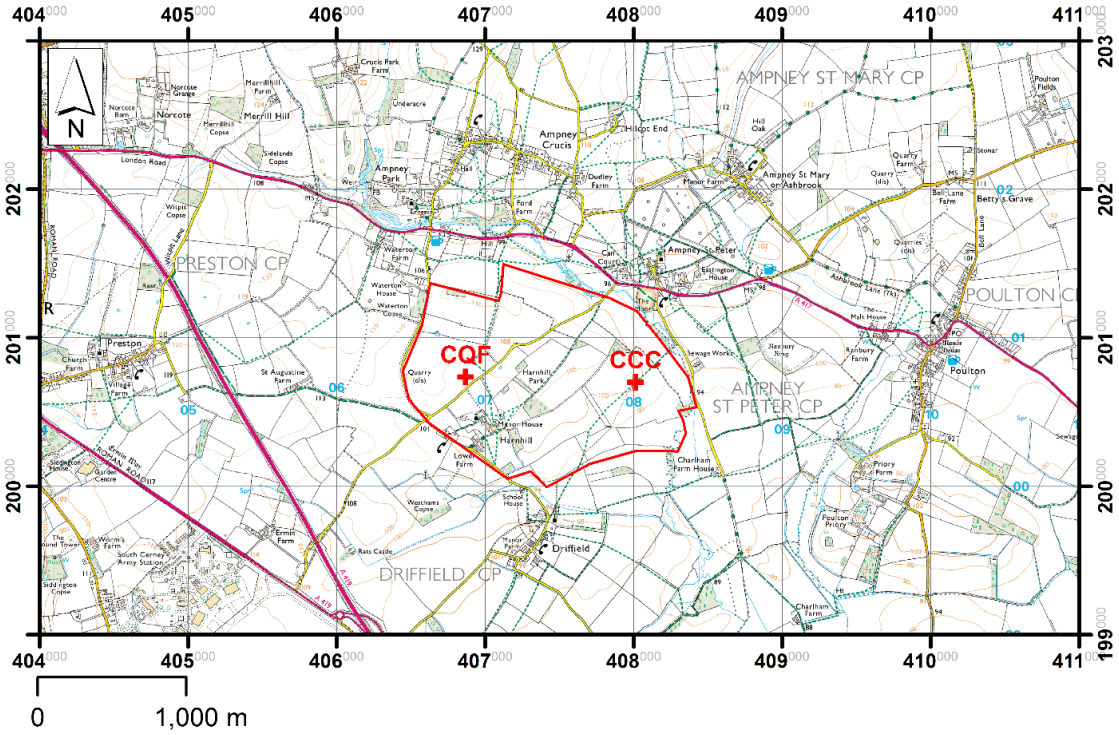

Figure 4.2 The DART research sites at Cirencester. The red line denotes the study area used in analysis Method 3, the ground conditions approach (Section 7.6). Mapping (Ordnance Survey, 2013a).

The research location at Cirencester is at Harnhill Farm, which is owned by the Royal Agricultural University (RAU) and is located approximately 4km to the south-east of the town of Cirencester. The two research sites, Cirencester Quarry Field (CQF) at National Grid Reference SP 08015 00700, and Cirencester Cherry Copse (CCC) at National Grid Reference SP 06872 00736, are located as shown in Figure 4.2.

4.3.2.2 Hydrological and Topographical Setting

Both CQF and CCC lie within the arc of the southerly flowing Ampney Brook as shown in Figure 4.3. An easterly flowing drainage channel to the south of the research sites joins the brook approximately 1 km to the south of CCC. A number of small ponds are located near CQF, which lie within an outcrop of mudstone.

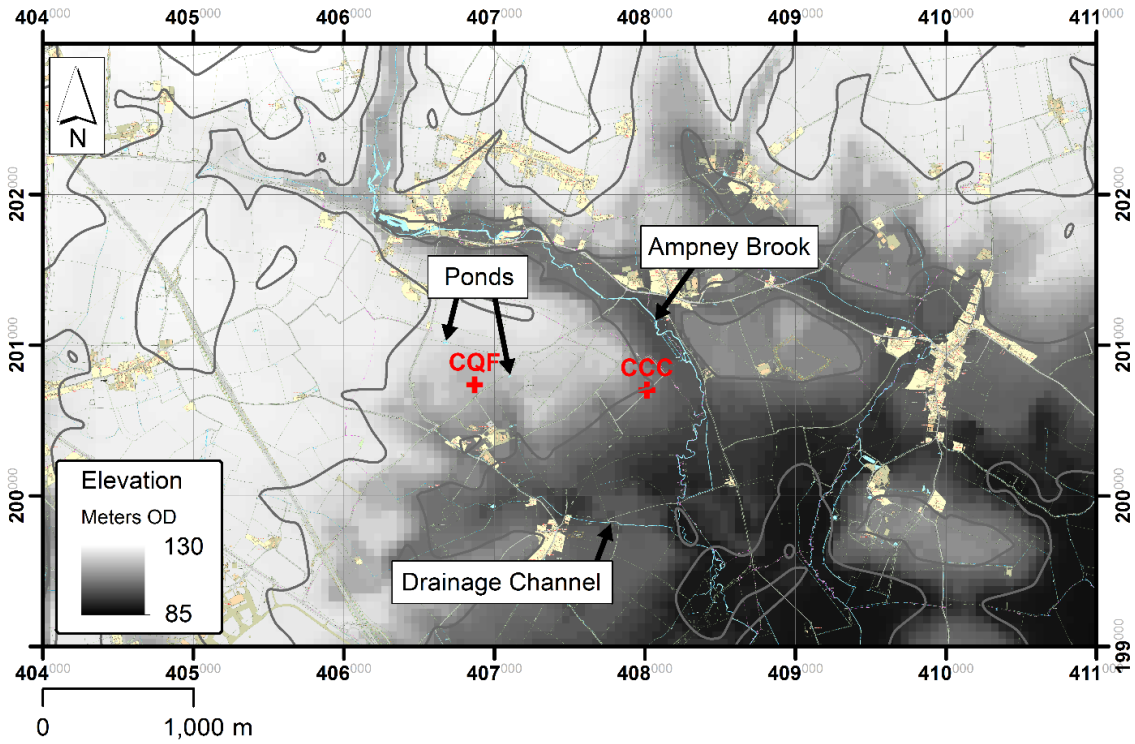

Figure 4.3 Hydrology and topography of the area around Cirencester. Mapping and terrain (Ordnance Survey, 2013c, 2013e, 2013g).

CQF is located at 118m OD in an area with a gentle slope down to the south-east towards the drainage channel. CCC is located at 90m OD on ground which slopes down to the east towards Ampney Brook.

4.3.2.3 Geological and Geotechnical Setting

Figure 4.4 shows the bedrock, superficial and linear geology of the area around Harnhill.

The area is underlain by Mid-Jurassic limestones and mudstones of the Great Oolite Group. The Forest Marble Formation outcrops to the north-west of the area and comprises silicate mudstone with limestone units (British Geological Survey, 2012). CQF is located in an area of Forest Marble Mudstone, which is the parent material of the overlying soils. It is a stiff fine-grained soil, with predominantly clay minerals, subordinate silica and no reported calcium carbonate content. The parent material is laminated and bedded with a fine-grained matrix and degraded rock fragments (British

Geological Survey, 2015d). Forest Marble limestones outcrop on the lower ground surrounding the research site.

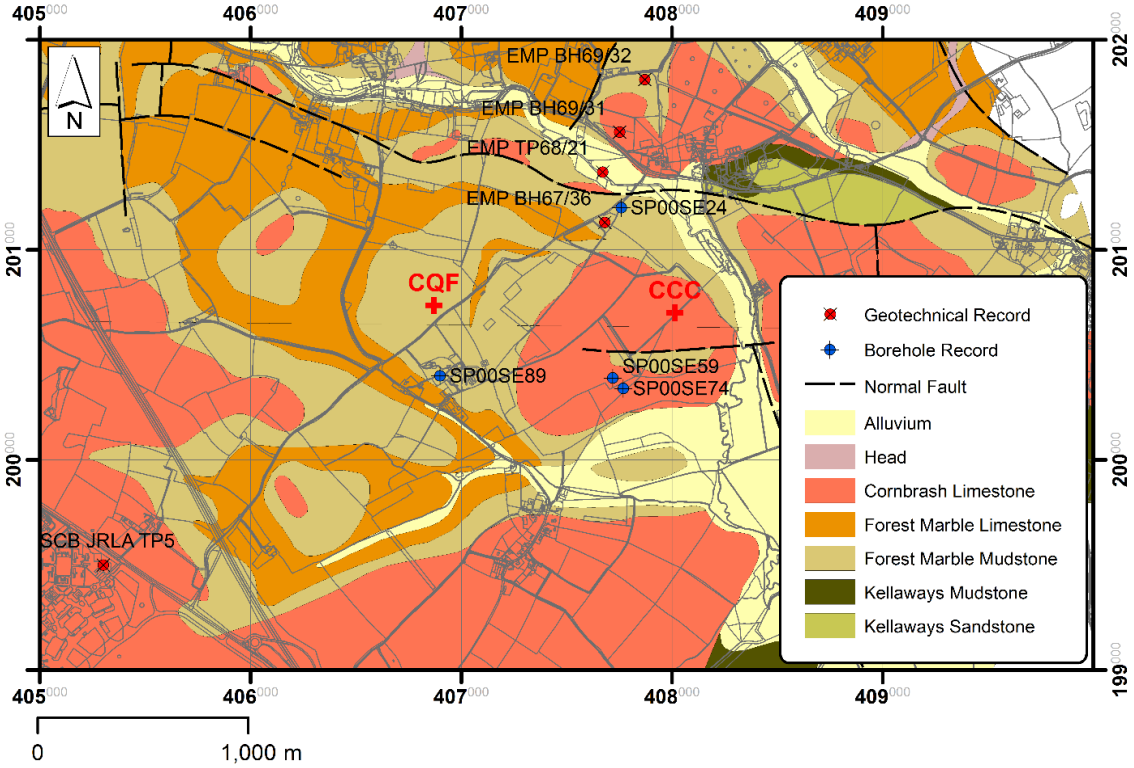

Figure 4.4 Bedrock and superficial geology in the area around Harnhill. Mapping (British Geological Survey, 2009a, 2009b; Ordnance Survey, 2013c). Borehole and geotechnical properties record locations are based upon records provided by British Geological Survey (NERC).

Limestones of the Cornbrash Formation overlie the Forest Marble at a disconformity. They typically comprise medium to fine grained, poorly bedded limestones. CCC lies within an outcrop of the Cornbrash Limestone within the arc of Ampney Brook to the north and east. This Cornbrash Limestone is the parent material of the overlying soil at CCC, which has bedding features and jointing. The soil is firm, well graded, calcareous, with a dominant sand and fine-grained matrix with degraded rock fragments (British Geological Survey, 2015d). A number of normal faults are inferred nearby. An east-west fault 190m to the south of CCC has an upthrow on its southern side allowing the underlying Forest Marble mudstone to outcrop.

The borehole records referenced in this section (shown on Figure 4.4) are openly available from the BGS website (British Geological Survey, 2015c). Approximately 1km to the north-east of CQF, within the outcrop of the Forest Marble mudstone, a deep borehole (SP00SE24) encountered the Forest Marble Formation to a depth of 8.5mbgl. The upper 0.9m comprises soils described as brown topsoil with limestone, overlying brown clay and grey limestone to 4.0mbgl and dark grey clay and beds of grey limestone to 8.5mbgl. Approximately 350m to the south of CQF a borehole (SP00SE89) describes the strata underlying the topsoil simply as grey rock to a depth of 9.6mbgl.

Approximately 450m to the south-west of CCC, two trial pit records (SP00SE59 and SP00SE74) are located within the outcrop of the Cornbrash limestone, south of the fault. They encountered fine-coarse gravel and cobbles of limestone, in a matrix of firm brown silty sandy clay, underlying shallow (15-20cm) gravelly topsoil.

Four records from the NGPPD (British Geological Survey, 2015b) to the north of the research sites describe the soils at 0.5mbgl as silty clays, with plastic limits of 26-28 and liquid limits of 52-60 (EMP BH69/32, EMP BH69/31 and EMP TP68/21), and clayey silt with a plastic limit of 24 and a liquid limit of 44 (EMP BH67/36). A single record from the database to the southeast of the research sites describes the soils at 1.5mbgl as stiff clay with limestone laminations, with a plastic limit of 20 and a liquid limit of 42 (SCB JRLA TP5). No nearby records hold any further geotechnical data.

4.3.2.4 Hydrogeological Setting

The Great Oolite Group is classified as a highly productive aquifer, with virtually all groundwater flowing through fractures and discontinuities in the rock (British Geological Survey, 2015a). However, the mudstone units of the Forest Marble Formation in the upper part of the group confine the aquifer (Sumbler et al., 2000).

The groundwater level at the nearby Ampney St Peter Observation Borehole (SP00SE24) typically varied between 84m and 96m OD between 1970 and 1976. This large variation in the groundwater level shows that groundwater response to recharge and drainage events is rapid (Sumbler et al., 2000). No groundwater was encountered in the boreholes in the Cornbrash Formation (SP00SE59 and SP00SE74) near to CCC, which were drilled to a maximum of approximately 1.4mbgl.

4.3.2.5 Historical and Archaeological Setting

Evidence exists of occupation of the area of Cirencester back to the Neolithic, though the area is most well-known for early Roman settlement when Cirencester was known as Corinium Dobunnorum. There is a wealth of Roman remains in the area, including a villa in the field of CCC, which has been scheduled by HE (see Figure 4.5).

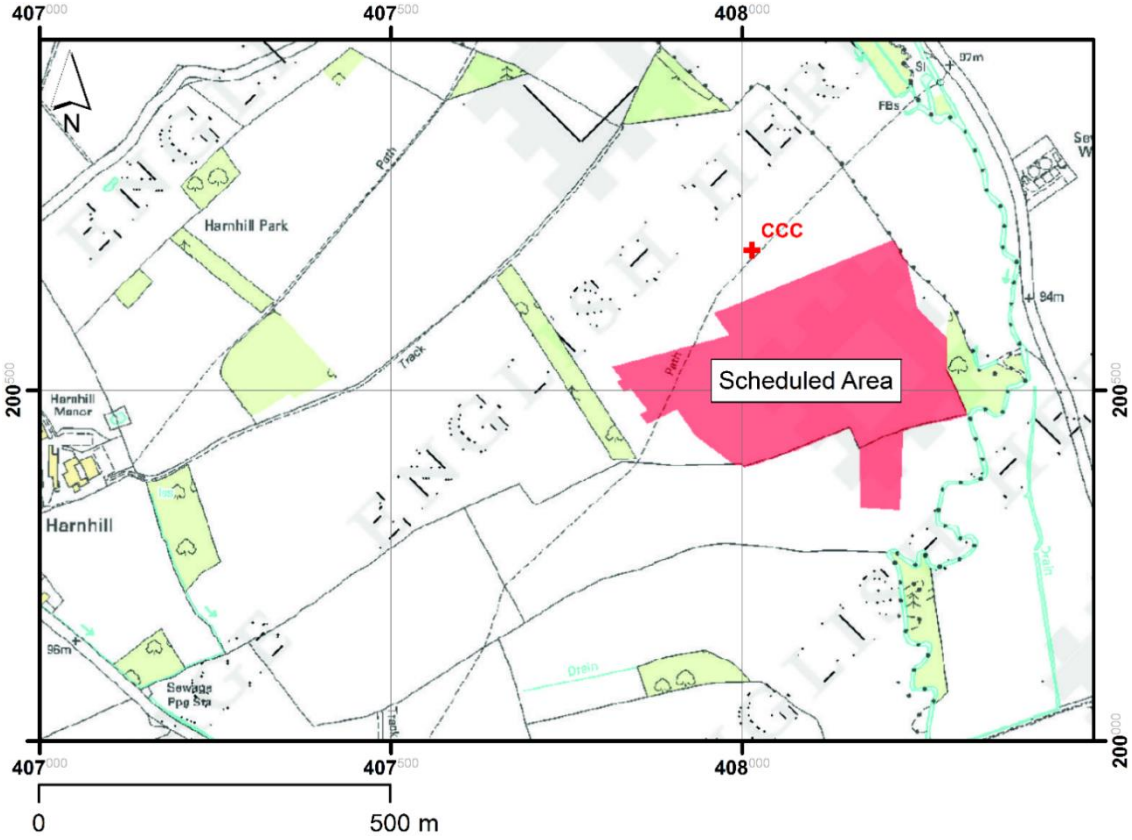

Figure 4.5 Scheduled area near Cirencester Cherry Copse. (Historic England, 2011).

The archaeological record held by HE is available via the Pastscape website (Historic England, 2015b). All features listed in this record within a 2km radius of the centre of the research location that have been identified as cropmarks are given in Table 4.1. Where they are available, the dates of the images taken where the cropmarks were seen has been included. The locations of these records have been plotted in Figure 4.6 using the coordinates given by EH, which are accurate to between 1-100m.

The mapped geographical locations and geometry of buried archaeological features and levelled earthworks (not including upstanding earthworks or sites) of the research location held by HE are shown in Figure 4.7.

The historical maps in the region of the research locations which have been studied are listed in Table 4.2 and key maps reproduced in Figure 4.8. A quarry 360m to the west of CQF, which is now disused and overgrown, is present on the 1884 map. The CQF research site is located at the junction of two field boundaries present in 1884, which were removed between 1938 and 1960. A track 100m to the northeast of CQF along the line of the old field boundaries was removed between 1974 and 1977. The 1884 map shows that CCC is also located along a northwest – southeast trending historical field boundary, which perpendicularly intersects a track 10m to the south-east of the site. The boundary was removed between 1903 and 1921. Between 1938 and 1960 further field boundaries were removed near to the site, although the track is still present. Both CQF and CCC were assumed to be related to the field boundaries on which they are located, either as part of the boundary itself or possibly field drainage ditches aligned along the boundary.

The Esso Midland Pipeline crosses the area from north to south and was installed in 1985 (Smith and Cox, 1986). The location of the pipe is shown in Figure 4.9.

Table 4.1 Archaeological records created from aerial imaging of cropmarks within a 2km radius of the Cirencester research location. Information from (Historic England, 2015b).

Reference Number	*Image Date(s)*	*Brief Description*	*Geology*
1	10/04/1946 01/12/1952 18/10/2004	Shrunken settlement	Shallow Forest Marble Limestone
2	10/04/1946 28/05/1947 14/05/1948 01/12/1952 29/03/1965 14/09/1973 30/10/1967	Ridge and Furrow	Shallow Forest Marble Limestone
3	28/05/1947 19/07/1990	Water meadow	Alluvium
4	06/09/1946	Deserted medieval village	Alluvium
5	04/06/2006	Prehistoric rectangular enclosure	Shallow Forest Marble Limestone
6	10/04/1946	Water meadow	Shallow Cornbrash Limestone
7	28/05/1947	Water meadow	Deep Clay
8	01/07/1975 27/07/1975 19/07/1990	Prehistoric field system	Shallow Cornbrash Limestone
9	01/07/1975 27/07/1975	Ring ditch	Shallow Cornbrash Limestone
10	No Date Given	Roman enclosures	Alluvium
11	No Date Given	Roman enclosures	Alluvium
12	No Date Given	Roman settlement	Alluvium
13	No Date Given	Roman settlement	Deep Clay
14	No Date Given	Prehistoric or Roman field boundary	Alluvium
15	28/05/1945	Curvelinear enclosure	Shallow Cornbrash Limestone
16	13/07/1972 19/07/1990	Linear ditches	Alluvium
17	19/07/1990	Linear ditch	Shallow Cornbrash Limestone
18	19/07/1990	Linear ditches	Alluvium
19	19/07/1984 19/07/1990	Trackway	Alluvium
20	10/04/1946 01/12/1952 05/10/1971 14/09/1973	Ridge and Furrow	Shallow Forest Marble Limestone
21	No Date Given	Linear ditches	Alluvium
22	No Date Given	Post medieval drainage system	Alluvium
23	No Date Given	Enclosures and trackways	Alluvium
24	No Date Given	Drain of unknown date	Alluvium
25	No Date Given	Post medieval boundary	Alluvium
26	24/07/1976	Round barrow	Shallow Cornbrash Limestone
27	04/06/1990	Roman double ditched enclosure	Shallow Cornbrash Limestone
28	24/07/1976	Iron Age farmstead	Deep Clay
29	24/07/1976	Iron Age /Roman enclosures	Deep Clay
30	25/06/1970 24/07/1976	Roman boundaries	Shallow Cornbrash Limestone

31	19/07/1990	Roman road	Shallow Cornbrash Limestone
32	19/07/1990	Roman field system	Shallow Cornbrash Limestone
33	24/07/1976	Enclosure	Shallow Cornbrash Limestone
34	06/01/2000	Medieval shrunken village	Deep Clay
35	No Date Given	Bronze age round barrow	Shallow Forest Marble Limestone
36	No Date Given	Prehistoric/Roman enclosures	Shallow Cornbrash Limestone
37	01/07/1975 03/07/2006	Iron Age /Roman enclosures	Shallow Forest Marble Limestone
38	24/07/1976	Bronze age round barrow	Shallow Cornbrash Limestone
39	No Date Given	Ditches	Shallow Forest Marble Limestone
40	No Date Given	Field system	Shallow Cornbrash Limestone
41	No Date Given	Medieval gravel pits	Shallow Cornbrash Limestone
42	No Date Given	Enclosure	Kellaways Clay
43	No Date Given	Bronze age round barrow	Shallow Cornbrash Limestone
44	25/06/1970	Roman villa and enclosures	Shallow Cornbrash Limestone
45	03/07/2006	Iron Age/Roman enclosure	Shallow Cornbrash Limestone
46	03/07/2007	Iron Age/Roman enclosure	Shallow Cornbrash Limestone
47	03/06/2011	Ring ditch	Shallow Forest Marble Limestone
48	03/06/2011	Building of uncertain date	Deep Clay
49	No Date Given	Bronze age dispersed barrow cemetery	Shallow Cornbrash Limestone
50	01/07/1975	Iron Age/Roman enclosure	Deep Clay
51	04/06/1990	Iron Age enclosure	Shallow Cornbrash Limestone
52	21/07/1971	Medieval field boundary	Shallow Forest Marble Limestone
53	18/07/1969	Bronze age barrow	Shallow Cornbrash Limestone
54	18/07/1969	Bronze age barrow	Shallow Cornbrash Limestone
55	25/06/1970 12/07/1999	Bronze age barrow	Shallow Cornbrash Limestone
56	30/07/1969	Bronze age ring ditches	Shallow Cornbrash Limestone
57	18/07/1969	Iron Age enclosure	Shallow Cornbrash Limestone
58	30/07/1969	Iron Age ditch	Shallow Cornbrash Limestone
59	03/07/2006	Ring ditch	Deep Clay
60	01/07/1975 04/06/1990	Field boundary	Deep Clay
61	01/12/1952	Water meadow	Shallow Forest Marble Limestone

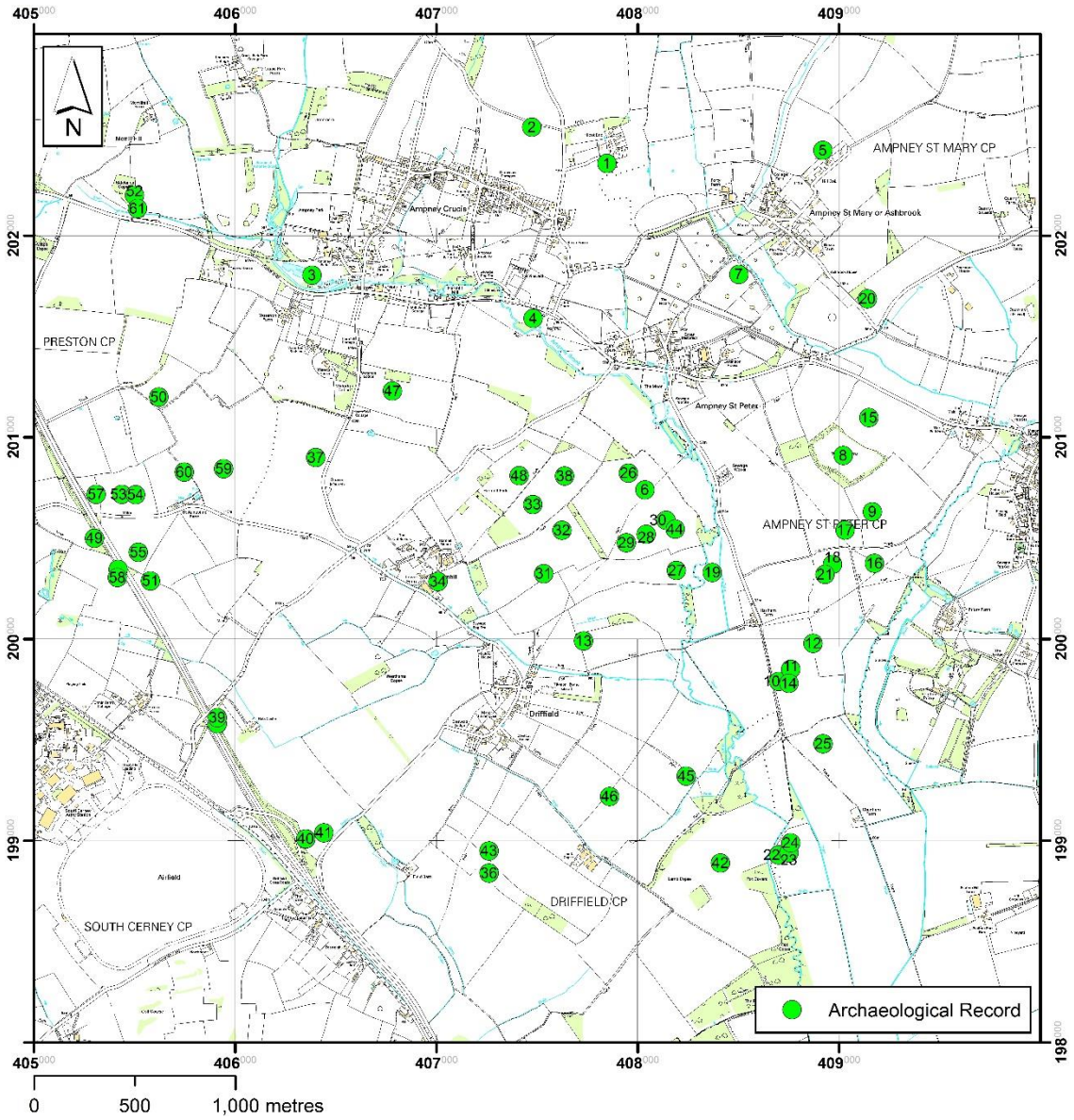

Figure 4.6 Locations of buried archaeological features identified from crop marks within a 2km radius of the centre of the research location. Locations are taken from pastscape (Historic England, 2015b), mapping (Ordnance Survey, 1982).

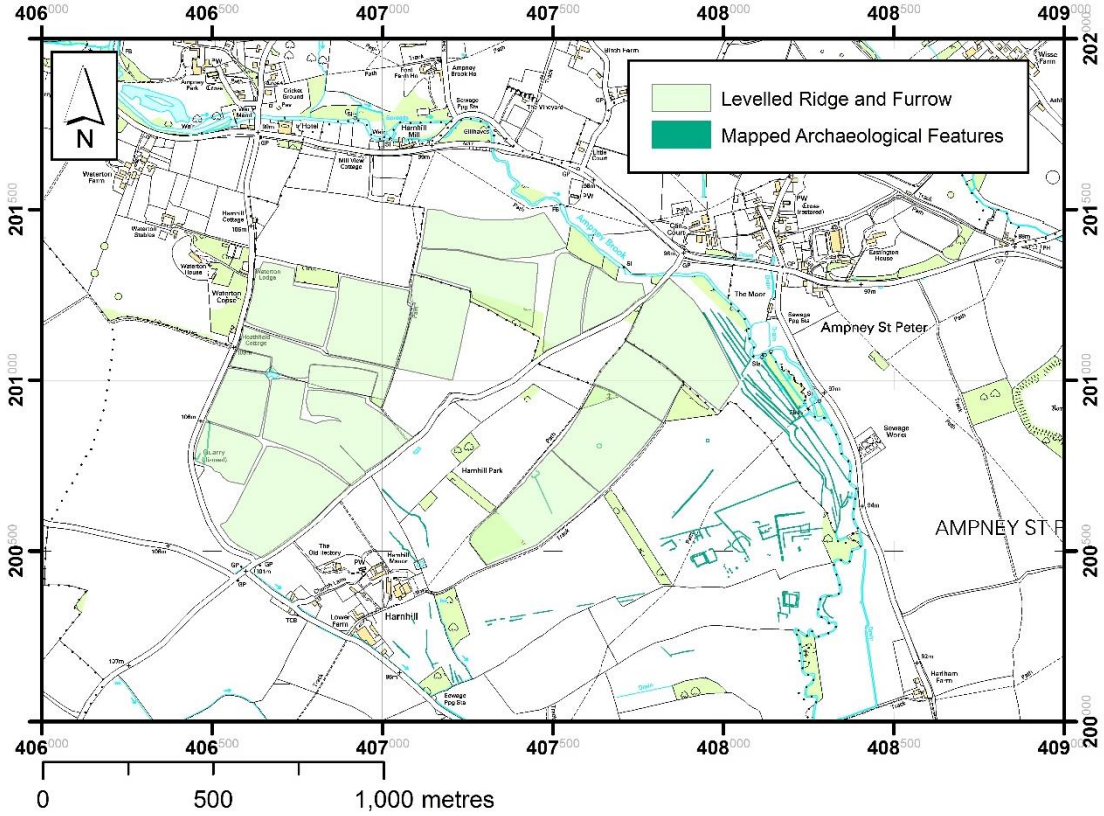

Figure 4.7 Data from the archaeological record which has been mapped (GIS layers provided by EH). Mapping (Ordnance Survey, 1982).

Table 4.2 Historical maps reviewed in the Cirencester Area. Mapping from Landmark Information Group, UK, using: EDINA Historical Mapping Service <digimap.edina.ac.uk>.

Mapping	*Scale*	*Edition*	*Publication Date*	*Reproduced*
County Series	1:2500	1st Edition	1884	Figure 4.8
County Series	1:10560	1st Edition	1888-91	
County Series	1:2500	1st Revision	1902-03	
County Series	1:10560	1st Revision	1903	
County Series	1:2500	2nd Revision	1921	Figure 4.8
County Series	1:10560	2nd Revision	1924	
County Series	1:10560	3rd Revision	1938	
National Survey	1:10560	1st Imperial Edition	1960	Figure 4.8
National Survey	1:10560	1st Imperial Revision	1974	
National Survey	1:2500	1st Edition	1977	
National Survey	1:10000	Latest Metric Edition	1982	
OS Mastermap	1:2000		Current	Figure 4.8

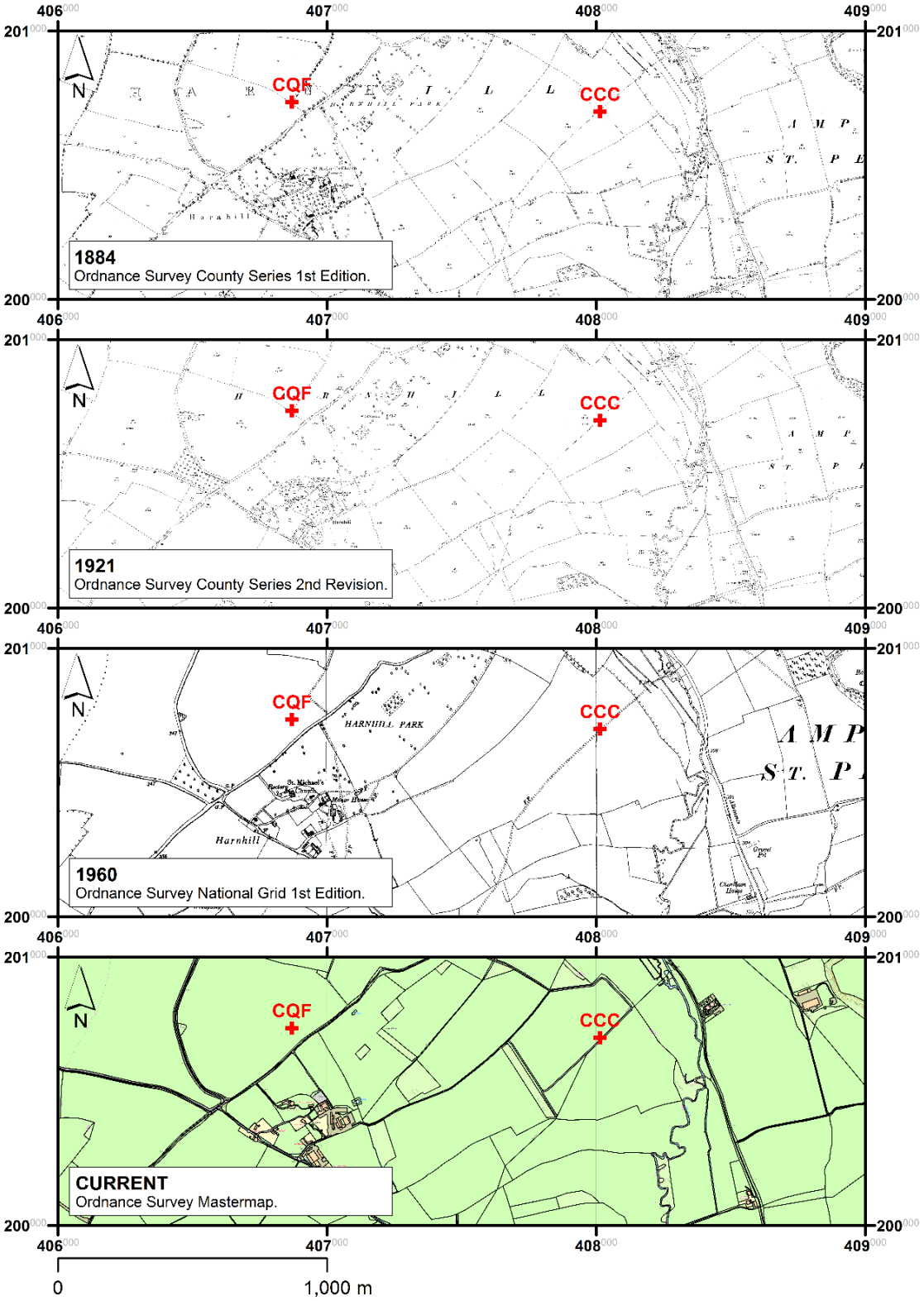

Figure 4.8 Review of historical maps in the Cirencester Area. Mapping (Ordnance Survey, 1884, 1921, 1960, 2013c).

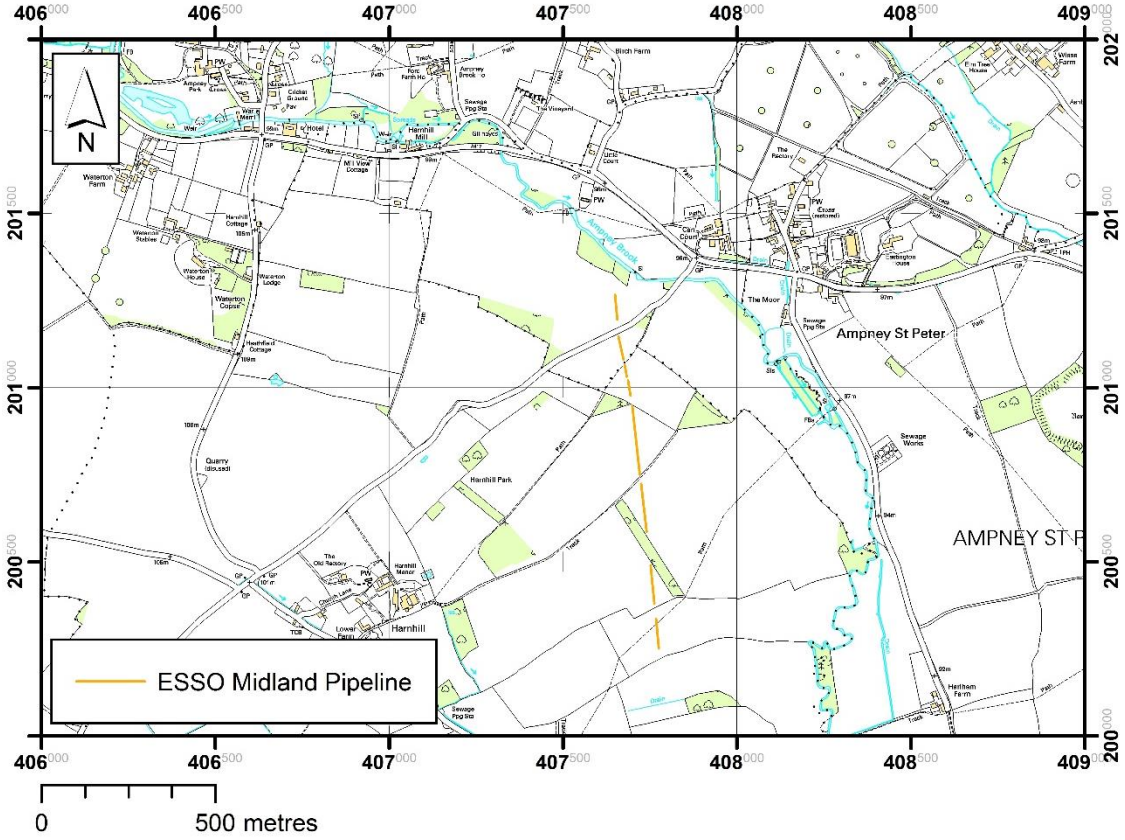

Figure 4.9 Location of the ESSO Midland Pipeline. Mapping (Ordnance Survey, 1982)

4.3.3 Research Location at Diddington

4.3.3.1 Geographical Setting

The village of Diddington is located in Cambridgeshire in the eastern side of the UK and was chosen by the DART Project as the area typically has a low rainfall, lying in the river valley of the Great Ouse, which is one of the driest river basins in the UK (Worssam and Taylor, 1969). The research location is at Lodge Farm, which straddles the A1 and the two research sites; Diddington Clay Field (DCF) at National Grid Reference TL 17627 65673, and Diddington Pasture Field (DPF) at National Grid Reference TL 19173 65262, are located either side of the road as shown in Figure 4.10.

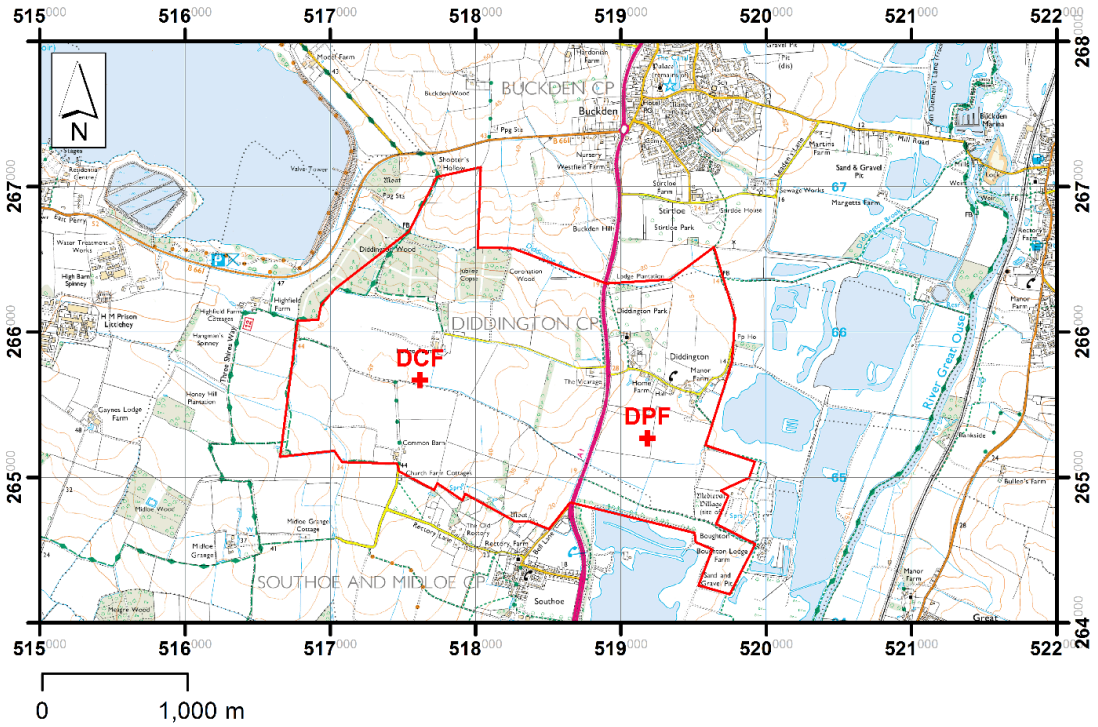

Figure 4.10 The DART research location and sites at Diddington. The red line denotes the study area used in analysis Method 3, the ground conditions approach (Section 7.6). Mapping (Ordnance Survey, 2013b).

4.3.3.2 Hydrological and Topographical Setting

The hydrology and topography of the area are shown in Figure 4.11. Lodge Farm is located on the western side of the Great Ouse River valley. The river flows towards the northeast approximately 3.2km and 1.6km to the west of DCF and DPF respectively. Diddington Brook is a west to east flowing tributary of the Great Ouse located in a stream valley approximately 1.0km to the north of both DCF and DPF. In 1965 the tributary was dammed to form Grafham Water Reservoir, approximately 1.2km north-west of DCF. Historic quarries on the western banks of the River Ouse have been flooded forming a number of lakes adjacent to the river.

DCF is located at 45.8m OD on relatively level ground. Within a 200m radius of the site, the ground level varies from 43.7-46.7m OD. Outside this radius to the north the ground level falls towards Diddington Brook, to the south-east falls to the river valley and to the

west it climbs slightly. DPF is located at 16.9m OD again on relatively level ground with a very gradual slope down to the east towards the river valley.

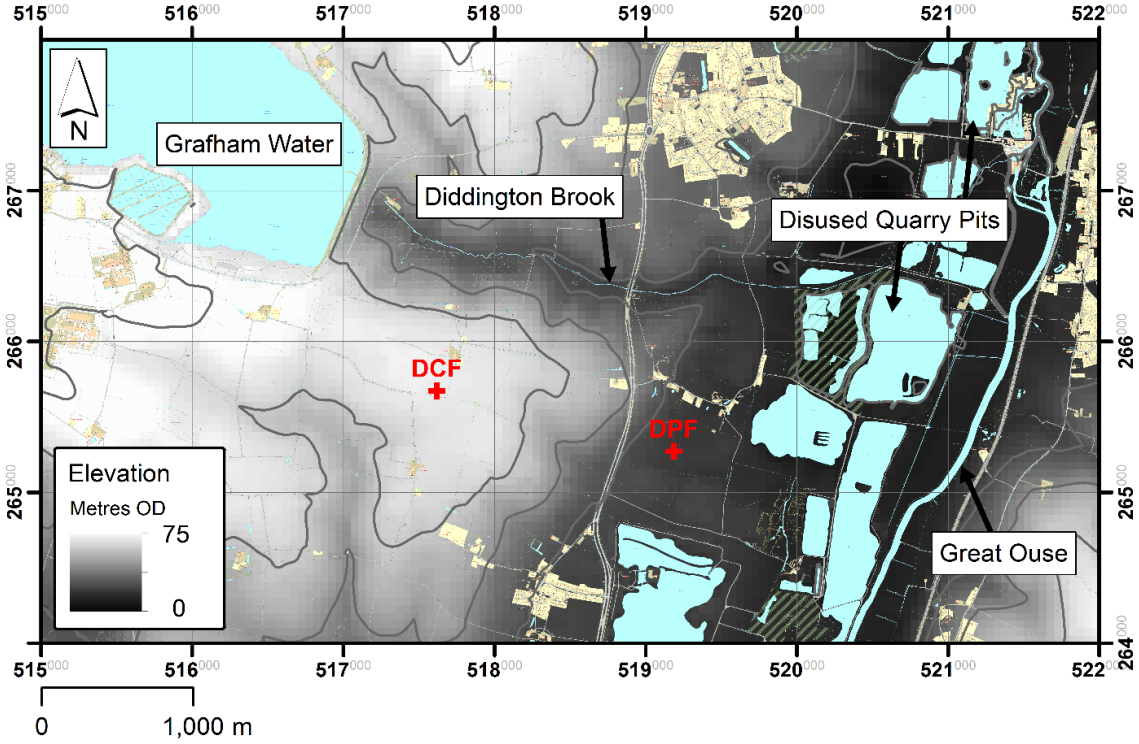

Figure 4.11 Hydrology and topography of the area around Diddington. Mapping and terrain (Ordnance Survey, 2013d, 2013f, 2013h).

4.3.3.3 Geological and Geotechnical Setting

Figure 4.12 shows the bedrock and superficial geology of the area around Diddington.

The area is underlain by Mid-Late Jurassic mudstone of the Oxford Clay Formation. The rock comprises up to 70m thickness of bluish grey fossiliferous clay with pyrite crystals (Gatliff, 1981). The mudstone outcrops to the north of the research sites in the stream valley of Diddington Brook.

DCF lies within an area where the mudstone is mantled by Mid-Pleistocene glacial till. The till is a very stiff diamicton of clay with sand and gravel. It is predominantly silica clay with variable clastic carbonates and some carbonate cement. It is heterogeneous

with weak or discontinuous bedding or locally structureless, with varying zones of matric clastic dominance (British Geological Survey, 2015d).

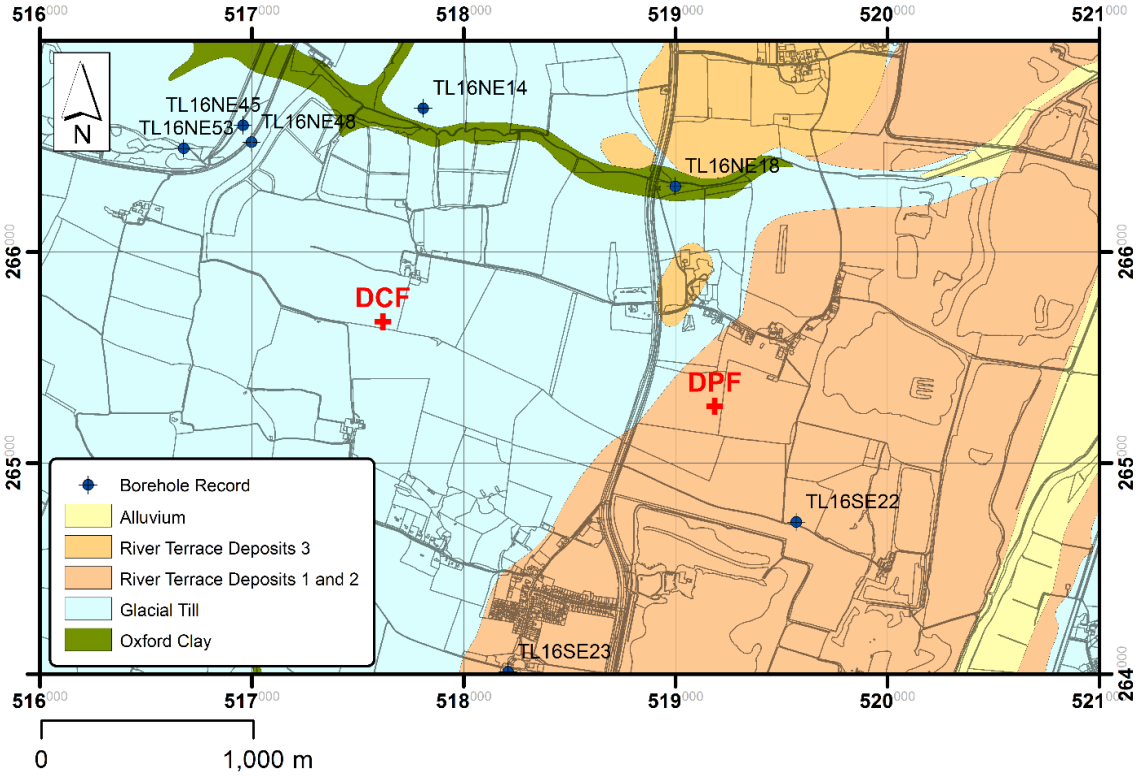

Figure 4.12 Bedrock and superficial geology in the area of Diddington. Mapping (British Geological Survey, 2009a, 2009b; Ordnance Survey, 2013d). Borehole locations are based upon records provided by British Geological Survey (NERC).

In the valley of the River Ouse in the eastern part of the area, the till is overlain by river terrace deposits 1 and 2, which are undifferentiated on the superficial geology map. DPF lies within this area. The deposits are unconsolidated sands with gravel which display lamination and bedding features. They are predominantly silica with no reported carbonate content (British Geological Survey, 2015d).

The borehole and trial pit records referenced in this section are openly available from the BGS website (British Geological Survey, 2015c). Approximately 1km to the northwest of DCF (TL16NE45, TL16NE48 and TL16NE53), and approximately 1-1.5km to the north and northeast of DCF in the stream valley of Diddington Brook (TL16NE14 and TL16NE18), the boreholes encountered till underlying the surface soils. The maximum

proven depth of the till (TL16NE48 only) is to approximately 27mbgl, directly overlying the mudstone bedrock. The top few metres are typically described as mottled brown and grey clay, with gravel and chalk. Near to the top of the strata the clay is described as firm to very stiff, and at depths of below 0.75-2.3mbgl, the clay becomes stiff to very stiff.

Approximately 0.7km to the south-east of DPF (TL16SE22) beneath the surface soils, river terrace deposits overlie the till at a depth of 3.0mbgl. The borehole record indicates that the upper deposits (to 1.2mbgl) are orange-brown clayey very gravelly coarse-medium sand, over yellow clayey gravelly coarse-medium sand. 1.6km south-east of DPF (TL16SE23) river terrace deposits were encountered below the surface soils to a depth of 1.6mbgl, overlying the till. The upper deposits (to 1.1mbgl), are orange and yellow clayey coarse-medium sand and fine gravel, over yellow slightly clayey medium sand and fine-medium gravel.

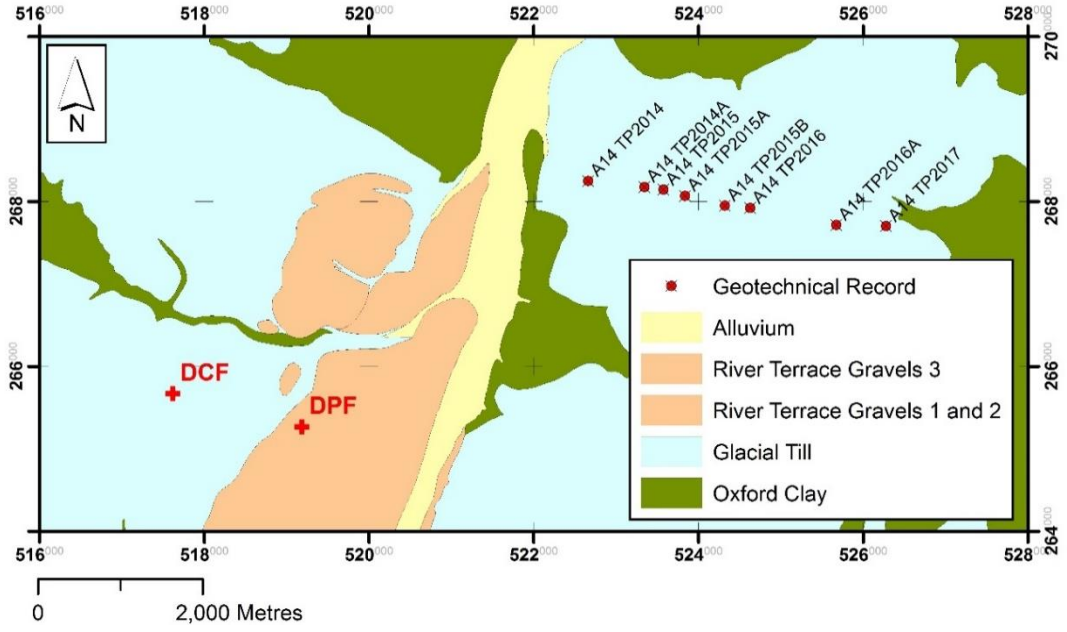

Figure 4.13 Bedrock and superficial geology in the area of Diddington. Mapping (British Geological Survey, 2009a, 2009b; Ordnance Survey, 2013d). Geotechnical properties record locations are based upon records provided by British Geological Survey (NERC).

Records from the NGPPD (British Geological Survey, 2015b) are available for a number of boreholes drilled approximately 5.5-9.0km to the northeast of the research location (Figure 4.13). Those boreholes which are drilled into the superficial till deposits (the unit in which DCF lies) have laboratory testing information at 1.1-2.0mbgl. The soils are described as firm to stiff sandy clay with flint, quartz and chalk gravel, with plastic limits of 17-20 and liquid limits of 46-53. The particle size distribution data show clay contents of 40% and sand contents of 54-58%. No geotechnical laboratory information is available from the river terrace deposits in which DPF lies.

4.3.3.4 Hydrogeological Setting

The underlying mudstone of the Oxford Clay Formation is classed as "rock with essentially no groundwater" (British Geological Survey, 2015a). The till is relatively impermeable and infiltration is limited (Environment Agency, 2010). A borehole to the north-west of DCF (TL16NE48) drilled through the till and into the Oxford Clay to a depth of 29.1mbgl did not encounter groundwater. This lack of infiltration capacity is likely to result in rain runoff at DCF where the till underlies the surface soils, particularly at times when the soils are already saturated.

The river terrace deposits at DPF are dominated by sands and gravels, bound at the base by relatively impermeable clays. They are likely to have a storage capacity for water with fluctuating levels from rainfall, river flow and runoff from the clay-dominated soils to the west. Boreholes through the river terrace deposits to the south-east of DPF (TL16SE22 and TL16SE23, Figure 4.13) found water at 17.0m OD (0.9m bgl) and at 19.6m OD (2.6m bgl).

4.3.3.5 Historical and Archaeological Setting

There is evidence of settlement in the area up to 4000 years ago, when well-draining river terraces in the area were favoured locations (Friends of Paxton Pits, 2014). During the Iron Age, flooding covered the area in up to 300mm of silt and farming settlements were abandoned and later re-established. Another abandonment during the Roman period may have also been due to flooding.

Aggregate quarrying of the gravels to the east and south of the research location along the Great Ouse began in the 19th Century and the area named Paxton Pits. As demand for construction materials increased during the Second World War, the operation was ramped up. Extraction ceased in 2010, though licences for further extraction in the area have been granted. Some of the now flooded quarries have been handed over to Paxton Pits Nature Reserve.

The archaeological record held by EH is available via the Pastscape website (Historic England, 2015b). All features listed in this record within a 2km radius of the centre of the research location that have been identified as cropmarks are given in Table 4.3. Where they are available, the dates of the images taken where the cropmarks were seen has been included. The locations of these records have been plotted in Figure 4.14 using the coordinates given by HE, which are accurate to between 1-100m. Mapping of the area using geographical information systems, as yet has not been carried out by HE.

The recent history of the area near to the sites on a field scale has been studied using historical maps. A list of the maps reviewed is provided in Table 4.4 and key maps have been reproduced in Figure 4.15. Historical maps show that little has changed since Ordnance Survey mapping began in 1888, other than field boundaries. The field in which DCF lies was historically subdivided, with a field boundary approximately 300m to the

west removed between 1970 and 1980. DPF is located at the site of an old east-west field boundary which was also removed between 1970 and 1980.

Table 4.3 Archaeological records created from aerial imaging of cropmarks within a 2km radius of the Diddington research location. Information from (Historic England, 2015b).

Reference Number	*Image Date(s)*	*Brief Description*	*Geology*
1	29/06/2011	Iron Age/Roman settlement enclosure	Till
2	No Date Given	Group of ring ditches	River Terrace Deposits 1&2
3	No Date Given	Cursus	River Terrace Deposits 1&2
4	28/11/1992	Parallel ditches	Till
5	No Date Given	Ring ditches and square enclosures	River Terrace Deposits 1&2
6	16/06/1970	Ring ditch	River Terrace Deposits 1&2
7	23/06/2005	Prehistoric settlement	River Terrace Deposits 1&2
8	23/06/2005	Iron Age/Roman settlement	River Terrace Deposits 1&2
9	17/06/2006	Late prehistoric settlement	Till
10	29/06/2011	Late prehistoric/Roman settlement	Till
11	29/06/2011	Medieval encolsures or field boundaries	Till
12	23/06/2005	Ring ditch or tree enclosure	River Terrace Deposits 1&2
13	29/06/2011	Prehistoric settlement	River Terrace Deposits 1&2
14	29/06/2011	Iron Age/Roman settlement	Till
15	29/06/2011	Iron Age/Roman settlement	River Terrace Deposits 1&2
16	29/06/2011	Late prehistoric/Roman settlement	Till
17	No Date Given	None	River Terrace Deposits 1&2
18	10/08/1945	Quarrying	River Terrace Deposits 1&2
19	No Date Given	Ring ditch and enclosures	River Terrace Deposits 1&2
20	No Date Given	Ring ditch and enclosures	River Terrace Deposits 1&2
21	10/06/1970	Ring ditch and enclosures	River Terrace Deposits 1&2

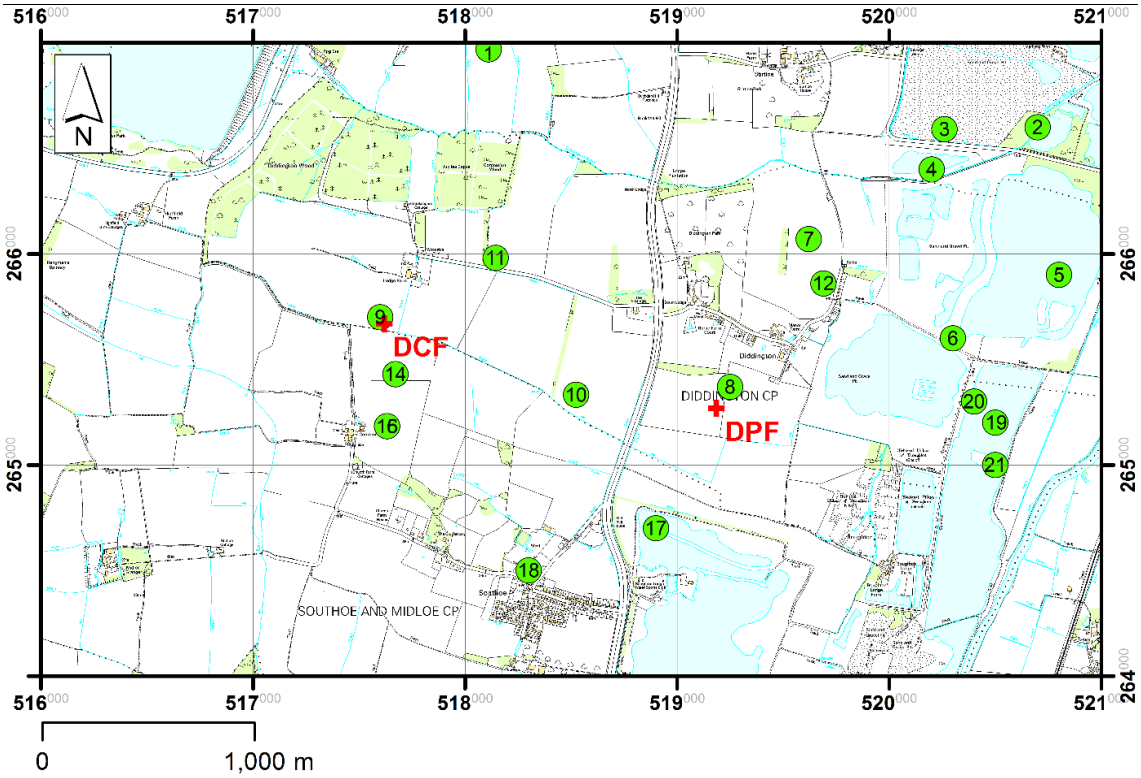

Figure 4.14 Locations of buried archaeological features identified from crop marks within a 2km radius of the centre of the research location. Locations are taken from pastscape (Historic England, 2015b), mapping (Ordnance Survey, 1984).

Table 4.4 Historical maps reviewed in the Diddington Area. Mapping from Landmark Information Group, UK, using: EDINA Historical Mapping Service <digimap.edina.ac.uk>.

Mapping	*Scale*	*Edition*	*Publication Date*	*Reproduced*
County Series	1:2500	1st Edition	1888	Figure 4.15
County Series	1:10560	1st Edition	1888-92	
County Series	1:2500	1st Revision	1901	
County Series	1:10560	1st Revision	1902	
County Series	1:2500	2nd Revision	1926	
County Series	1:10560	2nd Revision	1927	
County Series	1:10560	3rd Revision	1938-53	
National Survey	1:10560	1st Imperial Edition	1958	
National Survey	1:10560	1st Imperial Revision	1970	Figure 4.15
National Survey	1:2500	1st Edition	1980	
National Survey	1:10000	Latest Metric Edition	1984	Figure 4.15
OS Mastermap	1:2000		Current	Figure 4.15

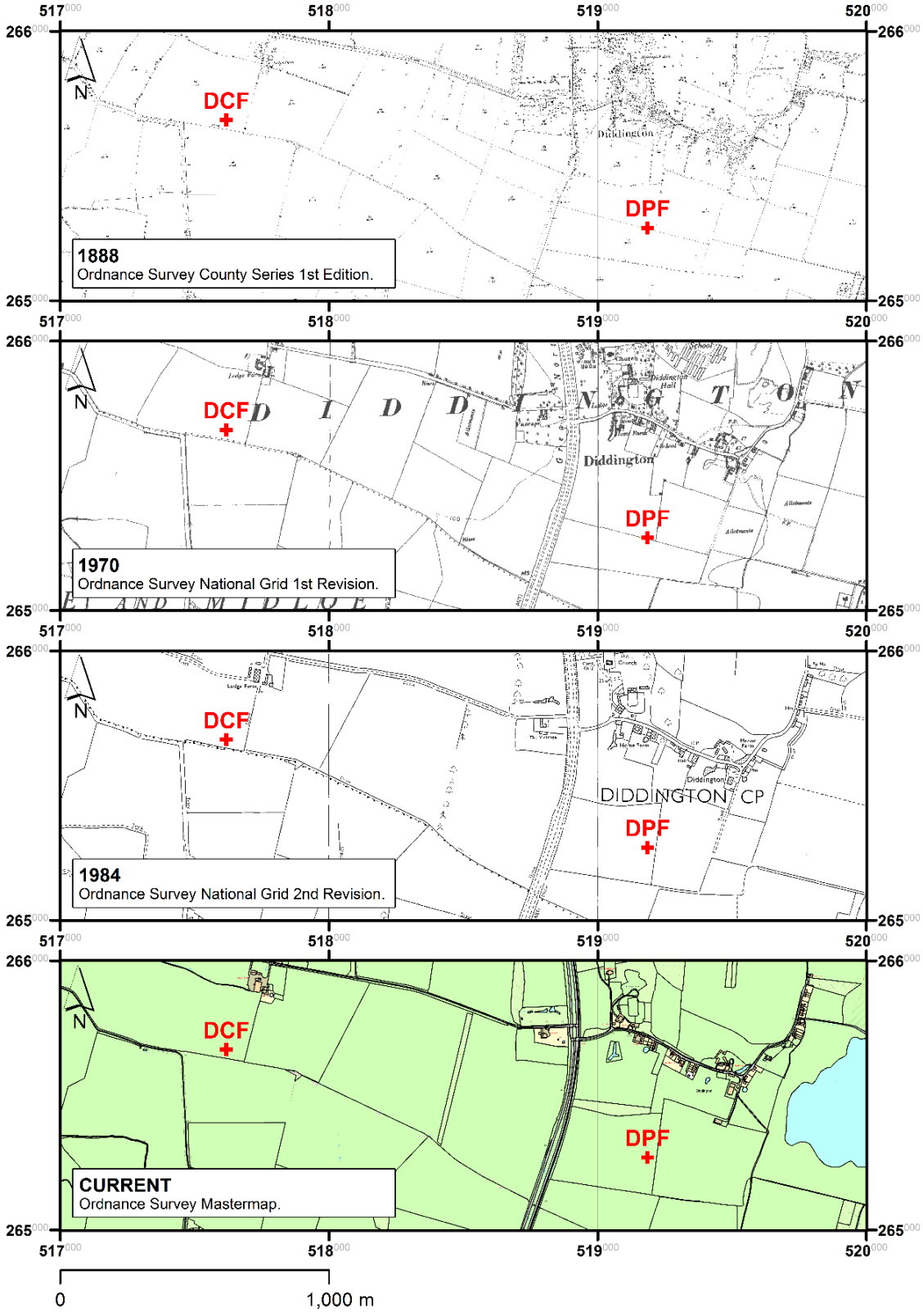

Figure 4.15 Review of historical maps in the Diddington Area. Mapping (Ordnance Survey, 1888, 1970, 1984, 2013d).

4.4 SITE INVESTIGATIONS

4.4.1 Locating the Ditch Features

The DART Project carried out site investigations at each of the four research sites in order to target excavations at suitable subsurface ditch features.

Initially, each research site was surveyed using a Barrington 601-2 dual sensor fluxgate gradiometer system by Rob Fry (University of Bradford) and David Stott (University of Leeds) on behalf of the DART Project. The results are shown in Figures 4.16 (a-d). Two further sites were investigated at Harnhill Farm, but were ruled out: one due to the proximity to a road, which may have invited unwanted attention to the costly monitoring equipment that was to be installed. The other due to scheduling by HE of the area (see Section 4.3.2). Additional information on the investigations at Harnhill, including the survey methods used and the discounted sites is available in a report written for the landowners (Fry, 2011). The sites at Harnhill Farm were surveyed on 24-27th January 2011 and 10th April 2011, and at Lodge Farm on 7-10th March 2011.

The subsurface linear features identified by the fluxgate gradiometer survey were further investigated using borehole surveys by ARCA Consultancy, led by Keith Wilkinson (University of Winchester), on behalf of the DART project. CQF was investigated on 3rd March 2011, DCF on 9-10th March 2011, and DPF on 16th March 2011. However, due to time constraints, the linear feature at CCC was not investigated in this way. Between 5 and 7 boreholes were drilled in a line across and perpendicular to the features using an Atlas Copco Cobra TT percussion hammer (the borehole locations are shown on Figures 4.16 (a-d)). This gave an initial understanding of the geometry of the features, which were all considered to be infilled ditches (Wilkinson, 2013).

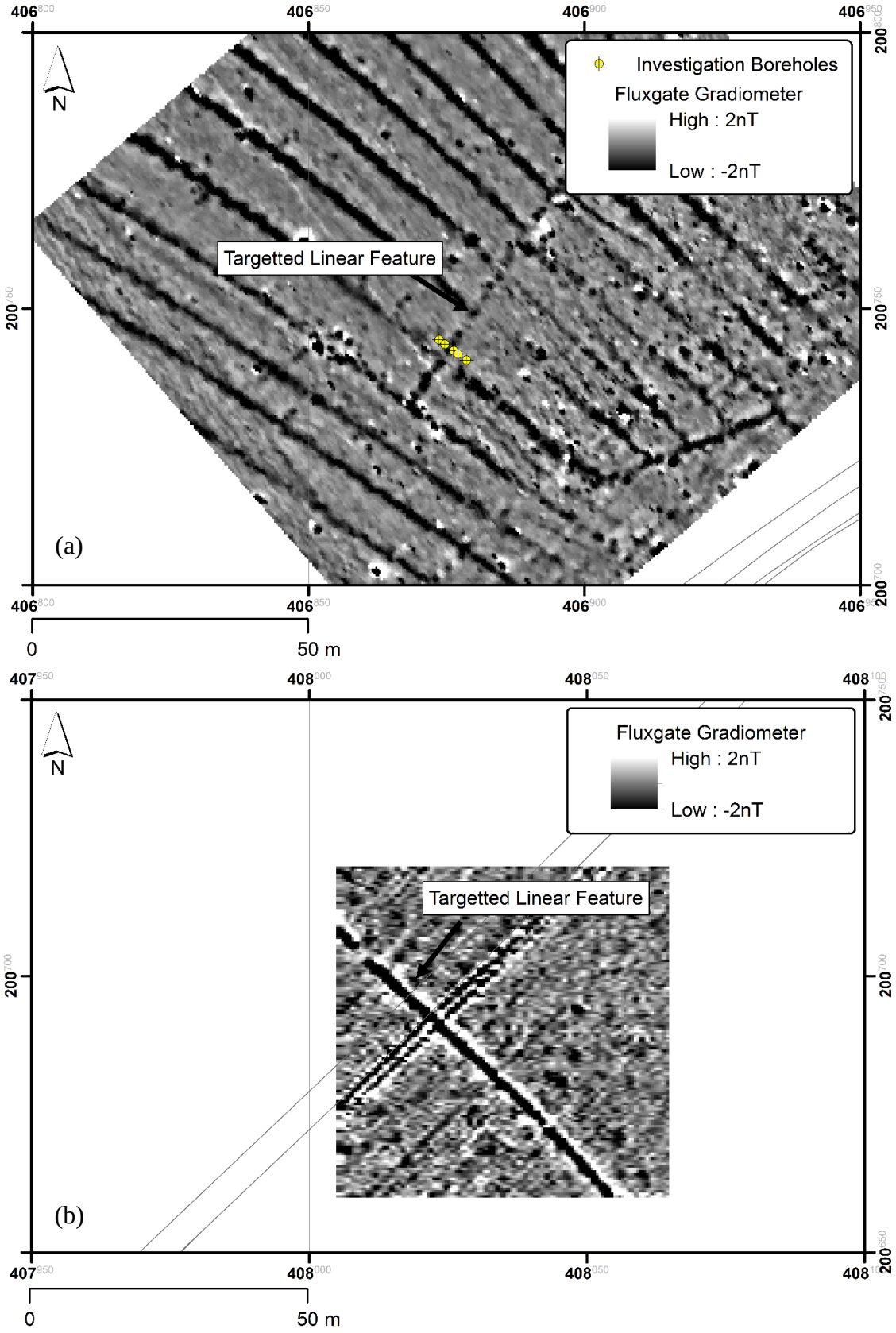

Figure 4.16 . Results of the initial investigations. Magnetometer survey results and borehole survey locations.

(a) CQF (b) CCC

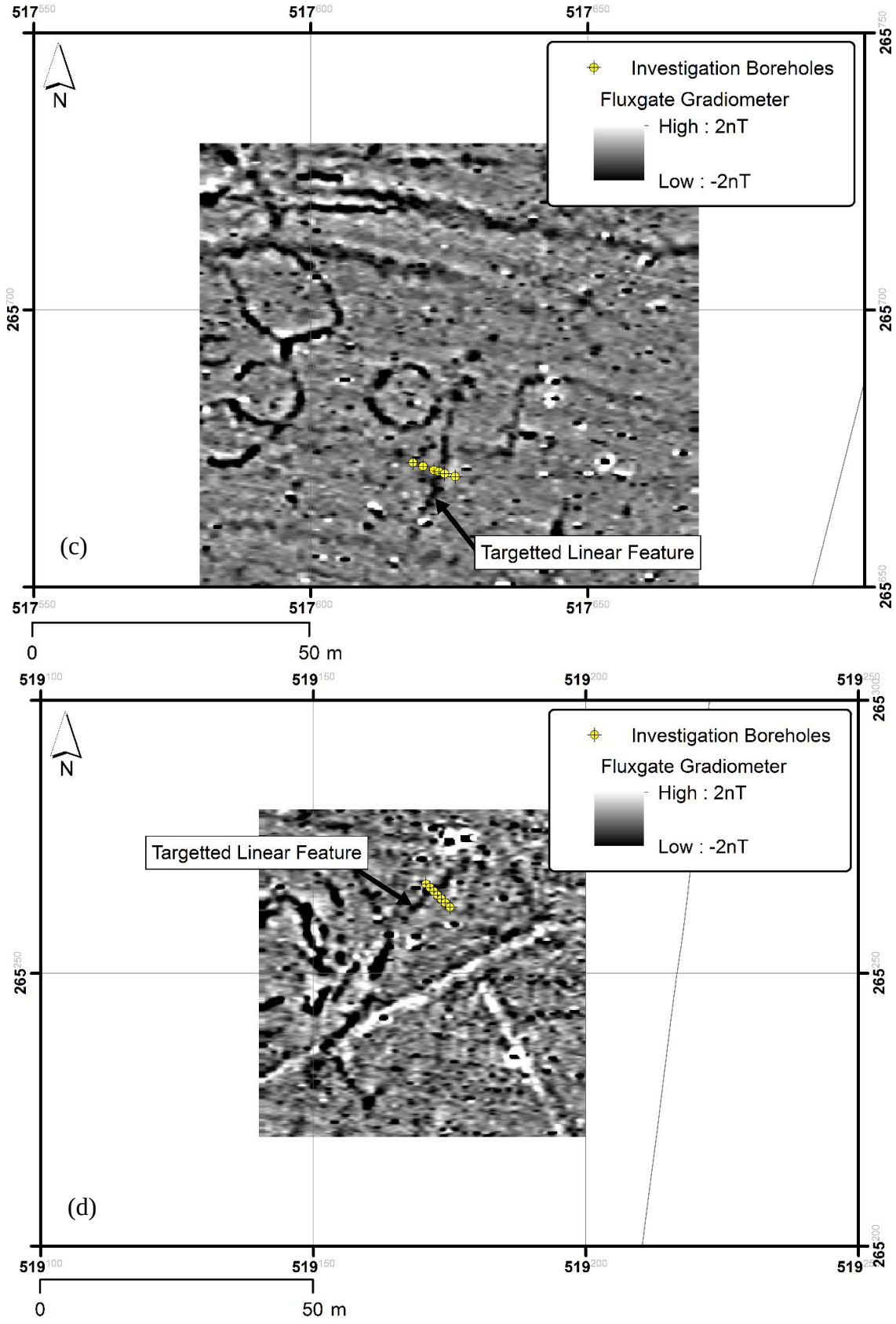

Figure 4.16 (cont.) Results of the initial investigations. Magnetometer survey results and borehole survey locations.

(c) DCF (d) DPF

4.4.2 Excavation Strategy

In order to accurately log the ditch geometry, sample the soils and install semi-permanent monitoring equipment, trenches were excavated at each site revealing a cross section of the ditch feature. Excavations were carried out by Rob Fry (University of Bradford) and David Stott (University of Leeds) using archaeological methods. The topsoils, subsoils and ditchfills were removed by hand and the trenches were then excavated by mechanical digger to below the level of the base of the ditch. The locations of the trenches are shown in Figures 4.17 (a-d), with photographs of the sections shown in Figures 4.18 (a-d). Diagrammatic cross sections drawn by the DART project team using archaeological methods, have been adapted and reproduced in Figures 4.19 (a-d), to show information relevant to this study.

4.4.3 Excavation Findings

4.4.3.1 Cirencester Quarry Field

The linear feature targeted in CQF formed part of the historical field boundary system seen in Figure 4.8. The ditch was cut into clays of the Forest Marble Mudstone and overlain by clayey topsoil. The feature was found to be a maximum of approximately 1.3m wide at the top and 0.6m deep, from approximately 0.3mbgl to 0.9mbgl. Two partially silted up clay drainage pipes were located at the base of the ditch cut, which dated to within the last 150 years (Wilkinson, 2013). Permission was granted by the landowner to cut through the pipes as they were disused. A second active concrete lined drain capped with paving slabs was found perpendicular to the ditch alignment, approximately 2m to the southwest of the section D-D' (Figure 4.19(a)). The two ditchfills typically comprised sandy clays, likely to be locally derived and reworked.

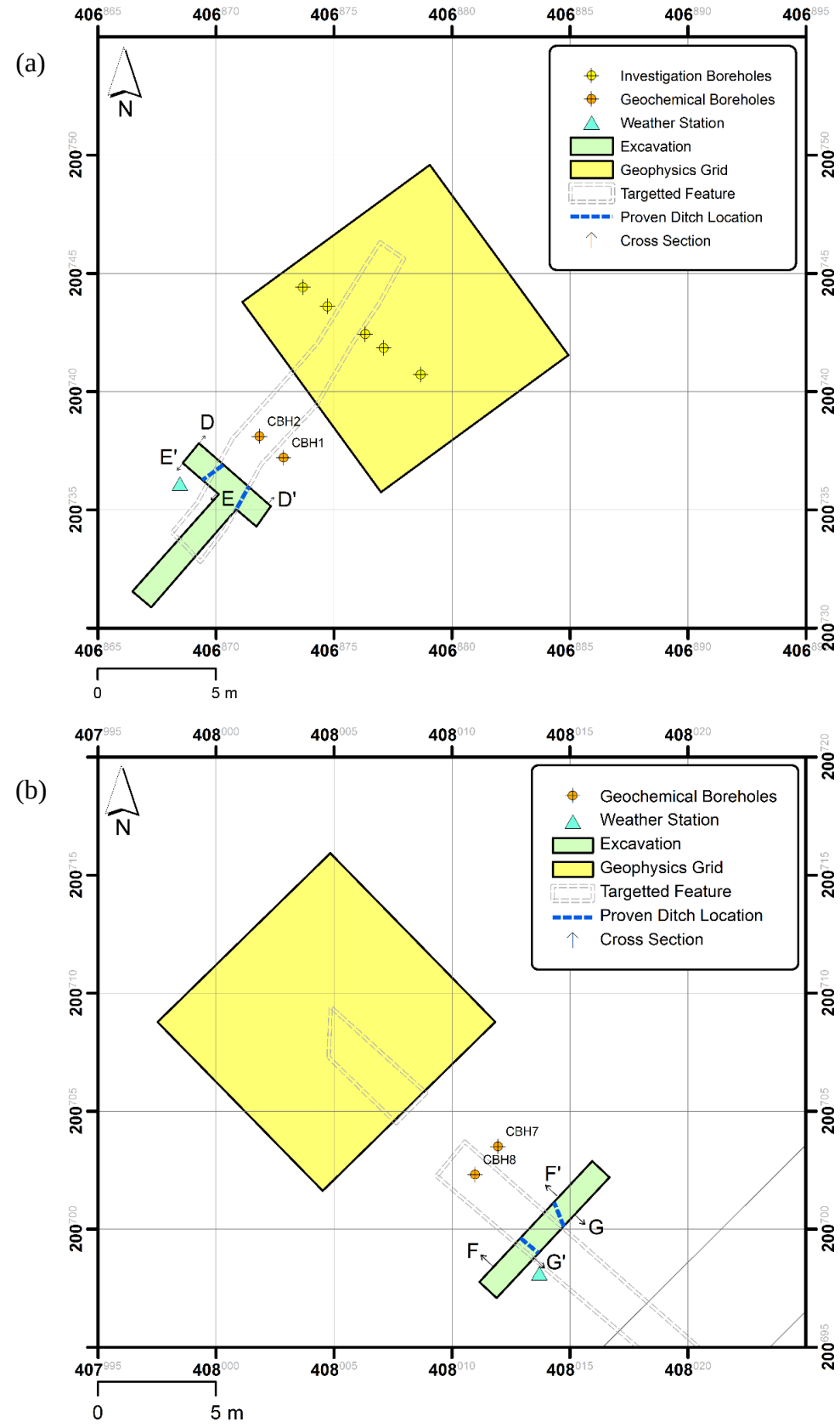

Figure 4.17 Plan of the site investigations and monitoring locations.

(a) CQF (b) CCC

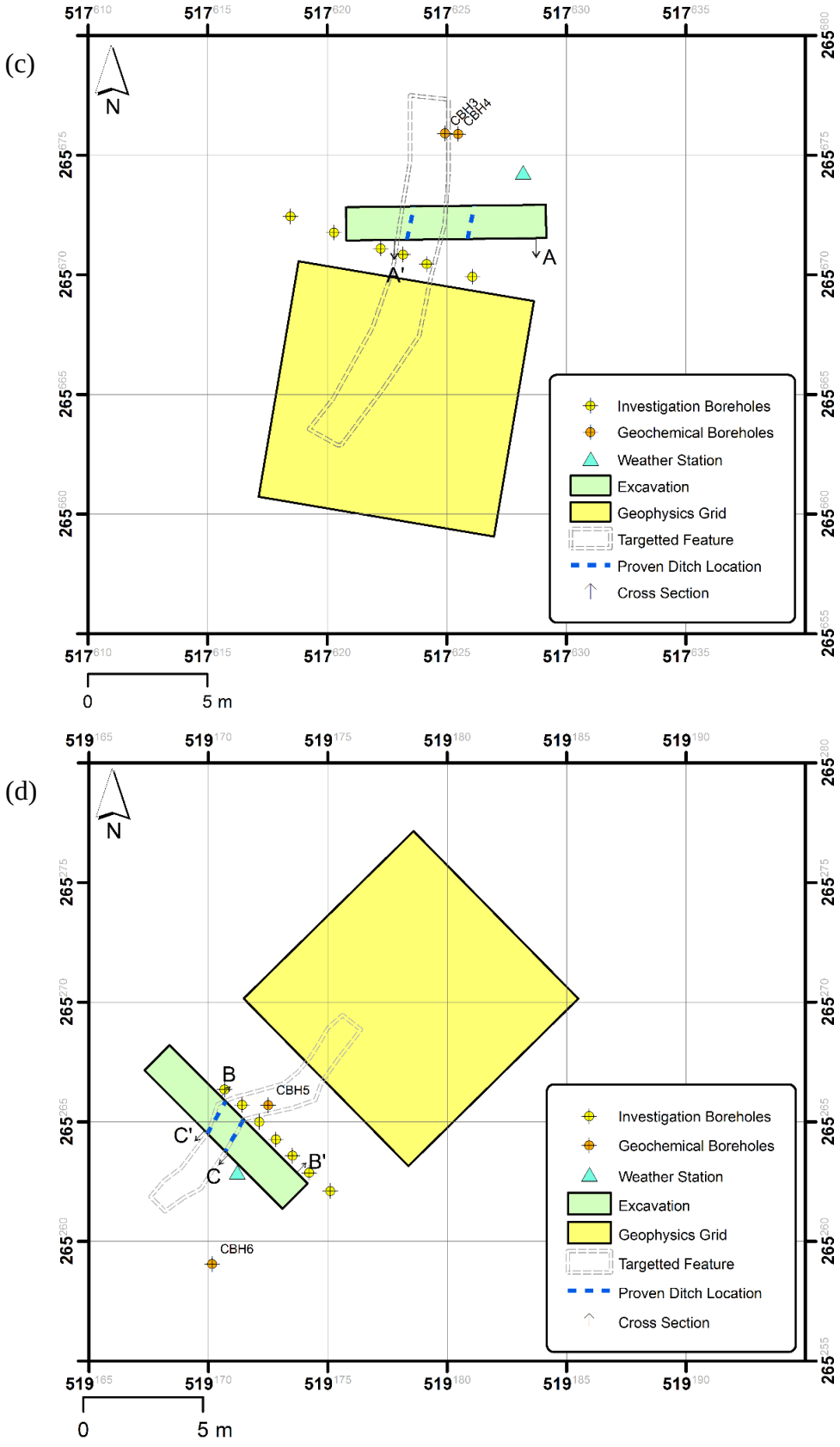

Figure 4.17(cont.) Plan of the site investigations and monitoring locations.

(a) DCF (b) DPF

Figure 4.18 The infilled ditches photographed in the trench section.

(a) CQF (b)CCC

Figure 4.18(cont.) The infilled ditches photographed in the trench section.

(c) DCF (Photograph by D. Boddice) (d)DPF

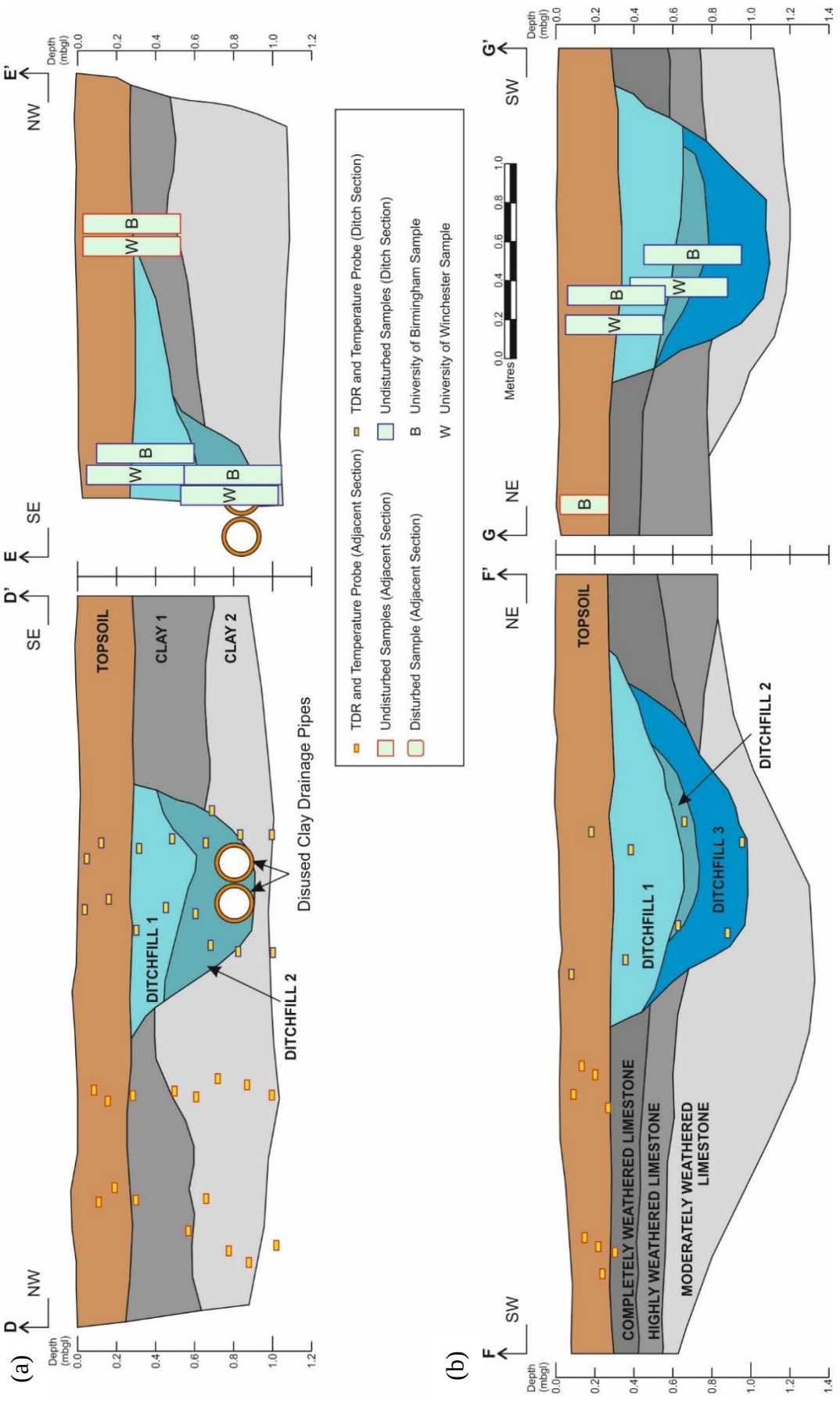

Figure 4.19 Excavated cross sections. (a) CQF (b) CCC

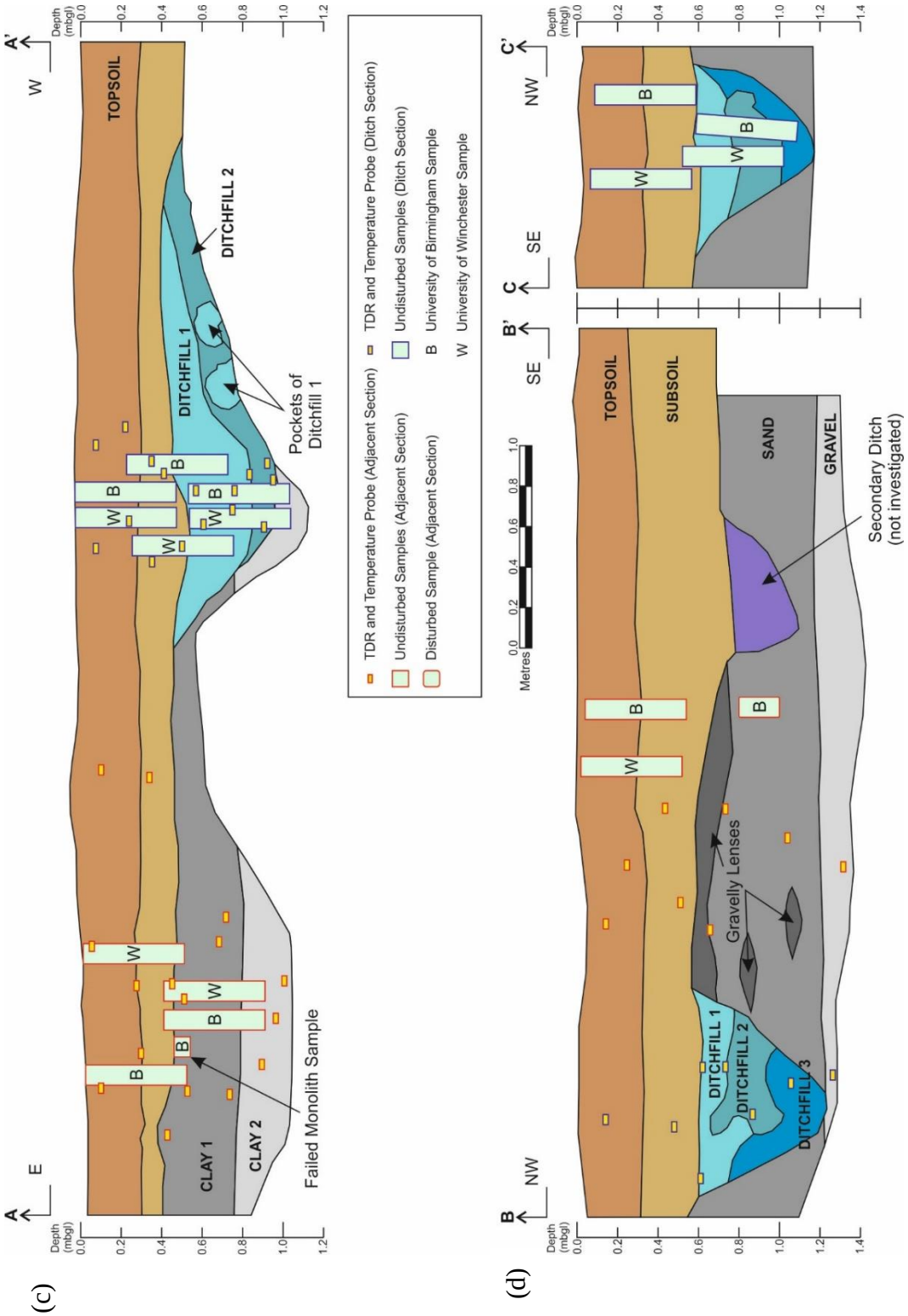

Figure 4.19(cont.) Excavated cross sections. (a) DCF (b) DPF

4.4.3.2 Cirencester Cherry Copse

At CCC, the targeted feature could be identified at the ground surface as a cropmark as shown in Figure 4.20 and followed the line of an historical field boundary (Figure 4.8). The feature was cut into the Cornbrash Limestone, which displayed a weathering profile overlain by silty gravelly topsoil. The ditch measured a maximum of approximately 1.9m in width at the top and was 0.7m in depth from 0.3mbgl to 1.0mbgl. The three ditchfills comprised poorly sorted gravelly silts and silty gravels. The ditchfills contained fragments of glass and charcoal and a tin can, and was dated from 100 to 150 years ago (Wilkinson, 2013).

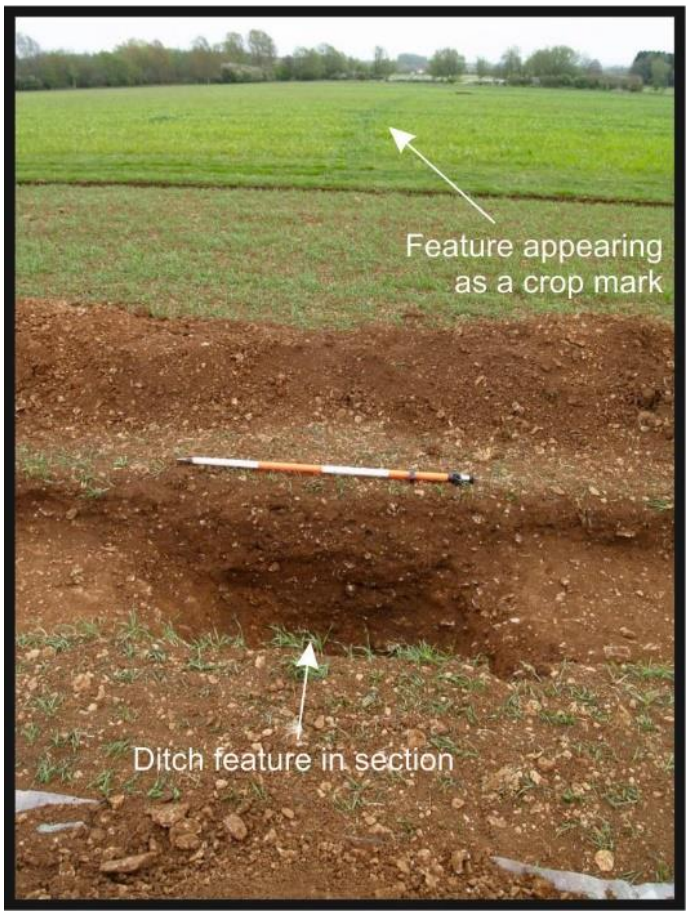

Figure 4.20 Cirencester Cherry Copse, the location of the ditch feature can be seen at the surface as a crop mark. (Photograph by Keith Wilkinson).

4.4.3.3 Diddington Clay Field

The infilled ditch feature at DCF was cut into gravelly clay till, which underlies clay topsoil and subsoil. The ditch was found to be a maximum of 2.5m wide at the top and approximately 0.5m in thickness, stretching from 0.5mbgl, underlying the subsoil, to a maximum of 1.0mbgl. The lower ditchfill comprised organic clay and the upper ditchfill is visually similar to that of the adjacent till, indicating that they are likely to be derived locally and reworked. All the soils contained significant quantities of chalk, most notably in the sand fraction. Ceramic fragments were present in the lower ditchfill and a nearby excavation of a second infilled ditch (not included as part of this study) contained Romano-British and Iron Age pottery (Wilkinson, 2013).

4.4.3.4 Diddington Pasture Field

At DPF the initial investigations were carried out near to an area where an historic field boundary was located (Section 4.3.3). However, the orientation of the targeted feature did not match that of the boundary and was not considered to be directly related. The ditch feature was cut into sandy river terrace deposits overlain by silty topsoil and a significant depth of firm to stiff silty subsoil, likely to be a product of historical flooding. The ditch was approximately 1.0m wide at the top, and 0.6m in depth, stretching from 0.6mbgl, underlying the subsoil, to 1.2mbgl. The three ditchfills comprise very sandy silts and are visually similar in nature other than in colour. Fragments of pottery (up to boulder size), charcoal and bone were found within the feature, probably of prehistoric age (Wilkinson, 2013).

4.4.4 Geotechnical Logging

The geotechnical characterisation compares the soils within the ditch feature with the nearby surrounding soils. The general model considered the buried ditch feature and

nearby soils in two vertical sections. The DS, with relevant information on any figures coloured blue, encompassed the soils and/or rock overlying and underlying the feature, recorded to the base of excavation. The AS has relevant information on any figures coloured red. The base of the AS was chosen such that the soil was equivalent to the base of the DS. The logs through the sections are given in Figures 4.21(a-d), where, to make discussion easier, each soil horizon has been given a name loosely based on the geotechnical description (e.g. "Clay 1"). The full geotechnical descriptions of each of these soil horizons are given on the logs.

4.4.5 Sampling Strategy

Samples were retrieved from site for geotechnical characterisation. To preserve the geometry of the sections and obtain undisturbed samples for laboratory testing, where possible, monolith tins measuring 500x100x100mm were inserted into the wall of the trench using a sledgehammer (Figure 4.22). The trench wall was collapsed by excavation behind the tins to retrieve the samples. The samples were trimmed to the size of the monolith tins and sealed at site. In the AS at CCC is was not possible to insert a monolith tin because of the presence of shallow rock. In the sand in the AS at DPF the non-cohesive nature of the soils caused the sample to collapse during retrieval. Therefore, samples of the Topsoil at CCC AS and the Sand at DPF AS, were taken as bulk disturbed. The locations of the samples taken are shown on the cross sections in Figures 4.19(a-d), and represented on the logs in Figures 4.21(a-d), where undisturbed samples are labelled as UD and bulk disturbed samples as BD. A similar sampling strategy was applied by the University of Winchester for laboratory testing using geoarchaeological methods.

Where significant overlap of the monolith tins occurred, the duplicate soil horizon was treated as a second sample to allow for comparison of results. Where only a small overlap

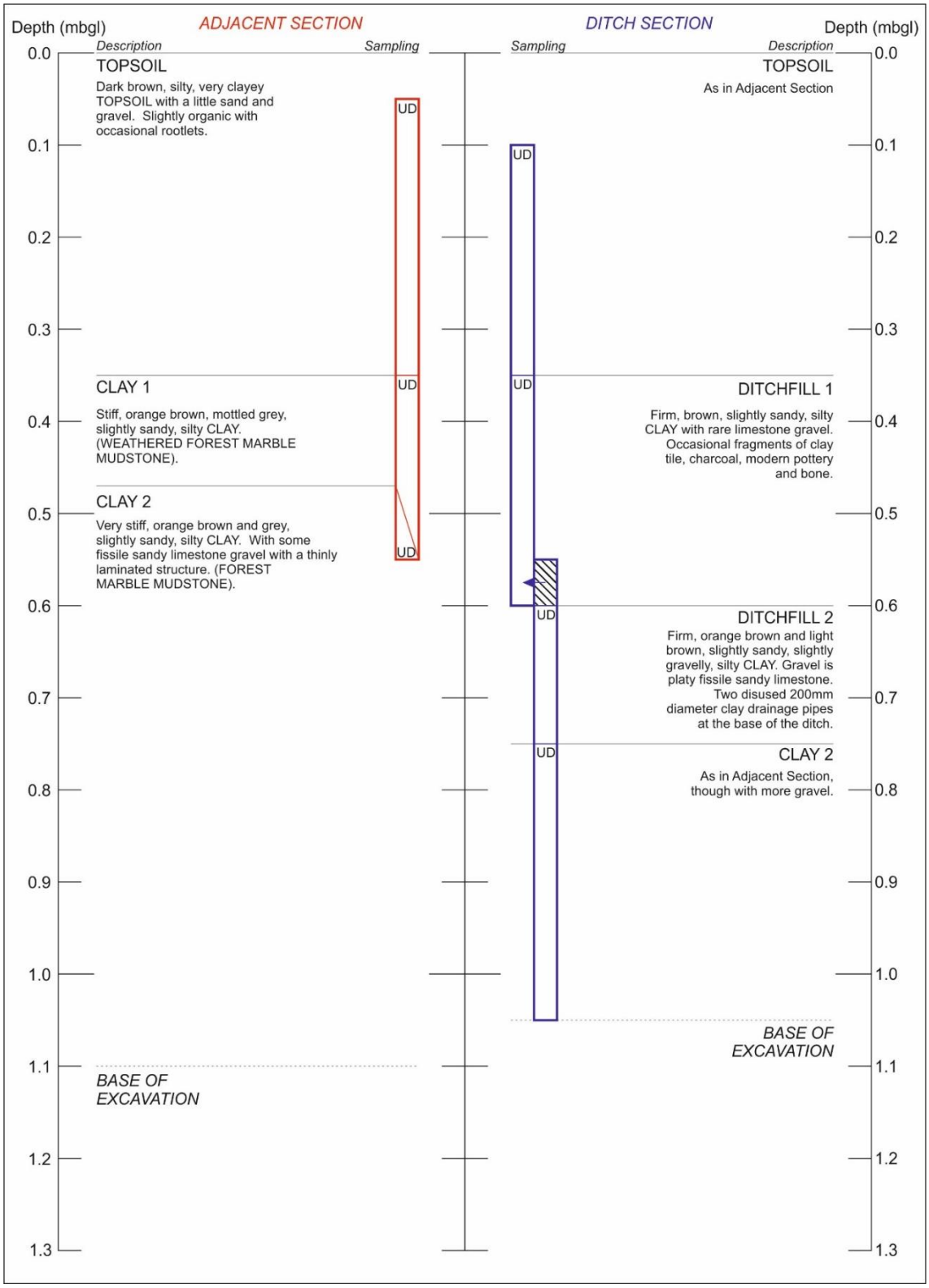

Figure 4.21 Adjacent and ditch section excavation logs.

(a) CQF

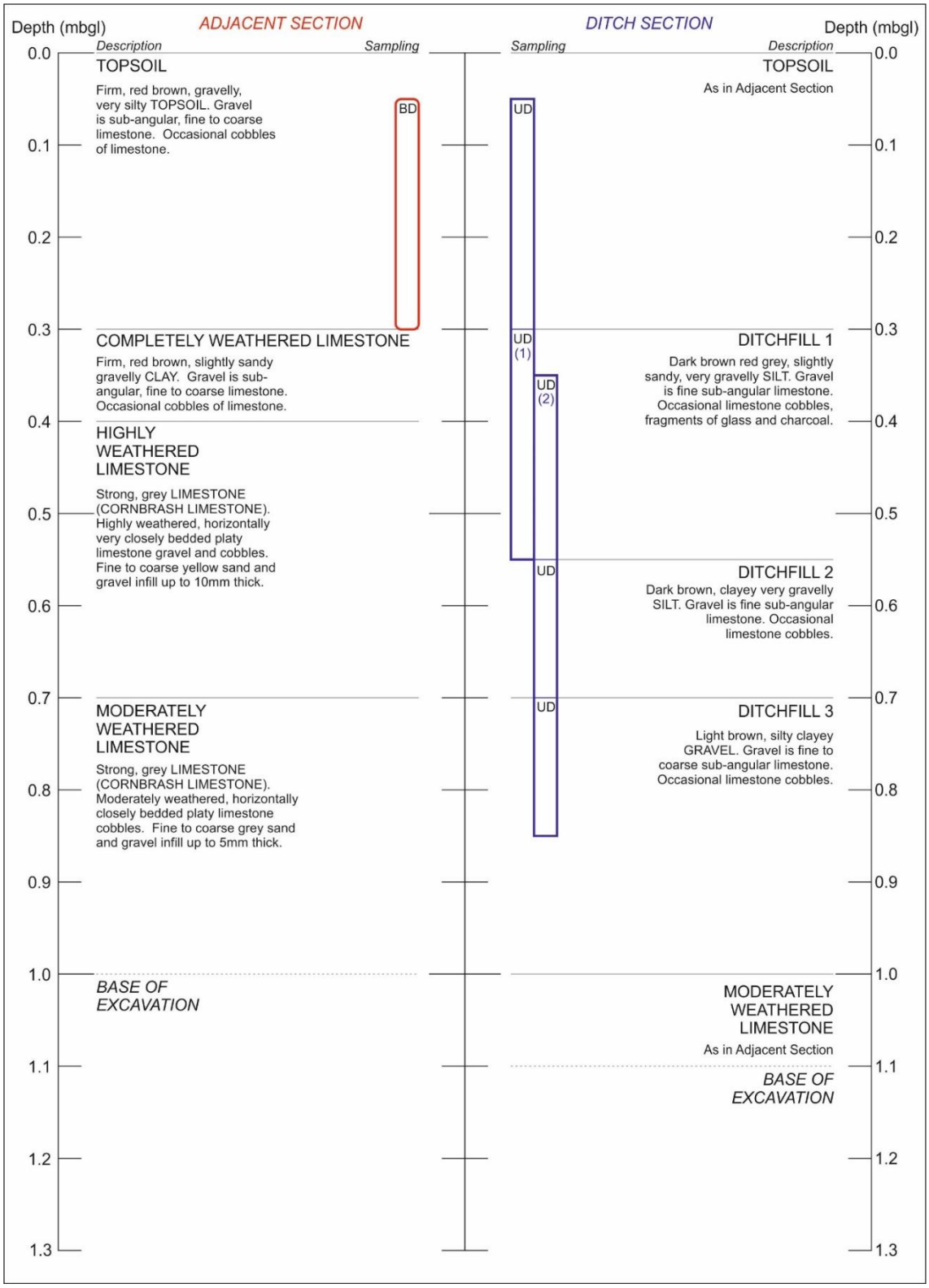

Figure 4.21(cont.) Adjacent and ditch section excavation logs.

(b) CCC

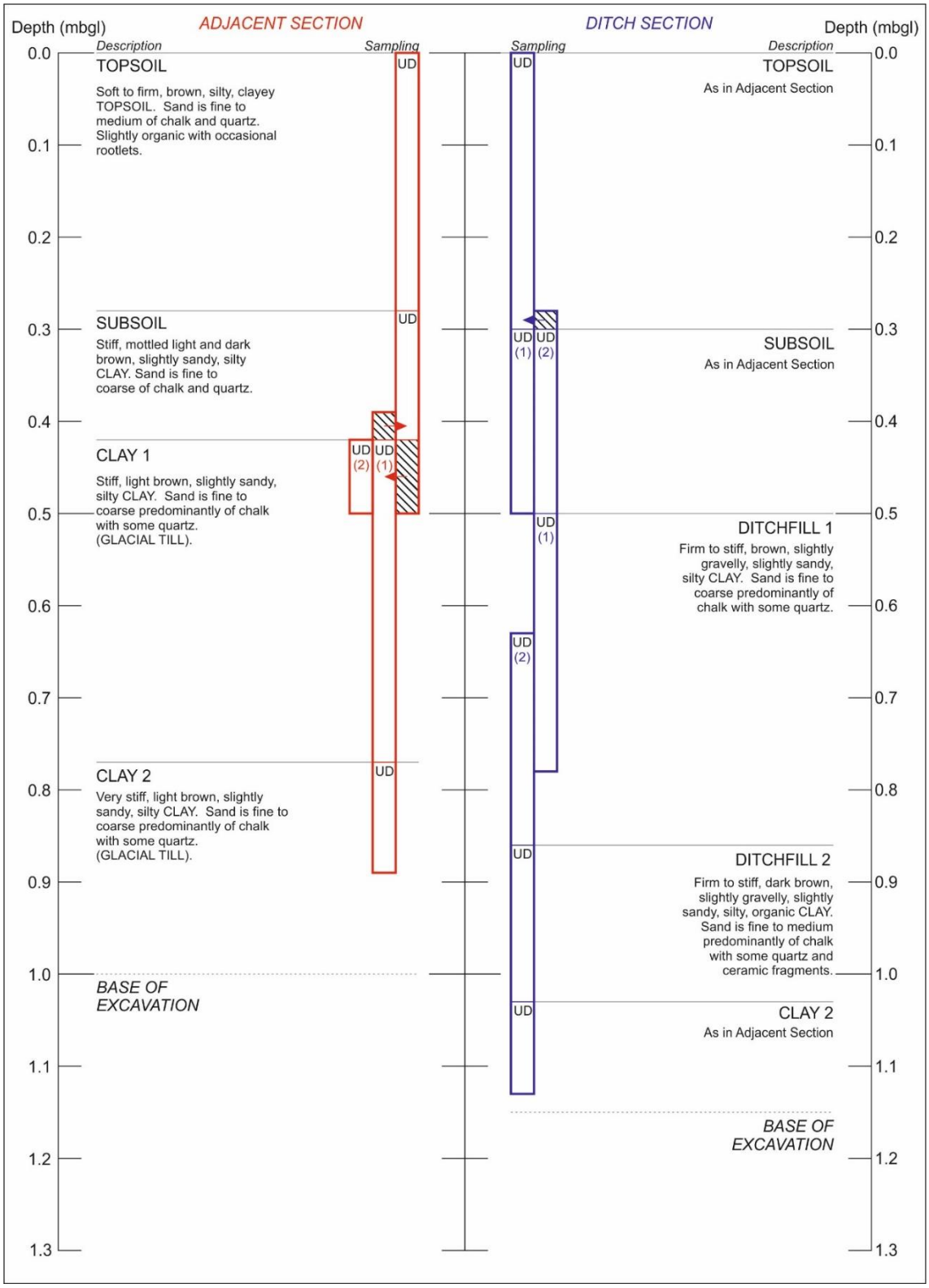

Figure 4.21(cont.) Adjacent and ditch section excavation logs.

(c) DCF

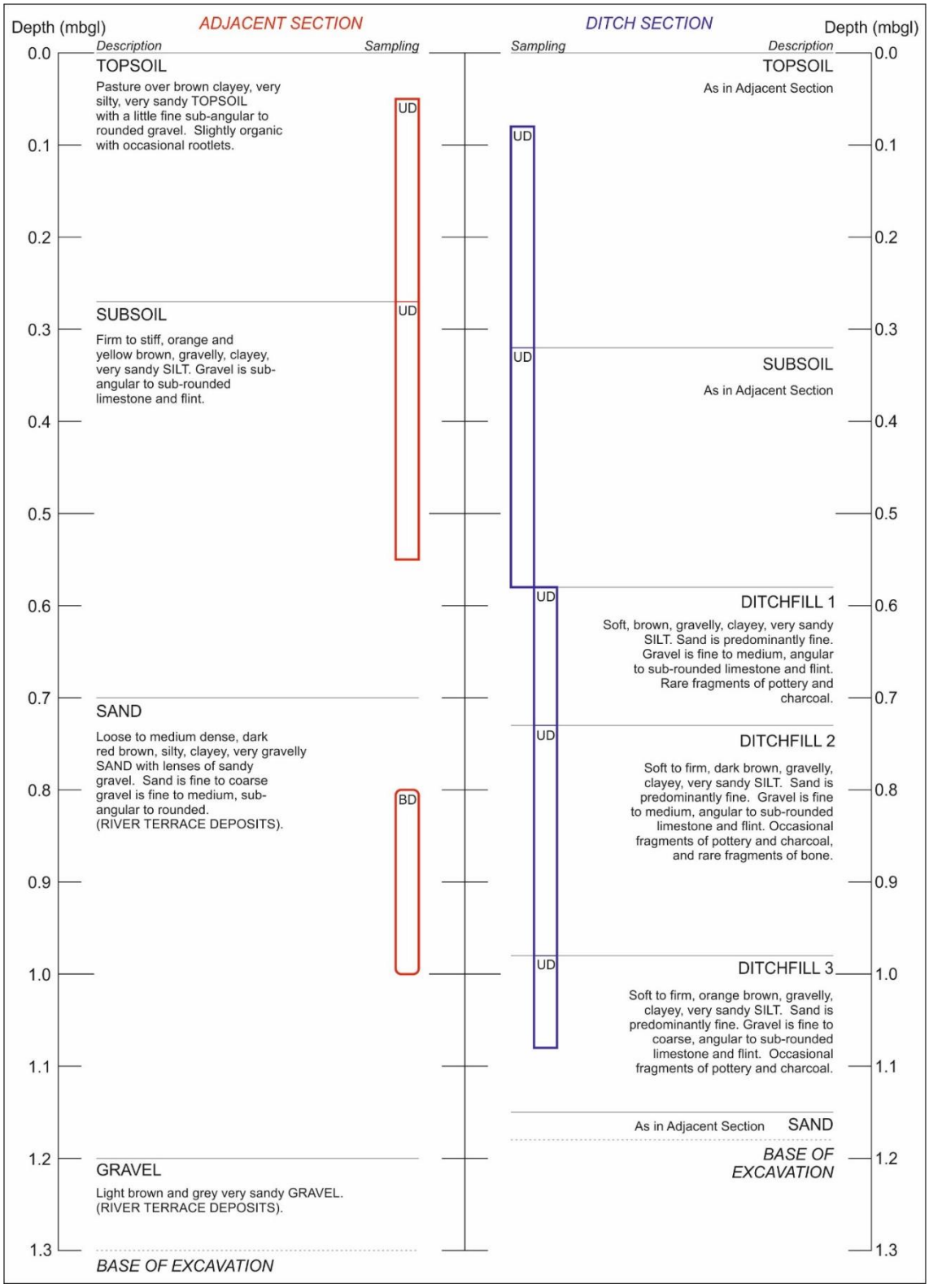

Figure 4.21(cont.) Adjacent and ditch section excavation logs.

(d) DPF

occurred, the duplicate horizons were combined to form a single sample, as shown on the geotechnical logs.

Geochemical samples were retrieved from boreholes (labelled CBH) at the locations shown in Figure 4.17(a-d) for commercial geochemical testing.

Further bulk samples were also taken by the University of Birmingham in order to synthesise various soil conditions (Boddice, 2014).

Figure 4.22 Soil sampling using monolith tins at CQF.

4.5 LONG-TERM MONITORING

4.5.1 Introduction

The DART Project carried out intensive study of the four research sites over a monitoring period of at least 1 year. This included continuous monitoring of soil water, temperature and weather, regular geophysical and spectroradiometry surveys, and aerial imagery. The raw data from each of these are openly available via the DART Portal (DART, 2013).

The subsequent sections provide an overview of the monitoring conducted at each of the research sites.

4.5.2 Soil Water and Temperature

Prior to backfilling the excavated trenches, a number of probes were inserted into the trench sides in profiles through both the adjacent and ditch sections at the locations shown on the cross sections in Figures 4.19(a-d). Each probe location comprised a Time Domain Reflectometry (TDR) probe coupled with a temperature probe, as shown in Figure 4.23.

The TDR probes measure both the electrical conductivity and electrical permittivity of the soil, and post-processing of the data returns a volumetric water content. This aspect of the DART Project is extensively reported by Boddice (2014).

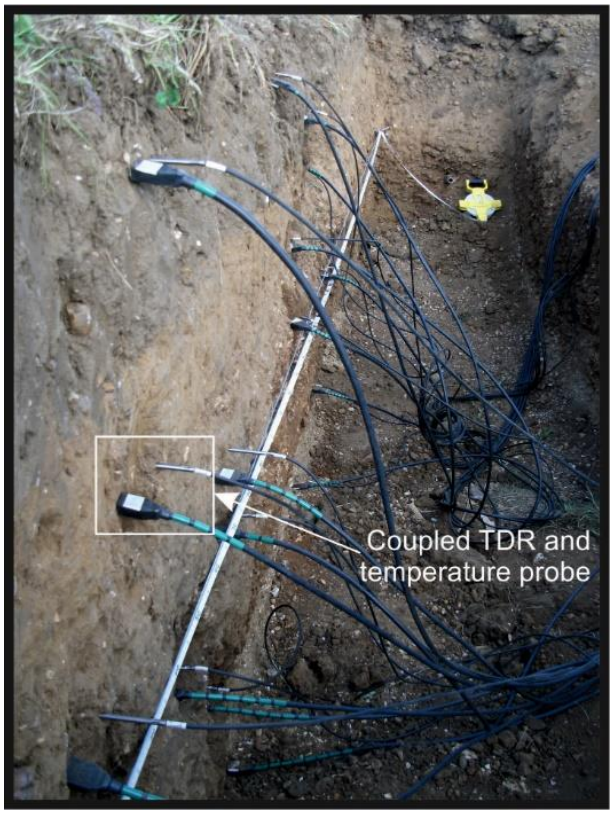

Figure 4.23 TDR and temperature probes in place at DPF prior to backfilling.

At the research sites located in clay-dominant soils (DCF and CQF), 16 coupled probes were installed though the adjacent section and another 16 in the ditch section to allow for increased data collection in the "difficult" clay soils. At DPF and CCC, 8 coupled probes were installed through each section. At CCC the presence of shallow bedrock did not allow for probes to be inserted into the weathered limestone, therefore all 8 coupled probes were inserted above 0.4mbgl in the overlying soils. Readings were taken from each probe hourly throughout the monitoring period.

The temperature and TDR probes were powered by car batteries charged by solar power, and the data collected by a datalogger. All the electronic control was housed in a partially buried aluminium case, and a bespoke mounting was designed to support the solar panels (see Figures 4.24 and 4.25). The monitoring station was designed by D. Boddice (University of Birmingham) and is reported in Boddice (2014).

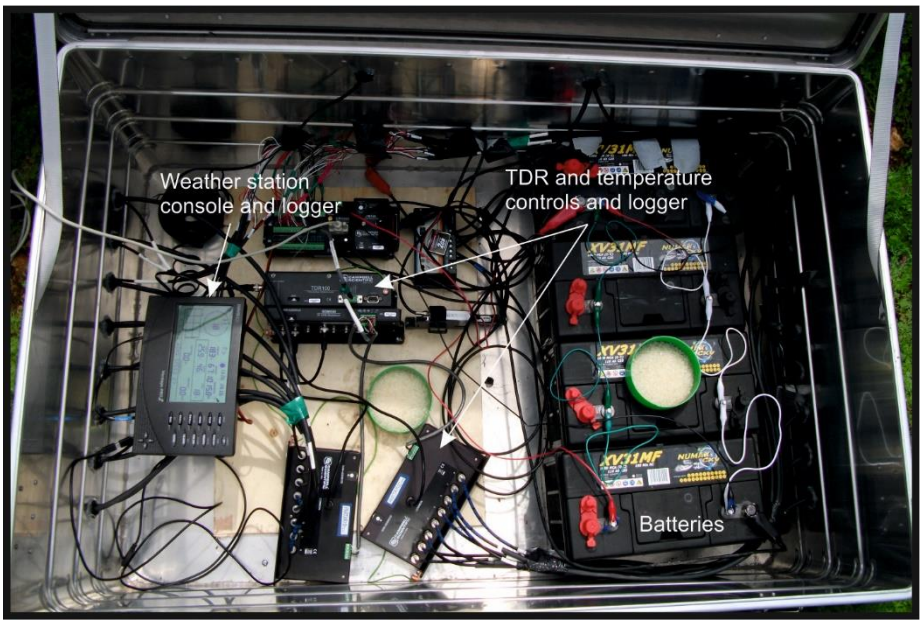

Figure 4.24 The monitoring box with weather station console and datalogger, TDR, multiplexers and datalogger, batteries, and solar panel control.

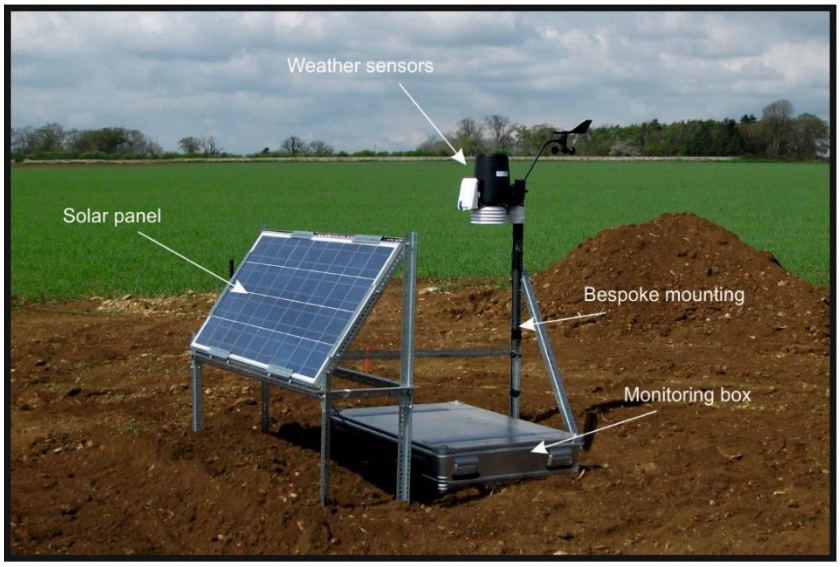

Figure 4.25 The completed monitoring station with monitoring box, and mounted solar panel and weather station.

4.5.3 Weather

Each of the four research sites was installed with a cabled Vantage Pro 2 (Davis Instruments) weather station at the locations shown in Figures 4.17(a-d). Each weather station comprised a 2mm cup rainfall gauge, an anemometer (measuring wind speed and direction) and a temperature and humidity sensor. In addition, one station at each location (DCF and CQF) also had a solar radiation sensor. The sensors were located at 1.2m above ground level as part of the integrated mounting system for the monitoring station, and cabled from the sensor to the datalogger housed in the monitoring box. Each of the weather stations was powered by battery, but also linked to the solar power unit as backup. Data from each of the sensors was recorded every half hour throughout the monitoring period.

4.5.4 Aerial Surveys

Aerial surveys were commissioned by the DART Project during the monitoring period. The National Environment Research Council (NERC) completed two aerial surveys of each of the research locations (23/03/2012, 20/06/2012), and the Environment Agency

(EA) completed one survey (27/06/2011). These surveys included hyperspectral images in addition to those within the visible spectra. Only the images within the visible range have been used in the study, though further work relating to the hyperspectral range is available in Stott (2014).

Oblique aerial images in the visible spectrum were taken on behalf of the DART Project. 10 flights were made over the Cirencester research location with images taken by Bob Bewley and 8 flights over the Diddington research location with images taken by Rog Palmer.

4.6 CHAPTER SUMMARY

This chapter has presented the methods and results of data acquisition and fulfils Objective 2 of the study. The two research locations were the subject of a desk study, investigating; the geographical, the hydrological and topographical; the geological and geotechnical; hydrogeological; and historical and archaeological settings.

The buried features at each of the four research sites, two at each research location, were intrusively investigated in conjunction with the DART Project. The features were revealed in section through excavation, and profiles through the AS and DS were logged and sampled.

Long-term monitoring of the features and adjacent soils was carried out by the installation of TDR and temperature probes, and a weather station at each of the four research sites. Throughout the monitoring period, aerial images were commissioned by the DART project.

The following chapter describes the geotechnical characterisation of the research sites using samples retrieved during the site investigation.

CHAPTER 5. GEOTECHNICAL CHARACTERISATON

5.1 INTRODUCTION

This chapter presents the results of geotechnical characterisation of the soils retrieved from the research sites. The results have been used in to compare the differences between the soils in vertical sections through the buried ditch features, the ditch section (DS), and through the soils adjacent to the buried ditch feature, the adjacent section (AS), to provide background data.

The geotechnical characterisation assesses the density (both dry and particle), the Particle Size Distribution (PSD) and the plasticity. In addition the organic content has been assessed.

The results have been used as inputs into the hydrogeological model proposed in Chapter 6, which compares the soil water characteristics of the vertical sections in relation to the appearance of cropmarks over the buried features. The variation of those properties used as soil inputs into the hydrogeological model have been assessed to provide information for the sensitivity analysis.

Laboratory analysis of geotechnical properties is moving towards automated techniques, such as computerised gas pycnometers and laser diffraction methods for determination of PSD. These techniques have a number of advantages over the traditional methods. Data for use in a commercial capacity requires testing to industry standards; however, these automated methods are increasingly used in research (Rawlins, 2014).

In addition to British Standard testing of the soils, a gas pycnometer (to determine particle density) and laser diffraction (to determine PSD of the fine fraction) have been used for comparison. The advantages of both these methods are a significant reduction in both

testing times and hands-on operator time; the required specimen sizes are smaller; and they offer the ability to take numerous readings from a specimen with a high accuracy and precision of results. The gas pycnometer method is covered by American Standards (American Society for the Testing of Materials, 2000); however, it has not yet entered British Standards. Laser Diffraction has been shown to commonly underestimate the clay fraction when compared with standard sedimentation techniques (e.g. Campbell, 2003; Kerry et al., 2009)

This study suggests that information from databases such as the BGS (British Geological Survey) NGPPD (National Geotechnical Physical Properties Database) can be used as inputs into models. The methods used for determination of the geotechnical properties may impact on the results. There should be awareness that if the database holds data arising from differing methods, there may be data which is not comparable. The particle density results from the gas pycnometer and the PSD of the fine fraction have been compared with tests carried out to British Standards to determine if they are equivalent.

The following section gives an overview of the testing strategy for geotechnical characterisation of the site soils. This is followed by sections which present the results of testing of density parameters, PSD and plasticity of the site soils, and the results of organic and mineral analysis.

5.2 METHODOLOGY

Laboratory testing was carried out to determine the both the dry density (where possible) and particle density of site soils. Analysis was carried out in general accordance with BS1377-2 (British Standards Institute, 1990), using the water displacement method (dry density) and the small pycnometer method (particle density). For comparison, the

particle density was also determined by the gas pycnometer method, presented in ASTM D5550-06 (American Society for the Testing of Materials, 2000).

The bulk density of soils is calculated as a stage within the determination of dry density. However, because the sample storage method in monolith tins can allow for movement of water between soil types, the bulk density has not been considered as a true representation of conditions at the time of sampling, and the results have not been presented.

Dry density determination was carried out on all soil types where UD samples could be taken. Where a soil type was non-cohesive and an UD sample was not obtainable, no test could be carried out. Particle density was determined for all the site soils using both the small pycnometer and gas pycnometer methods. Calculations for sedimentation methods for determination of PSD of the <63μm fraction are dependent on particle density. However, since heavier minerals are preferentially found in the finer size classes (Rubey, 1933), the use of the average particle density across all size classes would incur a bias in the results. Therefore, the particle density of the <63 μm fraction only was also determined for use in sedimentation calculations.

The gas pycnometer method has a number of advantages over the small pycnometer method: sample sizes required for testing are smaller; and hands-on operator time is significantly less. Testing times for the small pycnometer method are lengthy, and repeat testing may be required should results not be precise in the first instance. Using the gas pycnometer method, many readings can be taken of a single specimen allowing for variability analysis. The gas pycnometer method is not covered by British Standards, although, it is being increasingly used in research. Results of particle density

determination using the gas pycnometer method have been compared with those from the small pycnometer method.

Analysis of the PSD was undertaken at the University of Birmingham and was carried out in general accordance with BS1377:2 (British Standards Institute, 1990). The wet sieving method (Sv) was used for the coarse fraction (>63μm), and sedimentation by the hydrometer method (SH), with guidance from the calibration methods described in Head (1992), for the fine fraction (<63μm).

PSD of fine fractions can also be determined using Laser Diffraction (LD). Although this method does not meet standards, it is being increasingly used, particularly in a research capacity, because of the significantly reduced testing time and the small specimen sizes required.

For comparison with the SH results, LD was carried out using a Mastersizer 2000 and Hydro 2000s feeder (Malvern Instruments Ltd.) at the University of Warwick. The instrument offers a detection range of 0.02 - 2000μm, however, a different percentage light obscuration is required for samples based on the expected range of particle sizes within these limits. Therefore, best results are achieved when a small range of particle sizes is tested at a time. Since results were available from Sv for the fraction >63μm, the fraction <63μm was tested.

Testing to determine the plastic limit (PL), liquid limit (LL) of the soils was carried out in accordance with BS1377-2 (British Standards Institute, 1990). The LL was determined using the cone penetrometer method (definitive method). The plasticity index (PI) was calculated from the results of testing. The Total Organic Matter content (TOM) of the soils was determined using the loss on ignition method by ALcontrol Laboratories.

Undisturbed samples (UD) were retrieved from site using monolith tins. Where UD samples could not be taken, either due to the non-cohesive nature of the soils or the presence of rock, BD samples have been analysed. This allowed for locational consistency of the samples ensuring that, where possible, tests were carried out on samples through the vertical sections both adjacent to and within the buried ditch features for comparison. Where sequential monolith tins used to collect samples overlapped and significant portions of a soil type were present in both (DCF Subsoil (DS)), DCF Ditchfill 1 and CCC Ditchfill 1), duplicate samples of the soil type were tested. If the quantity of a soil type was insignificant in one or both of the monolith tins, the samples were treated as one. The samples used for analysis are shown on Figures 4.21(a-d).

Test-specific laboratory methods, including any deviations from the standards and relevant calculations of errors, are included in Appendix A. The results of the geotechnical characterisation are presented in the following section.

5.3 RESULTS

5.3.1 Dry Density

The number of tests carried out for each soil type was limited by the number of undisturbed specimens which could be obtained. Up to four specimens from each soil type were tested, as could be extracted undisturbed from the UD samples. Results were averaged to give a single value of dry density representative of the complete depth for each soil type. A diagrammatic representation of the results is given in Figures 5.1(a-d).

The average range of data for repeated tests on specimens of a soil type was 0.17 Mg/m^3 with a minimum 0.01 Mg/m^3 and a maximum of 0.60 Mg/m^3. Though sample variation may have contributed to the wide ranges of data, the small specimen sizes may have introduced errors in the results.

5.3.2 Particle Density by the Small Pycnometer Method

BS1377:2 (British Standards Institute, 1990) states that the average of two results for each specimen should be taken if they differ by no more than 0.03 Mg/m^3. Where two initial results did not meet this condition, further tests were carried out. A maximum of 10 tests on different specimens were carried out on each sample which required retesting until a consistent dataset was achieved. A diagrammatic representation of results of testing both the fraction <63 μm and all size fractions is given in Figures 5.2(a-d). These data have been compared in Section 5.3.4.

The range of results for tests which did not meet the condition of being within 0.03Mg/m^3 was 0.12-0.14 Mg/m^3, which was considered to be due laboratory error, sample variation or a combination of the two. However, after the introduction of measures to combat the laboratory errors (see Appendix A), results of the initial tests were consistently within the 0.03 Mg/m^3 limit required by the standard with the exception of just one sample requiring further testing. This indicates that the primary cause of error is more likely to have been methodological.

5.3.3 Particle Density by the Gas Pycnometer Method

The gas pycnometer method is described, and an assessment of expected error has been included, in Appendix A. The results have been compared with those from the small pycnometer method in the next section.

The expected error was found to be <±0.02 Mg/m^3. Where two results for a soil type were available (there was a total of nine soil types), the difference between results were all within the expected error with the exception of CCC Ditchfill 1, which had a difference of 0.21 Mg/m^3. In this case it is sample variation that is the likely cause of the wide range.

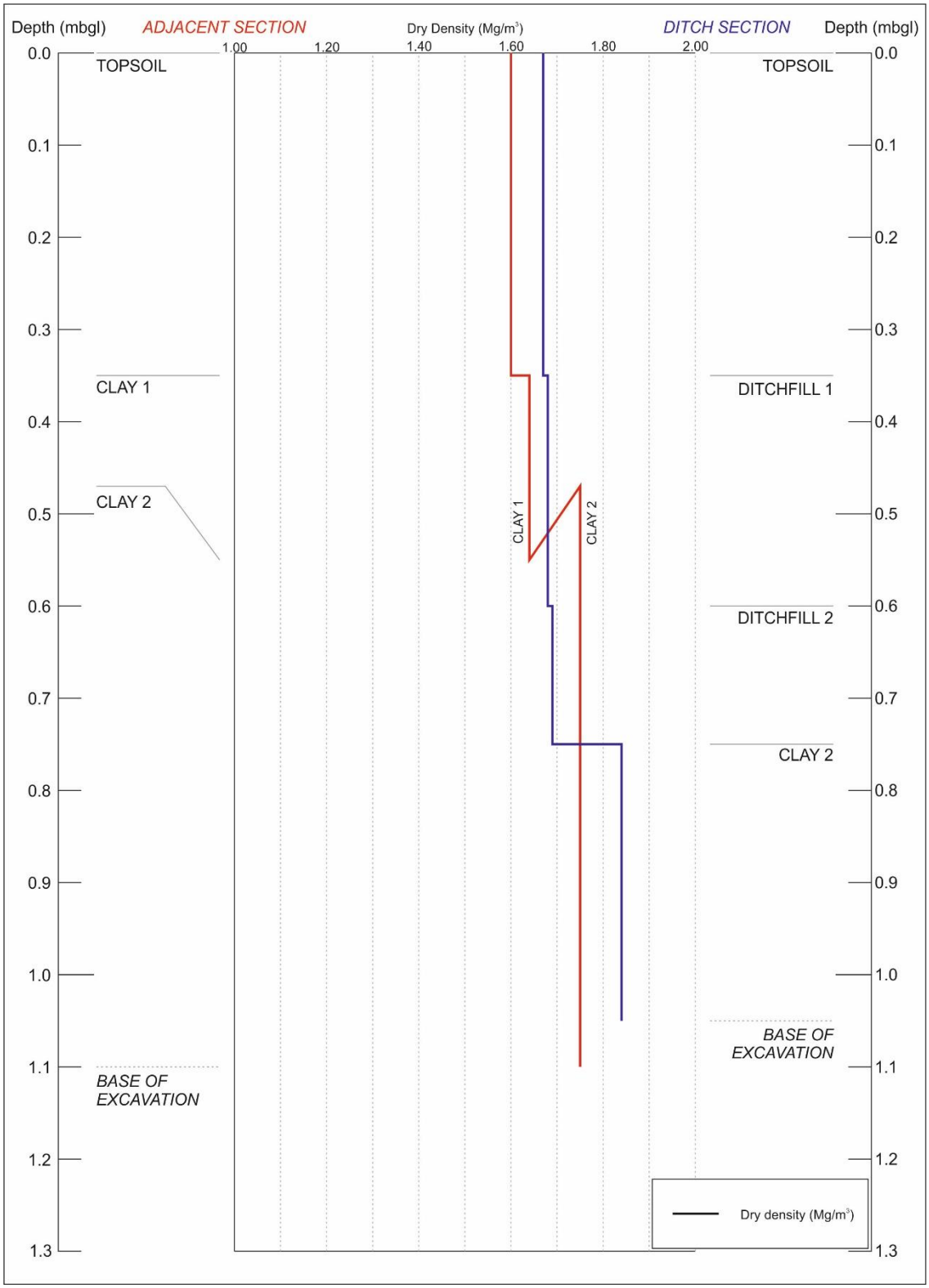

Figure 5.1 Results of determination of dry density by the water displacement method for the AS and DS.

(a) CQF

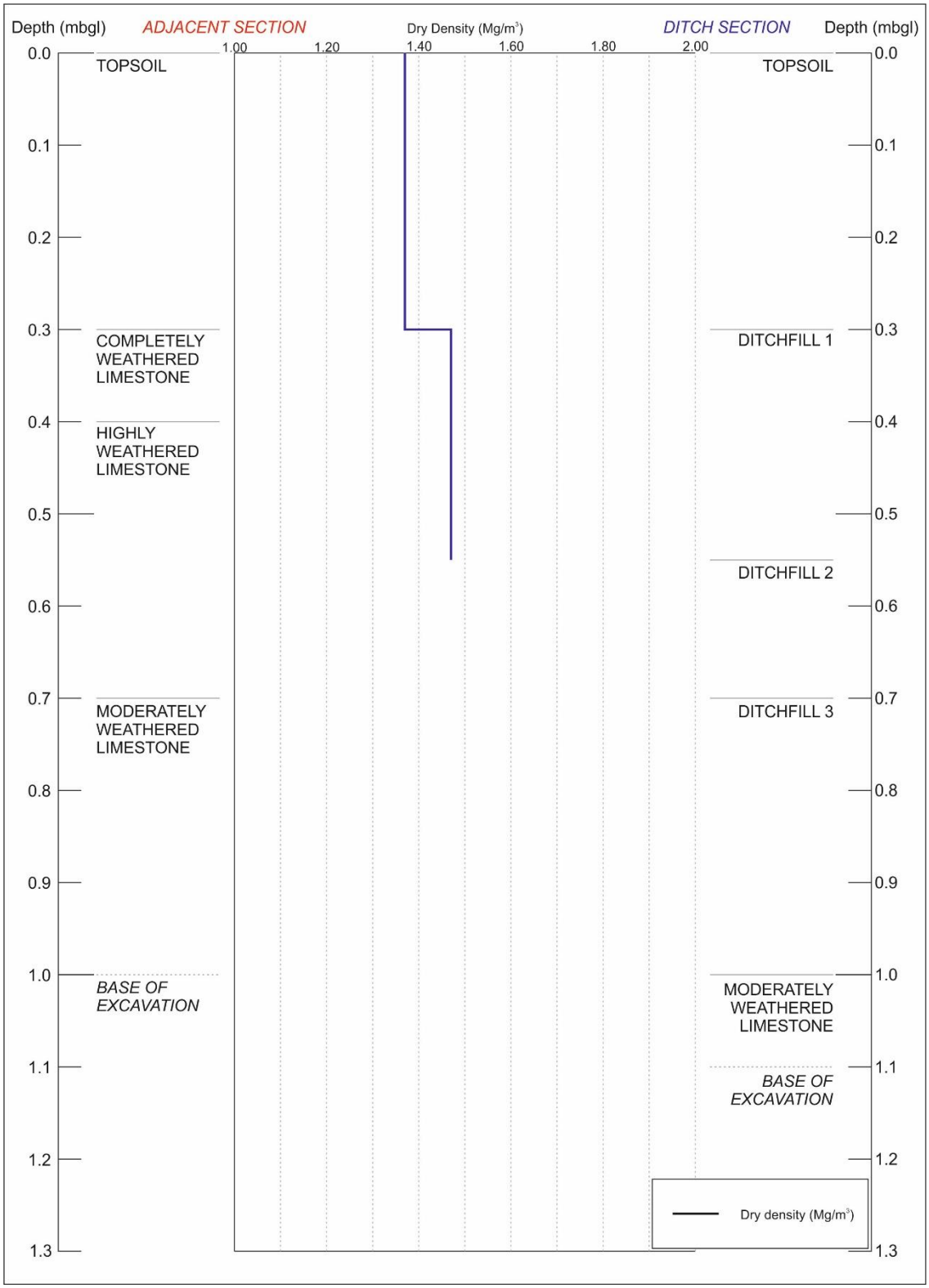

Figure 5.1(cont.) Results of determination of dry density by the water displacement method for the AS and DS.

(b) CCC

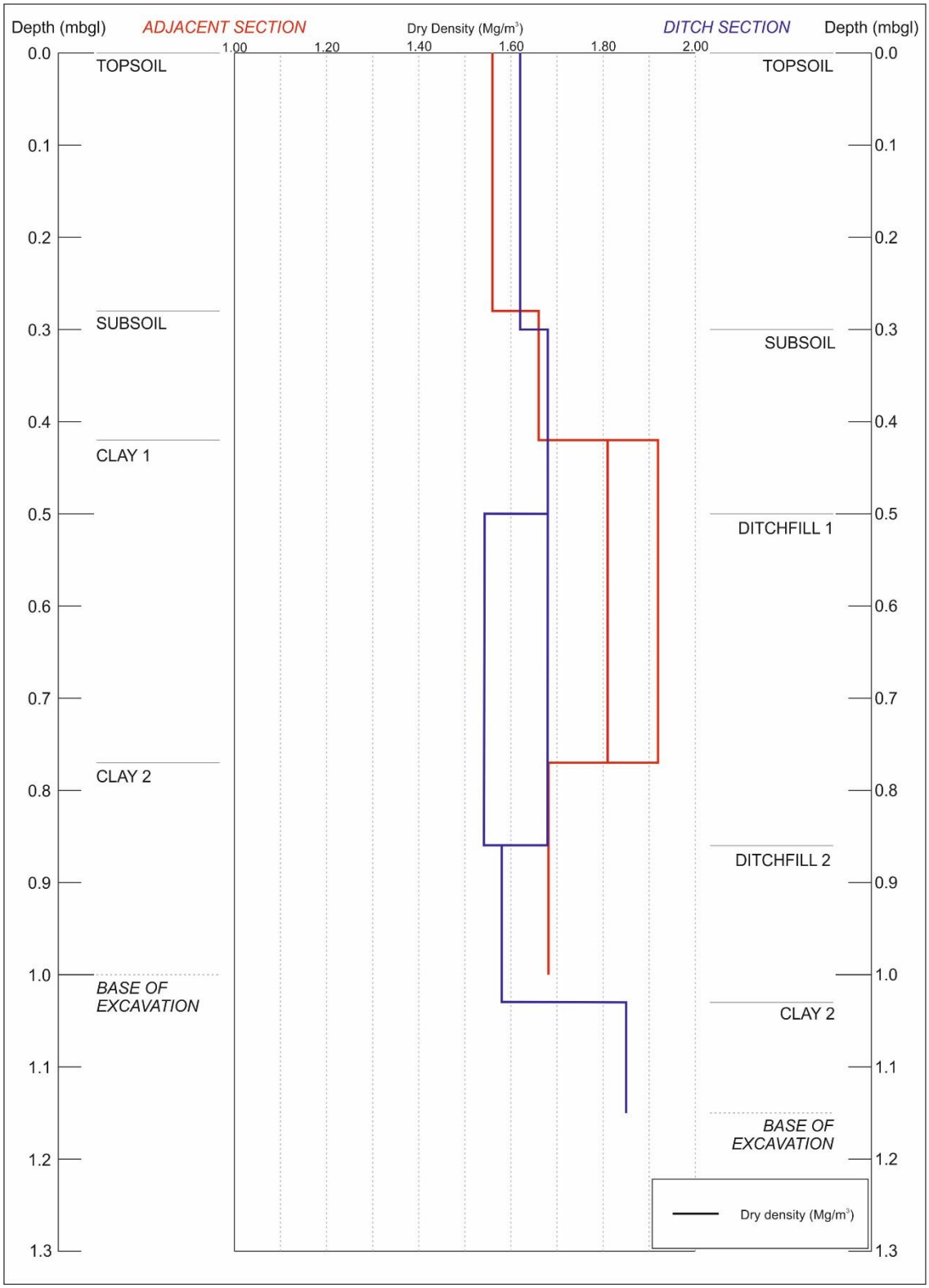

Figure 5.1(cont.) Results of determination of dry density by the water displacement method for the AS and DS.

(c) DCF

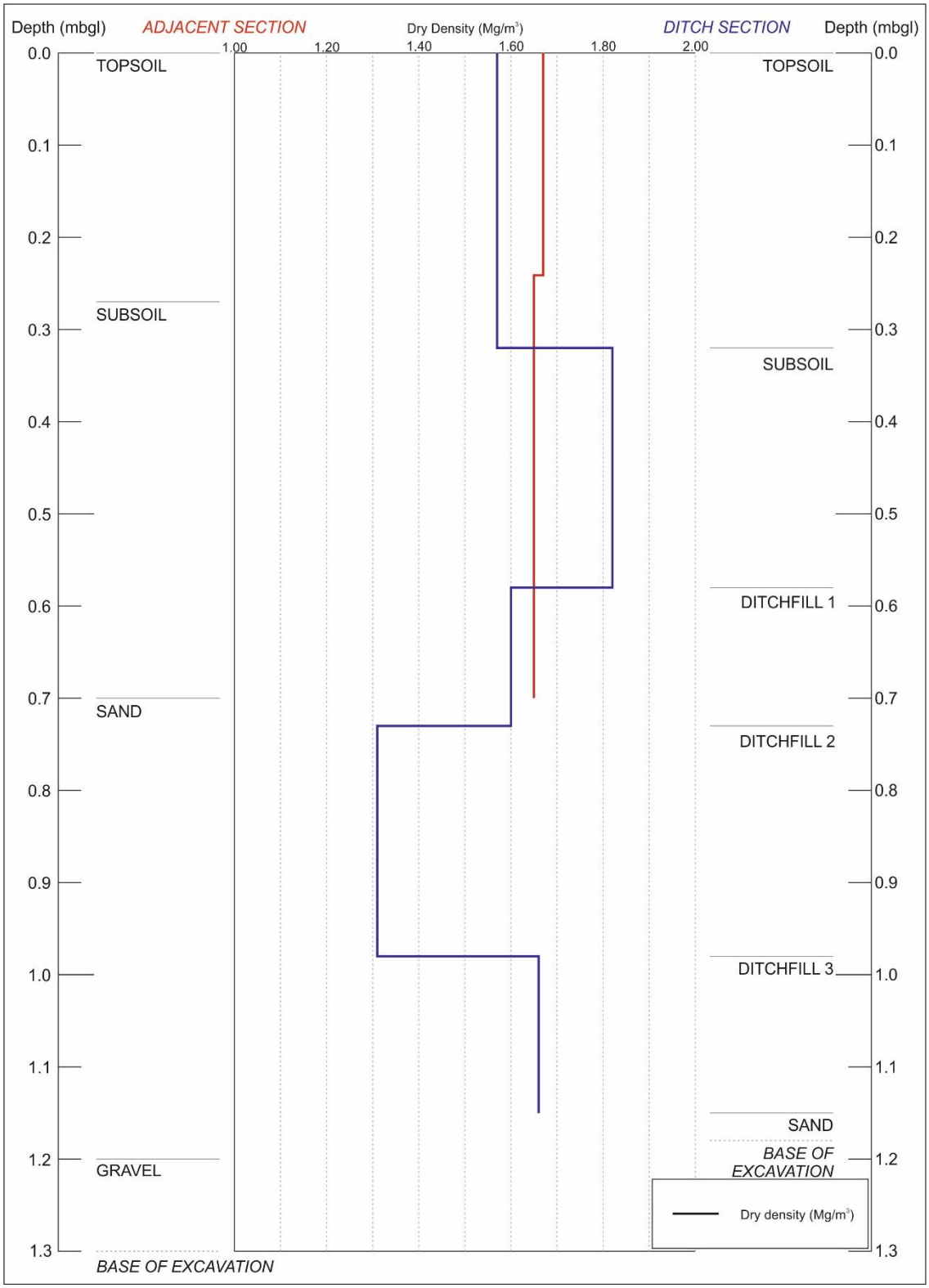

Figure 5.1(cont.) Results of determination of dry density by the water displacement method for the AS and DS.

(d) DPF

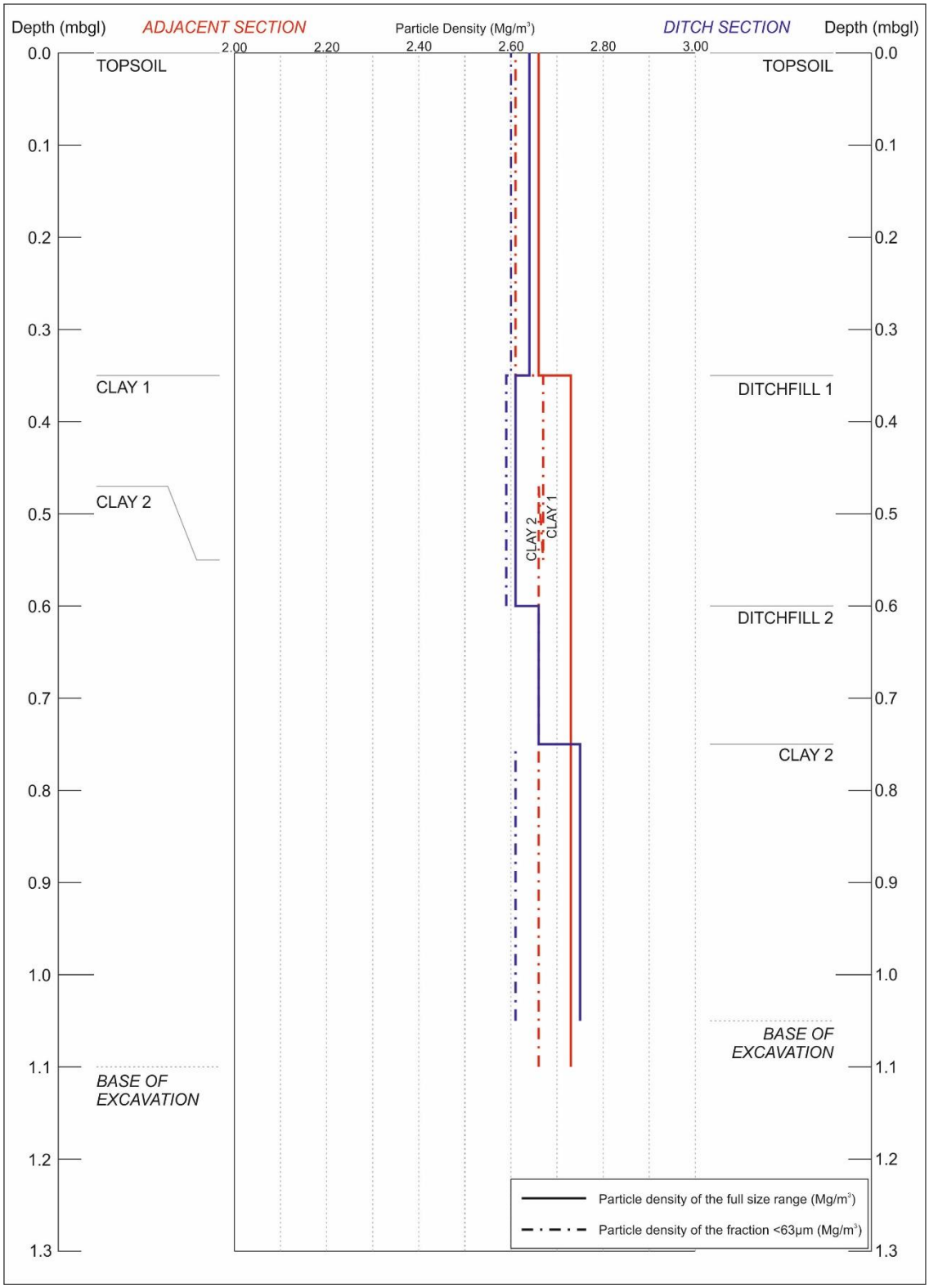

Figure 5.2 Results of determination of particle density by the small pycnometer method for the AS and DS.

(a) CQF

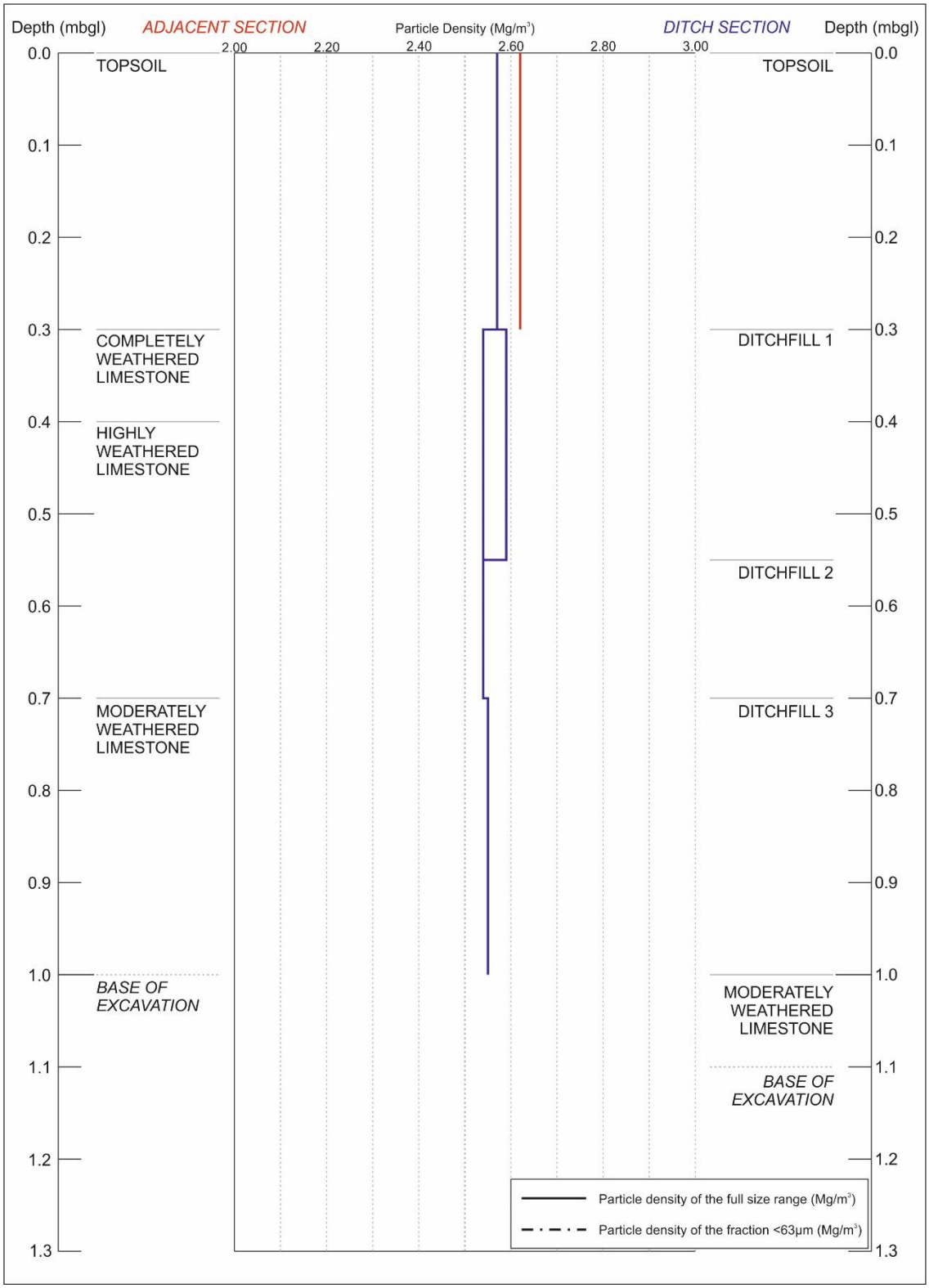

Figure 5.2(cont.) Results of determination of particle density by the small pycnometer method for the AS and DS.

(b) CCC

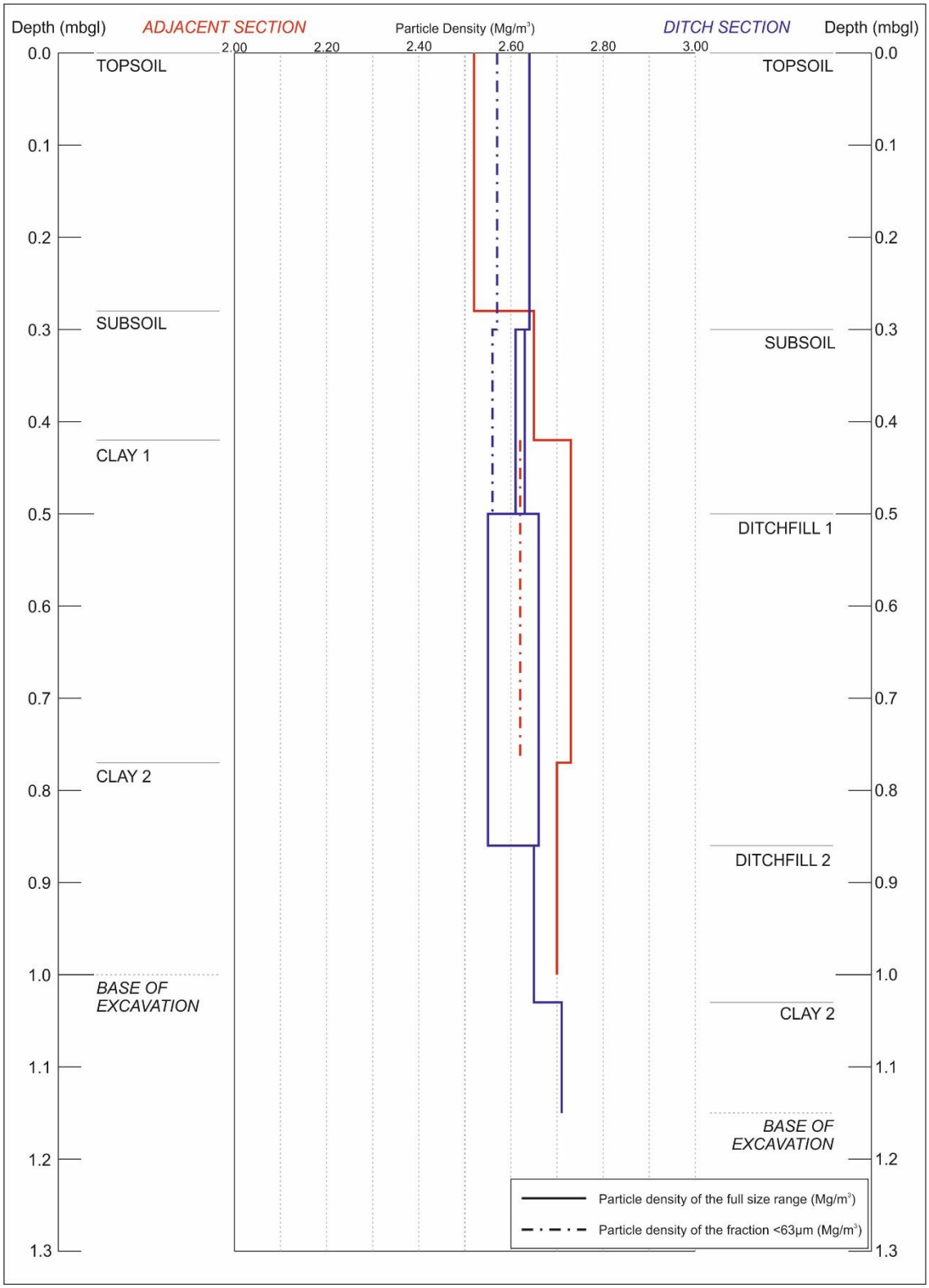

Figure 5.2(cont.) Results of determination of particle density by the small pycnometer method for the AS and DS.

(c) DCF

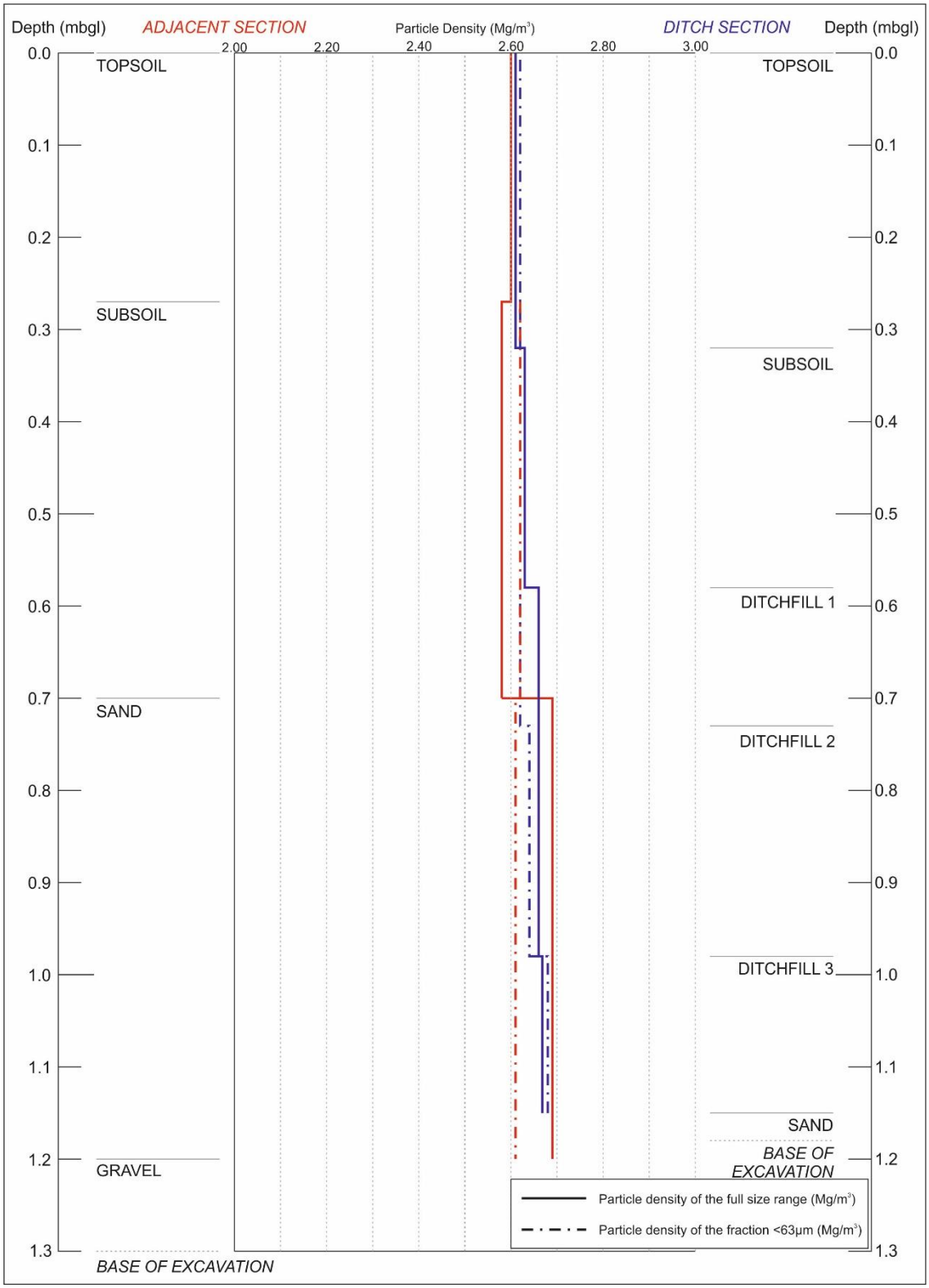

Figure 5.2(cont.) Results of determination of particle density by the small pycnometer method for the AS and DS.

(d) DPF

5.3.4 Particle Density Data Comparisons

5.3.4.1 Analysis Method Comparison

Figure 5.3 shows a comparison of the results obtained using the gas pycnometer method with those of the small pycnometer method. For the results across the full size range, the sites from which the soils were retrieved have been indicated. Those soil selected for comparison of the fines fraction have also been plotted. Dashed lines have been added at ±0.03Mg/m^3 from the 1:1 line.

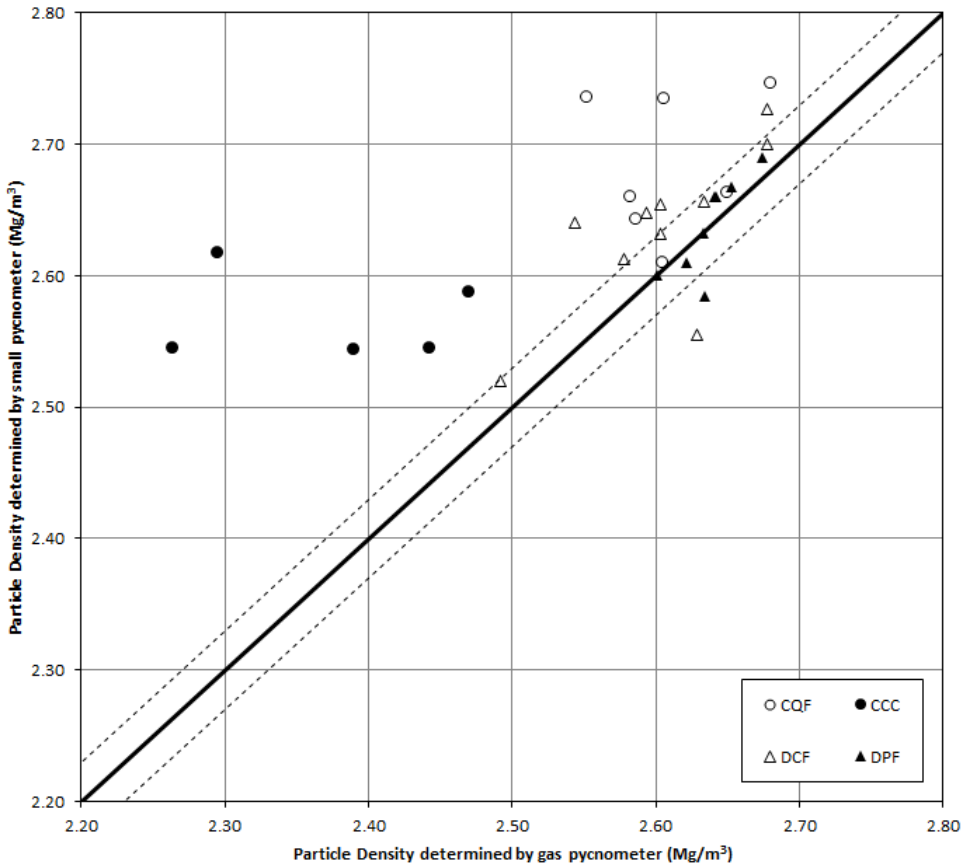

Figure 5.3 Comparison of the particle density results of gas pycnometer and small pycnometer methods.

With one exception (from DCF), the results across all particle sizes for the clay sites (DCF and CQF) all recorded higher particle densities when tested with the small pycnometer method, with the largest differences in the clay soils. Soils from DPF were

typically within ±0.03 Mg/m^3. The largest differences were seen in the soils from CCC, which all recorded significantly higher results (0.11-0.37 Mg/m^3) using the gas pycnometer method.

Since the mass for both methods is determined using the same technique, an explanation for this difference may be inherent in the different mediums used to determine volume, deaired water for the small pycnometer method, and helium for the gas pycnometer method. A water molecule has a diameter of approximately 3Å, whereas a helium atom has a diameter of approximately 0.5Å. Pore throat diameters between these values would therefore allow the exchange to helium, but not to water. The larger the exchange volume, the lower the determined specimen volume, resulting in a higher calculated density. Therefore, these higher values in the small pycnometer method may be due to the presence of a high number of pore throat sizes in the composition of the soils with a diameter of 0.5-3Å.

5.3.4.2 Fractional Differences in Particle Density

Rubey (1933) found that heavier minerals are preferentially found in the finer size classes. Therefore, a comparison of the average particle density across all particle size ranges was compared to that of the fraction <63µm, using the results of testing with the gas pycnometer method. Figure 5.4 shows the results of the comparison in terms of the soil type and which test site the soils were retrieved from. Dashed lines have been added at ±0.03Mg/m^3 from the 1:1 line.

The soils retrieved from the clay sites (DCF and CQF) typically had a slightly higher particle density (of up to +0.5 Mg/m^3) in the fine fraction than across all particle size ranges. However, DCF Clay 2 and CQF Clays 1 and 2 showed a significantly higher density (up to +0.14 Mg/m^3) in the fine fraction, indicating that the clay matrix is

composed of heavier minerals than the coarse fraction. No significant differences were noted in the results for the DPF soils which were all were within ±0.03 Mg/m^3. All the soils from CCC had a markedly higher (up to +0.29 Mg/m^3) particle density in the fines fraction. The CCC soils also had typically higher proportions of organic matter than the soils from other sites, which may be preferentially found in the coarse fraction, reducing the average particle density when measured across all size ranges.

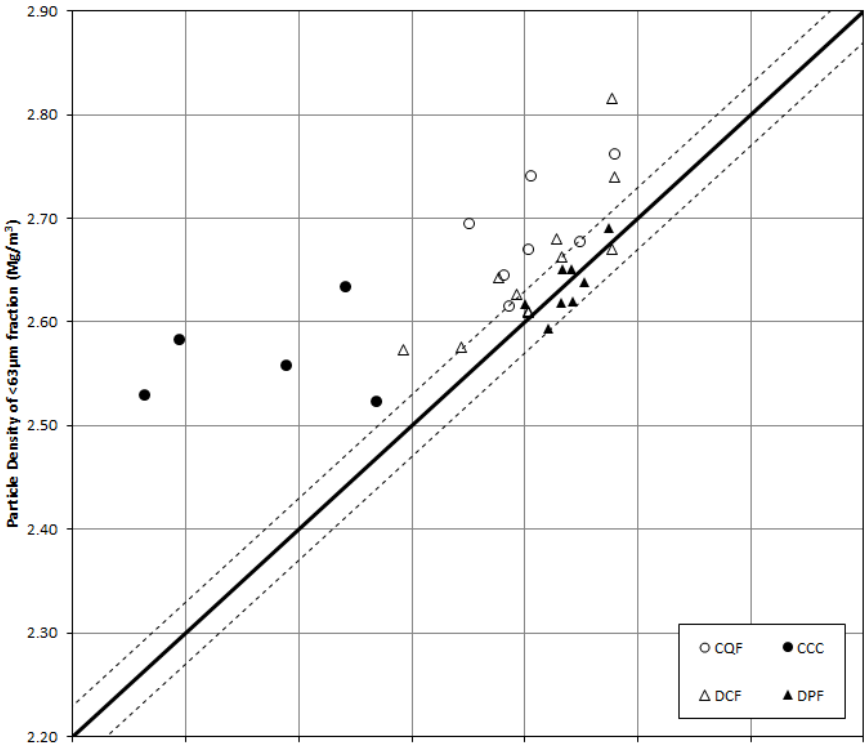

Figure 5.4 Comparison of the particle density of all size fractions and the fine fraction.

5.3.5 Particle Size Distribution by the Sieve Method

The sieve method with some deviation from the standard, and an assessment of sample variation, has been reported in Appendix A. A diagrammatic representation of the results is given in Figures 5.5(a-d).

Precision of the data was tested where possible and was found to be 5%. Sample variation was found to be <10% in the gravel fraction and <3% in the sand fraction. The wider

variations in the gravel fraction may have been due to limitations on sample sizes. (Appendix A).

5.3.6 Particle Size Distribution by the Sedimentation by Hydrometer

The calibrations, raw data and calculations relating to the SH analysis are provided in Appendix A. A diagrammatic representation of the results is given in Figures 5.6(a-d).

To assess the repeatability of the SH test, three specimens were tested twice by remixing the sedimentation column after the initial test. Differences between the percentages in both the clay and silt fractions was <1%.

Precision and repeatability were found to be within 2%. Differences outside this range were assumed to be from sample variation.

5.3.7 Particle size Distribution by the Laser Diffraction Method

The LD method was applied to samples to assess if the results were comparable with those from the SH method. Figure 5.7 shows the comparison of the percentages within the silt and clay fractions for the two methods. The graph shows that there are significant differences in the results. With few exceptions (DPF Sand and CCC Topsoil), percentages in the silt fraction are significantly higher, in the extreme cases (CQF Clay 1 and CQF Fill 1), values recorded using LD are more than double that of the SH results. A relationship between the clay fraction percentages recorded by the two methods is evident. A best fit line to the data shows a relationship where LD returns values which are approximately 1/3 of the SH value.

5.3.8 Plasticity by the Plastic Limit and Cone Penetrometer Method

Diagrammatic representations of the plasticity is given in Figures 5.8(a-d).

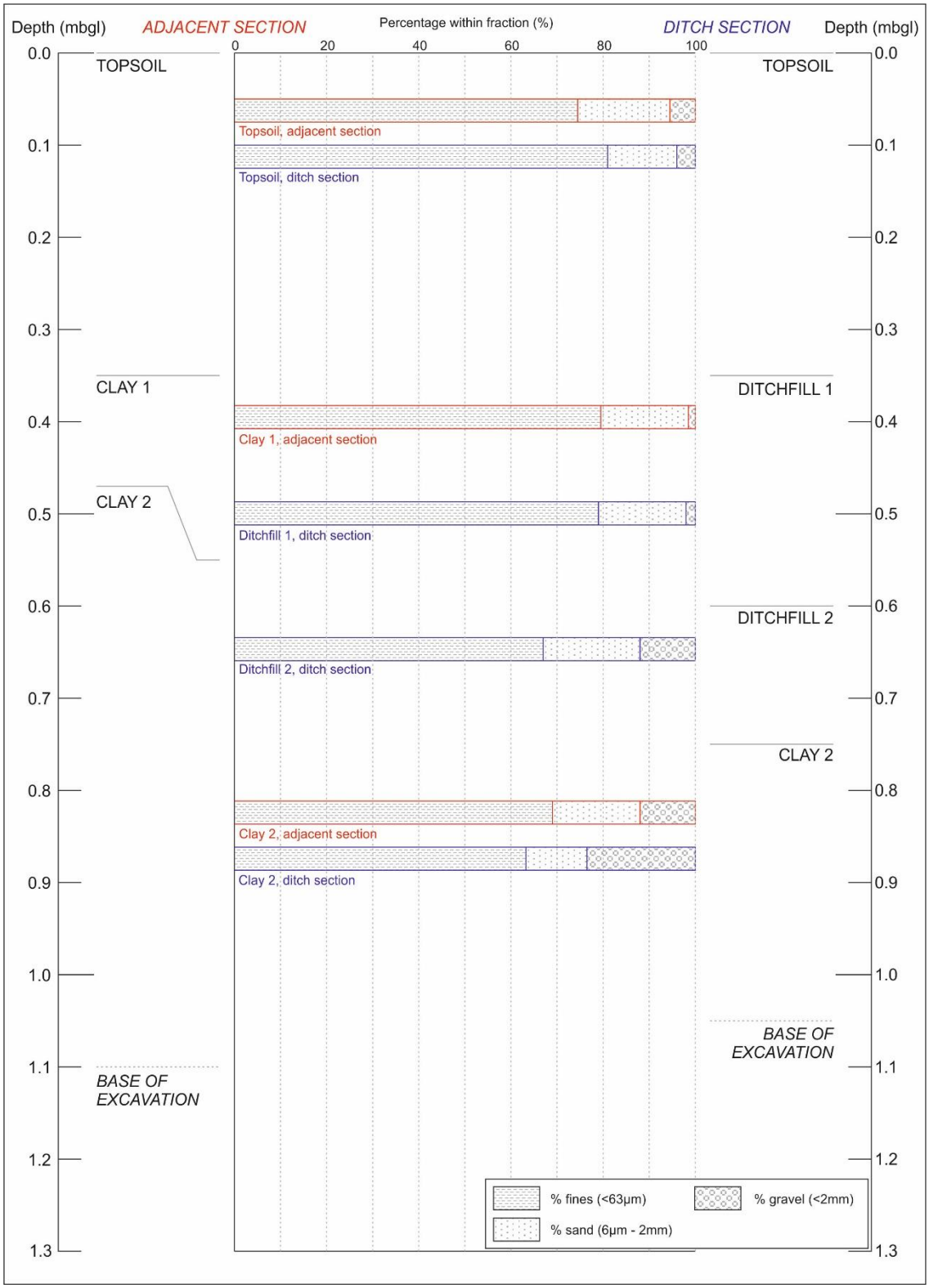

Figure 5.5 Results of determination of PSD by the sieve method for the AS and DS.

(a) CQF

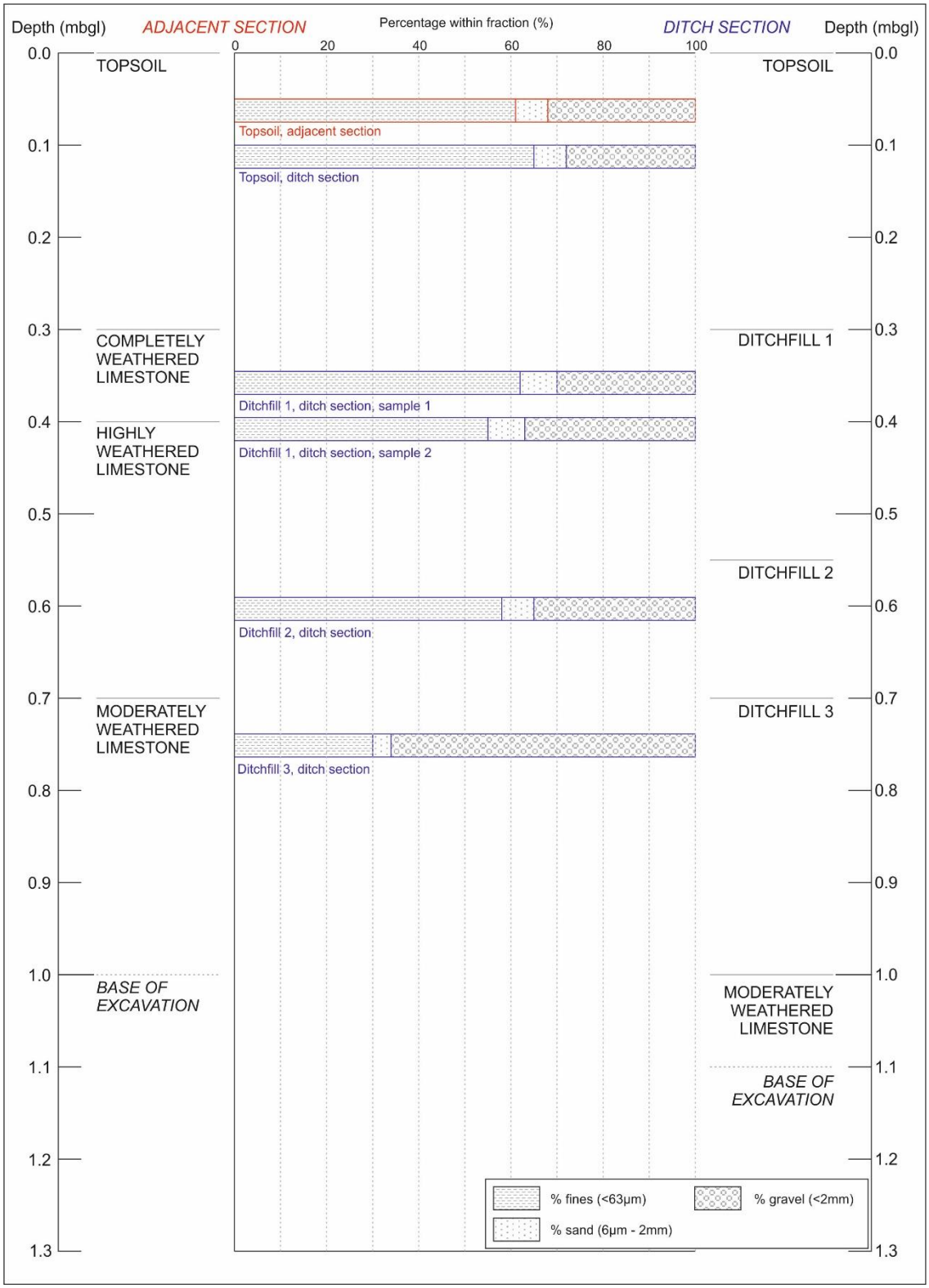

Figure 5.5(cont.) Results of determination of PSD by the sieve method for the AS and DS.

(b) CCC

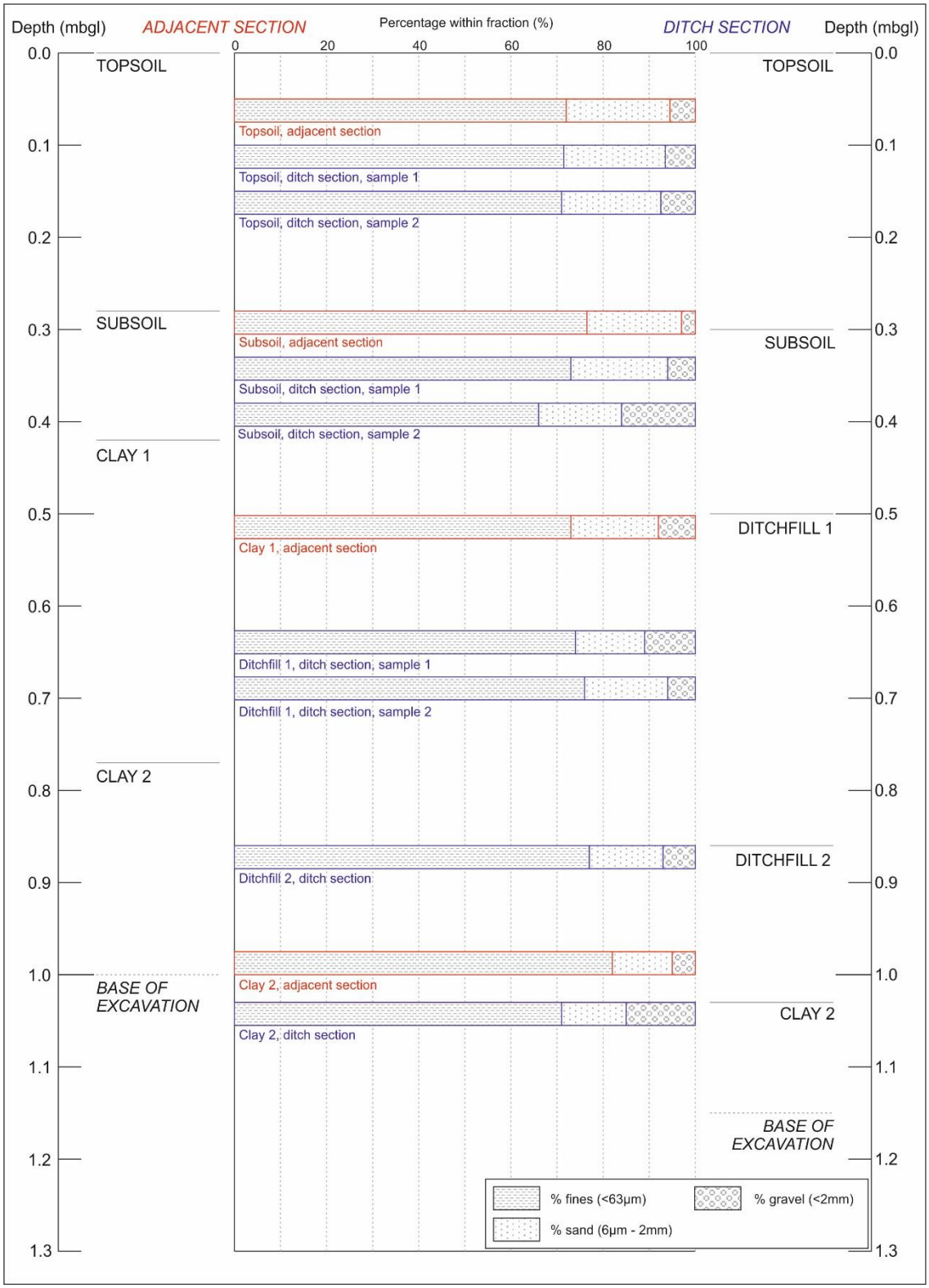

Figure 5.5(cont.) Results of determination of PSD by the sieve method for the AS and DS.

(c) DCF

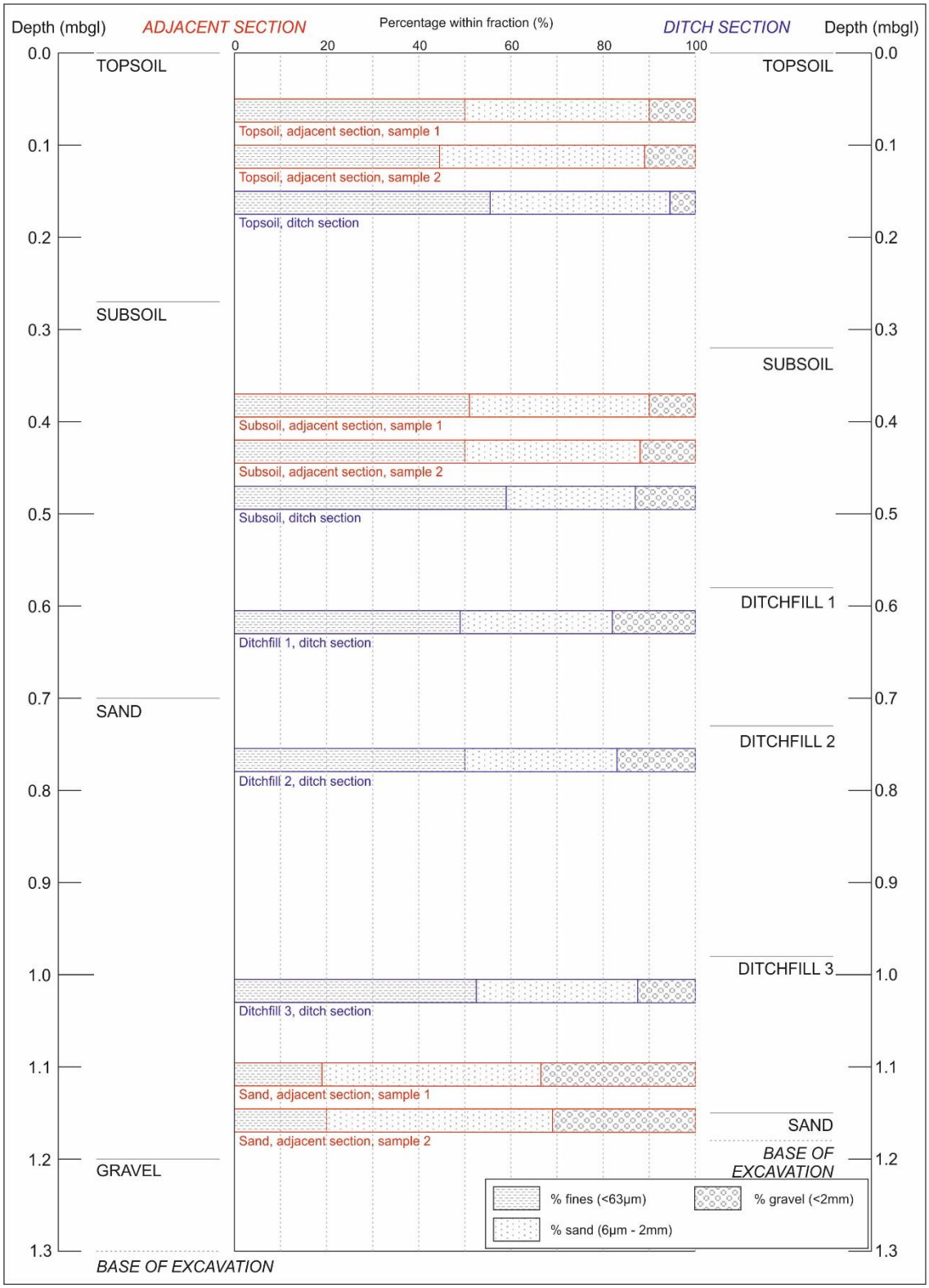

Figure 5.5(cont.) Results of determination of PSD by the sieve method for the AS and DS.

(d) DPF

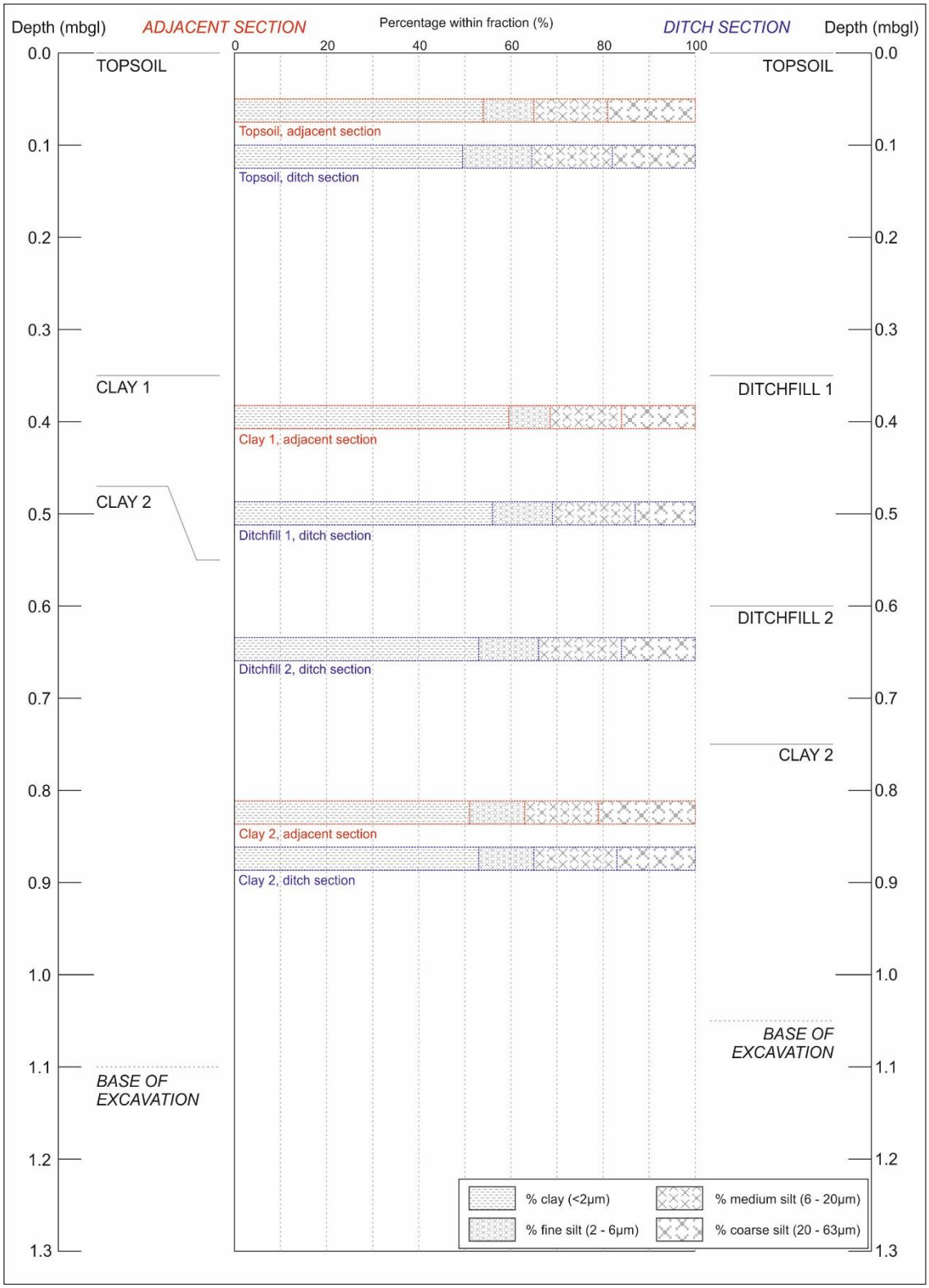

Figure 5.6 Results of determination of PSD by the sedimentation by hydrometer method for the AS and DS.

(a) CQF

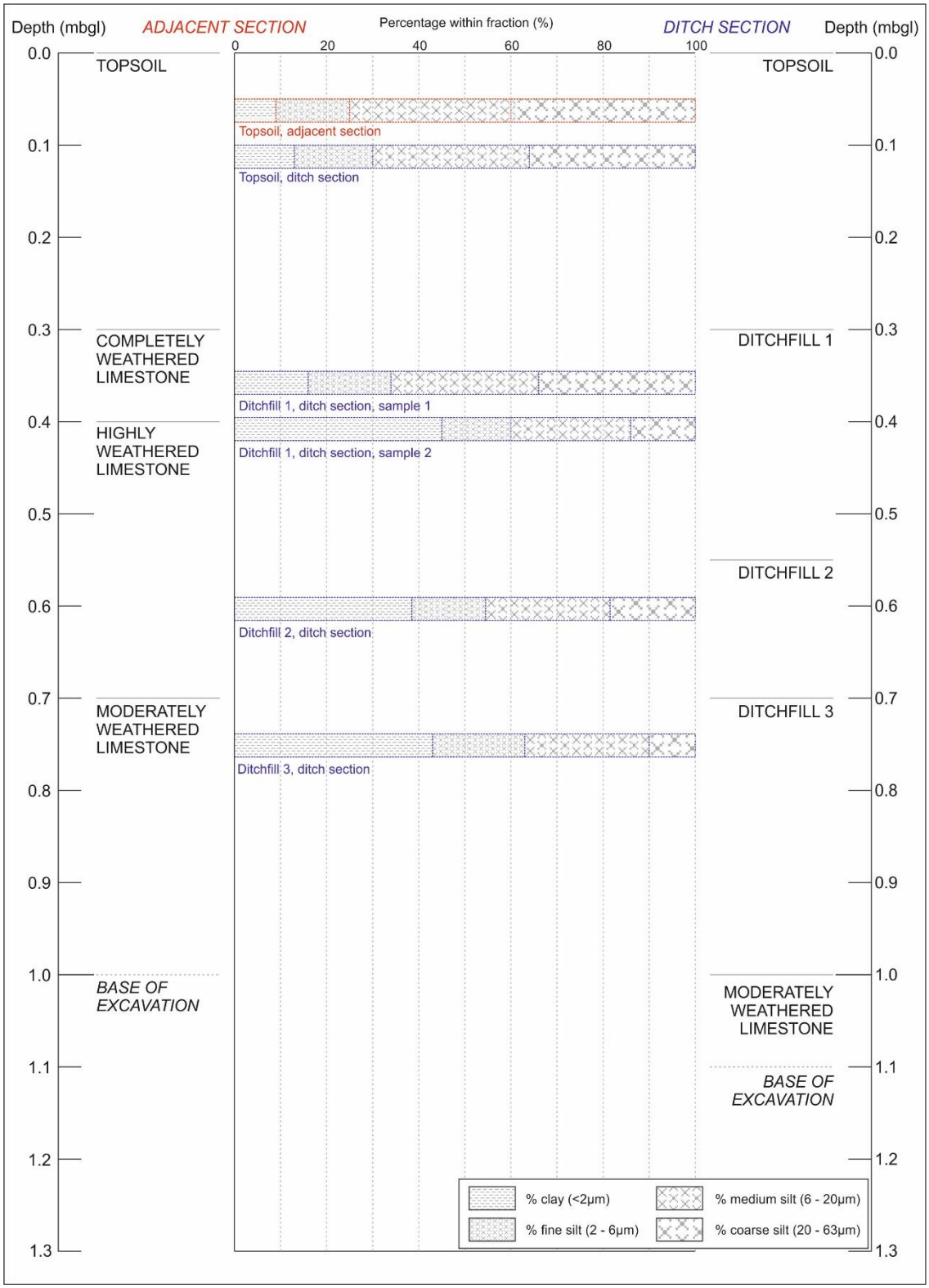

Figure 5.6(cont.) Results of determination of PSD by the sedimentation by hydrometer method for the AS and DS.

(b) CCC

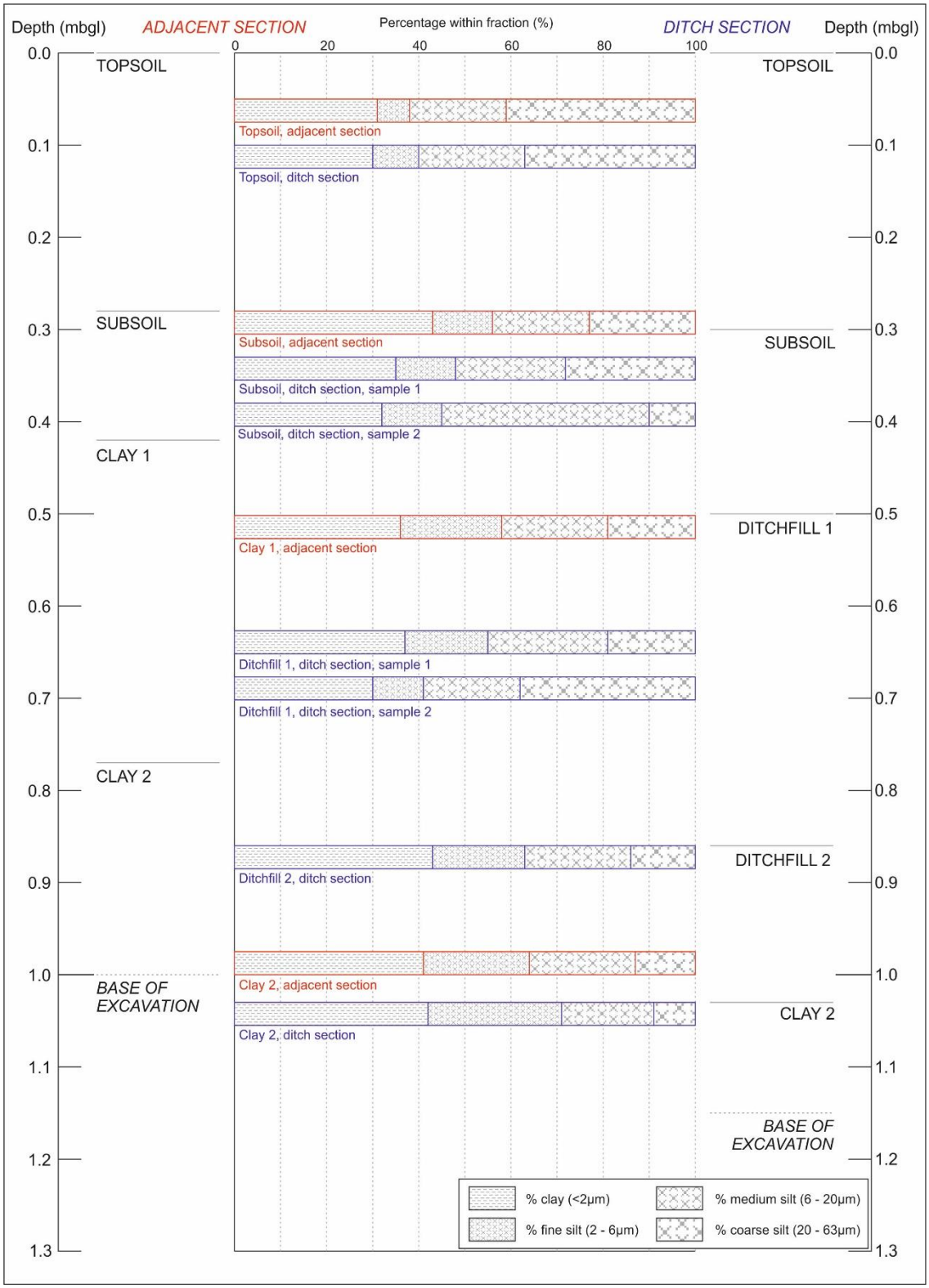

Figure 5.6(cont.) Results of determination of PSD by the sedimentation by hydrometer method for the AS and DS.

(c) DCF

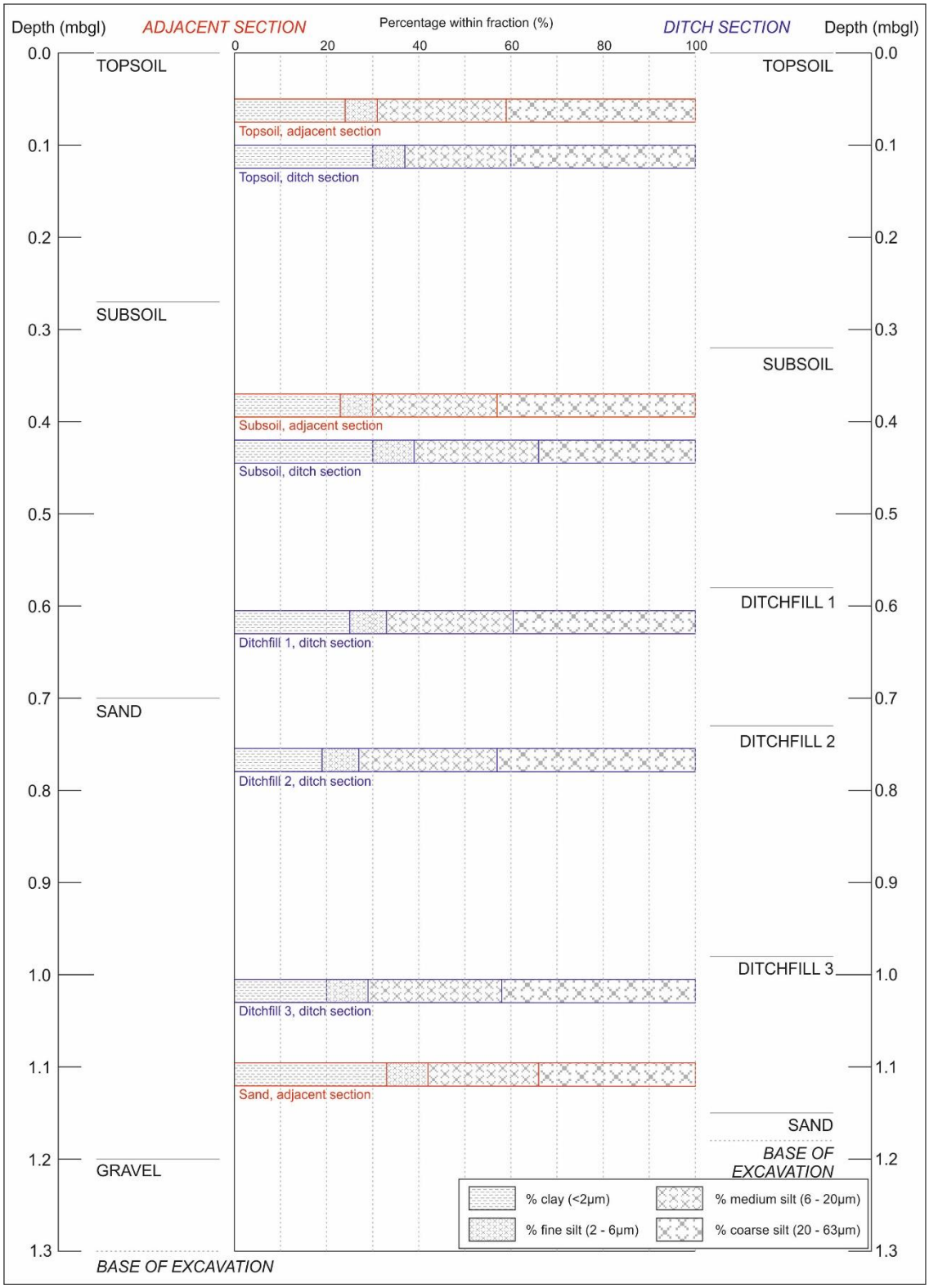

Figure 5.6(cont.) Results of determination of PSD by the sedimentation by hydrometer method for the AS and DS.

(d) DPF

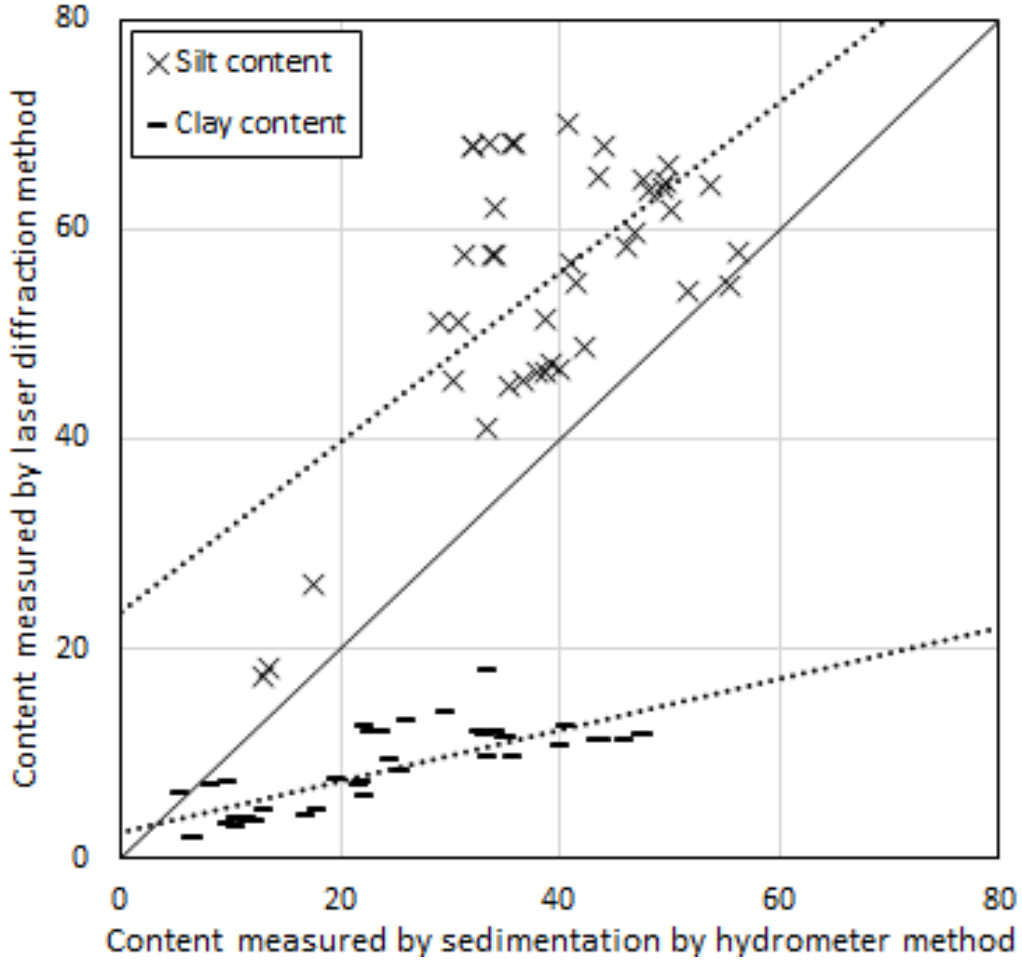

Figure 5.7 Comparison of the results of testing using the sedimentation by hydrometer method and the laser diffraction method for the proportions in the silt and clay fractions

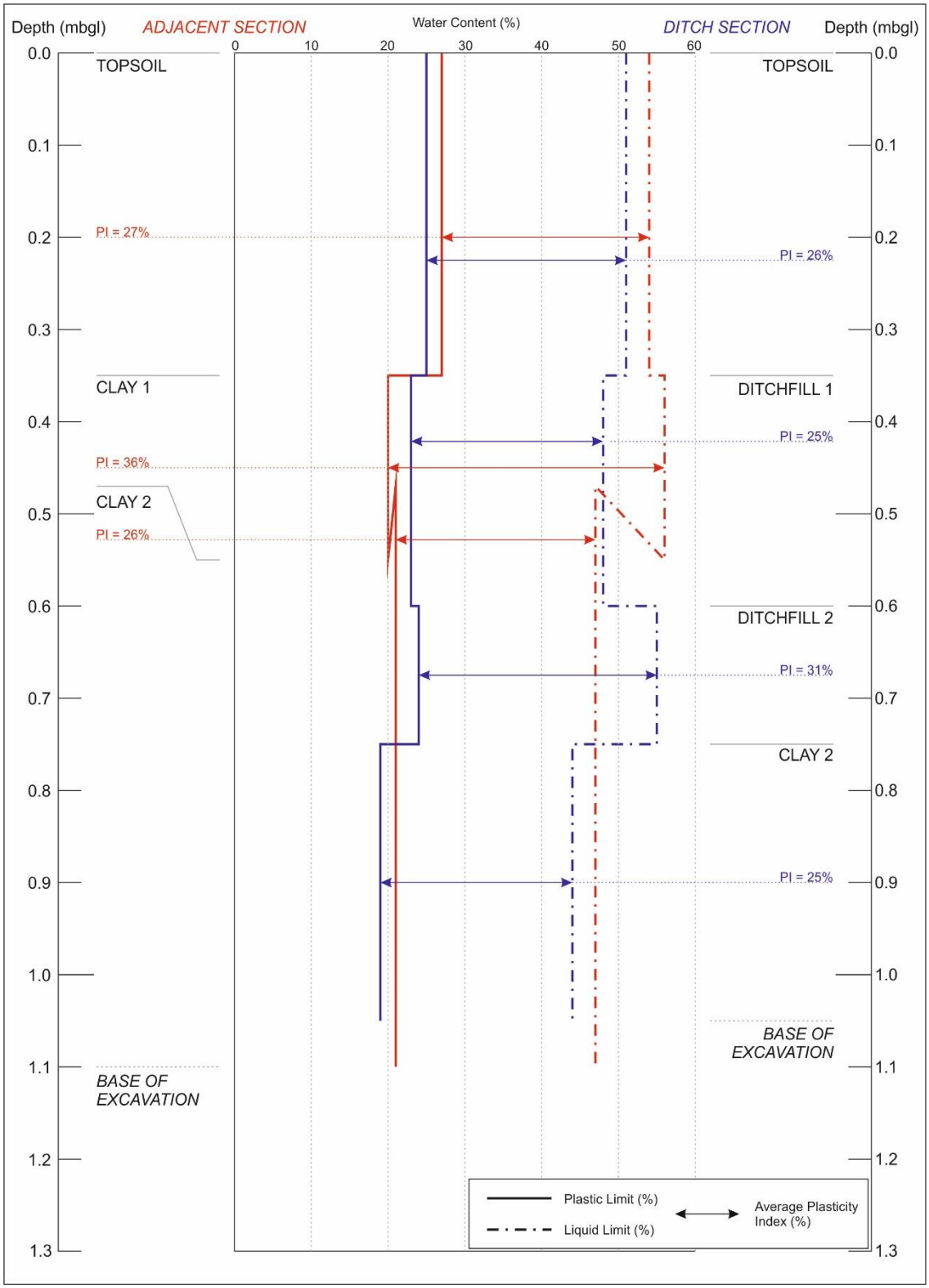

Figure 5.8 Results of plasticity testing by the plastic limit and cone penetrometer methods for the AS and DS.

(a) CQF

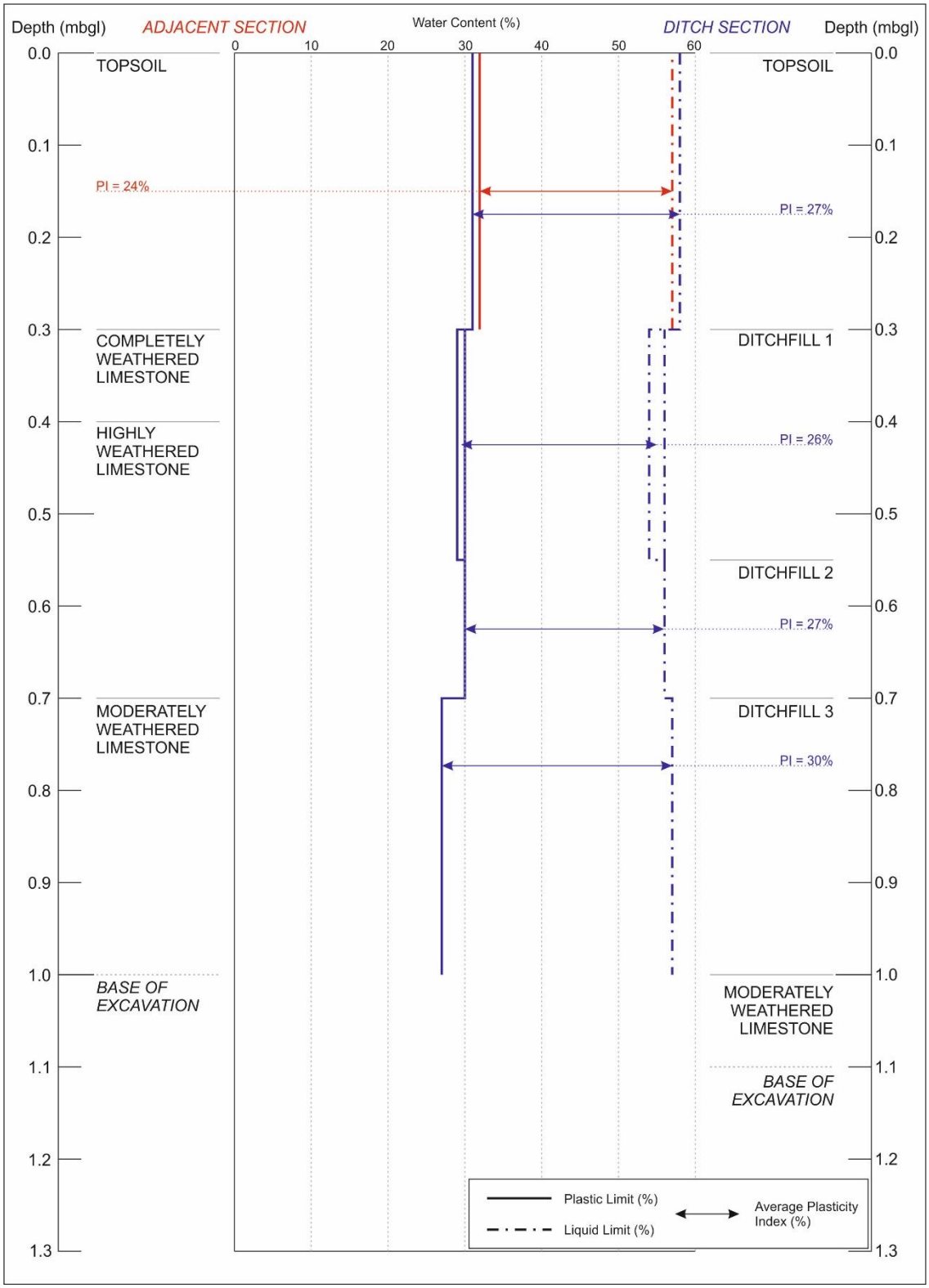

Figure 5.8(cont.) Results of plasticity testing by the plastic limit and cone penetrometer methods for the AS and DS.

(b) CCC

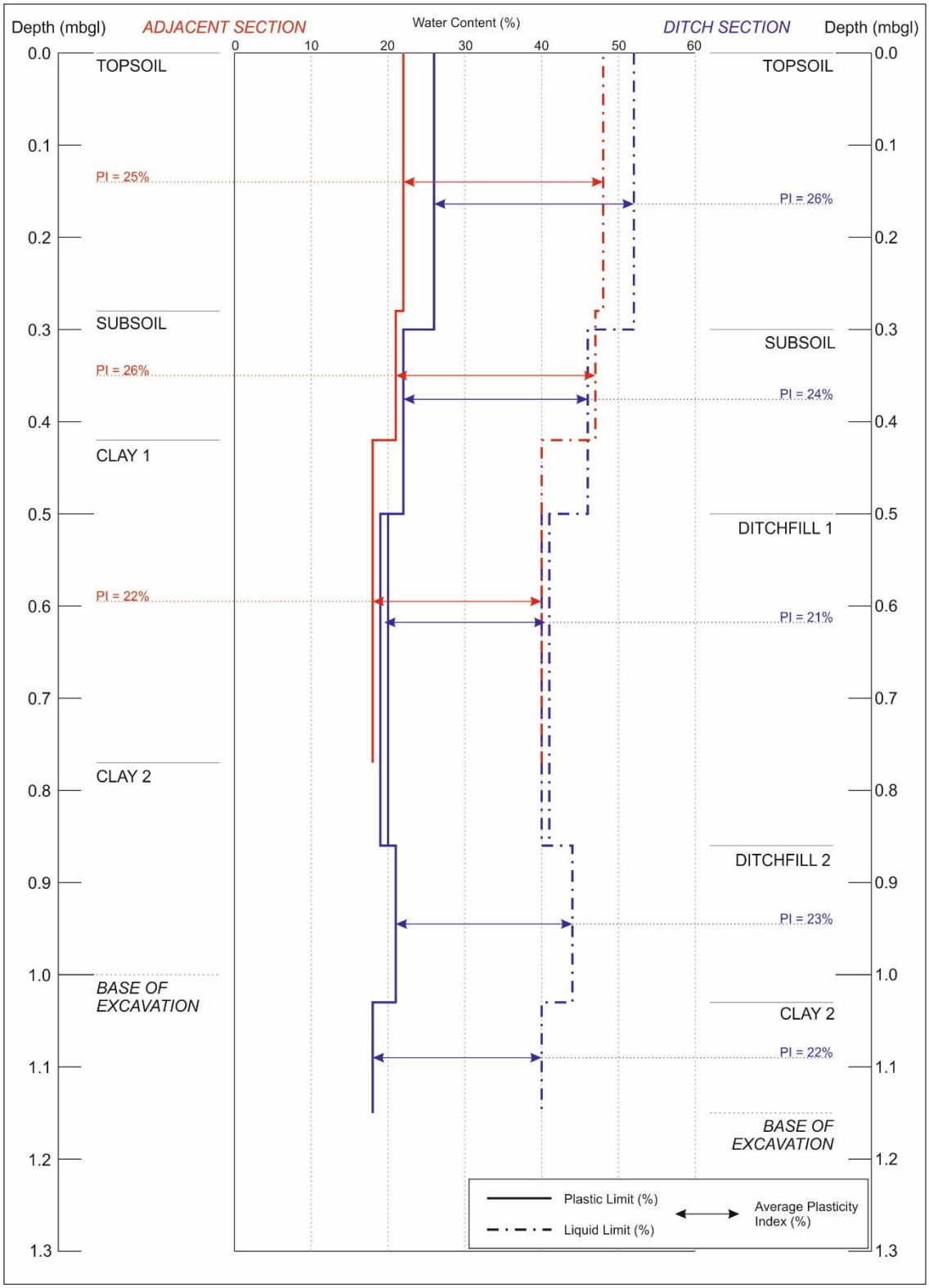

Figure 5.8(cont.) Results of plasticity testing by the plastic limit and cone penetrometer methods for the AS and DS.

(c) DCF

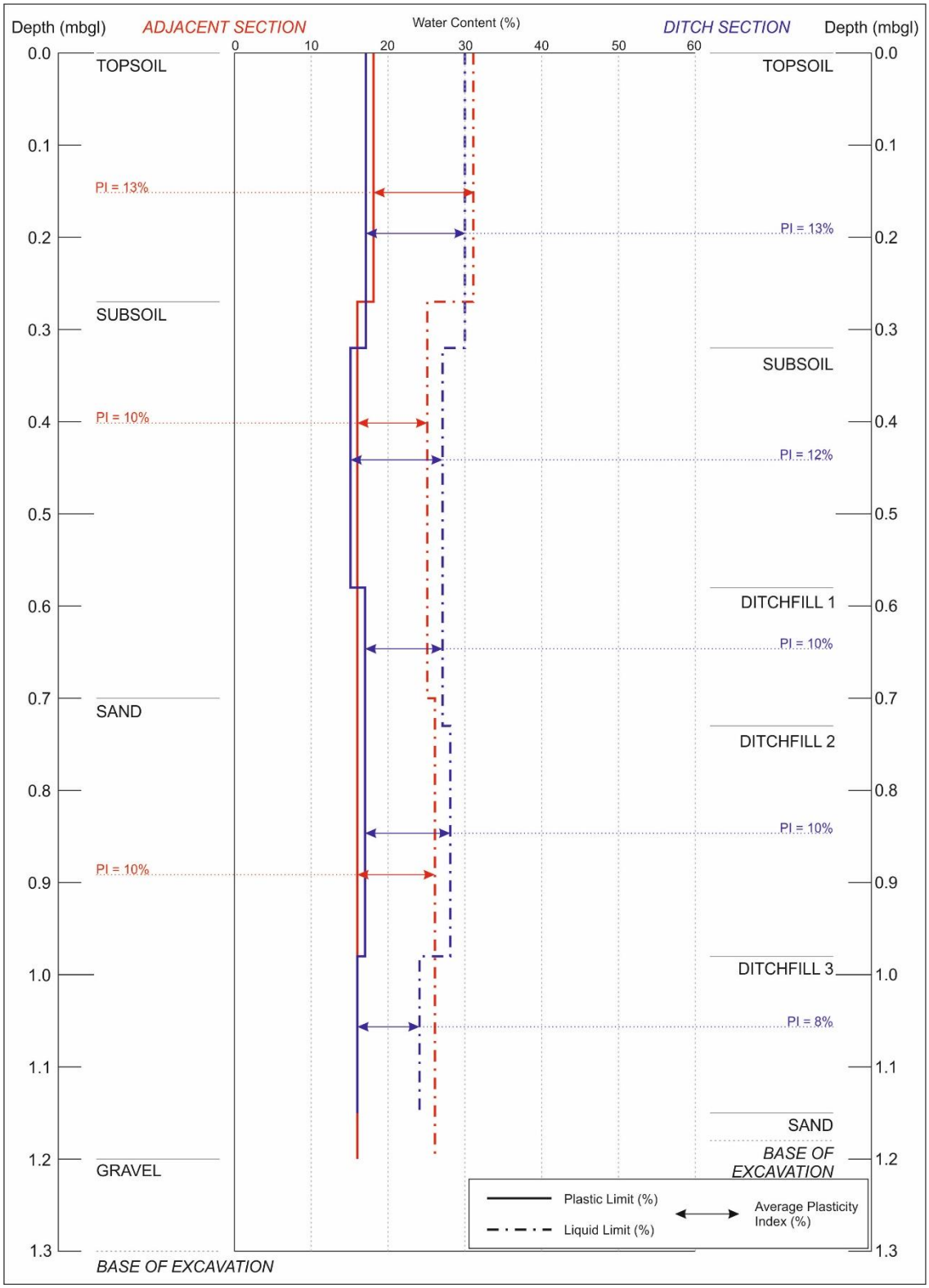

Figure 5.8(cont.) Results of plasticity testing by the plastic limit and cone penetrometer methods for the AS and DS.

(d) DPF

5.3.9 Organic Content by the Loss on Ignition Method

Organic content affects the behaviour of soils, changing the plasticity characteristics. The Total Organic Matter content (TOM) of the soils was determined using the loss on ignition method by ALcontrol Laboratories. The tested samples were retrieved from boreholes at the locations shown in Figures 4.17(a-d). Not all soil horizons recorded in the sections were distinct in the recovered cores. Where necessary assumptions were made in the data, for example in each of the ditch sections, separate ditchfills were indistinct and a single results was taken to represent all ditchfills in the section. A diagrammatic representation of the results are shown in Figures 5.9(a-d).

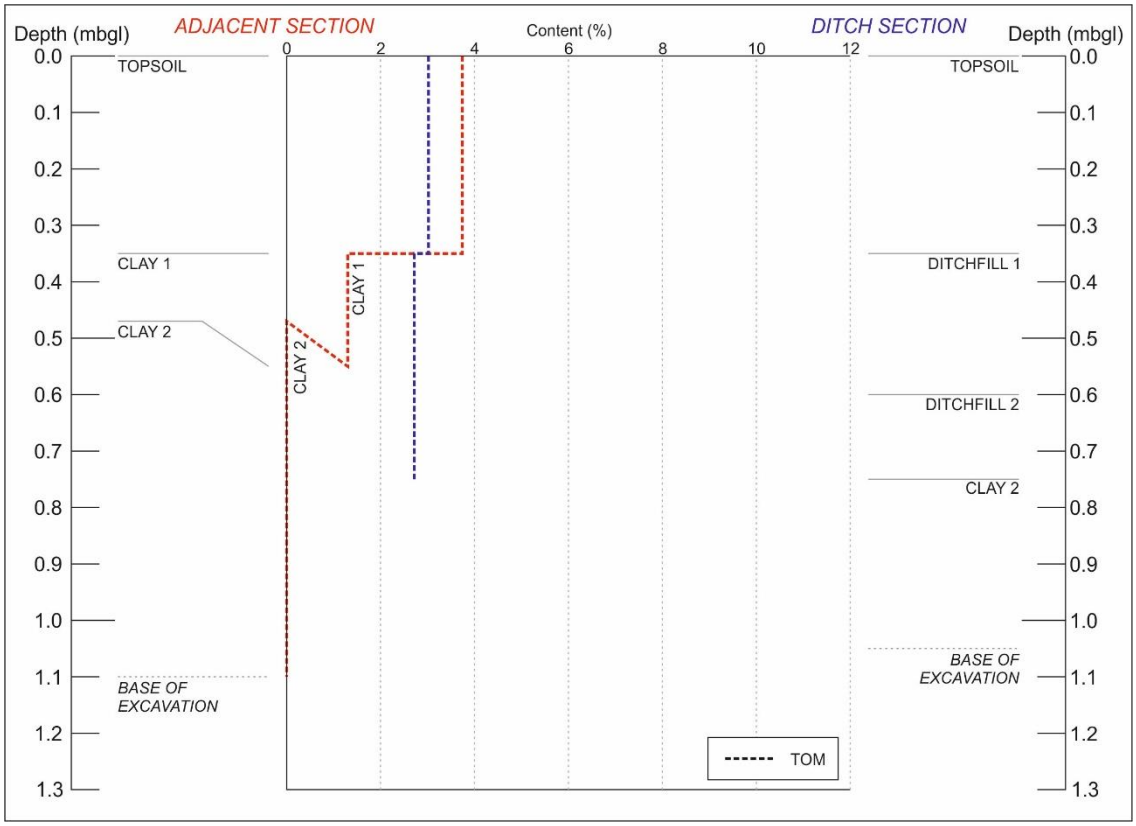

Figure 5.9 Results of testing for organic matter by the loss on ignition method for the AS and DS.

(a) CQF

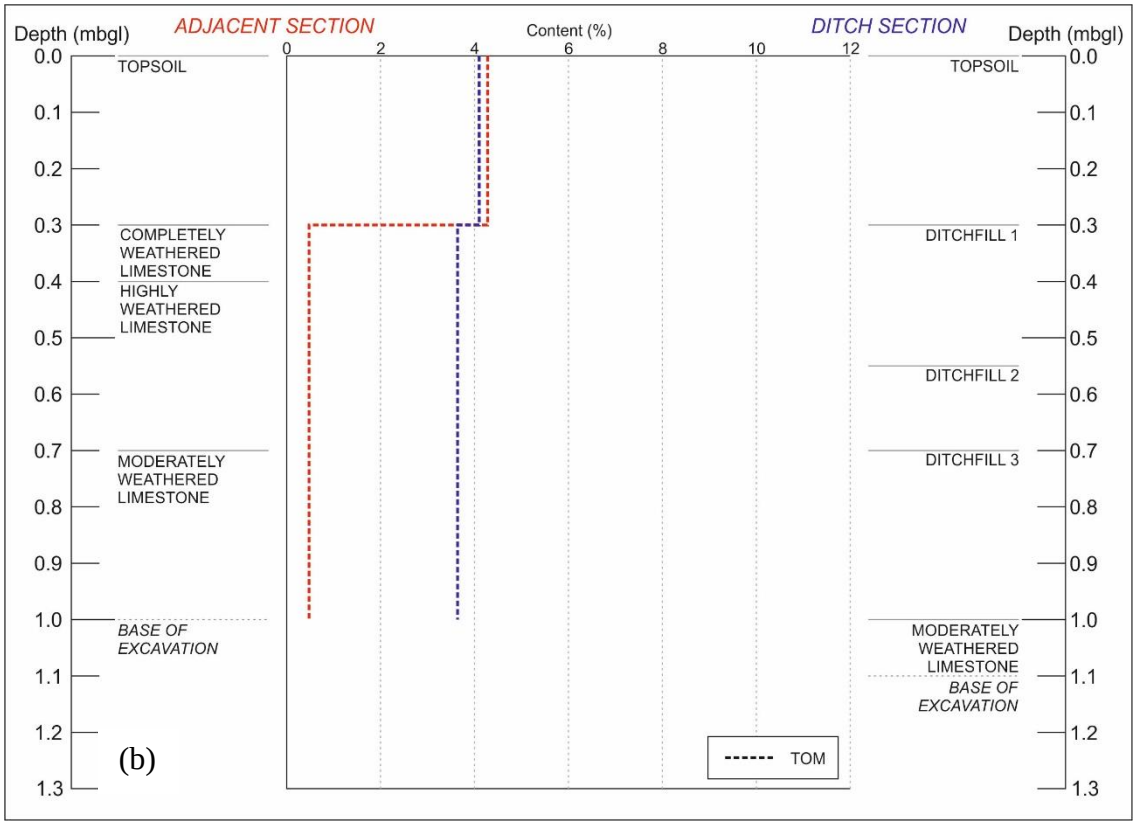

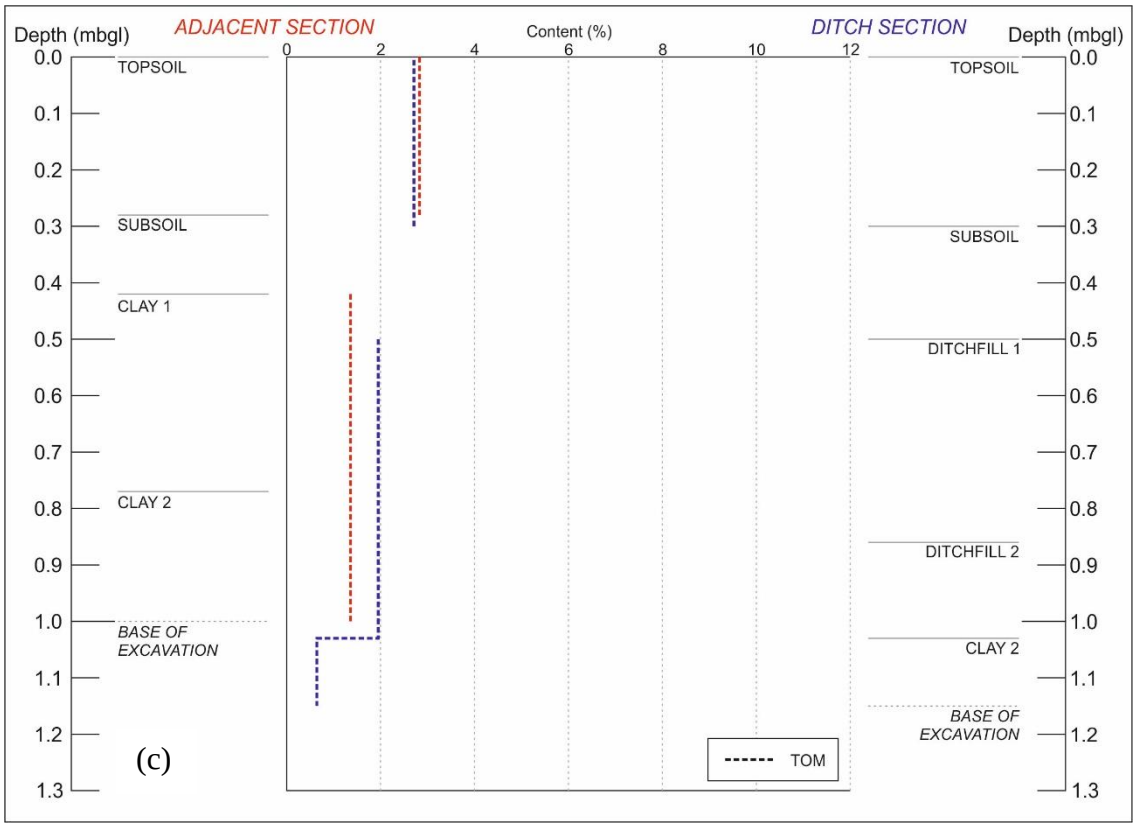

Figure 5.9(cont.) Results of testing for organic matter by the loss on ignition method for the AS and DS.

(b) CCC (c) DCF

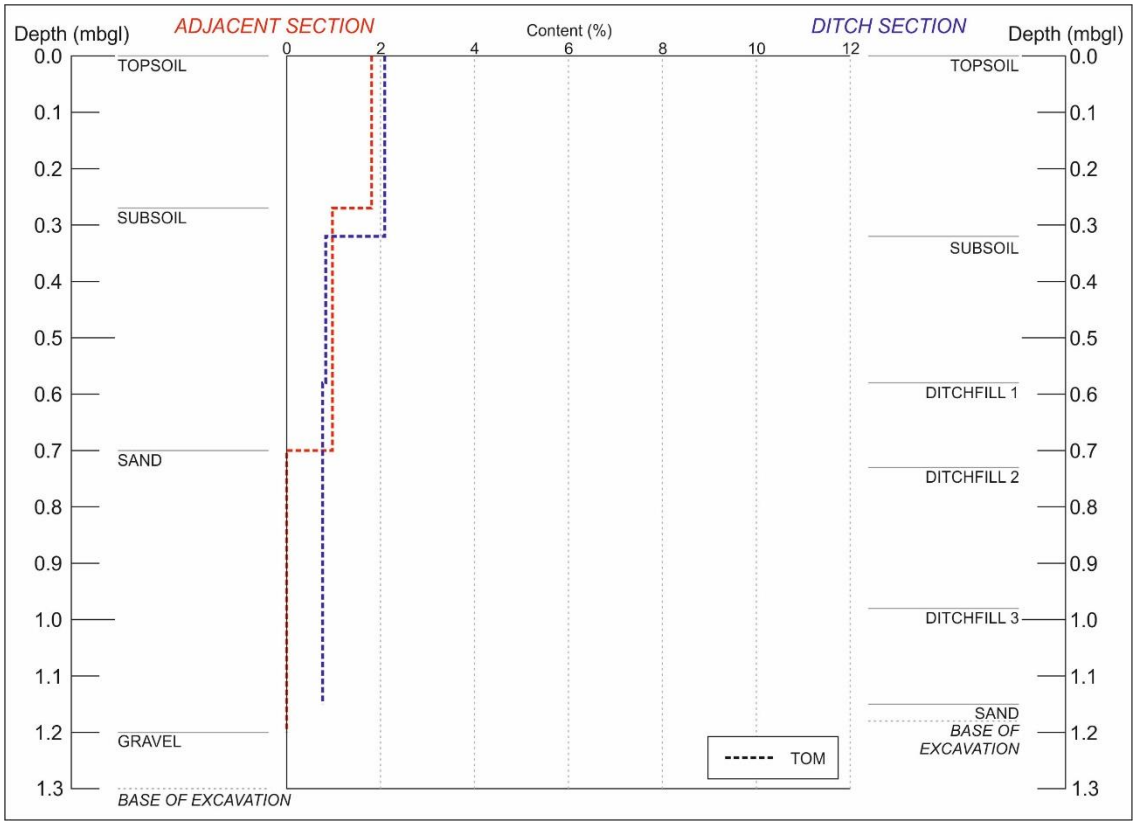

Figure 5.9(cont.) Results of testing for organic matter by the loss on ignition method for the AS and DS.

(d) DPF

5.4 SECTION COMPARISONS

5.4.1 CQF

There were no significant differences between the AS and DS in density or PSD. Perhaps the most noticeable geotechnical difference between the two sections was in plasticity. At the Ditchfill 1 level, the *PI* of the soil was 11% less in the DS than the AS, and ditch soils were more similar with the topsoil than the adjacent Clay 1. At the Ditchfill 2 level, the *PI* was greater in the DS than in the adjacent Clay 2 soil, with the ditchfill being more similar to Clay 1. Organic contents were higher in the ditch than in the adjacent clay soils.

5.4.2 CCC

Comparisons between the sections at CCC was not possible. The presence of limestone in the AS ruled out testing using soil classification methods.

5.4.3 DCF

At DCF, the most notable difference between the sections was the dry density of the soils. Between 0.50mbgl and 0.75mbgl Ditchfill 1 was up to 0.35 Mg/m^3 less than the adjacent Clay 1. At this level, particle densities were also lower but by a lesser magnitude, indicating a difference in the porosity of the soils. The PSD was similar at all depths, and differences in plasticity parameters were negligible where comparable at the ditch level.

5.4.4 DPF

The dominating difference at DPF is the PSD. The AS contained much higher proportions of gravel and sand than the ditchfills, which had higher silt and clay contents. Differences in plasticity and particle density were small at all depths.

5.5 CHAPTER SUMMARY

This chapter has presented the results of geotechnical characterisation of the soils retrieved from the DART research sites. The density (dry and particle), PSD, plasticity and organic properties of the soils in vertical sections both through and adjacent to the buried ditch features has been determined and compared. This fulfils Objective 3 of this study. A summary of all the results is given in Table 5.1.

The results have a significant finding related to the use of LD for determination of PSD. The LD method has advantages over the SH method: smaller sample sizes are required; many readings can be taken in less time. However, comparison of the results from the

SH method and the LD method showed that there were significant differences in the values obtained. In the case of the soils in this study, results of percentages within the silt and clay fractions using the LD method are not considered representative of results tested to the British Standard. In later analysis, it is suggested that database soil data can be used for inputs into hydrogeological models. If these databases include PSD data from LD methods, the results may incur error.

The geotechnical soil properties of CCC could not be compared due to the presence of rock. Of the other three research sites, the dominating differences at CQF were found to be plasticity, at DCF it was density and porosity, and at DPF it was PSD.

The resulting data have been used in the next chapter as inputs into a model to determine the differences in the soil water characteristics through and adjacent to the buried ditch features.

Table 5.1 Summary of the results of the geotechnical characterisation

	Soil Horizon	Depth m	Dry Density Mg/m^3	Particle Density Mg/m^3	Gravel %	Sand %	Silt %	Clay %	Plastic Limit	Liquid Limit	Plasticity Index	Organic Matter %
CQF	AS	Topsoil	0.00-0.35	1.60	2.66	5.6	19.7	34.2	40.4	27	54	27	3.7
		Clay 1	0.35-0.55	1.64	2.73	1.6	18.7	32.2	47.5	20	56	36	1.3
		Clay 2	0.47-1.10 (base unproven)	1.73	2.73	12.4	18.6	33.8	35.2	21	47	26	<0.35
	DS	Topsoil	0.00-0.35	1.67	2.64	4.4	14.8	40.8	40.0	25	51	26	3.0
		Ditchfill 1	0.35-0.60	1.68	2.61	2.1	18.6	35.1	44.3	23	48	25	2.7
		Ditchfill 2	0.60-0.75	1.69	2.66	11.9	21.1	31.3	35.7	24	55	31	2.7
		Clay 2	0.75-1.05 (base unproven)	1.84	2.75	23.4	13.3	29.7	33.5	19	44	25	<0.35
CCC	AS	Topsoil	0.00-0.30		2.62	32.1	7.0	55.5	5.3	32	57	24	4.3
		Completely Weathered Limestone	0.30-0.40										
		Highly Weathered Limestone	0.40-0.70										
		Moderately Weathered Limestone	0.70-1.00 (base unproven)										
	DS	Topsoil	0.00-0.30	1.37	2.57	27.9	7.4	56.4	8.3	31	58	27	4.1
		Ditchfill 1	0.30-0.55	1.47	2.57	33.7	8.1	40.6	17.6	30	55	26	3.6
		Ditchfill 2	0.55-0.70		2.54	35.2	7.1	35.5	22.2	30	56	27	3.6
		Ditchfill 3	0.70-1.00		2.55	65.7	3.7	17.5	13.1	27	57	30	3.6
		Moderately Weathered Limestone	1.00-1.10 (base unproven)										0.5
DCF	AS	Topsoil	0.00-0.28	1.56	2.52	5.5	22.4	49.8	22.4	22	48	25	2.8
		Subsoil	0.28-0.42	1.66	2.65	2.9	20.5	43.7	32.9	21	47	26	
		Clay 1	0.42-0.77	1.86	2.73	7.8	19.3	46.6	26.2	18	40	22	1.4
		Clay 2	0.77-1.00 (base unproven)	1.85	2.70	5.2	13.3	48.1	33.4				0.6
	DS	Topsoil	0.00-0.30	1.62	2.64	7.0	21.7	49.9	21.4	26	52	26	2.7
		Subsoil	0.30-0.50	1.68	2.62	11.0	19.6	45.8	23.6	22	46	24	
		Ditchfill 1	0.50-0.86	1.61	2.61	8.6	16.3	50.0	25.1	20	41	21	2.0
		Ditchfill 2	0.86-1.03	1.58	2.65	6.6	15.9	44.2	33.3	21	44	23	2.0
		Clay 2	1.03-1.15 (base unproven)	1.85	2.71	15.3	13.9	41.1	29.7	18	40	22	0.6
DPF	AS	Topsoil	0.00-0.27	1.67	2.60	10.7	42.1	35.8	11.3	18	31	13	1.8
		Subsoil	0.27-0.70	1.65	2.58	11.1	38.7	38.7	11.5	16	25	10	1.0
		Sand	0.70-1.20		2.69	32.2	48.1	13.3	6.5	16	26	10	<0.35
		Gravel	1.20-1.30 (base unproven)										<0.35
	DS	Evaporative Layer	0.00-0.32	1.57	2.61	5.6	38.8	38.9	16.7	17	30	13	2.1
		Subsoil	0.32-0.58	1.82	2.63	12.8	27.8	41.6	17.8	15	27	12	0.8
		Ditchfill 1	0.58-0.73	1.60	2.66	18.1	33.0	36.7	12.2	17	27	10	0.8
		Ditchfill 2	0.73-0.98	1.31	2.66	17.4	32.9	40.3	9.4	17	28	10	0.8
		Ditchfill 3	0.98-1.15	1.66	2.67	12.5	34.9	42.0	10.5	16	24	8	0.8
		Sand	1.15-1.20 (base unproven)			32.2	48.1	13.3	6.5	16	26	10	<0.35

CHAPTER 6. MODELLING SOIL WATER CHARACTERISTICS

6.1 INTRODUCTION

The aim of this chapter is twofold. Firstly, two analyses have been made using data acquired from site investigation and monitoring: the determination of the mechanisms of appearance of cropmarks by a comparison of the soil water in the AS and DS; and the relationship of SMD to cropmark appearance. The second aim is to determine whether the results of these two analyses can be reproduced using progressively less measured data, replacing costly data acquisition methods with desk study information.

The analysis of both the mechanisms of cropmark appearance and the relationship of SMD to cropmark appearance require definition of the term "cropmark appearance". The chapter begins by introducing a grading system of how cropmarks appear visually. The newly defined system is presented in Section 6.2.

Before addressing the data analyses, an empirical method was required to determine the SWCC of site soils for conversion of VWC to suction. An assessment of empirical methods has been included in Appendix B. From this assessment it was concluded that the method presented by Saxton and Rawls (2006) (SR method) was appropriate for use in the case of this research.

Section 6.4 presents the results of the two analyses using measured data, with some empirical calculations. The first analysis is a comparison of the difference in suction between the AS and DS, and the appearance of the cropmark, to determine, where possible, the mechanisms of appearance. The second analysis compares the background SMD and the appearance of the cropmark to determine the more general conditions in

which cropmarks appear. A detailed method is provided along with the results and discussion for each analysis.

The remainder of the chapter is focused on determining whether using simulated data and database inputs in place of measured data can reproduce the results of the two analyses. The first step was to model the VWC determined by the TDR data from the monitoring stations. The SPAW (Soil Plant Air Water) model, based on the empirical SWCC equations used for conversion of VWC to suction, was chosen for this process. It uses data inputs in three categories: soil data, which could be obtained from the geotechnical characterisation; crop data, which was supplied by the landowner (the Cirencester research location only); and weather data, which was measured by the weather stations at each research site. The structure, inputs and outputs of the SPAW model are described in Section 6.5.

To assess if the SPAW model was able to reproduce the VWC and SMD calculated from TDR, it was tested using a sub-set of data. This test revealed inconsistencies in the output data, which was investigated using a sensitivity analysis (Section 6.6). Although the cause of the inconsistency was identified, it could not be corrected in the model computation. A method of correcting the results to compensate for the inconsistency was found for the tested subset of data. The refinement of the model is presented in Section 6.7.

The refined model was found to be unable to reproduce results using measured data with enough accuracy for analysis of the comparison of sections, and hence for determination of the mechanisms of cropmark appearance. However, in the tested case, the model was able to give results which could be used for analysis of background SMD with cropmark appearance. The model was applied to datasets from the research sites where possible.

The model output was tested against using database values to replace the measured soil, crop and weather inputs into the SPAW model. Using these inputs to reproduce the model output would negate the need for any intrusive investigation, with all data from desk study sources. Section 6.8 presents the results of this analysis.

6.2 A GRADING SYSTEM FOR CROPMARK APPEARANCE

Analyses throughout this study include comparison of datasets with "cropmark appearance". The concept of cropmark appearance is subjective and is difficult to measure. It was necessary to define a grading system whereby a value can be applied to the visual appearance of the crop over a known buried feature. A simple method where cropmark appearance can be given one of three grades has been derived. The definitions of the grades "not visible", "indicative" and "mappable" are given below.

Not Visible

There is no indication of any cropmark.

Indicative

A cropmark is present but indistinct. For example, the cropmark may be noticed if the observer is searching a specific location where a buried feature is known to be present, whereas the cropmark may not be apparent to a prospective observer with no knowledge of the feature.

Mappable

A cropmark which is easily visible and would reveal the geographical location of an underlying buried feature to a prospective observer.

Three examples of these grades are shown in Figures 6.1(a-d), 6.2(a-d) and 6.3(a-d).

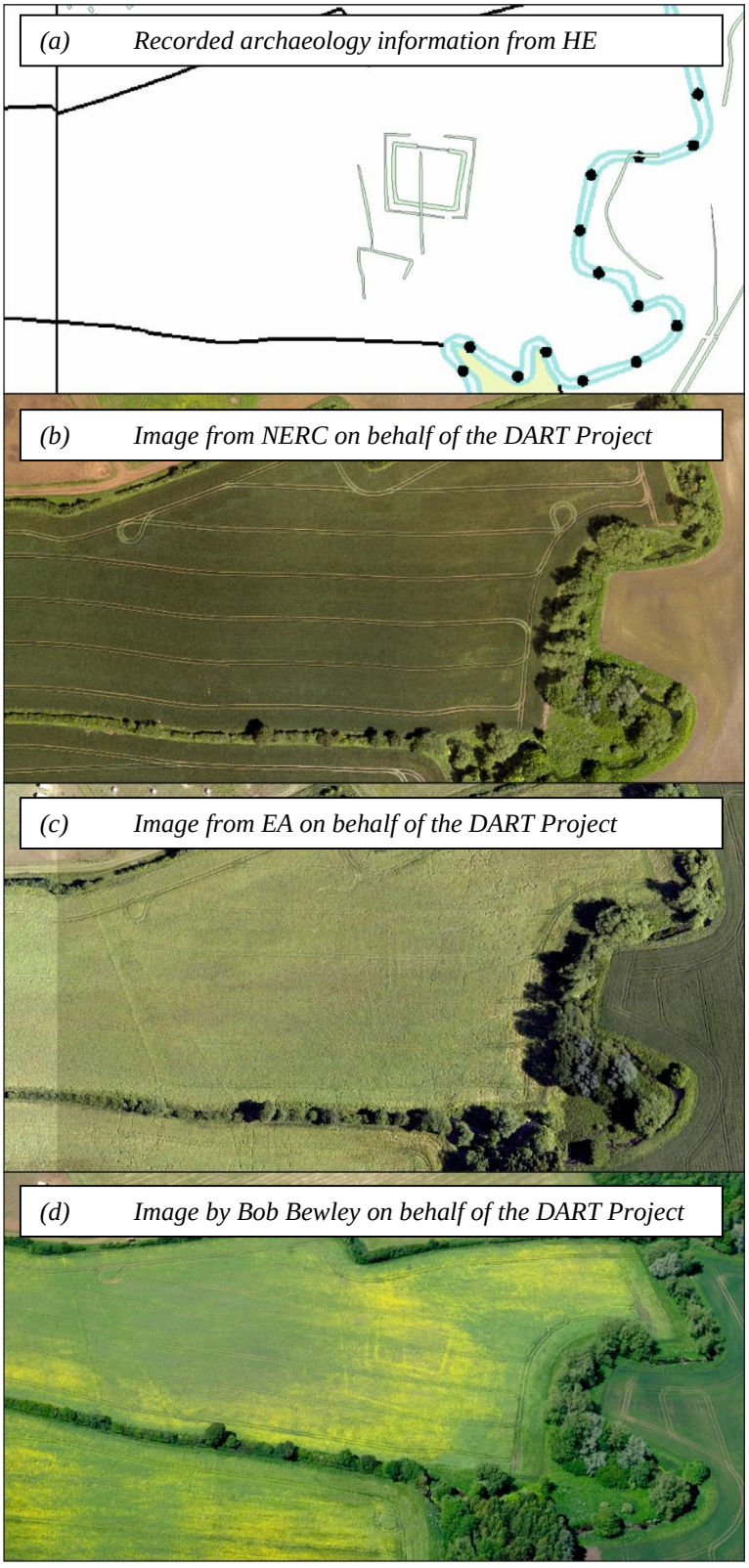

Figure 6.1 Example of grading levels of cell appearance.

(a) Location of recorded archaeology features
(b) Not visible (c) Indicative (d) Mappable

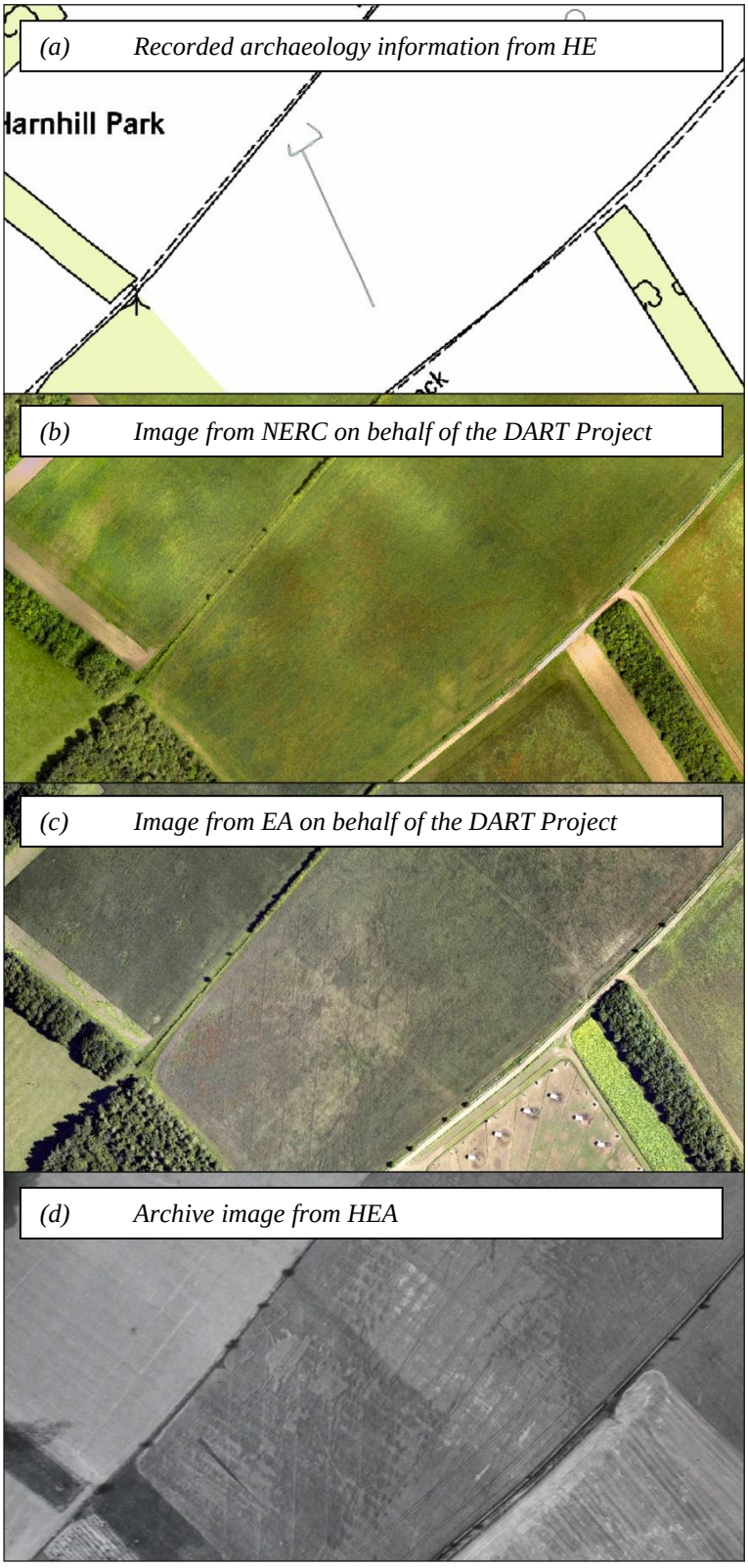

Figure 6.2 Example of grading levels of cell appearance.

(a) Location of recorded archaeology feature
(b) Not visible (c) Indicative (d) Mappable

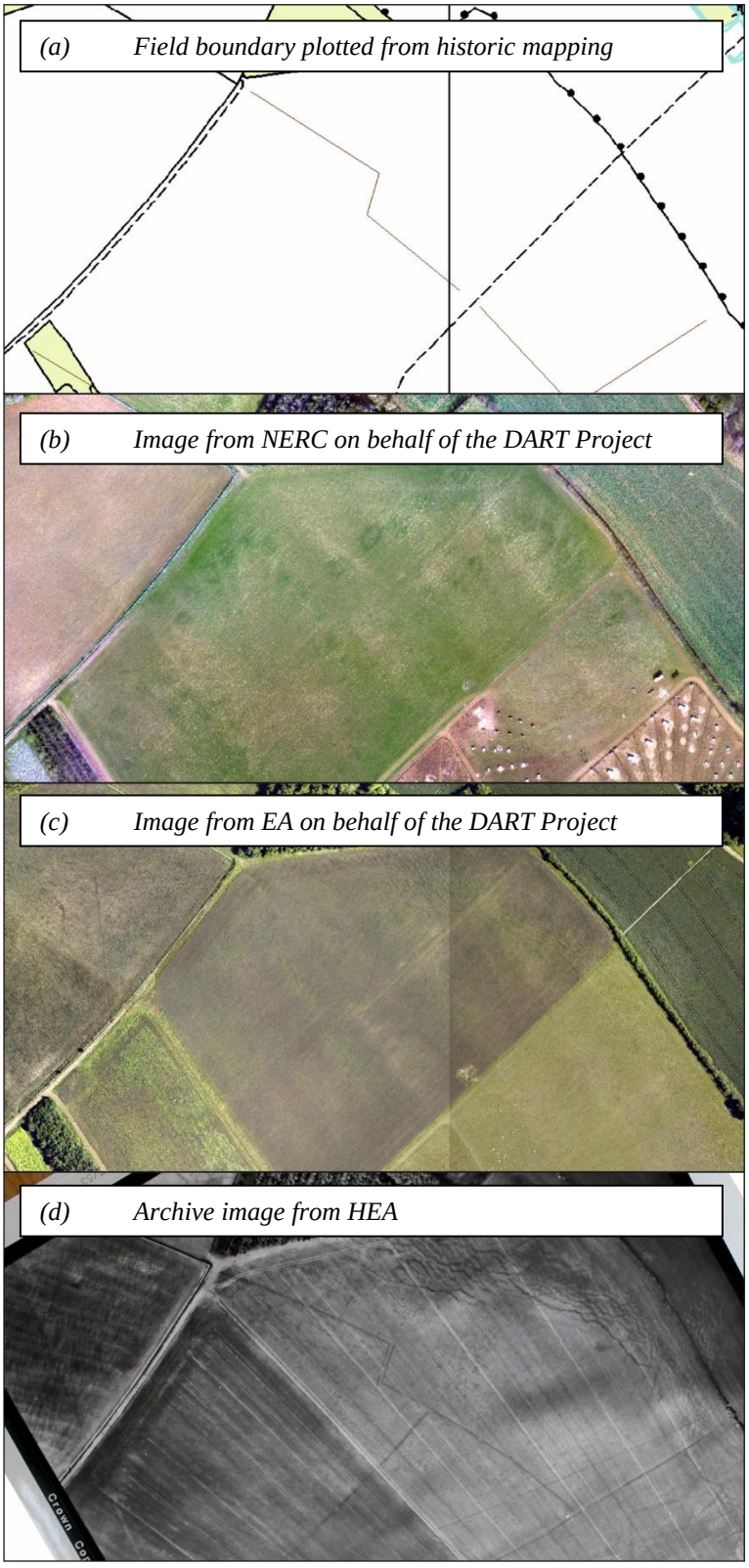

Figure 6.3 Example of grading levels of cell appearance.

(a) Location of field boundary feature
(b) Not visible (c) Indicative (d) Mappable

Aerial images of the research sites taken during the monitoring period were reviewed and a grade applied to the appearance of the cropmark. The resulting dataset was a dated grade of appearance for each of the research sites for use in the two analyses (section comparisons and background SMD).

6.3 DATA DEFINITIONS

This section defines the terminology of the data used for analysis in this section.

Cropmark Appearance

The grade of appearance of a cropmark at a known date (see Section 6.2).

Measured Soil Data

The soil data inputs for empirical calculation of the SWCC and modelling of VWC were obtained from the geotechnical characterisation. The parameters used are taken from testing of PSD, density and organic matter.

The gravel content, *R*, and sand content, *S*, were assigned values based on the results of sieve testing, and clay content, *C*, as determined by hydrometer. The model is based on the Unified Soil Classification System (USCS) where the PSD does not include gravel, but considers the soil as a matrix of particles below 2mm diameter with gravel inclusions. This differs from the BSI classification system used for geotechnical testing. Therefore, values of *S* and *C* for each soil horizon as determined by laboratory testing were adjusted accordingly to compensate for this difference. *R* was not changed. These PSD parameters have been expressed as a decimal percentage throughout.

The organic matter content *OM* was assigned values as determined by external laboratory testing and are expressed as a percentage.

The empirical method requires values for the dry density of the matrix (the fraction of soil <2mm), ρ_m. This could not be determined by laboratory testing, though results were available for dry density, ρ_d, where undisturbed samples could be retrieved. The assumption that $\rho_m = \rho_b$ has been made.

TDR VWC

The monitoring stations at each of the research sites recorded hourly TDR waveforms for each of the buried probes. The permittivity of the soil was determined from the waveform response of the TDR, and was converted to VWC using the Topp equation (Topp et al., 1980). The VWC of all probes located within a single soil horizon in sections through and adjacent to the buried ditch features were averaged to give a single hourly value. This data was then averaged to give daily values. This process was carried out by Dan Boddice (University of Birmingham) as part of the DART Project. This acquisition of VWC data is outside the scope of this study but the process of obtaining data from TDR monitoring and relevant VWC calculations are covered extensively in Boddice (2014).

TDR SMD

The SMD calculated from TDR VWC. The calculation also requires FC, empirically calculated from measured soil data using the SWCC.

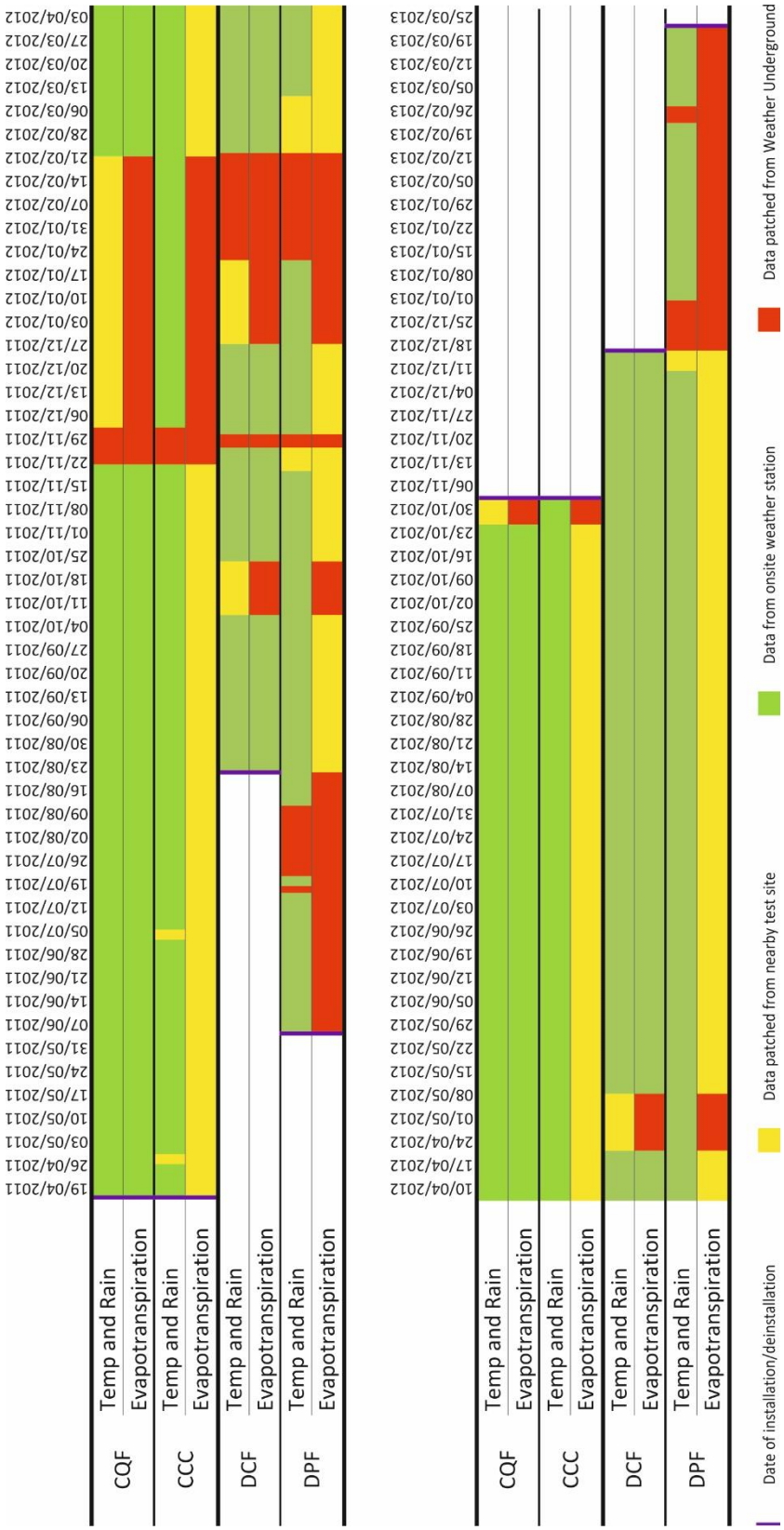

Figure 6.4 Sources of weather data throughout the monitoring period at each test site.

Measured Weather Data

The weather stations at the research location recorded half hourly readings of minimum, maximum and average temperatures, and rainfall. One station at each research location had a solar radiation sensor (CQF and DCF). For these stations, evapotranspiration is calculated internally using a modified version of the Penman-Monteith equation (Davis Instruments, 2001). For the research sites where there was no solar radiation sensor (CCC and DPF), values of evapotranspiration were taken from the other station at the research location. Where gaps in the data occurred due to temporary failure of one of the stations at a test location, the data was patched using the other nearby station. At times where both stations at a location failed, data was patched from the nearest station data available (IGLOSCIR1 for Cirencester, and ICENTRAL25 for Diddington) from Weather Underground (The Weather Channel, 2012). Figure 6.4 shows the data sources for the duration of the monitoring period (data patches with a duration less than 24 hours have not been included). All data were converted to daily totals or averages.

Known Crop Data

The RAU (landowner) provided crop data for the CQF and CCC test sites, comprising the crop type, dates of drilling (planting) and dates of harvest for the duration of the monitoring period. This information was not available for the sites at Diddington (DCF and DPF).

6.4 ANALYSIS USING MEASURED DATA

6.4.1 Section Comparisons

6.4.1.1 Method

This section determines the differences in soil suctions between the AS and DS at each of the research sites to increase understanding of the mechanisms of formation of cropmarks. It uses TDR VWC and converts the results to suctions for comparison. The suctions and differences between sections are plotted throughout growing seasons for the research sites and have been analysed in conjunction with cropmark appearance.

Four datasets have been analysed with the start and end date of each determined by crop rotations and the extent of the monitoring period, hereafter known as a growing season.

1. CQF 2011, stretching from the 20th April 2011 (after installation of the monitoring station) to the 31st July 2011 (post-harvest of the crop). This growing season has a crop of winter wheat, which was drilled in the autumn of 2010, before monitoring began.
2. CQF 2012, stretching from the 14th March 2012 (the date of drilling of spring wheat) to 12th September 2012 (post-harvest of the crop).
3. DCF stretching from 25th August 2011 (shortly after the drilling of winter wheat) to 25th June 2012 (before the harvest of the crop). The dates of drilling and harvest were unavailable for this research site. The last aerial image was taken on the 20th June 2012, which indicated the crop had not been harvested before the end of the analysis period.
4. DPF, stretching from 9th June 2011 (after installation of the monitoring station) to 19th June 2012 (the last time the research site was imaged).

The CCC research location comprised weathered rock in the AS. It was therefore not possible to insert probes into the section and no TDR VWC data could be provided. As such, no analysis could be carried out.

The sections were compared at two (DCF and DPF) or three (CQF) depth levels bounded at the base by a rooting depth dependent on the type of crop.

1. Above the ditch. The soil from the ground surface to a level at the upper extent of the ditchfills. At this depth soils in the AS and DS sections are similar, comprising topsoils homogenised by ploughing, and in some cases continuous subsoils deposited since the infilling of the ditch.
2. The ditch level. The depth of soil from the top of the ditchfills to base of the ditch (CQF and DCF) or to 1.0m (DPF). At DPF, where there is permanent pasture, although the ditchfills extend deeper the 1.0m limit is applied as it is equal to the maximum depth of AWC (available water capacity) for grass, as used for calculation in the MORECS model (Hough and Jones, 1997). This level directly compares the differences where ditchfills are adjacent to the undisturbed soil.
3. Below the ditch, from the base of the ditch to a maximum depth of 1.2m. This is only applicable to CQF. The 1.2m limit is equal to the maximum depth of AWC for wheat, as used for calculation in the MORECS model (Hough and Jones, 1997). No probes were inserted vertically below the ditch at DCF, therefore no data were available for the DS and no comparison with the AS is possible.

The daily TDR VWC in each of the soil horizons was converted to suction, Ψ, using the SR method (Appendix B) with soil inputs as determined by the geotechnical characterisation. The SWCC has a semi-logarithmic relationship where suctions are plotted on a log scale against normal VWC. To allow for this relationship, the sections

have been compared as the logarithm base 10. The calculations below give an idea of the ranges of Log suctions.

Field capacity	Ψ = 33 kPa	$Log_{10}\Psi$ = 1.52
Permanent wilting point	Ψ = 1500 kPa	$Log_{10}\Psi$ = 3.18

To compare each depth level in the section, a weighted average of $Log_{10}\Psi$ was calculated using Equation 6.1, based on the thicknesses of the soil horizons present within the level, to give a single value. The resulting dataset is therefore a daily value of $Log_{10}\Psi$ for each level within each section.

$$Log_{10}\Psi_j = \frac{\sum_{l=1}^{n}\left[T_l \times Log_{10}\Psi_{j(l)}\right]}{\sum_{l=1}^{n} T_l} \qquad [\ 6.1\ ]$$

Where Ψ_j is the suction at time j (kPa)
$\Psi_{j(l)}$ is the suction of layer l at time j (kPa)
T_l is the thickness of layer l (cm)
and n is the number of layers

The $Log_{10}\Psi$ of the AS and DS throughout each growing season has been compared with cropmark appearance.

6.4.1.2 Results

Figures 6.5(a-e), 6.6(a-e), 6.7(a-d) and 6.8(a-d) show the results of this analysis for CQF 2011, CQF 2012, DCF and DPF respectively.

Figure 6.5(a) gives the plot of $Log_{10}\Psi$ calculated from TDR VWC in the AS and DS above the ditch level (0-350mm bgl) for CQF 2011. There are periods during the growing season where data is missing, this is due to temporary failure of the monitoring stations

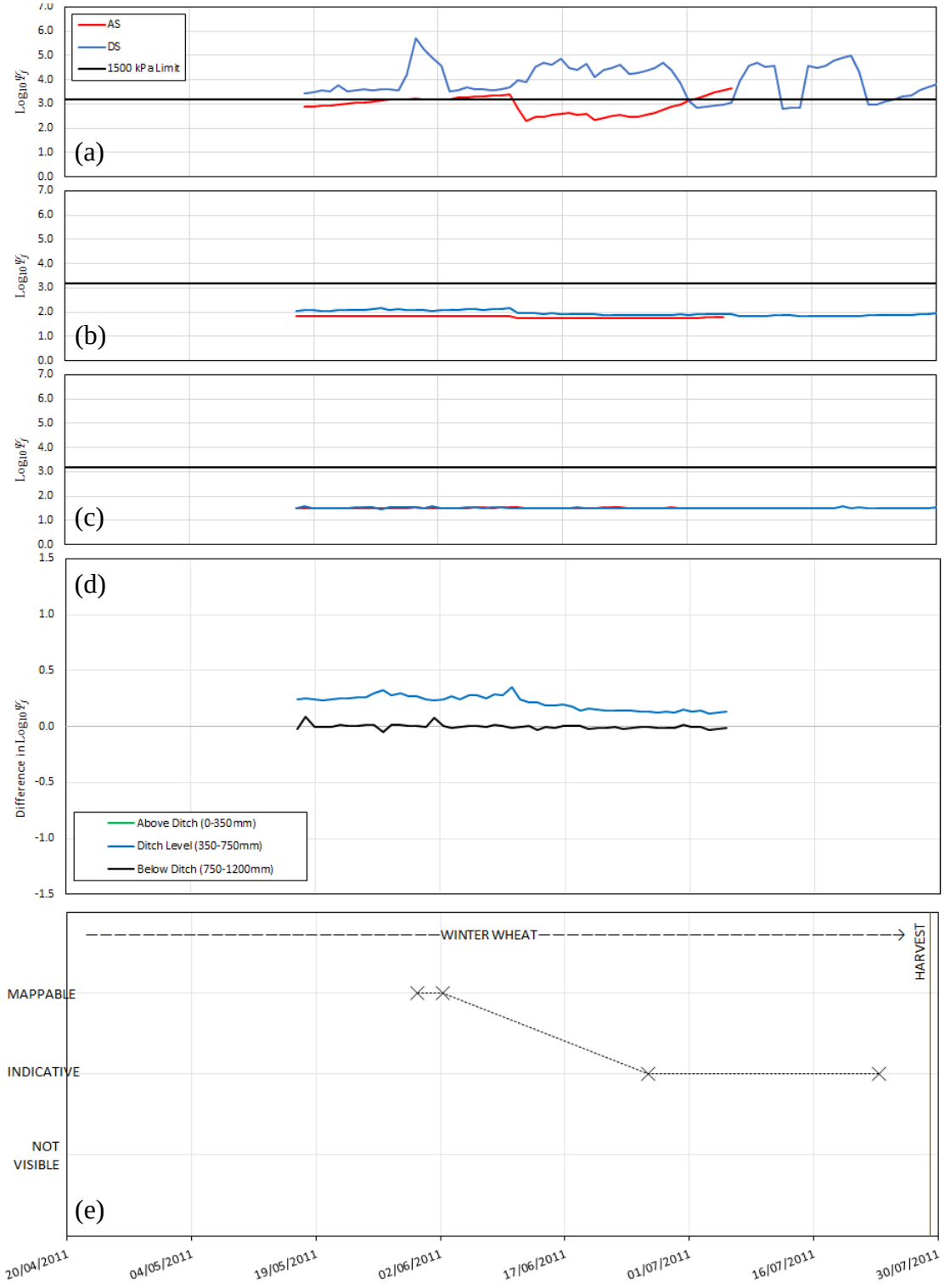

Figure 6.5 Results of comparison of suctions between the AS and DS for the CQF 2011 growing season.

(a) Suctions at the level above the ditch (b) Suctions at the ditch level

(c) Suctions at the level below the ditch (d) Difference in suctions

(e) Cropmark appearance

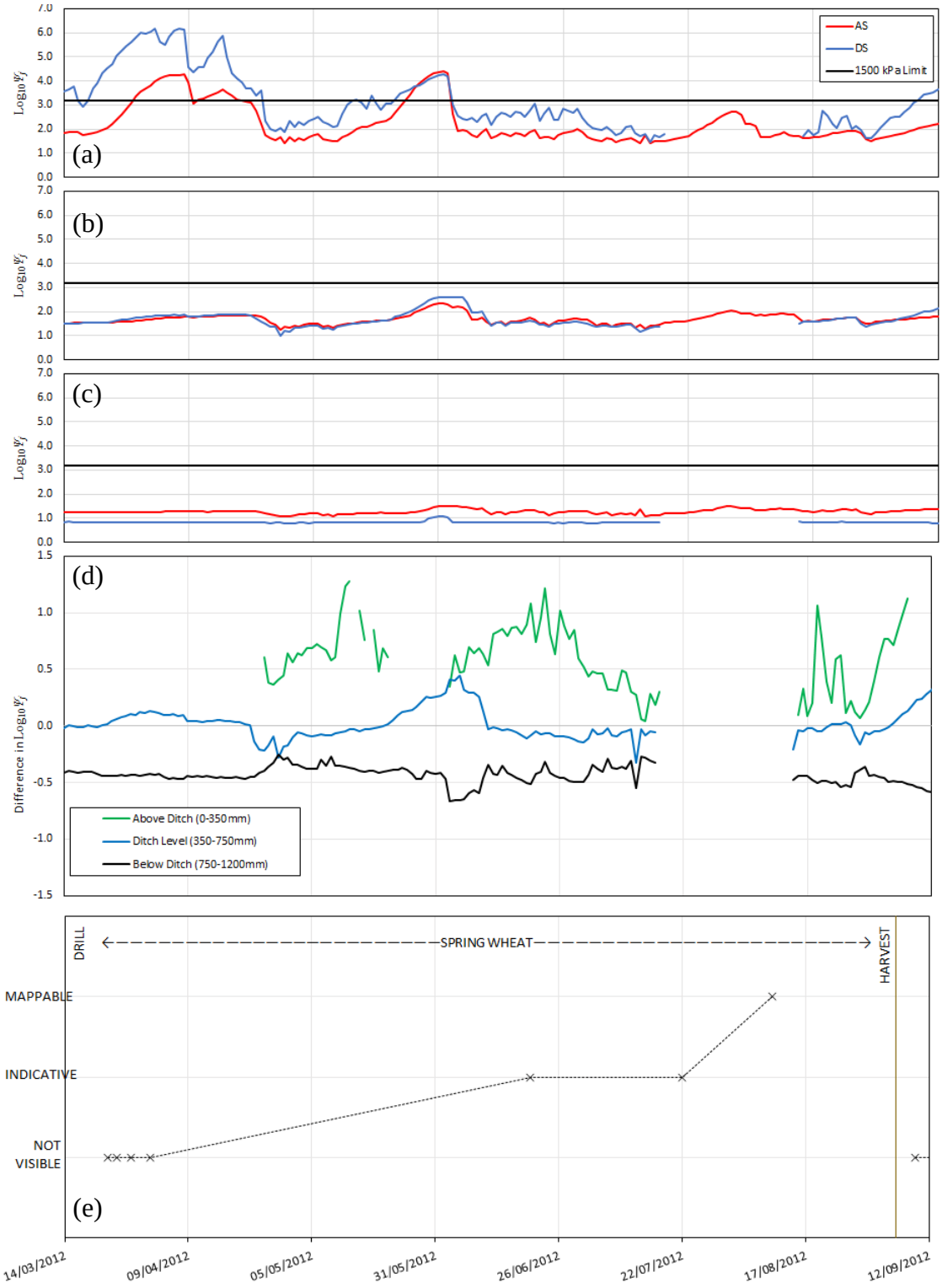

Figure 6.6 Results of comparison of suctions between the AS and DS for the CQF 2012 growing season.

(a) Suctions at the level above the ditch (b) Suctions at the ditch level

(c) Suctions at the level below the ditch (d) Difference in suctions

(e) Cropmark appearance

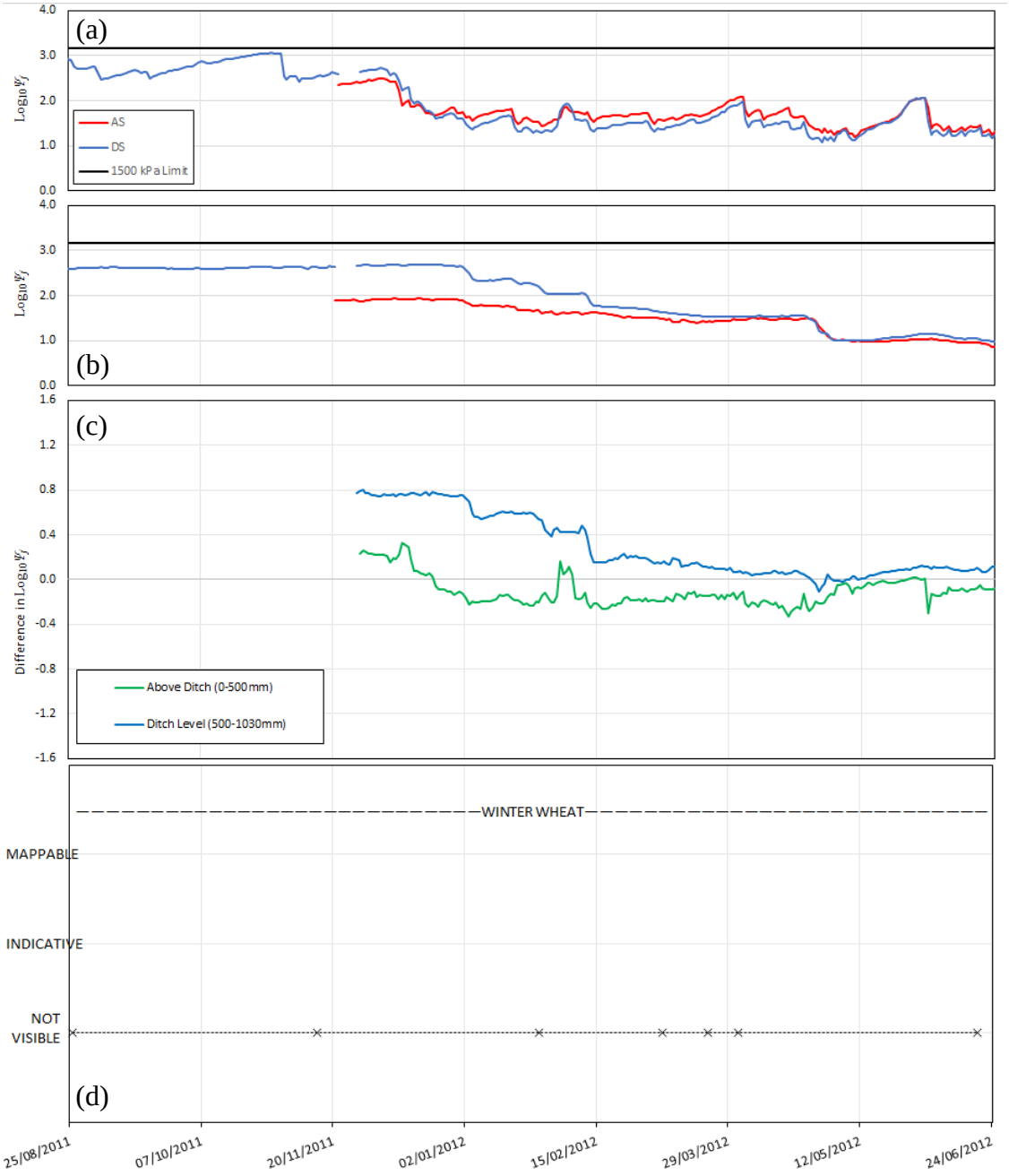

Figure 6.7 Results of comparison of suctions between the AS and DS for the DCF growing season.

(a) Suctions at the level above the ditch (b) Suctions at the ditch level

(c) Difference in suctions (d) Cropmark appearance

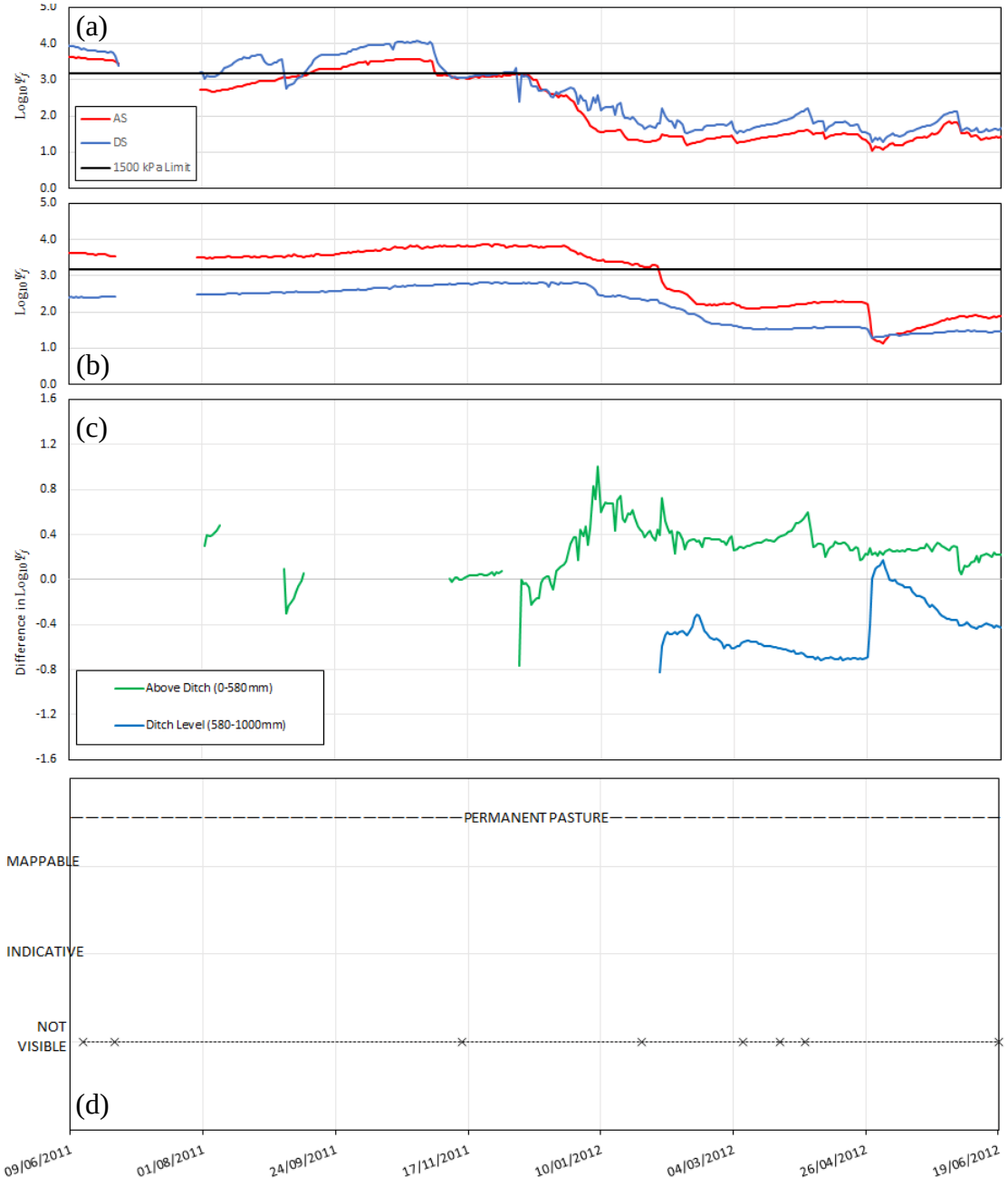

Figure 6.8 Results of comparison of suctions between the AS and DS for the DPF growing season.

(a) Suctions at the level above the ditch (b) Suctions at the ditch level

(c) Difference in suctions (d) Cropmark appearance

(for information see Boddice, 2014). The plot also includes a 1500 kPa limit at $Log_{10}\Psi = 3.18$. The SR method does not provide a calculation method where suctions are greater than 1500 kPa. Where $Log_{10}\Psi < 3.18$, the results have been calculated using the SR method for suctions between 33 and 1500 kPa. This gives an indication of high suctions above this limit: however, any comparison of the differences between the sections at times when either section is at this threshold would not be valid. Figures 6.5(b-c) give the equivalent results for the ditch level (350-750 mmbgl) and below the ditch level (750-1200 mmbgl).

Figure 6.5(d) plots the differences in $Log_{10}\Psi$ between the AS and DS at each of the levels. This comparison in not possible where TDR VWC data is missing or $Log_{10}\Psi > 3.18$ in either section. In the case of CQF 2011, no comparison can be made at the above ditch level.

Figure 6.5(e) gives information on the crop and cropmark appearance.

Figures 6.6(a-e), 6.7(a-d) and 6.8(a-d) give the equivalent data for CQF 2012, DCF and DPF respectively. Although DCF and DPF are not compared below the ditch level.

6.4.1.3 Discussion

Figures 6.5(a-c), 6.6(a-c), 6.7(a-b) and 6.8(a-b) show that there are much greater fluctuations in $Log_{10}\Psi$ at the level above the ditch than there are at deeper levels. This is to be expected as losses and gains of water in the deeper soils is only through redistribution and transpiration, whereas surface soils are also subject to water exchange with the air from rainfall and evaporation.

Drying of the surface soils causes suctions to exceed the 1500kPa limit of the SR method at times throughout the monitoring period in both the AS and DS during both growing

seasons at CQF (Figures 6.5(a) and 6.6(a)). During the CQF 2011 growing season no comparison can be made for the level above the ditch as $Log_{10}\Psi$ does not drop below the limit for both the AS and DS (Figures 6.5 d)). The other three growing seasons all have times where the above ditch level are comparable. Figure 6.6(d) shows that, for the CQF 2012 growing season, Δ $Log_{10}\Psi$ fluctuates between 0.04-1.28. Figure 6.8(c) shows that the DPF growing season also has wide range of Δ $Log_{10}\Psi$, fluctuating between -0.80 and 1.00. These differences at these above ditch levels are generally greater than seen at the deeper levels and may contribute to differential growth of the crop; however, the spatial variability of water content in the surface soils may also contribute to this high fluctuation.

Röver and Kaiser (1999) studied the spatial heterogeneity in plough soils over a 63x60m area. On two dates, 81 samples were taken at 7m intervals in a grid pattern. The plough soil was found to have a variability in GWC of up to 4.3%. The daily GWC of the topsoil at each of the research sites throughout the full monitoring periods (not limited to the growing seasons) was calculated from VWC measured by TDR and dry density values from the geotechnical characterisation. The difference in GWC between the AS and DS was found to have median values of 3.3%, 2.2% and 0.5% for CQF, DCF and DPF respectively. At CQF differences in GWC were above the 4.3% natural variation as determined by Röver and Kaiser (1999) on 28% of days. At DCF this difference was only exceeded on 5% of days, and never at DPF. Therefore the differences were typically within the range of natural variation of the plough soil.

Although the water content (and therefore suctions) in the soils will be affected above the ditch level by differences in the redistribution of water in the AS and DS, natural spatial variation of the topsoil water content may mask differences in $Log_{10}\Psi$ that are

directly due to the different soil water characteristics of the feature and adjacent soils at the ditch level.

Differential growth resulting in a cropmark are due to the presence of the feature soils, and as such, a comparison of differences at the ditch level where adjacent soils differ not only from natural variation could be expected to have the greatest influence in the appearance of cropmarks.

Soils at the ditch level were, at times, comparable for all growing seasons although monitoring station failure caused gaps in the data. The 1500 kPa limit of the SR method was exceeded in the AS for the majority of the DPF growing season (Figure 6.8(b)), with only the latter part being comparable.

Although the ditch level is expected to have the greatest influence on cropmark appearance, where the soils below the ditch are within the maximum rooting depth (1200mm for wheat), as they are at CQF, soils below the ditch level may also influence crop growth. Below the ditch level, in CQF 2011, differences in suctions between the AS and DS remained >±0.10. During CQF 2012, suctions directly below the ditch were consistently >0.20 lower than in the adjacent soils where the sections could be compared. One explanation for this difference between the CQF 2011 and CQF 2012 data is that the wet winter of 2011/2012 and the subsequent wet year may have caused water to become perched in the voids of the disused pipe at the base of the ditch increasing the VWC of the soils immediately below.

The following paragraphs discuss the results of the analysis for each growing season.

CQF 2011

The comparable data for CQF 2011 stretches for a total of 50 days from 17th May – 6th July, during which time, suctions are higher in the DS than the AS at the ditch level and differences in the soils below the ditch level are small ($\Delta \text{Log}_{10}\Psi$ <±0.10) (Figures 6.5(b-c)). From the beginning of this period to 15th June, the $\Delta \text{Log}_{10}\Psi$ is between 0.20 and 0.40. In this period a mappable cropmark was recorded twice, on the 31st May and 3rd June (Figure 6.5(e)). The images show the cropmark to be greener and darker than the surrounding area, indicating a positive cropmark, where there is enhanced growth above the feature compared with the surrounding area. Higher suctions in the feature soils would be expected to inhibit growth, resulting in a negative cropmark. A speculative explanation is that the reduced ability of the crop to access water at the ditch level results in roots growing deeper at a faster rate to fulfil the needs of the crop, gaining access to the soil water held at lower suctions (Figure 6.5(b-c)) below the ditch level earlier, although there is no evidence to support this. Confirmation of this theory would require monitoring of the crop rooting depth, which was outside the scope of both this research and the DART Project. This could be achieved by comparison with a control section where no crops are present, monitored by TDR, to quantify the water loss due to plant uptake at specific depths. After the 15th June, there are lesser differences of 0.10-0.20, where an image taken on 27th June recorded the cropmark as indicative.

CQF 2012

Four images taken in the early part of the CQF 2012 growing season (21st March – 3rd April) did not show any indication of a cropmark (Figure 6.6(e)). The crop, drilled

on the 14th March, had not reached emergence at this time and images taken on all four dates indicate bare soil.

The image taken on 20th June shows the cropmark at CQF as indicative (Figure 6.6(e)). The crop above the ditch appears greener than the surrounding crop, indicating increased growth and a positive cropmark. At this point, the $Log_{10}\Psi$ at the ditch level had been less in the DS than the AS for a total of 9 days, which would give crops easier access to water, possibly enhancing growth. However, prior to this, $Log_{10}\Psi$ was higher in the DS by up to 0.45 for 20 days, which could have inhibited comparative growth with the surrounding crop. Should this be the case a negative cropmark would be expected. However, at the level below the ditch $Log_{10}\Psi$ is less in the DS, possibly from perched water in voids from the disused pipe. Should the crop have access to this water, a positive cropmark would be expected. After this image date, suctions remained lower at both the ditch and below ditch level until a gap in the DS data, during which, the cropmark was again recorded as indicative (22nd July).

The cropmark was recorded as mappable on 10th August; however, this is during the gap in the DS data and comparison of the sections in the lead up to and at the time of imaging is not possible. An image taken after harvest on the 9th September did not record any visible cropmark; however as with the early 2012 images, no crop was present.

DCF

The analysis period for DCF is from 25th August 2011 to 25th July 2012, however comparison of the sections was only possible from 29th November, due to data gaps. Winter wheat, drilled in August 2011 was present on the site throughout the full analysis period, though no images taken recoded any indication of a cropmark.

Winter wheat is drilled in autumn and enters a stage of dormancy over winter where crops do not develop. This period can last for around 3 months, before growth resumes in spring. An image taken on 15th November 2011 did not show any indication of a cropmark (Figure 6.7(d)). Although there are high differences in $Log_{10}\Psi$ (>0.40) at the ditch level from December through to mid-February (Figure 6.7(c)), it could be expected that there would be no change in the crop until dormancy ends.

The 2012 astronomical spring began on the 20th March and images taken near this date (8th March, 23rd March and 2nd April) again showed no indication of a cropmark (Figure 6.7(d)). Although growth may have resumed at this point, the $\Delta Log_{10}\Psi$ may be too low to have caused differential growth, or the crop has not had time to respond to the differences. The $\Delta Log_{10}\Psi$ remained typically <0.10 until the final image was taken of DCF on 20th June 2012, the crop appears well developed, however, there is still no indication of a cropmark. No image was taken in the late summer where crops reach the latter stages of development and cropmarks are known to be most common.

DPF

DPF was in permanent pasture throughout the growing season and no images recorded any indication of cropmark (Figure 6.8(d)). $Log_{10}\Psi$ were above the limit of the SR method for the majority of the growing season and comparisons were not possible until 3rd February 2012 (Figure 6.8(c)), when $Log_{10}\Psi$ dropped below 3.18 in both the AS and DS. At this time the $\Delta Log_{10}\Psi$ at the ditch level was >-0.40 and remained below -0.30 until 28th April, where a sudden drop in the $Log_{10}\Psi$ of the AS after high rainfall reduced the difference (Figure 6.8(b)). Although the $\Delta Log_{10}\Psi$ was high

during the spring, pasture is known to be less visibly responsive unless very dry weather causes parching and plants become discoloured.

6.4.1.4 In Summary

Comparisons of suctions at the level above the ditch may be affected by the natural variation of water contents in the plough soil.

The CQF 2011 growing season recorded a positive cropmark which was, at times, both indicative and mappable. The comparison of suctions showed that $Log_{10}\Psi$ was higher in the DS at the ditch level, indicating that crops rooted in the feature would have more difficulty accessing water and a negative cropmark could be expected. However, although there may be explanations for this discrepancy relating to the rooting patterns of the crops, there is no evidence for the cause in the data available.

The CQF 2012 growing season also showed a positive cropmark which was, at times, both indicative and mappable. Where images recoded no visible cropmark, no crop was present above ground level and images were of bare soil. The cropmark was recorded as indicative at a time where the $Log_{10}\Psi$ in the DS had been significantly lower at the below ditch level, possibly from water in the voids remaining in the disused pipe.

The DCF growing season did not record any indication of cropmarks in the winter wheat. During a period of dormancy of the crop $\Delta\ Log_{10}\Psi$ were high, though at the time the crop resumed growth $\Delta\ Log_{10}\Psi$ was less.

The permanent pasture at DPF did not show any indication of a cropmark through the growing season, even though $\Delta\ Log_{10}\Psi$ were shown to be high, where comparable. Cropmarks are known to be less common on grasses, and extreme dry weather is need to stress the plants causing discolouration.

This analysis shows that monitoring of the water content in buried features and comparing them as $Log_{10}\Psi$ with the surrounding soils, and with aerial image data, can provide information on the appearance of cropmarks. Where data have allowed (at CQF), mechanisms of cropmark formation can be suggested. At DCF and DPF even though no indication of cropmarks were recorded, the data can still provide information on the conditions in which cropmarks do not form.

6.4.2 Cropmark Appearance and SMD

6.4.2.1 Method

This analysis compares the background SMD, represented by the AS data, with cropmark appearance.

Aerial surveyors plan flights using SMD over an area as an indicator of likely cropmark appearance. When SMD reaches above 50mm, cropmarks are expected to be more likely in areas of free-draining or shallow soils. At over 150mm cropmarks are expected to be more likely in soils which are clay-dominated. This section compares the SMD calculated from the TDR VWC data at each of the image dates with the appearance of the cropmarks at each of the research sites, where possible.

The SMD used by aerial surveyors represents an average over an area (40x40km square), therefore, it is the background SMD which is of importance. The composition of any features within this area is unknown. The AS at each site has been used to represent the background soils across an area near to the feature, generally corresponding to the geological unit, and all calculations have been applied to this section.

The SMD at time j, δ_j, is represented by Equation 6.2. This equation is true where SMD is positive; however, SMD cannot be negative. Where $\theta_j > \theta_{33}$, SMD is always given the value of 0mm.

$$\delta_j = [\theta_{33} - \theta_j] Z_r \qquad [\ 6.2\ ]$$

Where θ_{33} is the VWC at FC (33 kPa suction) (decimal percentage),
θ_j is the VWC at time *j* (decimal percentage),
and Z_r is the rooting depth (mm).

The Z_r for each of the sections was assigned as the maximum depth of AWC (Hough and Jones, 1997) for the crop present. Where the crop was wheat, this was 1200mm, and where there is permanent pasture, the rooting depth was 1000mm.

The FC of each of the soil horizons was determined from the SWCC where Ψ = 33 kPa, using the SR method, with soil inputs as determined by the geotechnical characterisation.

A weighted average VWC, θ_j, within the rooting depth was calculated using Equation 6.3.

$$\theta_j = \frac{\sum_{l=1}^{n} [T_l \times \theta_{j(l)}]}{\sum_{l=1}^{n} T_l} \qquad [\ 6.3\ ]$$

Where θ_j is the VWC at time *j* (decimal percentage),
$\theta_{j(l)}$ is the VWC of layer *l* at time *j* (decimal percentage),
T_l is the thickness of layer *l* (cm),
and *n* is the number of layers.

Similarly, a weighted average field capacity, θ_{33}, within the rooting depth was calculated using Equation 6.4.

$$\theta_{33} = \frac{\sum_{l=1}^{n} [T_l \times \theta_{33(l)}]}{\sum_{l=1}^{n} T_l} \qquad [\ 6.4\ ]$$

Where θ_{33} is the FC at time *j* (decimal percentage),
and $\theta_{33(l)}$ is the FC of layer *l* at time *j* (decimal percentage).

Substitution of Equations 6.3 and 6.4 into Equation 6.2 gives Equation 6.5.

$$\delta_j = \frac{\sum_{l=1}^{n} [T_l \times \theta_{33(l)}] - \sum_{l=1}^{n} [T_l \times \theta_{j(l)}]}{\sum_{l=1}^{n} T_l} \times Z_r \qquad [\ 6.5\ ]$$

Since $Z_r = \sum_{l=1}^{n} T_l$, the SMD, δ_j, can be simplified to Equation 6.6.

$$\delta_j = \sum_{l=1}^{n}\left[T_l \times \theta_{33(l)}\right] - \sum_{l=1}^{n}\left[T_l \times \theta_{j(l)}\right] \qquad [\ 6.6\ ]$$

The SMD of the background soil (AS) at each of the image dates was compared with cropmark appearance.

6.4.2.2 Results and Discussion

Figure 6.9 shows the TDR SMD at times when the cropmark was not visible, indicative or mappable at each of the sites. From the current knowledge, it would be expected that mappable cropmarks would be recorded at CQF and DCF only when high SMD of >150mm occurs. This is not the case: the three images which recorded the cropmark as mappable were taken at TDR SMD of 50mm or less. The SMD when the cropmark at CQF was indicative was always <40mm. When the CQF cropmark was not visible, TDR SMD reached 60mm, although the four images taken at TDR SMD between 20 and 60mm are all known to be on bare soil.

DCF did not display any indication of a cropmark at any of the image dates, although the crop was known to be present throughout the monitoring period. The range of TDR SMD at the image dates was from 0-50mm, which agrees with the current knowledge of likely cropmark appearance.

Although DPF is located on free-draining soils, where cropmarks are expected to appear at SMD of >50mm, there was no indication of a cropmark in grass where high TDR SMD of >100mm occurs. However, the site is in permanent pasture, which is known to be less visibly responsive to changes in water content, and therefore, suctions. In the field next to the DPF research site, also located on river terrace gravels, crop was present, and buried features were known to be present within 60m of the research site. The same

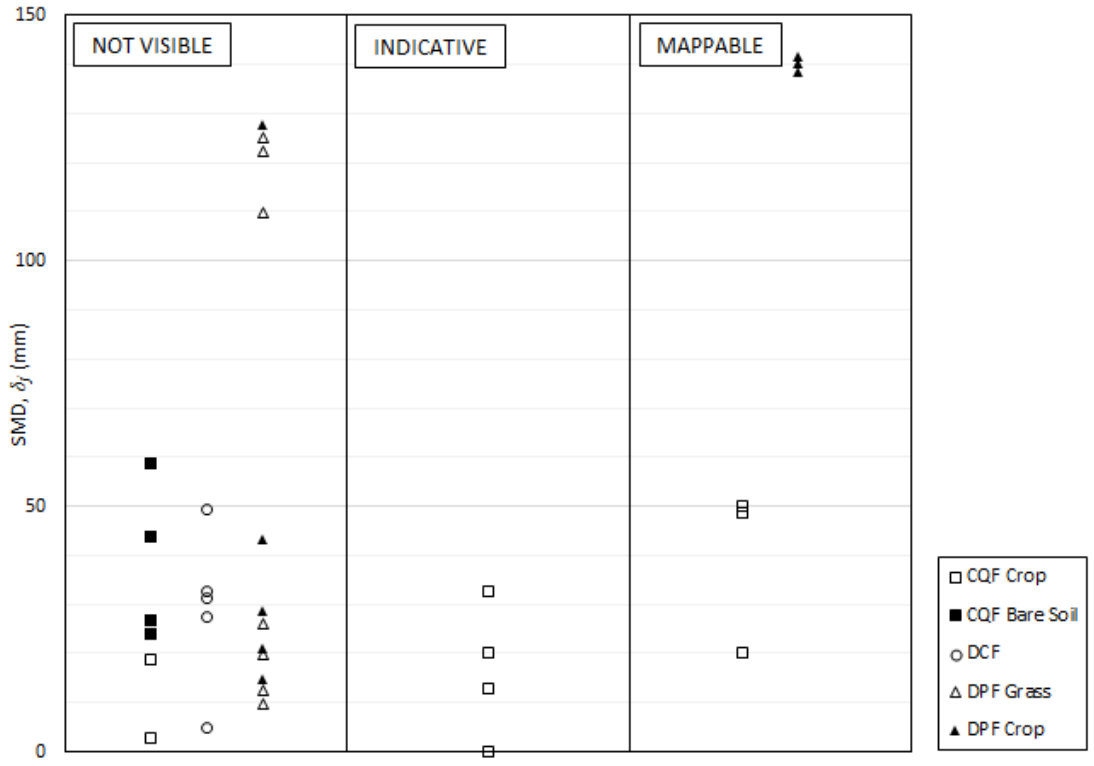

Figure 6.9 The appearance of cropmarks at CQF, DCF and DPF against TDR SMD.

analysis was applied to images taken of this field, using TDR SMD from DPF AS with a rooting depth of 1200mm. The results have been included in Figure 6.9 and show that three images taken at TDR SMD of approximately 140mm recorded a mappable cropmark. The cropmark was recorded as not visible on four occasions at TDR SMD of <50mm, and once at approximately 130mm. Noting that the assumption has been made that the VWC in the DPF AS represents the background VWC of the nearby cropmark, approximately 60m away, this is in general accordance with current knowledge.

This section has used measured data to assess the differences in suctions between the AS and DS, and the background SMD at times where the appearance of cropmarks could be graded. They have shown that monitoring the VWC of buried features and the background adjacent soils over a period can reveal information about both the mechanisms of appearance of cropmarks and the SMD at times when cropmarks are not

visible, indicative or mappable. The remainder of this chapter assesses whether using a model to simulate VWC, with soil, weather and crop inputs, can provide similar information. The following section describes the model and calculations used for this analysis.

6.5 THE SPAW MODEL

6.5.1 Application in this Study

The SPAW model was designed by the USDA (U.S. Department of Agriculture) Agricultural Research Service in cooperation with The Department of Biological Systems Engineering (Washington State University). The model was chosen for its simplicity in assessing vertical soil water budgets on a small scale, without the complication of lateral flow. It was designed for agricultural purposes and gives a variety of outputs relating to soil hydrogeology and soil chemistry as daily or monthly data, as well as the effect of hydrogeological regimes on crops, such as stress and yield. It also has the direct application of evaluating the daily status of VWC for individual soil layers within a profile (Saxton et al., 2006), the simulated equivalent of the TDR VWC.

The SPAW model uses the relationships in the SWCC, calculated using the SR method to simulate vertical hydrogeological budgets. The model, and a book chapter which describes the model (Saxton and Willey, 2005) are both available for free download from <http://hydrolab.arsusda.gov/SPAW/SPAWDownload.html>.

It comprises two computational modules: the Soil Water Characteristics Module, which has soil parameters as inputs to predict the SWCC and properties, such as hydraulic conductivity; and a simulator, which uses the soil water characteristics along with additional weather and crop data to evaluate hydrologic processes. These modules and the computational methods are defined in Appendix B.

6.5.2 Data Inputs

6.5.2.1 Soil

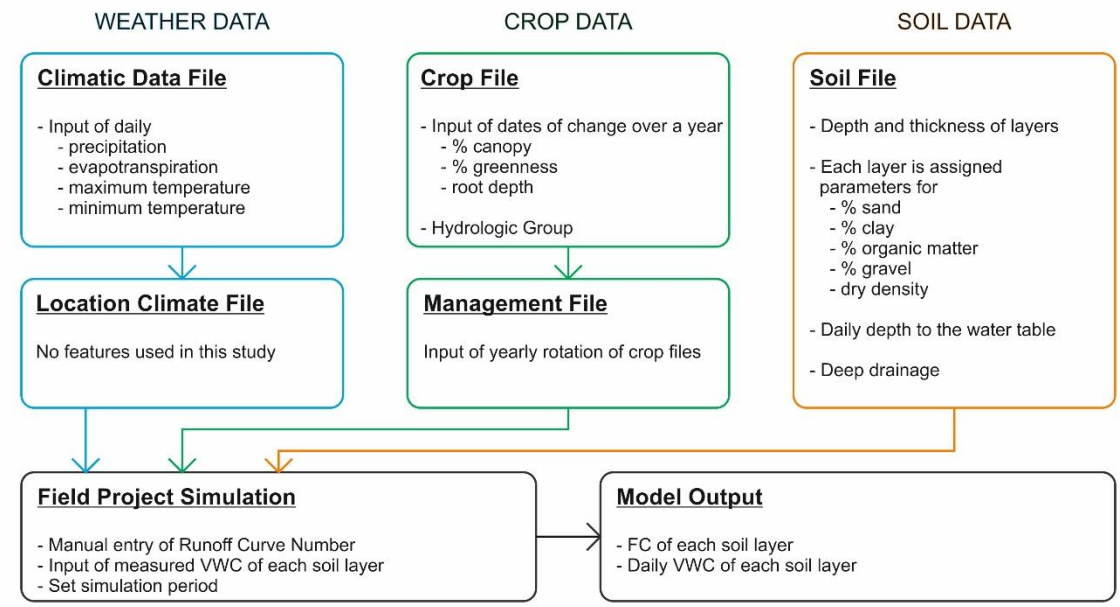

Figure 6.10 The general structure of a field project in the SPAW model.

A schematic of the format of the simulator field project model with the input parameters, outputs and features used in this analysis is shown in Figure 6.10.

Soil data files were constructed for sections both adjacent to and through the ditch features at each of the four research sites. The soils are inputted in layers each with depths below ground level as determined by excavation of the sections (Figures 4.21(a-d)). The parameters which are assigned to each of the layers are sand content, *S*, clay content, *C*, organic matter, *OM*, gravel content, *R* and the matric dry density, ρ_m. An example of a soil input file is shown in Figure 6.11. The soil parameters were set using the data acquired from laboratory testing in the geotechnical characterisation (Table 6.1). General information on the construction and inputs of the soil files is described below.

Each of the soil horizons in the sections were assigned thicknesses and depths below ground level as determined by the site investigations. Due to restrictions on the

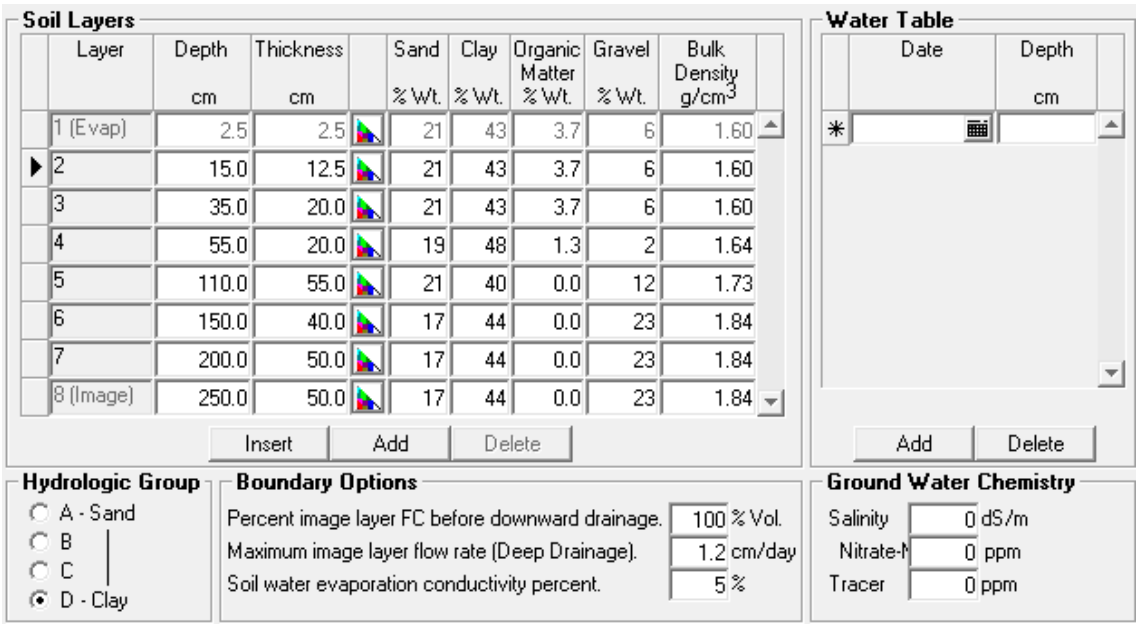

Figure 6.11 Example of a soil file in the SPAW model (CQF AS).

thicknesses of layers in the model, where the thickness of a horizon exceeded that allowed, it was necessary to assign a number of layers to represent a single horizon (Table 6.1).

The model includes an evaporative layer fixed at the top 25mm, which is automatically assigned the parameters of the immediately underlying layer, forming part of the topsoil horizon. The proven soils at the base of each section were assumed to continue to a depth of 2.0m. The model includes an image layer below the base of the section which was set to a thickness of 0.5m, and is automatically assigned the parameters of the immediately overlying soil layer.

Some site specific soil inputs are given in the following paragraphs.

Where only disturbed samples were available due to a lack of cohesion (CCC Ditchfills 2 and 3 and Limestones, and DPF Sand and Gravel), typical values were assigned.

At CQF, Clay 2 is present in the AS over a significant depth (from 0.55mbgl to an unproven depth >1.1mbgl), therefore, for the purposes of the model, it has been divided

into an upper, “Clay 2 (up)”, and lower “Clay 2 (lo)” layer. Laboratory testing of Clay 2 in the AS was carried out on samples taken from the top of the layer and the results of have been assigned to Clay 2 (up). As no results were available from deeper in the section, Clay 2 (lo) has been assigned the values determined by laboratory testing from the DS, which may be more representative of the conditions at this depth.

The model allows only inputs of soils, with no provision made for rock. Therefore, at CCC where a weathering profile of limestone was present, values which best described the rock using soil parameters were assigned. The values used were based on visual inspection, where the weathered limestone rock was assumed to be gravel (though the model limits this to a maximum of 60%), and the sand and clay inputs described the infill.

At DPF, the gravel at the base of the section was not proven in the DS, so it was assumed that the gravel would be present at a similar depth as the AS. However, due to the model constraints on the minimum thickness (100mm) of the sand layer above, a depth of 1.25mbgl was used as the top of the gravel layer. Neither the thin sand layer from the DS, nor the base gravel were tested in the laboratory. Therefore, the sand was assigned the same parameters as that of the sand in the AS, and the gravel was assigned parameters based on visual assessment.

Tests for organic matter were carried out on a limited number of soils as was available from recovery in boreholes. Typically, a single sample was taken from the topsoil, subsoil (if present) and the underlying soil or rock in the AS, and from the topsoil, subsoil and ditchfills in the DS. Gaps in the data are present for the subsoil at DCF, and the *OM* value of the underlying soil has been used. As only a single sample was tested from each of the ditches at all four sites, the results have been used to represent all ditchfills.

Table 6.1 The SPAW model soil data inputs.

		Soil Horizon	*Soil Layer*	*Depth (mm)*	*Thickness (mm)*	*C*	*S*	*R*	*OM (%)*	ρ_m *(Mg/m^3)*
Cirencester Quarry Field	Adjacent Section	Evaporative Layer	1	25	25	0.43	0.21	0.06	3.7	1.60
		Topsoil	2	150	125	0.43	0.21	0.06	3.7	1.60
			3	350	200					
		Clay 1	4	550	200	0.48	0.19	0.02	1.3	1.64
		Clay 2 (up)	5	110	550	0.40	0.21	0.12	0.0	1.73
		Clay 2 (lo)	6	150	400	0.44	0.17	0.23	0.0	1.84
			7	200	500					
		Image Layer	8	250	500	0.44	0.17	0.23	0.0	1.84
	Ditch Section	Evaporative Layer	1	25	25	0.42	0.15	0.04	3.0	1.67
		Topsoil	2	150	125	0.42	0.15	0.04	3.0	1.67
			3	350	200					
		Ditchfill 1	4	600	250	0.45	0.19	0.02	2.7	1.68
		Ditchfill 2	5	750	150	0.41	0.24	0.12	2.7	1.69
		Clay 2	6	105	300	0.44	0.17	0.23	0.0	1.84
			7	150	450					
			8	200	500					
		Image Layer	9	250	500	0.44	0.17	0.23	0.0	1.84
Cirencester Cherry Copse	Adjacent Section	Evaporative Layer	1	25	25	0.08	0.1	0.32	4.3	1.37
		Topsoil	2	150	125	0.08	0.1	0.32	4.3	1.37
			3	300	150					
		Completely Weathered Limestone	4	400	100	0.06	0.6	0.6	0.5	1.50
		Highly Weathered Limestone	5	700	300	0.06	0.75	0.6	0.5	1.60
		Moderately Weathered Limestone	6	100	300	0.06	0.9	0.6	0.5	1.70
			7	150	500					
			8	200	500					
		Image Layer	9	250	500	0.06	0.9	0.6	0.5	1.70
	Ditch Section	Evaporative Layer	1	25	25	0.11	0.1	0.28	4.1	1.37
		Topsoil	2	150	125	0.11	0.1	0.28	4.1	1.37
			3	300	150					
		Ditchfill 1	4	550	250	0.27	0.12	0.34	3.6	1.47
		Ditchfill 2	5	700	150	0.34	0.11	0.35	3.6	1.47
		Ditchfill 3	6	100	300	0.38	0.11	0.60	3.6	1.47
		Moderately Weathered Limestone	7	150	500	0.06	0.9	0.6	0.5	1.70
			8	200	500					
		Image Layer	9	250	500	0.06	0.9	0.6	0.5	1.70

Table 6.1(cont.) The SPAW model soil data inputs.

		Soil Horizon	*Soil Layer*	*Depth (mm)*	*Thickness (mm)*	*C*	*S*	*R*	*OM (%)*	ρ_m *(Mg/m^3)*
Diddington Clay Field	Adjacent Section	Evaporative Layer	1	25	25	0.24	0.24	0.05	2.8	1.56
		Topsoil	2	150	125	0.24	0.24	0.05	2.8	1.56
			3	280	130					
		Subsoil	4	420	140	0.34	0.21	0.03	1.4	1.66
		Clay 1	5	770	350	0.28	0.21	0.08	1.4	1.86
		Clay 2	6	1000	230	0.35	0.14	0.05	0.6	1.85
			7	1500	500					
			8	2000	500					
		Image Layer	9	2500	500	0.35	0.14	0.05	0.6	1.85
	Ditch Section	Evaporative Layer	1	25	25	0.23	0.23	0.07	2.7	1.62
		Topsoil	2	150	125	0.23	0.23	0.07	2.7	1.62
			3	300	150					
		Subsoil	4	500	200	0.27	0.22	0.11	2.0	1.68
		Ditchfill 1	5	860	360	0.27	0.18	0.09	2.0	1.61
		Ditchfill 2	6	1030	170	0.36	0.17	0.07	2.0	1.58
		Clay 2	7	1150	120	0.35	0.16	0.15	0.6	1.85
			8	1500	350					
			9	2000	500					
		Image Layer	10	2500	500	0.35	0.16	0.15	0.6	1.85
Diddington Pasture Field	Adjacent Section	Evaporative Layer	1	25	25	0.13	0.47	0.11	1.8	1.67
		Topsoil	2	150	125	0.13	0.47	0.11	1.8	1.67
			3	270	120					
		Subsoil	4	700	430	0.13	0.44	0.11	1.0	1.65
		Sand	5	1200	500	0.1	0.71	0.32	0.0	1.65
		Gravel	6	1500	300	0.06	0.5	0.5	0.0	1.65
			7	2000	500					
		Image Layer	8	2500	500	0.06	0.5	0.5	0.0	1.65
	Ditch Section	Evaporative Layer	1	25	25	0.18	0.41	0.06	2.1	1.57
		Topsoil	2	150	125	0.18	0.41	0.06	2.1	1.57
			3	320	170					
		Subsoil	4	580	260	0.2	0.32	0.13	0.8	1.82
		Ditchfill 1	5	730	150	0.15	0.4	0.13	0.8	1.60
		Ditchfill 2	6	980	250	0.11	0.4	0.17	0.8	1.31
		Ditchfill 3	7	1150	170	0.12	0.4	0.13	0.8	1.66
		Sand	8	1250	100	0.1	0.71	0.32	0.0	1.65
		Gravel	9	1500	250	0.06	0.5	0.5	0.0	1.65
			10	2000	500					
		Image Layer	11	2500	500	0.06	0.5	0.5	0.0	1.65

6.5.2.2 Weather

Measured weather data, comprising daily total rainfall, daily minimum and maximum temperatures and evaporation, was transferred to the model to create the four climatic data files, one for each test site. The location climate file allows the user to give default monthly evaporation data where high resolution data is unavailable. This feature was not used in this analysis as data were taken directly from the climatic data file.

6.5.2.3 Crop

Table 6.2 Example of data inputs into the crop file (CQF 2011).

Date	*Canopy (%)*	*Greeness (%)*	*Root Depth (mm)*
01/01/2011	20	100	300
09/03/2011	20		
10/03/2011	0	100	300
13/03/2011		0	
14/03/2011	0	100	0
27/03/2011	10		
04/04/2011			380
16/04/2011	50		
15/05/2011	80		760
24/06/2011			910
06/07/2011	94		
13/07/2011		100	
26/07/2011			1020
03/08/2011		70	
25/08/2011			1020
27/08/2011		0	
05/09/2011			300
07/09/2011	93		
05/09/2011	20		
12/09/2011	0		
22/09/2011	10		
31/12/2011	20	20	300

The model provides example crop files for a number of crop types, which provide typical values through a growing season for the percentage canopy, percentage greenness and root depth. The example wheat data were adjusted to the period of growth provided by the RAU to create crop files for CQF for 2011 and 2012. The management file is used to input the yearly rotation of crop files. For DCF, where crop data were unavailable, dated images were used to estimate the dates of drilling and harvest of the cereal, and the example wheat crop files adjusted accordingly. Since DPF was in permanent pasture throughout the simulation, the example file for permanent pasture was used. The simulation for DPF was also run using example crop files, since cropmarks were present during the modelling period in the adjacent field, also over River Terrace Deposits.

An example of the data inputs for a crop file are provided in Table 6.2. Data between input values are calculated by linear interpolation.

6.5.3 Data Outputs

Section 6.4.1 assessed the differences in the $Log_{10}\Psi$ between the AS and the DS, and the background SMD, represented by the AS, throughout growing seasons for the research sites. The model gives an output of daily VWC of each inputted soil layer, which has been post-processed to give the same data ($Log_{10}\Psi$ of the AS and DS, and SMD of the AS), to determine if the model can provide similar information in analysis as the measured data.

The model output of daily VWC for each soil layer is calculated from daily suction for each soil layer using the SR method. However, these daily suctions cannot be directly exported from the model. An additional computational model was created to revert the daily VWC back to suction using the SR method.

To recreate the section comparison analysis, replacing the measured data with modelled data, the daily $Log_{10}\Psi$ of the results were calculated for each soil layer and weighted averages taken to give a single daily $Log_{10}\Psi$ (using Equation 6.1) for each of the depth comparison levels as described in Section 6.4.1.

To recreate the analysis of cropmark appearance and SMD (Section 6.4.2), the daily VWC and field capacity model outputs to the maximum rooting depth were used as inputs into Equation 6.6.

6.6 TESTING THE MODEL

6.6.1 Initial Test

6.6.1.1 Methodology

Prior to running the analysis for section comparisons and cropmark appearance and SMD, an initial test was carried out to determine if patterns in the output data and post processed data were representative of patterns seen in data from TDR measurements. The model was tested against two datasets: the model output of VWC against TDR VWC; and the post-processed SMD of the background soils (AS) against the TDR SMD.

The CQF 2012 growing season was chosen for testing, the reasons being that CQF had both crop data provided by the landowner and complete soil files for both sections could be built from the results of the geotechnical characterisation, and the 2012 growing season had a much longer period of comparable data from the TDR.

Weather, crop and soil files (CQF AS and DS) were created as described in Section 6.5.2. The modelled daily VWC data from both the AS and DS were compared with the daily TDR VWC at four approximately equivalent depths: the topsoils; Clay 1 and Ditchfill 1; Clay 2 (upper) and Ditchfill 2; and Clay 2 (lower)/Clay 2 (below ditch). The modelled

SMD was calculated using Equation 6.6, with Z_r being 1200mm, the maximum depth of AWC for wheat (Hough and Jones, 1997).

6.6.1.2 Results

Figures 6.12(a-d) show the results of the simulation for the AS and DS at four depth levels. Across all depths, the soils were measured as more responsive than the shown in the modelled data, with increased frequency and amplitude. However, trends in the modelled data typically follow those of the TDR VWC at all depths. For example, there is a reduction in the VWC at all depths in the latter half of May, and subsequent increase at the beginning of June, seen in both measured and modelled data. However, the magnitude of the extremes differs, particularly in the topsoil (Figures 6.12(a)), where the modelled response to the dry spell is less. This significant difference in the magnitude of VWC fluctuation in the topsoils is also evident between mid-March and mid-April. The heterogeneity of topsoil may contribute to the greater changes in TDR VWC than in the simulation, where the modelled soils are assumed homogeneous.

This difference in the magnitude of fluctuations is also evident for the same two periods at the Clay 1/Ditchfill 1 level (Figures 6.12(b)), although to a much lesser extent. At the Clay 2/Ditchfill 2 level (Figures 6.12(c)), the magnitude of these fluctuations are approximately equal in the modelled and measured data throughout the simulation. However, the value of VWC is approximately 0.05 lower in the modelled data throughout the period. The Clay 2 (lower)/Clay 2 (below ditch) level (Figures 6.12(d)) has only small fluctuations in the measured data. In the modelled data, the AS shows almost no change throughout the period, whereas the DS shows periodic reductions from an upper limit of 0.34 VWC, reflecting the patterns seen in the levels above. The VWC value throughout is approximately 0.06 lower in both the AS and DS.

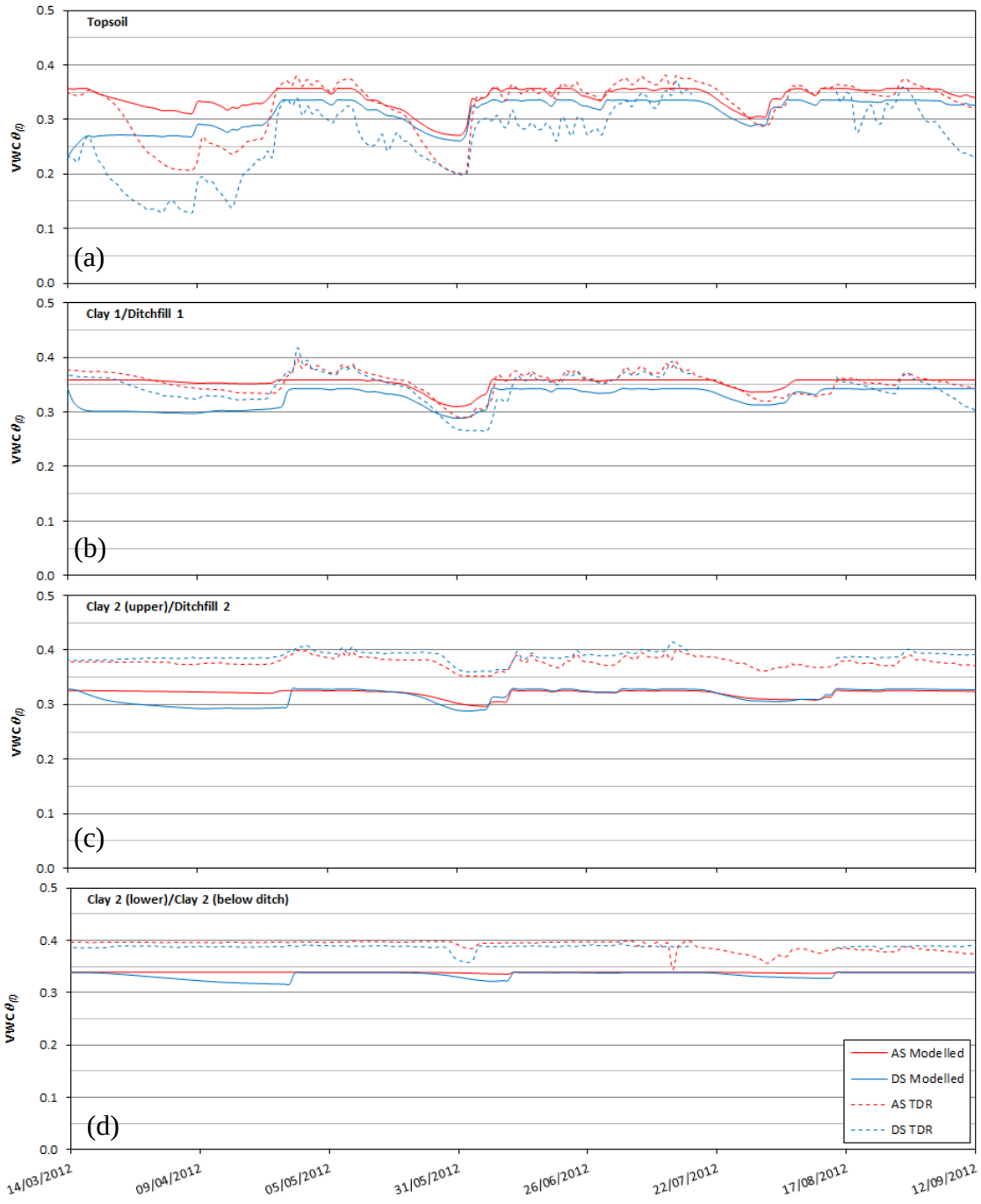

Figure 6.12 Comparison of simulated and TDR measured data in both AS and DS at approximately equivalent depths.

(a) Topsoils (b) Clay 1 and Ditchfill 1

(c) Clay 2(up) and Ditchfill 2 (d) Clay 2(lo) and Clay 2(DS)

One of the most notable features of the modelled VWC is that it displays a maximum limit that is lower than the maximum TDR VWC. This can be seen at all levels. This limitation does not allow trends to be followed where VWC is high or allow the TDR VWC value at the start of the simulation to be assigned correctly where it is higher than the limit value. At times when the VWC is below this limit, trends in the TDR VWC are reflected in the simulated data.

Figure 6.13 shows both the modelled SMD and TDR SMD. Trends in the data are again followed, where the time period (width) of peaks in the data are generally accurate. The magnitude of peaks are always less in the modelled SMD, although the comparative magnitude varies. The first major peak (8th April 2012) in the modelled data is one quarter of the magnitude of the TDR SMD, whereas the last major peak (1st August 2012) is two thirds of the equivalent TDR peak magnitude.

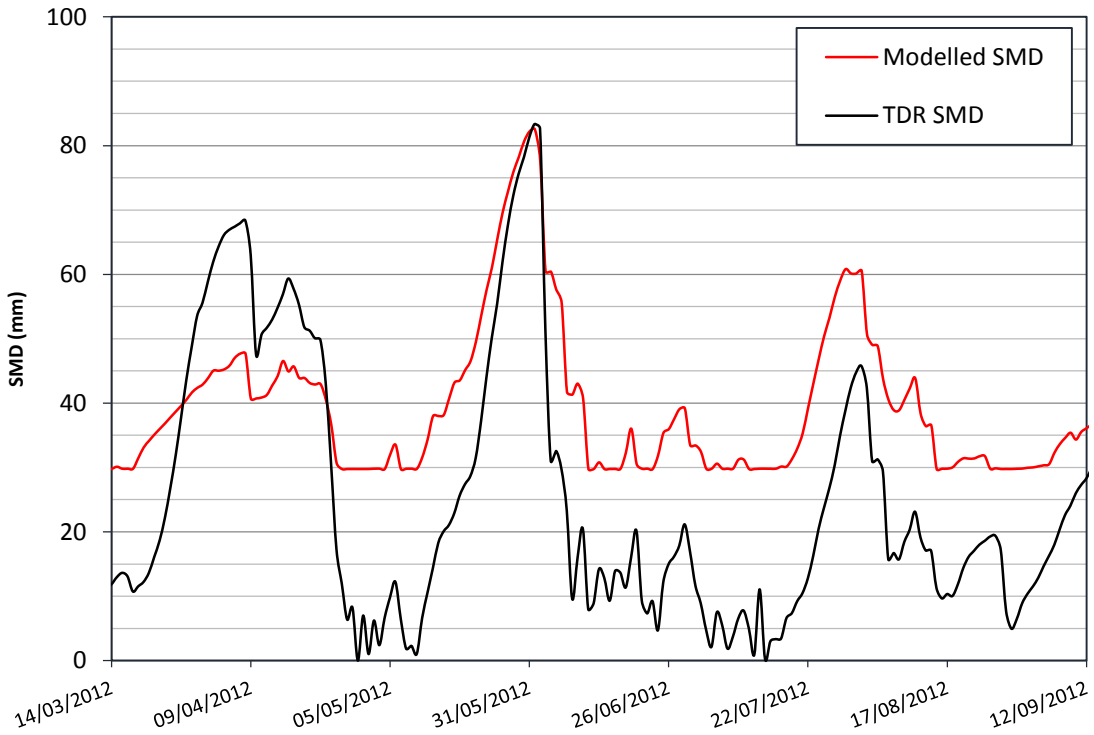

Figure 6.13 Comparison of modelled SMD and TDR SMD.

The most notable feature in the modelled SMD is a minimum value at 30mm below which the SMD never falls. The limitation to a maximum noted in the VWC test translates to a minimum SMD, δ_{min}. This should be at 0mm, when the VWC of soils are at or above FC, as is seen in the TDR SMD. Since θ_{33} is a constant for the section, where VWC is limited to a constant maximum, Equation 6.2 gives a constant δ_{min}. In this tested case, the maximum limit of VWC is lower than the θ_{33} by approximately 0.03, therefore soils can never reach 0mm SMD.

6.6.1.3 Discussion

Trends in both TDR VWC and TDR SMD are generally followed by the simulated data. Inconsistencies with the model output of VWC were noted where it was limited to a maximum. This translates into the post-processed SMD, causing δ_{min} to be >0mm. In the tested case, the limit is lower than θ_{33}, resulting in δ_j never reaching 0mm, even after prolonged rainfall.

At times when the VWC is limited to a maximum, the model reaches a steady state, where for all soil layers, the redistribution of water with the layer above (or infiltration at the ground surface) is equal to that of the redistribution with the layer below. The percolation into the image layer at the base of the section is 0mm for the complete duration of the simulation, so no water is lost or gained at the base of the section. The model calculates a daily infiltration as the daily rainfall minus losses (runoff and interception), where the soil capacity of the uppermost layers permits (Saxton et al., 2006). Figure 6.14 shows the surface exchange of water and percolation for the period from 16th August 2012 to 12th September 2012, where VWC is limited. Almost all rainfall was lost as runoff or interception, with only 3mm of a total 50mm of rainfall being infiltrated. With negligible

water exchange at the soil surface and no water exchange with the image layer (percolation), the section has become hydrostatic.

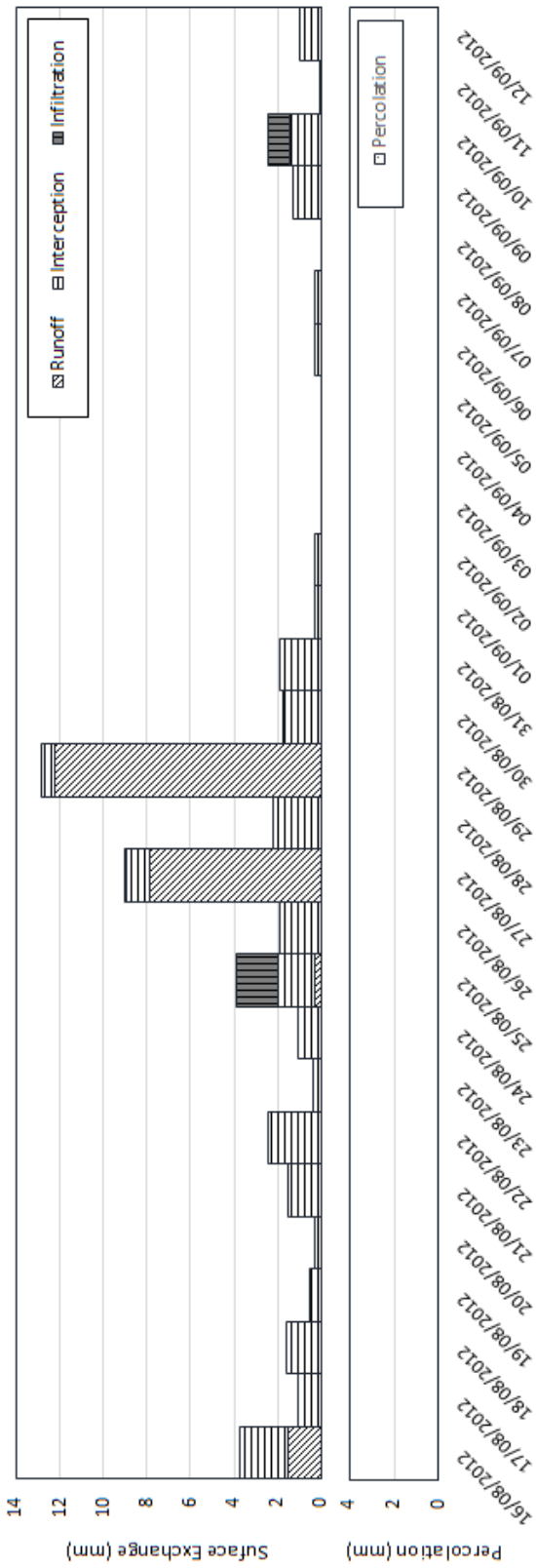

Figure 6.14 Modelled surface exchange of water and percolation data at times where VWC has reached a maximum limit.

To determine whether the VWC maximum limit was sensitive to model parameters which may affect exchange at either the surface or at the section base-image layer boundary, simulations were run varying: the calculation of runoff; the deep drainage parameters; and the depth to the water table.

To decrease the runoff, increasing the water available for infiltration, manual entry of the runoff curve numbers was used, as opposed to those determined by the model (using tabulated data from Rawls et al. 1992). The simulation was run using constant reduced input values of 20 and 50 for comparison with the results using the model runoff curve numbers of >70. The results of the simulation were unchanged, indicating that the runoff values are due to the inability of the uppermost soil to infiltrate additional water, as opposed to a high runoff curve number.

Deep drainage occurs at the base of the image layer when it is near saturation, and controls the movement of water to groundwater or interflow (Saxton et al., 2006). Hydraulic conductivity at the base of the image layer is set to 12mm/day. To assess if the simulated deep drainage changes with hydraulic conductivity, simulations with values of 0mm/day and 50mm/day were used. A parameter can also be set which controls the minimum VWC (as a percentage of θ_{33}) in the image layer required before deep drainage can occur. This value is set to 100% by default, reduced to 50% simultaneously with the change in hydraulic conductivity. In all cases, the outputs of the simulations were unchanged, indicating that, in this case, exchange of water at the base of the section is independent of hydraulic conductivity at the base of the image layer.

Since the model output is independent of both the runoff curve number and deep drainage parameters, the maximum limit must be determined by the input values of the soils.

No water table was encountered at CQF during the site investigations, therefore the base model was constructed with no water table depths. To assess whether including a water table at depths within the modelled section would have an effect on the simulated output, the model was run with water tables set to 1.0m and 1.5m. The output values of VWC were unchanged, even where soil layers were below the water table, where the VWC should be above θ_{33}.

The maximum limit of VWC is at the empirically calculated saturation, θ_s, but this is inconsistent with the empirical calculation of θ_{33} which should be at a lower VWC. The concept of FC is known to be an approximation (Hough and Hood, 2003), although the definition of the VWC at suctions of 33kPa has become widely accepted. A written definition of FC is the VWC after a wetting event where drainage becomes "very slow" (Nachabe, 1998). The tested sections become hydrostatic where the VWC has reached a maximum and drainage from not only the base of the section, but also redistribution between layers is 0mm/h. At this point the written definition of FC has been reached, and it could be considered equal to θ_s. Substitution of θ_s in the place of θ_{33} in Equation 6.2 as shown in Equation 6.7 would give SMD based on this written definition.

$$\delta_i = \left[\theta_s - \theta_j\right] Z_r \qquad [\ 6.7\ ]$$

Figure 6.15 shows the modelled SMD using θ_s as FC and the TDR SMD. This use of θ_s as FC as opposed to θ_{33} for calculation of SMD corrects the issue relating to δ_{min}, however, peak magnitudes remain variably lower than in the TDR SMD. Although δ_{min} = 0mm in this case, it does not address the inconsistency whereby $\theta_s < \theta_{33}$. To further investigate this inconsistency, a sensitivity analysis to the soil input parameters was carried out.

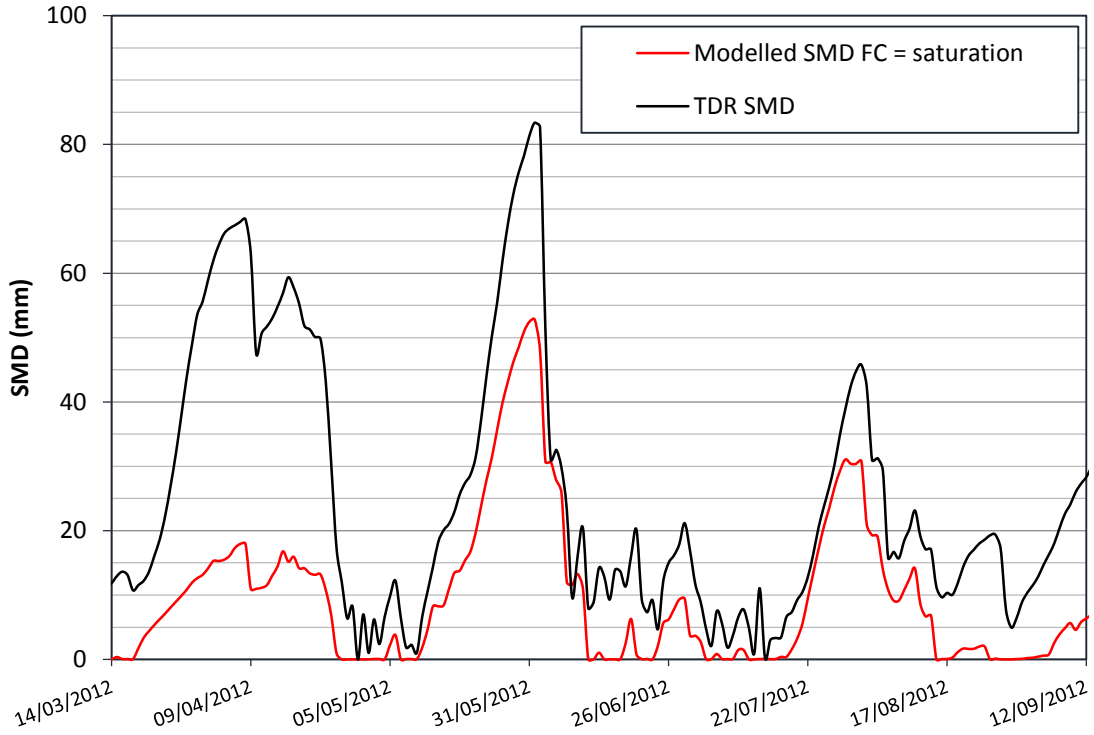

Figure 6.15 Comparison of modelled SMD where $\theta_{33} = \theta_s$, and TDR SMD.

6.6.1.4 In Summary

Where VWC is below θ_s, the modelled data followed trends in the TDR data. The magnitude of change in the VWC as soils are wetting and drying in the topsoil is much larger in the measured data, possibly due to the assumed homogeneity of the modelled topsoil. Below the topsoil actual values of the TDR VWC were typically higher than in the simulated data, as soils cannot exceed θ_s.

Where VWC is at θ_s, the soils have become hydrostatic. Varying of input parameters relating to water exchange at the surface and base of the section do not have any effect on the output. When the soils reach θ_s, any additional water into the section modelled by increasing potential infiltration (i.e. reducing the runoff), or the inclusion of a water table within the depth of the section, does not increase the VWC. However, the value of θ_s is inconsistent with the SWCC, and is lower than θ_{33}, resulting in SMD never reaching 0mm.

The trends in the TDR SMD are generally followed, although the magnitude of peaks is variably less. The minimum SMD is at 30mm, yet should be 0mm in prolonged wet conditions where soils are near θ_{33}. This is a result of the inconsistency found in the VWC. Using θ_s as FC, following the literal definition, for calculation of δ_j would give results where δ_{min} reached 0mm, as should be the case. However, this change in the definition of SMD does not account for the cause of θ_s.

The following section presents the results of a sensitivity analysis to determine the effects of varying soil inputs into the simulation, and further investigate the inconsistency found whereby $\theta_s < \theta_{33}$.

6.6.2 Sensitivity Analysis

6.6.2.1 Methodology

The previous section found that modelled data followed trends in both the TDR VWC and TDR SMD. However, the modelled soils reach saturation at a VWC lower than the field capacity. This resulted in the near surface soils being unresponsive to fluctuations in VWC at times when it is high, and VWC being consistently lower than was measured at greater depth. In calculation of SMD, the θ_s translates to a δ_{min} which cannot reach 0mm.

This section presents the results of a sensitivity analysis carried out to assess the dependency of the model output to soil parameters which are used in the empirical calculation of the SWCC (SR method), on which the SPAW model is based. The soil inputs are primarily *S*, *C* and *OM*, with adjustments made for *R* and ρ_m. The results of the sensitivity analysis have been used to further understand the reasons for the identified inconsistency in saturation and FC values, and to inform later analyses.

The sensitivity analysis has been carried out using the one factor at a time method, where only the parameter being assessed has been varied from a reference value and all other parameters are fixed.

Prior to assessing the sensitivity of VWC and SMD parameters, an initial analysis of the general effects of varying input parameters on the SWCC curve was carried out, using data from all 33 site soils.

To assess the model output of VWC and SMD, data from both the AS and DS from CQF have been used as references. Variations were made to the soil input parameters of *C*, *S*, *OM*, *R* and ρ_m and are further discussed in Section 6.6.2.2. For simulation, the value adjustments have been applied to all soil layers in the section, including those below rooting depth, which are not included in weighted average calculations but may affect the simulation. The data resulting from the same modelling period as that of the model test has been used (the CQF 2012 growing season).

For the section comparisons using the TDR data, the VWC was converted to $\mathrm{Log}_{10}\Psi$ using the SR method with input values as determined by the geotechnical characterisation. The same process would be applied to the model output of VWC should the analysis be carried out replacing TDR VWC with modelled VWC. Therefore, the analysis assesses the sensitivity of the direct model output of VWC to soil input parameters, without subsequent conversion to $\mathrm{Log}_{10}\Psi$.

The SMD of the AS has been used to represent the SMD of the background soils for comparison with cropmark appearance. The model test showed that there are two possible values which could be considered as FC, θ_{33} (the empirical definition) and θ_s (the literal definition) which are used in calculations of SMD. The sensitivity to the constant, δ_{min}, has been assessed for the AS and also the DS to provide additional data.

This is only relevant to calculations of SMD using θ_{33}, as, by definition, using θ_s returns $\delta_{min} = 0$. The time variable daily SMD, δ_j, returns different values depending on the definition of FC used in calculation, whereas the magnitude of peaks above δ_{min} have the same value and are independent of the FC definition. Peak magnitudes are equal to $\delta_j - \delta_{min}$ when using θ_{33} as FC, and equal to δ_j when calculated using θ_s as FC. The median, minimum and maximum changes from the reference peak magnitude throughout the simulation period were used for assessment of sensitivity. Only daily values where peaks of >10mm occurred have been included. Data closer to the δ_{min} were removed to avoid skewing of results by the large quantities of data near the minimum, allowing assessment of data only at times where more significant peaks were formed.

The following section defines the ranges of input values used for analysis.

6.6.2.2 Input Variables

The input values used for the sensitivity analysis are given in Table 6.3. The paragraphs below define the ranges used.

Clay Content

A number of datasets were available from laboratory testing for clay content from differing preparation and testing methods. The laser diffraction method typically recorded *C* values which were significantly lower (up to 0.40) than those determined by the sedimentation by hydrometer method (see Section 5.3.7). The sensitivity analysis was therefore carried out on an artificial set of *C* values reducing to 0.40 below the reference value, in increments of 0.10. This range includes the variability in clay content from the differing treatment and testing methods. A smaller range of inputs of ±0.05 and ±0.10 was also included to allow for more minor variations in the soils.

Table 6.3 Soil data inputs for the sensitivity analysis

Cirencester Quarry Field	Soil Horizon	Soil Layer	C				S				R				OM (%)				ρ_m (Mg/m^3)			
			-0.10	-0.05	Reference	+0.05	-0.10	-0.05	Reference	+0.05	-0.10	-0.05	Reference	+0.05	-2%	-1%	Reference	+1%	+2%	-0.2	-0.01	Reference	+0.1	+0.2
Adjacent Section	Evaporative Layer	1	0.33	0.38	0.43	0.48	0.53	0.11	0.16	0.21	0.26	0.31	0.00	0.01	0.06	0.11	0.16	1.7	2.7	3.7	4.7	5.7	1.40	1.59	1.60	1.61	1.80
	Topsoil	2	0.33	0.38	0.43	0.48	0.53	0.11	0.16	0.21	0.26	0.31	0.00	0.01	0.06	0.11	0.16	1.7	2.7	3.7	4.7	5.7	1.4	1.59	1.60	1.61	1.8
		3																									
	Clay 1	4	0.38	0.43	0.48	0.53	0.58	0.09	0.14	0.19	0.24	0.29	0.00	0.00	0.02	0.07	0.12	0.0	0.3	1.3	2.3	3.3	1.44	1.63	1.64	1.65	1.84
	Clay 2 (up)	5	0.3	0.35	0.4	0.45	0.5	0.11	0.16	0.21	0.26	0.31	0.02	0.07	0.12	0.17	0.22	0.0	0.0	0.0	1.0	2.0	1.53	1.72	1.73	1.74	1.93
	Clay 2 (lo)	6	0.34	0.39	0.44	0.49	0.54	0.07	0.12	0.17	0.22	0.27	0.13	0.18	0.23	0.28	0.33	0.0	0.0	0.0	1.0	2.0	1.64	1.83	1.84	1.85	2.04
		7																									
	Image Layer	8	0.34	0.39	0.44	0.49	0.54	0.07	0.12	0.17	0.22	0.27	0.13	0.18	0.23	0.28	0.33	0.0	0.0	0.0	1.0	2.0	1.64	1.83	1.84	1.85	2.04
Ditch Section	Evaporative Layer	1	0.32	0.37	0.42	0.47	0.52	0.05	0.1	0.15	0.2	0.25	0.00	0.00	0.04	0.09	0.14	1.0	2.0	3.0	4.0	5.0	1.47	1.66	1.67	1.68	1.87
	Topsoil	2	0.32	0.37	0.42	0.47	0.52	0.05	0.1	0.15	0.2	0.25	0.00	0.00	0.04	0.09	0.14	1.0	2.0	3.0	4.0	5.0	1.47	1.66	1.67	1.68	1.87
		3																									
	Ditchfill 1	4	0.35	0.4	0.45	0.5	0.55	0.09	0.14	0.19	0.24	0.29	0.00	0.00	0.02	0.07	0.12	0.7	1.7	2.7	3.7	4.7	1.48	1.67	1.68	1.69	1.88
	Ditchfill 2	5	0.31	0.36	0.41	0.46	0.51	0.14	0.19	0.24	0.29	0.34	0.02	0.07	0.12	0.17	0.22	0.7	1.7	2.7	3.7	4.7	1.49	1.68	1.69	1.7	1.89
		6																									
	Clay 2	7	0.34	0.39	0.44	0.49	0.54	0.07	0.12	0.17	0.22	0.27	0.13	0.18	0.23	0.28	0.33	0.0	0.0	0.0	1.0	2.0	1.64	1.83	1.84	1.85	2.04
		8																									
	Image Layer	9	0.34	0.39	0.44	0.49	0.54	0.07	0.12	0.17	0.22	0.27	0.13	0.18	0.23	0.28	0.33	0.0	0.0	0.0	1.0	2.0	1.64	1.83	1.84	1.85	2.04

Sand Content

In the geotechnical characterisation, where more than one specimen of the same section was tested the maximum range of *S* values was 0.05. Where the same soil horizon appeared in both sections (e.g. Topsoil), the maximum difference between values of *S* was 0.10. The sensitivity to *S* was tested by adjusting *S* by ± 0.05 and ± 0.10 to account for typical variation of the soil.

Gravel Content

In the geotechnical characterisation, where more than one specimen of the same section was tested, differences in *R* were in the region of approximately 0-0.10. The sensitivity of outputs to the *R* were tested by varying results by ±0.05 and ±0.10 in each of the soil layers where possible.

Organic Matter Content

Where two results of the same soil horizon in the both sections was available from laboratory testing, the maximum difference in *OM* was <1.0%. To assess the effect on the model output, the *OM* of the soils was varied by ± 1.0% and ± 2.0%. In Clay 2, where the soils had trace values and it was not possible to reduce *OM*, the input value was kept at zero.

Dry Density

The laboratory results from the geotechnical characterisation showed differences in ρ_m of up to 0.17 Mg/m^3, though typically nearer to 0.10 Mg/m^3, where either two samples of the same soil horizon or the same soil horizon in different sections were tested. The sensitivity of the model to dry density was tested by varying the dry density of the soils in all layers by ± 0.10 Mg/m^3 and ± 0.20 Mg/m^3.

6.6.2.3 Results

The results of varying soil parameters on the SWCC, VWC and SMD are given below.

The SWCC

The effect of varying the soil input parameters *C, S, OM* and ρ_m over the ranges given in the previous section on the SWCC has been assessed. Field soils typically sit within the suction range of 33kPa (FC) to 1500kPa. The SWCCs of all soils have been compared in this range. Figures 6.16(a-d) show the results for CQF AS Topsoil as an example, with the results of all other soils being comparable.

The SWCC is most sensitive to variations in *C*, where the largest effect is seen at the higher suctions (Figure 6.16(a)). Varying *C* by ±0.05 results in a direct change in VWC of ±0.027. At lower suctions, a change in *C* of the same magnitude results in a direct change of approximately ±0.022 in the tested range.

The larger reductions in *C*, which may be due to analysis methods, result in a more significant change (Figure 6.16(a)). The range of VWC between 33 kPa and 1500 kPa suction for the reference inputs is approximately 0.25-0.36. For a reduction in *C* of 0.20, this VWC range is 0.14-0.28, almost completely outside the reference range. Larger reductions do not overlap the reference range at all.

SWCC sensitivity to variations in *S* and *OM* is lower, where the range of inputs tested result in changes in VWC of typically less than ±0.01 (Figures 6.16(b-c)). Figure 6.16(d) shows that varying the density has negligible effect on the SWCC close to 1500 kPa, although there is a spread in the SWCC at lower suctions.

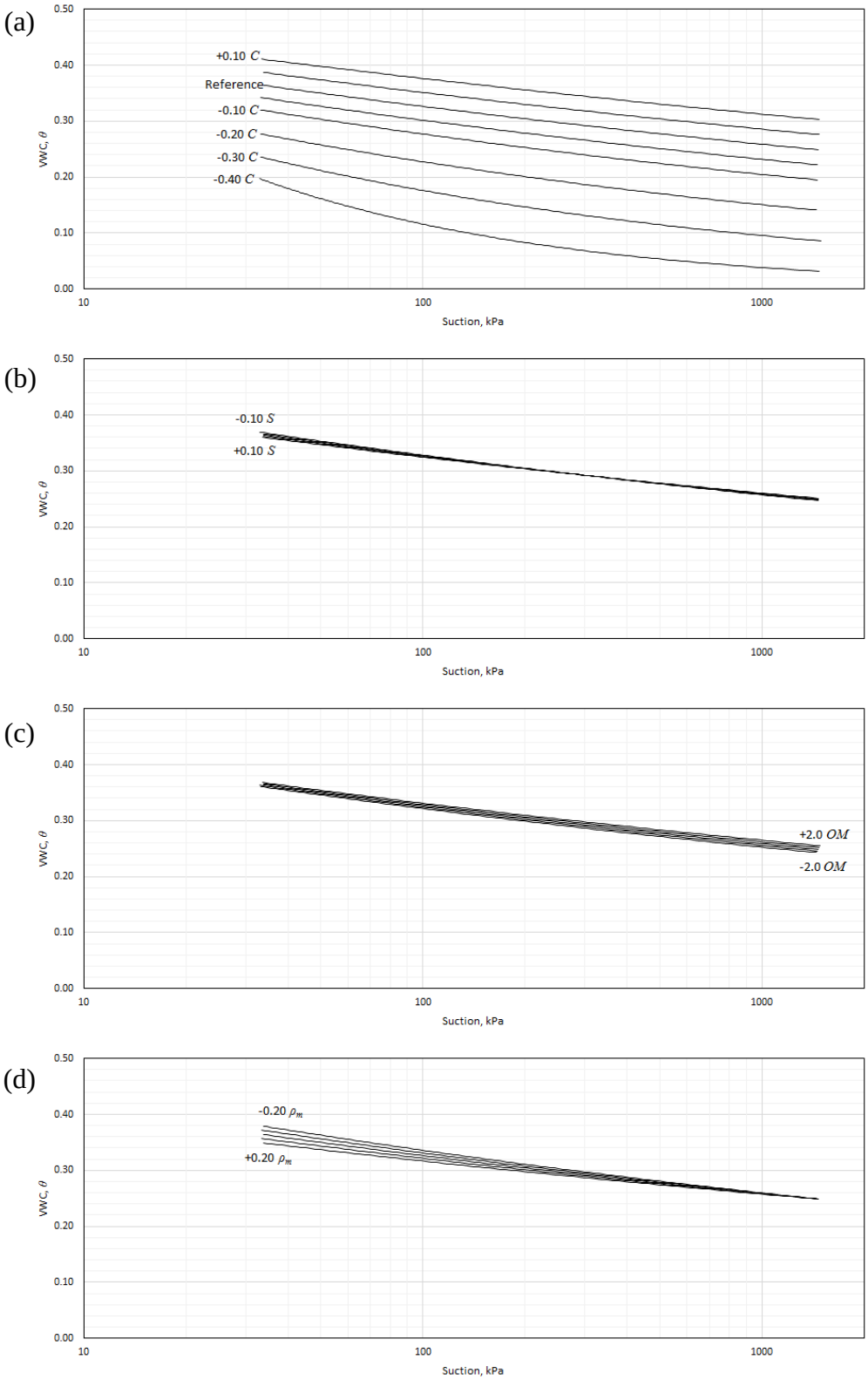

Figure 6.16 Sensitivity of the SWCC to soil input parameters, C, S, OM and ρ_m.

(a) Sensitivity to C (range, +0.10 to -0.40) (b) Sensitivity to S (range, ±0.10)

(c) Sensitivity to OM (range, ±2.0%) (d) Sensitivity to ρ_m (range, ±0.20 Mg/m^3)

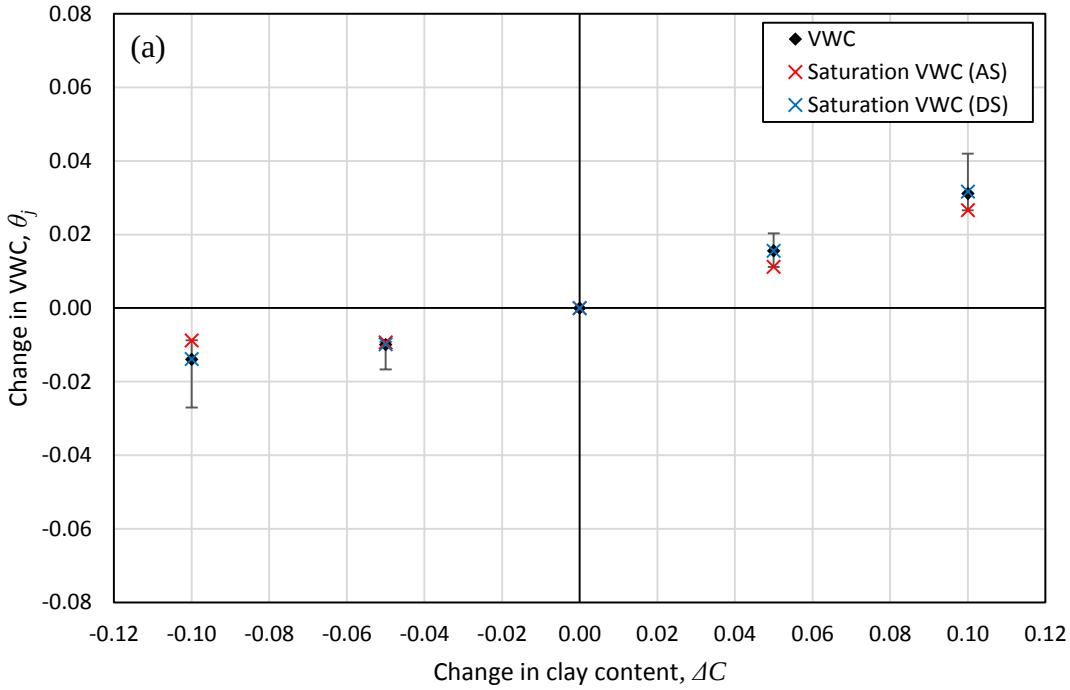

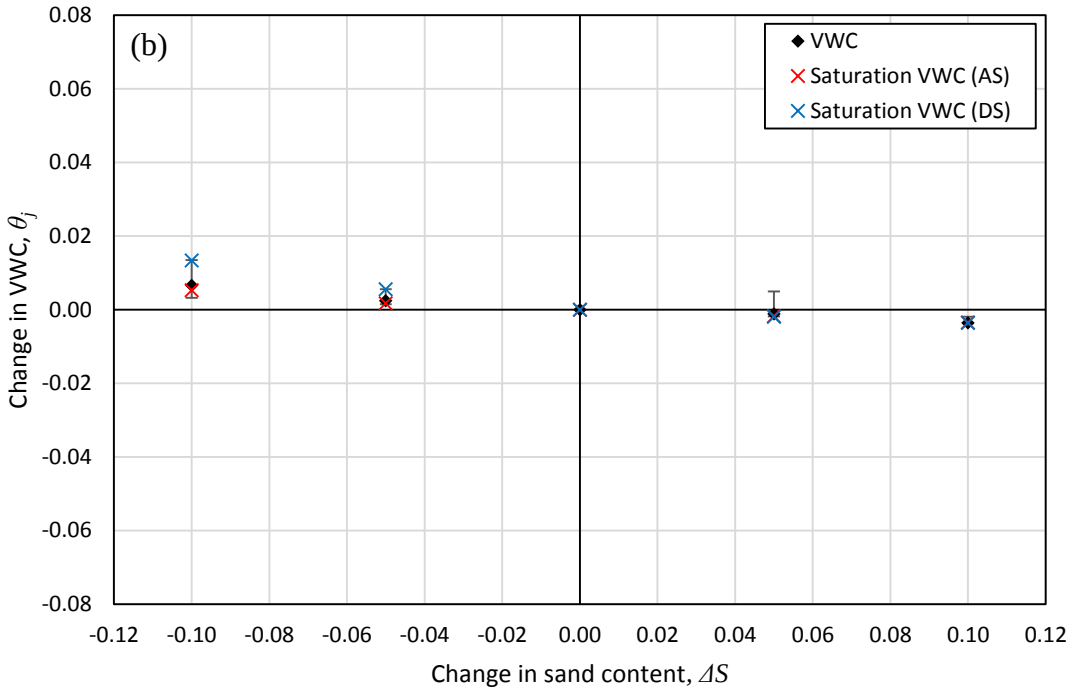

Figure 6.17 Sensitivity of daily VWC, θ_j, and saturation VWC, θ_s, to soil input parameters, C, S, OM and ρ_m.

(a) Sensitivity to C (range, ±0.10) (b) Sensitivity to S (range, ±0.10)

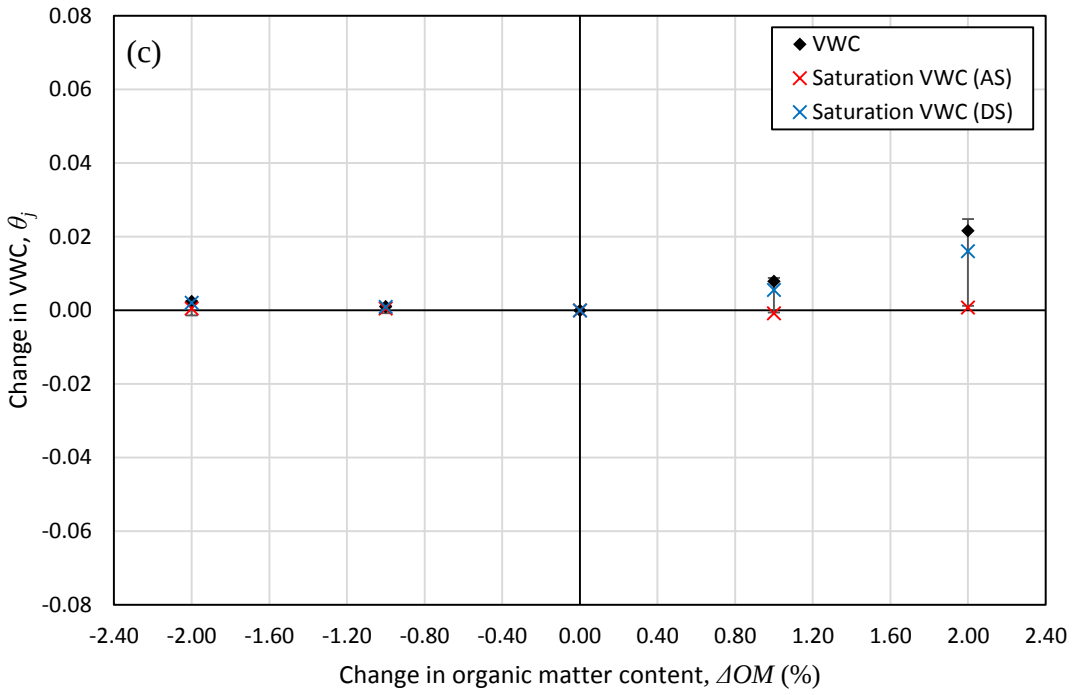

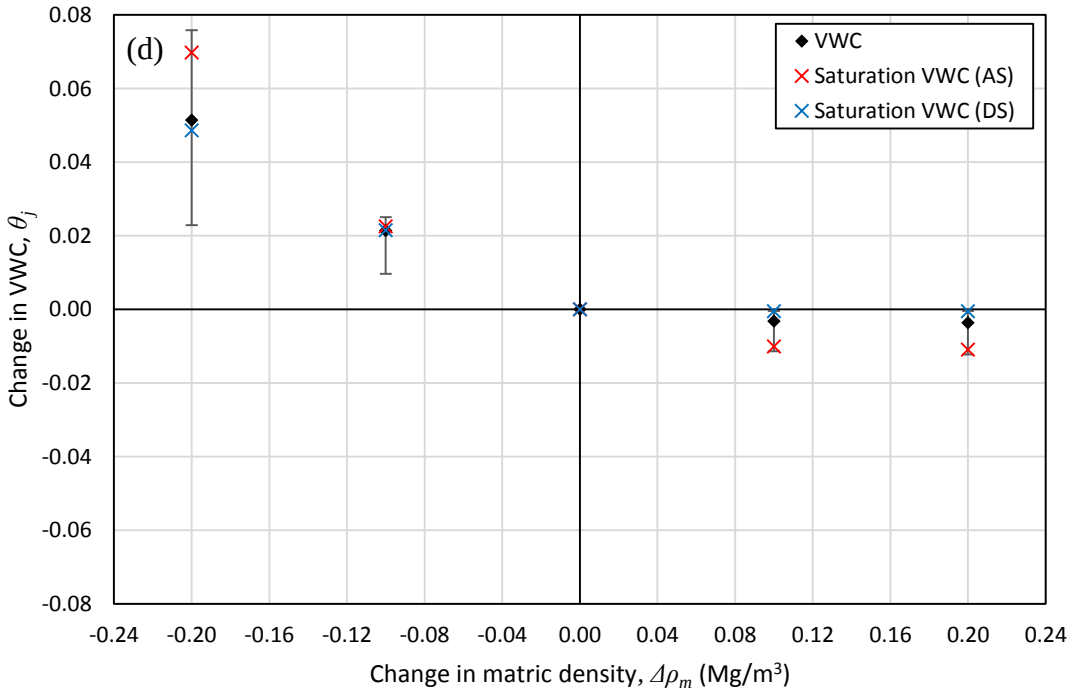

Figure 6.17(cont.) Sensitivity of daily VWC, θ_j, and saturation VWC, θ_s, to soil input parameters, C, S, OM and ρ_m.

(c) Sensitivity to OM (range, ±2.0%) (d) Sensitivity to ρ_m (range, ±0.20 Mg/m^3)

VWC

Figures 6.17(a-d) show the resulting data for the analysis for varying *C, S, OM* and ρ_m on both θ_j and θ_s. θ_s is independent of *R*, and sensitivity of θ_j to *R* is negligible and no figure has been presented. The constant, θ_s, has been assessed for AS and DS (two data points). As θ_j has numerous data points, the figures give a median value and range bars indicating the minimum and maximum values.

The results show that both θ_j and θ_s typically vary by <0.02 for the tested ranges of all soil input parameters, with a few exceptions. Increases in *C* and *OM* at the extreme of the tested range (0.10 and 2.0% respectively) also increase θ_j and θ_s by up to 0.03. Reductions in the tested range of ρ_m have a greater effect, increasing both θ_j and θ_s by up to 0.08.

SMD

Figures 6.18(a-d) show the resulting data for the analysis for varying *C, S, OM* and ρ_m on the minimum SMD, δ_{min}; and the peak magnitude above the δ_{min}. Sensitivity to *R* is negligible in both cases and has not been presented in the figure. The constant, δ_{min}, has been assessed for AS and DS. The figures give a median value and range bars indicating the minimum and maximum values for the peak magnitude.

Reductions in *C* (Figure 6.18(a)) typically cause reductions in the δ_{min} and the peak magnitude, whereas increases in *C*, typically cause increases in both SMD parameters. The effect of reducing *C* has the greatest effect on δ_{min}, with reductions of up to 30mm. Although peak magnitudes have wider ranges of change, the median sensitivity values are all <5mm.

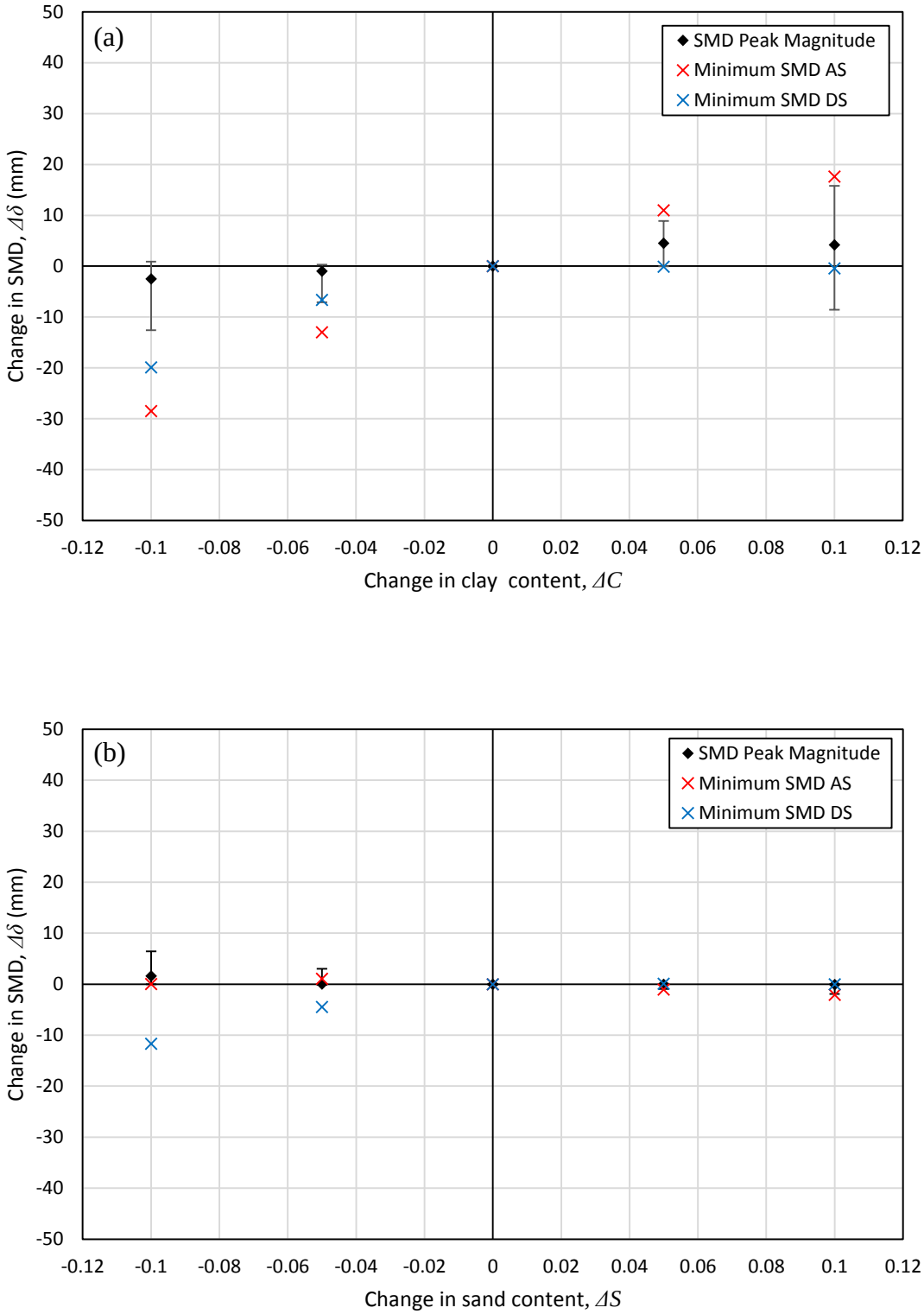

Figure 6.18 Sensitivity of SMD peak magnitude and maximum SMD, δ_{max}, to soil input parameters, C, S, OM and ρ_m.

(a) Sensitivity to C (range, ±0.10) (b) Sensitivity to S (range, ±0.10)

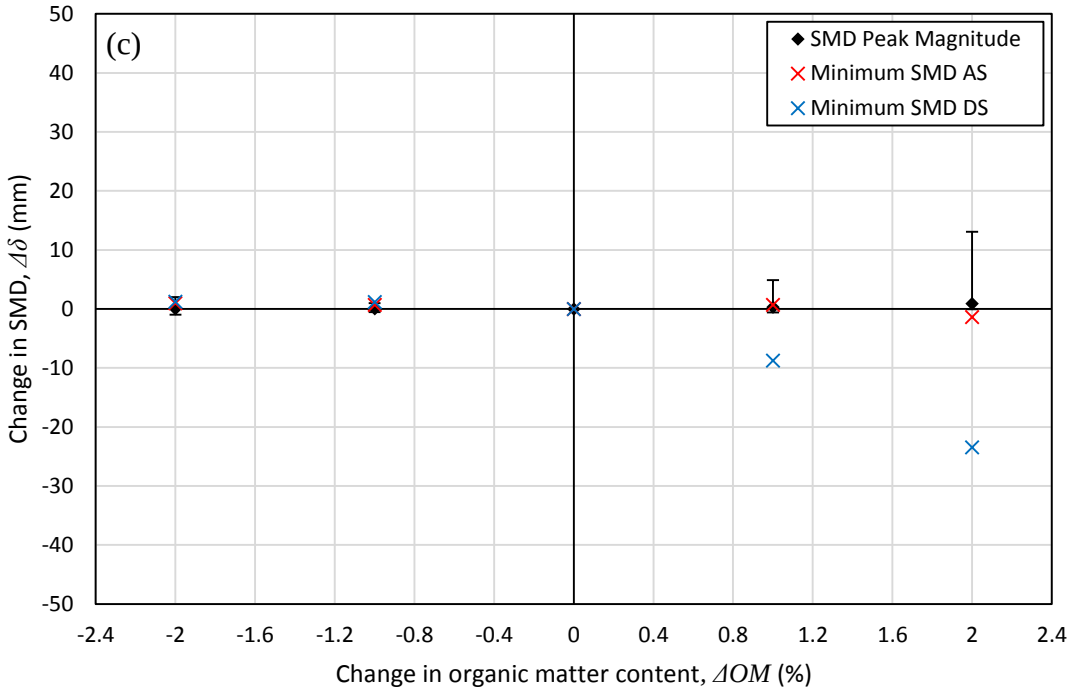

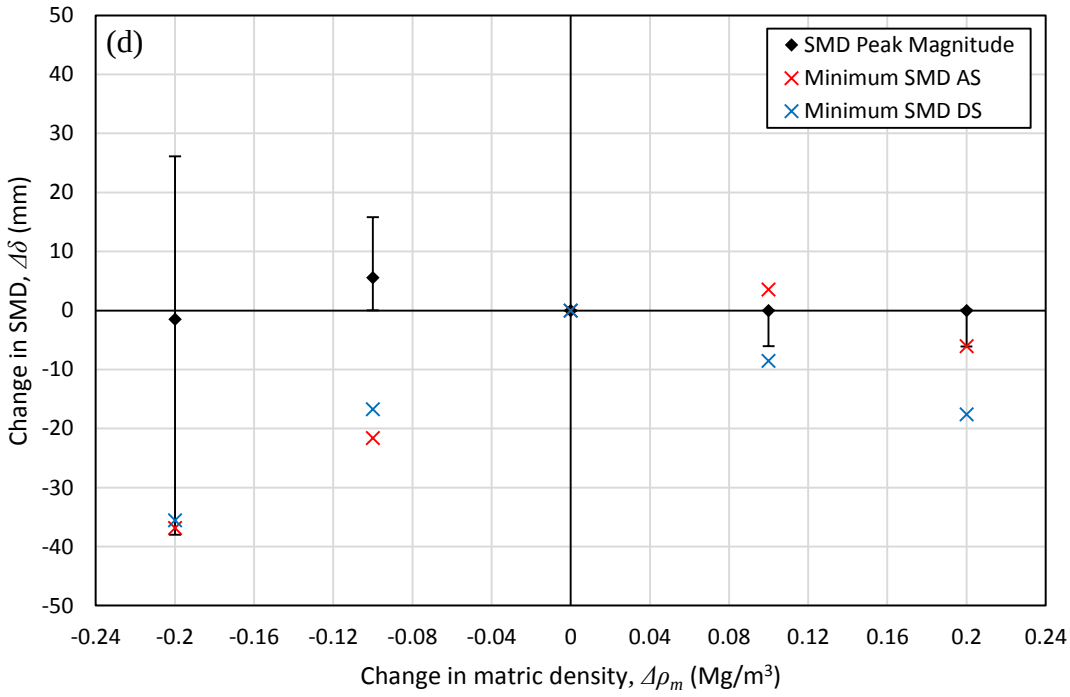

Figure 6.18(cont.) Sensitivity of SMD peak magnitude and maximum SMD, δ_{max}, to soil input parameters, C, S, OM and ρ_m.

(c) Sensitivity to OM (range, ±2.0%) (d) Sensitivity to ρ_m (range, ±0.20 Mg/m^3)

Varying *S* has a much smaller effect on both SMD parameters (Figure 6.18(b)), where the largest difference is seen in the δ_{min} where *S* is reduced; however, this is only noted in the DS, while sensitivity of δ_{min} in the AS is negligible.

Changes in both SMD parameters due to reductions in *OM* are negligible (Figure 6.18(c)). Increases, however, reduce the δ_{min} by up to -25mm in the DS, although this dependence is not seen in the AS. Median changes in peak magnitude are negligible across the tested range of *OM*, although increases in *OM* can also increase the peak magnitude.

Varying ρ_m has the most significant effect on both SMD parameters (Figure 6.18(d)). Varying ρ_m by the tested range resulted in changes to the δ_{min} of up to -35mm, with reduction causing the greatest change. The median changes in peak magnitude were all within ±6mm, however reductions in ρ_m of 0.20 Mg/m^3 had high maximum and minimum sensitivities of up to ±41mm.

6.6.2.4 Discussion

Significantly lower values of *C* were recorded from different analysis methods. The assessment of the sensitivity of the SWCC to these variations showed significant changes which at the extreme would cause the range of typical VWC likely in the field to only overlap by a negligible amount. As a result of this, using the SWCC based on *C* determined by different methods would not give applicable results, and have not been considered further.

The SPAW model is a soil based hydrogeological model and does not allow for rock inputs. As the AS at CCC comprises limestone with a weathering profile, it may have been possible to represent the rock as soils with a high gavel content. However, the SWCC is not dependent on gravel, and only negligible differences in SMD were seen by

varying this input in the sensitivity analysis, hence the SPAW model is unable to model the SMD at CCC.

The model test showed that δ_{min} was approximately 30mm, although it should be at 0mm at times when soils are at FC. This is a by-product of θ_s being lower than θ_{33}. Although this issue can be resolved by using the literal definition of FC, replacing θ_{33} with θ_s, it does not address the cause of $\theta_s < \theta_{33}$. Analysis of both θ_s and δ_{min} showed that reductions in ρ_m had the greatest effect on both parameters. The following paragraphs further investigate the effect of ρ_m on the model output.

Saxton and Rawls (2006) present the following equations for the calculation of θ_s and θ_{33} with adjustment for matric density inputs. They also provide a calculation for a default matric density that can be used if there are no known values.

$$\theta_{(33)DF} = \theta_{33} - 0.2\left(\theta_s - \theta_{(s)DF}\right) \quad [6.8]$$

$$\theta_{(s)DF} = 1 - \left({}^{\rho_m}/_{2.65}\right) \quad [6.9]$$

$$\rho_{m(default)} = 2.65(1 - \theta_s) \quad [6.10]$$

where $\theta_{33(DF)}$ is the VWC at 33 kPa suction (FC) adjusted for matric density inputs,
θ_{33} is the VWC at 33 kPa suction (FC) using a default matric density,
$\theta_{s(DF)}$ is the VWC at saturation adjusted for matric density inputs,
θ_s is the VWC at saturation using a default matric density,
and $\rho_{m(default)}$ is the default matric density (Mg/m^3).

Equations 6.8 and 6.9 for the calculation of $\theta_{33(DF)}$ and of $\theta_{s(DF)}$ using the measured values of ρ_m result in values of $\theta_{33(DF)}$ being greater than the $\theta_{s(DF)}$ for Clay 1, Clay 2(upper), Clay 2(lower) and Ditchfill 1. Saturation occurs at a lower VWC than the FC.

The SR method uses a standard particle density of 2.65 Mg/m^3 for calculation of $\theta_{s(DF)}$, on which $\theta_{33(DF)}$ is also dependent. The geotechnical characterisation measured higher

values of particle density for these soils. Using these measured values, Equations 6.8 and 6.9 return $\theta_{33(DF)}$ as lower than $\theta_{s(DF)}$, which would allow FC to be reached. This correction would translate to the weighted averages of FC and VWC allowing δ_{min} to be 0mm.

Although the cause of θ_s being lower than θ_{33} has been found to relate to the use of a standard particle density which is lower than measured values, it is not possible to use measured values for particle density in the simulation. Reconstruction of computational processes in the SPAW model would be required.

6.6.2.5 In Summary

This section has presented the results of a sensitivity analysis used to determine whether modelled VWC would give robust results which could be used firstly to compare the differences in suctions between sections through and adjacent to buried features, and secondly to determine the background SMD for comparison with cropmark appearance.

The analysis was performed, varying the soil input parameters of *C*, *S*, *R*, *OM* and ρ_m, by ranges determined from the geotechnical characterisation. The general effect on the SWCC and the parameters relating to VWC and SMD have been assessed for sensitivity.

The geotechnical characterisation found that different methods of determination can give a wide variation in clay content. The effect of using this wide range of input values had a significant effect on the SWCC, and it was concluded that using values obtained by methods other than British Standard were not applicable to this analysis.

Modelling of the SMD at CCC was not possible, as the SPAW model is not designed for rock inputs.

The initial test (Section 6.6.1) showed that the model output of VWC reached saturation below that of the FC, causing SMD to never reach 0mm. The sensitivity analysis showed that inputs of ρ_m had the greatest effect on both θ_s and δ_{min}. Further assessment of the calculations used to determine θ_s and θ_{33} showed that the use of a standard particle density of 2.65 Mg/m^3 when used alongside measured input values of ρ_m resulted in θ_s being less than θ_{33}. This issue could not be resolved within the SPAW model as particle density is an unchangeable parameter.

Although the inconsistency caused results to be inaccurate, the initial test showed that the model does follow trends in the measured data well. The following section attempts to refine the model to improve the output by the inclusion of a correction factor.

6.7 REFINING THE MODEL

6.7.1 Methodology

The previous sections found that, in the tested case (CQF 2012), modelled VWC and SMD followed trends in measured data well, although, values were inaccurate. The likely cause of this were inconsistencies in the soil density parameters, where the use of a standard particle density did not allow the measured values of matric density to be used for modelling without calculation error. For both VWC and SMD, the measured data would be better reflected if the graphs were shifted on the y-axis.

This section determines if it is possible to apply empirical correction factors to the simulation outputs to compensate for the inconsistency, allowing the model output to better reflect the measured data.

Initially, the tested case (CQF 2012) was used to determine the correction factors which shift the y-axis output of VWC and SMD, and whether the modelled results were robust for use in analyses of comparing sections and of background SMD.

The method of correcting data with a correction factor was then tested, where possible, against other growing seasons (CQF 2011, DCF and DPF) to determine if a single correction factor can be applied in all cases.

6.7.2 The Tested Case

Saxton and Rawls (2006) provide an empirical calculation of matric density, (Equation 6.10), which can be used as a default in the SPAW model. In the tested case (CQF 2012), the default values typically reduce the value of ρ_m by approximately 0.36 Mg/m^3, around 75-80% of the measured values.

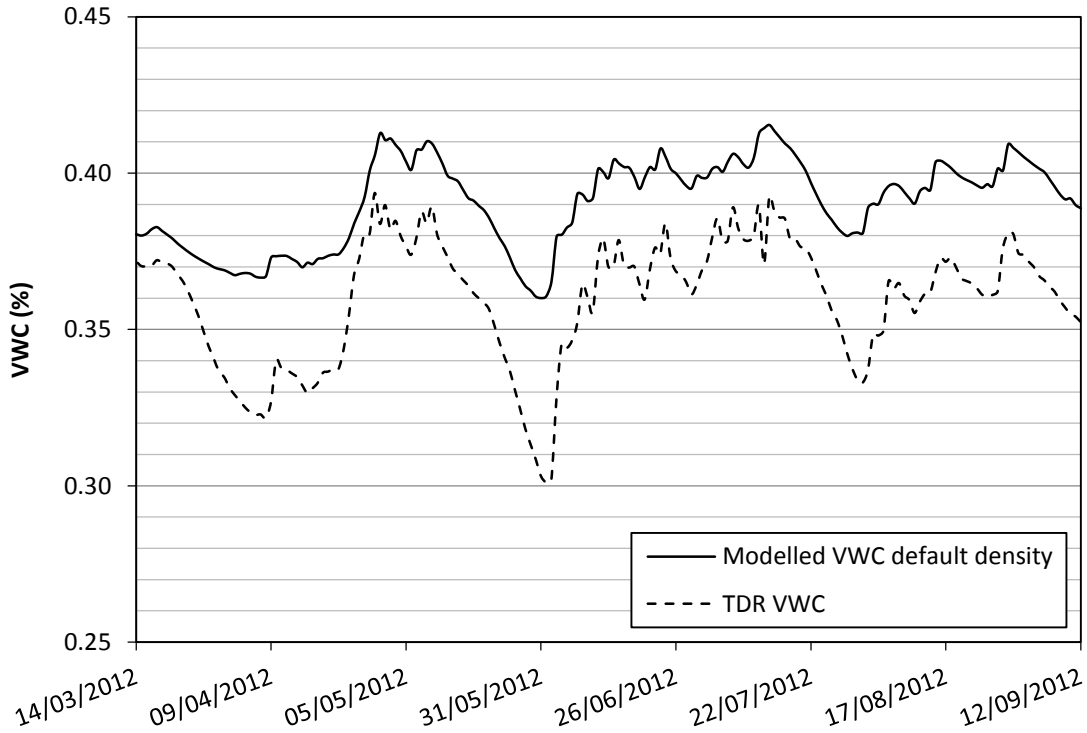

Figure 6.19 The VWC model output for CQF 2012 calculated using default density inputs.

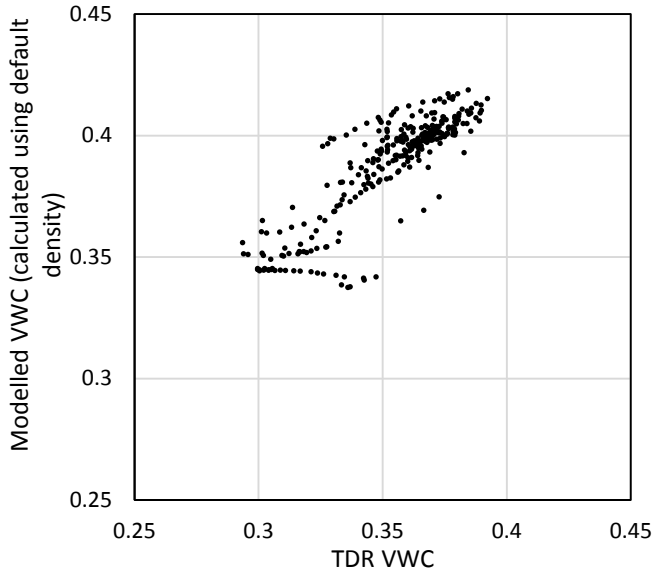

Figure 6.20 Comparison of TDR VWC with modelled VWC, calculated using default matric density.

The effect of using default values of ρ_m on the VWC for the AS is shown in Figure 6.19, along with the TDR VWC. After an initial period of settlement in the modelled data from the constraints of VWC at the beginning of the simulation, both trends and magnitudes of the fluctuations reflect those in the TDR VWC. However, the VWC values are higher throughout. Figure 6.20 shows a comparison of the TDR VWC and modelled VWC (with default ρ_m) using data from both the AS and DS, where the linear trend is θ_j (modelled) = $1.10\theta_j$ (measured). In the tested case, the modelled data can therefore be improved by using a correction factor of $0.91\theta_j$. The VWC modelled using this correction is within 0.04 of the measured data, with the 95th percentile within 0.03.

Figure 6.21 shows the modelled output of VWC using this correction factor. The figure includes dashed lines of the VWC ±0.03 for both the AS and DS, representing the range of the 95th percentile. After the initial settlement period, there is a significant overlap of the data, indicating that section comparisons of $\mathrm{Log}_{10}\Psi$ calculated from the VWC would not give robust results.

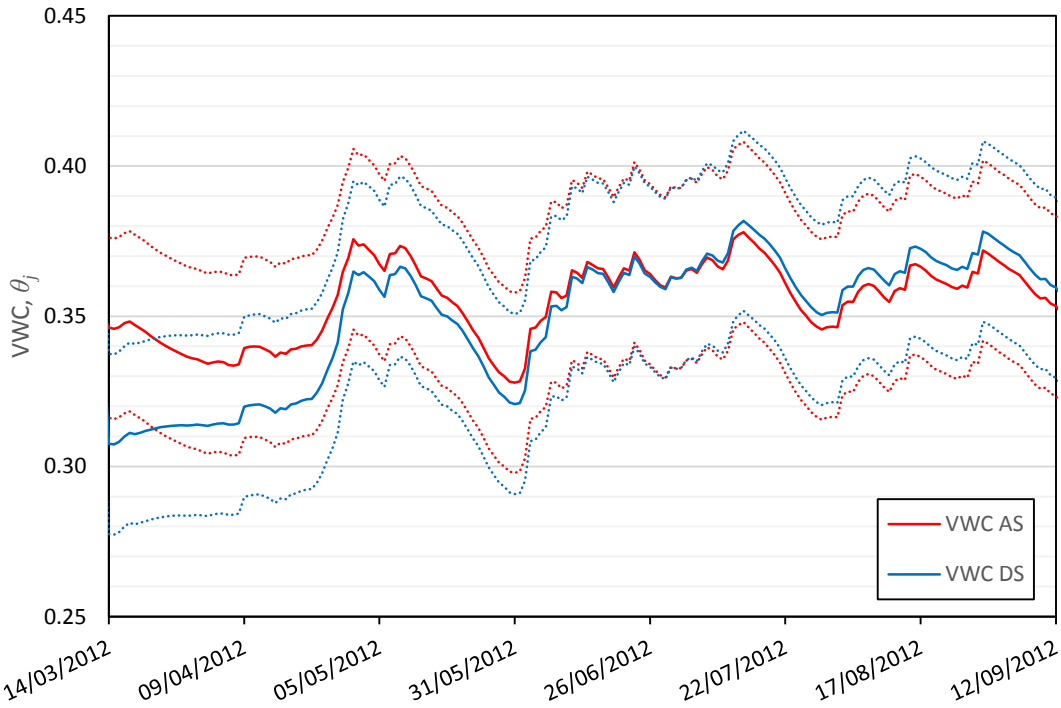

Figure 6.21 The modelled VWC of the AS and DS for CQF 2012 with a correction factor applied.

The previous paragraph shows that the simulation output with an empirical correction does not allow for comparison of sections. However, the background SMD was also found to follow trends in measured data and an empirical method of correcting the SMD data has also been assessed.

The effect of using default values of ρ_m on the SMD is shown in Figure 6.22, along with the TDR SMD. The VWC reaches above FC therefore δ_{min} = 0mm. There is an initial period of settlement of the modelled data, where SMD is marginally higher than that of the TDR SMD, after which peaks in SMD are significantly less. The soils are also not seen to be responsive at low SMD, remaining at 0mm where the TDR data shows minor peaks. A comparison of the resulting data with the initial settlement period (to the 2nd April 2012) and minor peaks (<10mm) removed (as was done for the sensitivity analysis) gives Figure 6.23, where the linear trend is δ_j (modelled) = 0.45δ_j (measured). Therefore,

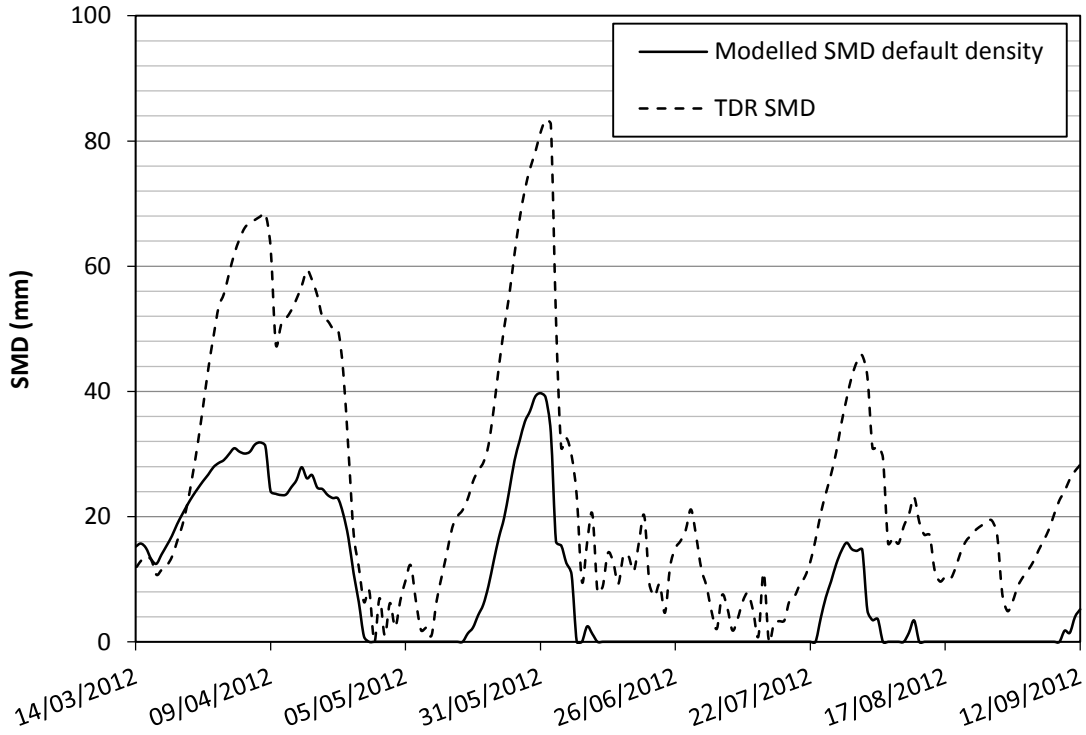

Figure 6.22 The SMD model output for CQF 2012 calculated using default density inputs.

in the tested case, at times when SMD is >10mm, the modelled data can be improved by using a correction factor of $2.22\delta_j$. The SMD modelled using this correction is within 18mm of the measured data, with the 95th percentile within 14mm and median of <3mm. Figure 6.24 shows the modelled output of SMD using this correction factor.

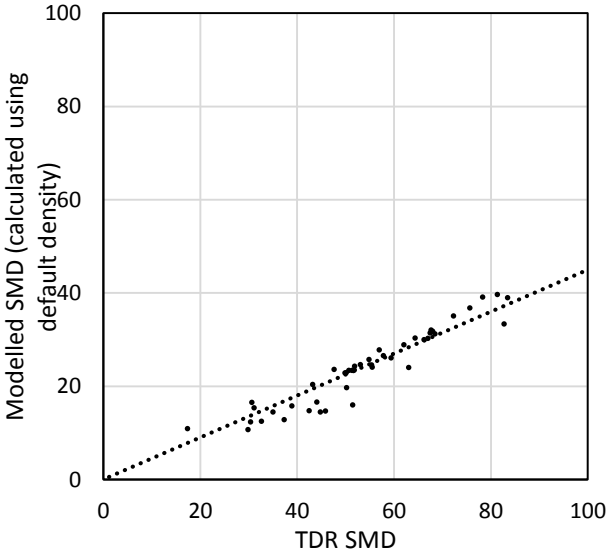

Figure 6.23 Comparison of TDR VWC with modelled VWC, calculated using default matric density.

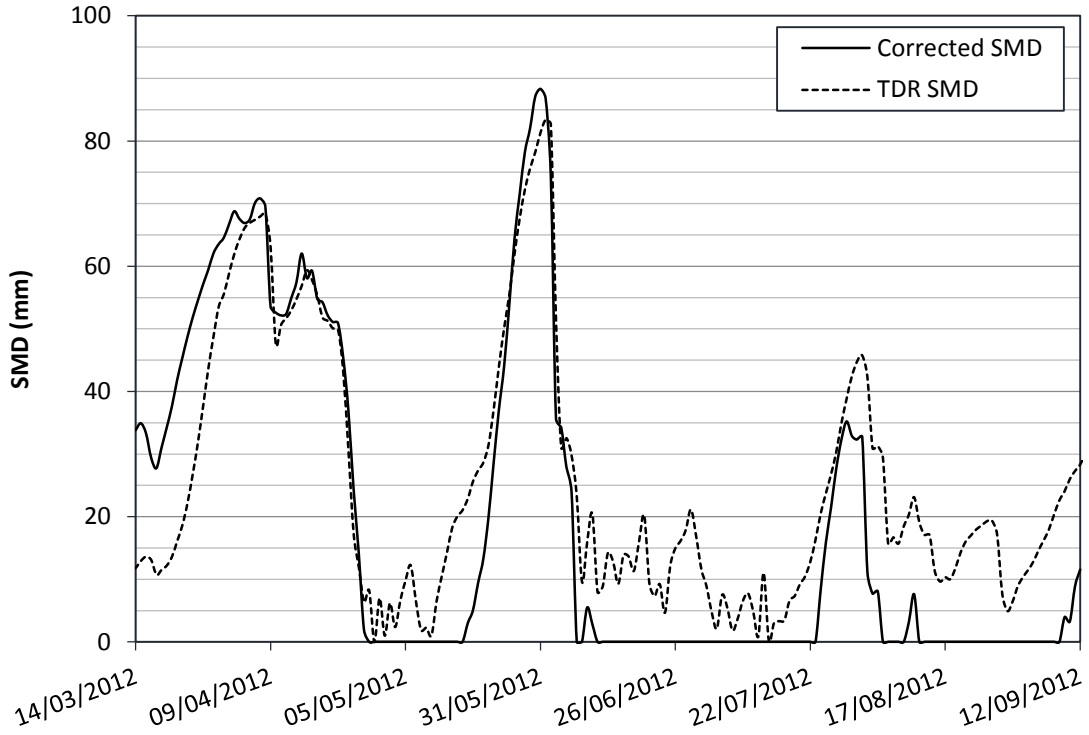

Figure 6.24 The modelled background SMD for CQF 2012 with a correction factor applied.

Figures 6.18(a-c) show that varying the soil input parameters of *C*, *S* and *OM* by the tested range, can alter the peak magnitude by up to 16mm, with this greatest sensitivity being from increases in *C* at the extreme of the tested range. However, median changes are within 5mm across the tested range for *C* and negligible for *S*, *R* and *OM*.

These analyses show that there is a sensitivity of <16mm for soil input parameters and <14mm for computational error (to the 95th percentile), and median sensitivity of <5mm for soil input parameters and <3mm for computational error. Therefore, for this tested case, SMD calculated using this method could conservatively be expected to be within 20mm of the TDR SMD. The current knowledge uses divisions of <50mm, 50-100mm and >100mm SMD to predict the likely appearance of cropmarks. Therefore, this model with an applied error of 20mm could provide useful data.

6.7.3 Wider Application

A method of correcting the modelled SMD was found for the tested case. Using default density inputs and applying a correction factor was found to give a SMD which could be expected to be within 20mm of the SMD calculated from TDR measurements.

The model with default density parameters was used to simulate SMD for CQF 2011, where crop and weather patterns vary but soil conditions are the same as the tested case. The uncorrected data has a higher SMD than the measured data for the available period. Applying the correction factor of 2.22 (as in the tested case) would increase the difference. A correction factor of 0.50 can be applied to bring the data within 15mm of the TDR SMD as shown in Figure 6.25.

The inconsistencies in the density parameters resulting in $\theta_{33(DF)}$ being greater than the $\theta_{s(DF)}$ was also the case for Clay 1 and Clay 2 at DCF. The model was therefore run using default values. Figure 6.26 shows the results of this analysis for the DCF growing season. In this case, a correction factor of 0.60 gives results typically within 20mm of the measured SMD, although at times the difference is up to ±30mm.

At DPF density input parameters did not cause any error, therefore the analysis was run using the measured data for ρ_m and a standard particle density (constrained by the model). Until the 3rd January 2012, it is not necessary to apply a correction factor for the modelled SMD to be typically within 20mm of the TDR SMD (Figure 6.27). At this time there is a greater drop in the TDR SMD than in the modelled SMD. Boddice (2014) suggested that this increase in VWC may be due to a rising water table, however he also states that equipment malfunction is possible, indicated by noisy data. Therefore, correcting modelled SMD to agree with TDR SMD, is not appropriate in this case.

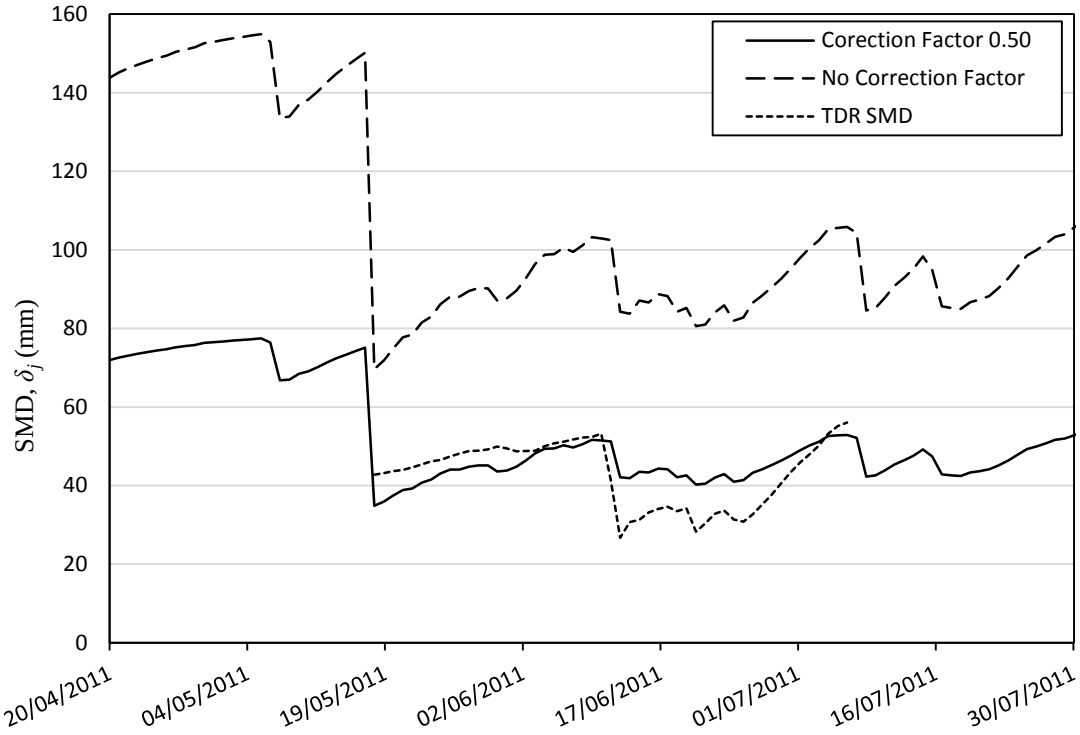

Figure 6.25 The modelled background SMD for CQF 2011 with no correction factor, and a correction factor of 0.50 applied.

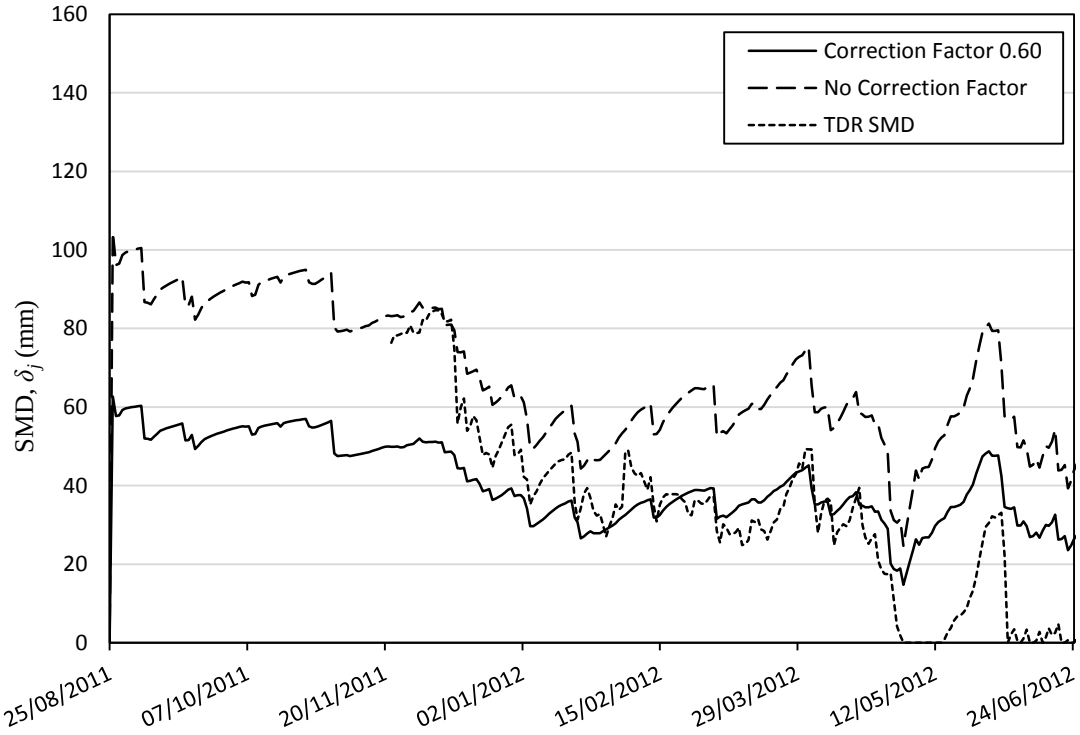

Figure 6.26 The modelled background SMD for DCF with no correction factor, and a correction factor of 0.60 applied.

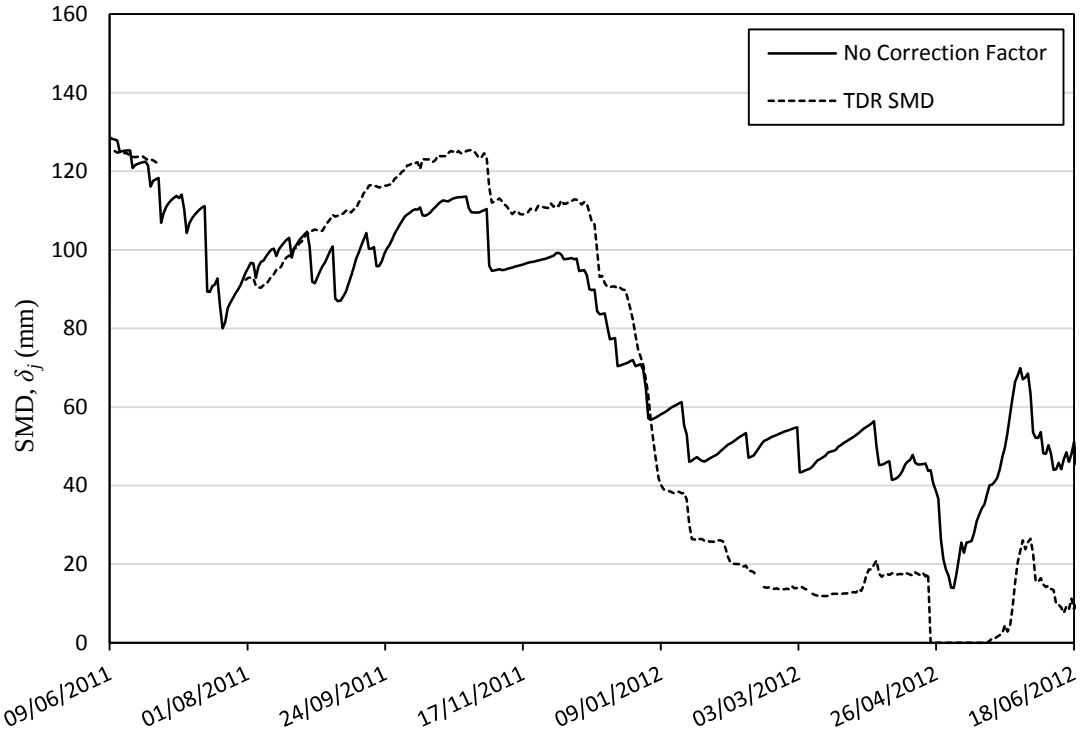

Figure 6.25 The modelled background SMD for DPF with no correction factor applied.

6.7.4 In Summary

This section has shown that, in the tested case, using the default matric density values calculated by the model for ρ_m as opposed to the higher measured values, applying a correction factor of 0.91 to the output of VWC gave results which were within 0.04 of the VWC measured by TDR. However, the differences between the sections were within this range. Therefore, although modelled results using this correction factor were accurate to 0.04, analysis of suctions calculated from the VWC would not give results which could be used to compare the sections.

For the tested case, using the default values for ρ_m the SMD was calculated from the VWC output. Applying a correction factor of 2.22 to the SMD and removing data where only minor peaks (<10mm) form, the modelled SMD was within 13mm (to the 95th percentile) of the SMD calculated from TDR measurements, with half of the data within

3mm. The current knowledge of cropmark appearance bases advice on bands of 50mm, therefore, this model with an applied error of 20mm using could provide useful data.

The method of correcting SMD for the inconsistency in density inputs was applied to other growing seasons. It was found that, even where the soil, crop and weather inputs were the same as the tested case (CQF 2011), a single correction factor was not applicable. As data were only available for three growing seasons where there are inconsistencies with the density input parameters, it is not possible to determine if there is any cause of the variation in the correction factor.

At DPF, where it was not necessary to use default density inputs as measured inputs did not cause error, the modelled SMD was found to be within 20mm of the TDR SMD for the applicable period.

6.8 MODELLING BACKGROUND SMD

6.8.1 Methodology

The previous sections showed that modelled SMD is within 20mm of the TDR SMD where density inputs do not result in error. Trends in the TDR SMD are followed where the calculated saturation VWC is below the FC, although values are inaccurate. This inconsistency cannot be overcome as the model uses a standard particle density of 2.65 Mg/m^3 which cannot be adjusted to measured values and reprogramming of the model would be necessary to directly correct this. The application of a correction factor can compensate for this issue, however no single factor fits all cases, and with only three datasets no further analysis is possible.

This section presents the modelled SMD output using soil, crop and weather inputs from database sources. The results have been compared with the model output where these

inputs are measured or known. To avoid computational inconsistencies, comparisons have been made using default density parameters. No correction factor has been applied to the outputs.

6.8.2 Database Soil Inputs

Analyses to this point have used soil input values measured in the geotechnical characterisation. This section assesses the modelled SMD output replacing the measured soil input values with soil information from the desk study, and compares the results.

To accurately reproduce measured outputs it was found that it was necessary to apply a correction factor to avoid calculation inconsistencies from density input parameters. For this assessment, the correction factor has not been applied and comparisons made with the direct outputs using default density parameters.

The BGS NGPPD held records for boreholes within the same parent materials as the locations of CQF and DCF (see Figures 4.4 and 4.13). The records, along with desk study data have been used to create soil sections for each research site, summarised in Table 6.4.

For CQF only a soil description was available, with record depth given as 0.5 mbgl. However a nearby borehole record (SP00SE24, approximately 1km away) found soils with a similar description to a depth of 4.0mbgl. Input values for *C*, *S*, and *R* were assigned to all depths in the modelled section based on the soil description. The soil descriptions for the till near DCF were similar for depths of up to 2.0m. The results of three PSD tests from samples taken at 2.0mbgl were available. The values of *C*, *S* and *R* were adjusted to fit the definitions used by the SPAW model and averaged to give a single value, and assigned to all depths in the modelled section.

Table 6.4 Soil model inputs from database sources.

		CQF	*DCF*
Data Source		EMP BH69/32	A14 TP2014A A14 TP2015A A14 TP2015B
Record Depth		0.50 mbgl	0.50-2.00 mbgl
Soil Description		Stiff grey-brown slightly sandy silty CLAY with occasional medium gravel-sized fragments of limestone with numerous rootlets at 0.50m.	Stiff fissured light grey mottled orange-brown slightly sandy CLAY with some subangular and subrounded fine to coarse flint and chalk gravel and rare cobbles.
0.0-0.5m	*C*	0.40	0.40
	S	0.20	0.17
	R	0.05	0.18
	OM	3.0 %	3.0 %
0.5-2.5m	*C*	0.40	0.40
	S	0.20	0.17
	R	0.05	0.18
	OM	0.0 %	0.0 %

For both CQF and DCF, the *OM* in the uppermost 0.5m was given a value of 3% as both are located in arable fields. Below this *OM* was assumed 0%. Default values of density were used, as was found to give the best results in modelling using measured soil inputs.

Figures 6.28(a-b) show the results of the analysis for CQF 2011 and CQF 2012 respectively along with the uncorrected SMD output using measured soil inputs. The SMD model output using database soil inputs is within 10mm of the output using measured soil inputs for CQF 2011 and within 3mm for CQF 2012. The equivalent data for DCF are shown in Figure 6.28(c), where using database soil inputs models SMD consistently between 5 and 30mm higher than the output using measured soil inputs. In this case, trends in the SMD are followed well and the graph indicates that the differences are systematic.

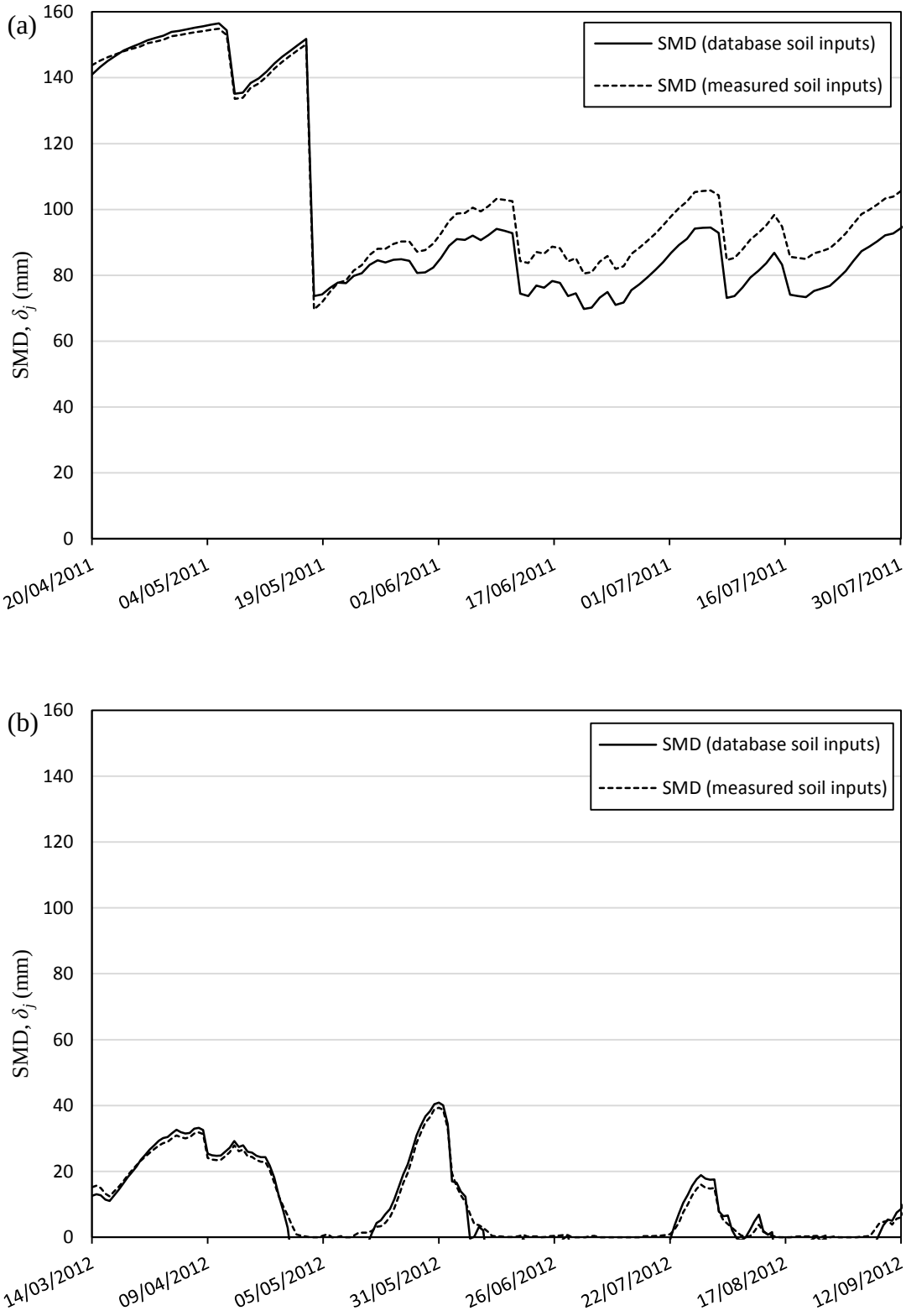

Figure 6.26 Modelling of SMD using soil database inputs.

(a) CQF 2011 (b) CQF 2012

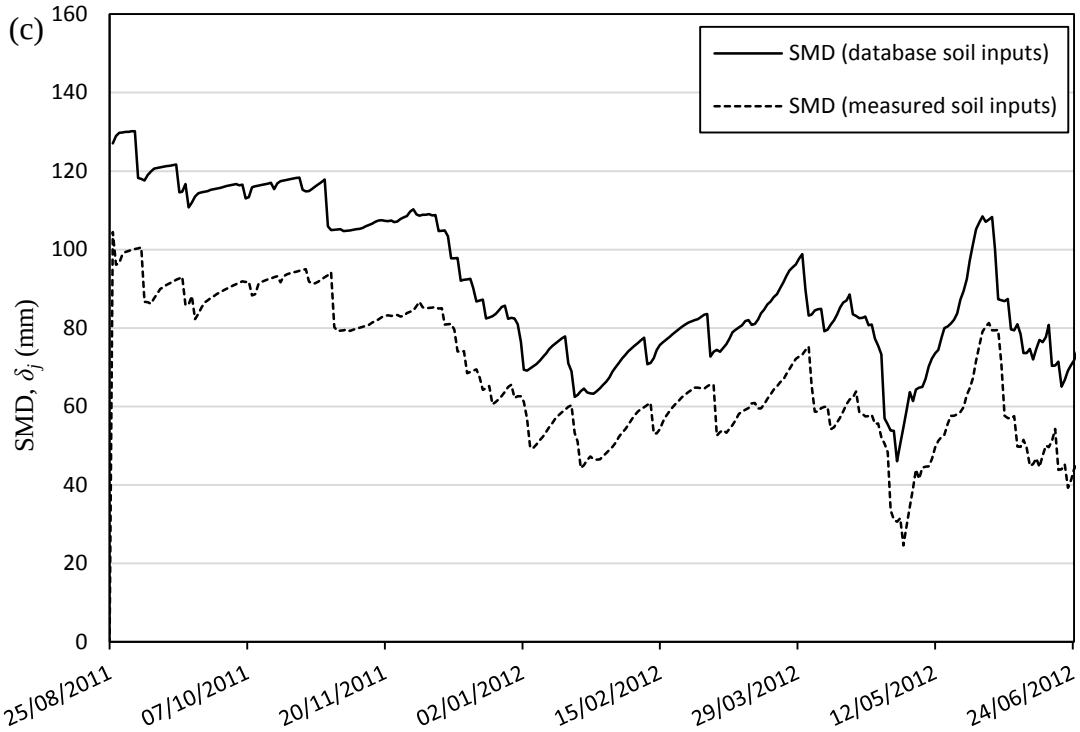

Figure 6.28(cont.) Modelling of SMD using soil database inputs.

(c) DCF

The borehole information on which the CQF soil section was built is <1km from the research location and soil inputs were similar to the measured data. The database records for DCF, although within the same soil unit, were <6km away, and most particularly *C* values were significantly greater (0.24-0.35 measured values and 0.40 database values) than was measured in the geotechnical characterisation. This wider variation in the soil parameters, possibly due to the distance from the research site, is the reason for the accuracy of the DCF data being lower than for CQF.

With only three growing seasons and two research sites, generalised comments cannot be made about the viability of using soil parameters obtained from databases as opposed to measured parameters from this analysis alone. However, the resulting differences in the SMD are directly related to the similarity of the database records to the point being measured and further information is available from the sensitivity analysis.

The sensitivity analysis showed that for the tested ranges of soil input parameters, SMD varied by a maximum of ±16mm for inputs of *C, S, R* and *OM*, with the highest sensitivity being to *C*. Default values of ρ_m are being used for both modelling methods. Although the sensitivity analysis used the one factor at a time method and combined variation of parameters may have a different effect, the median variation in *S, R* and *OM* across the tested range is negligible. Therefore, should the variability of soil parameters within a soil unit be within the tested range, the accuracy of the SMD can be indicated.

6.8.3 Example Crop Inputs

The SPAW model has a number of example crop files which can be used in place of known data. For CQF 2011 and CQF 2012 the crop file was created using known dates of drilling and harvesting. The DCF crop inputs were not known and example inputs have been used throughout all analyses. This section compares the results of using the example crop file for continuous spring wheat and compares the SMD output with that of the known crop inputs for CQF 2011 and CQF 2012. The database soil inputs have been used.

Figures 6.29(a-b) show the results of the analysis for CQF 2011 and CQF 2012 respectively. The SMD output follows a similar pattern as was seen with using database soil inputs (Figures 6.28(a-b)), with only very minor differences in the magnitude of peaks, however; using example crop inputs introduces a lag in the data of approximately 2 days.

The CQF crop files have a drilling date 30 days earlier than the example file, and a harvest date 11 days later. The earlier establishment of the crop is expected to be the cause of the time lag in SMD.

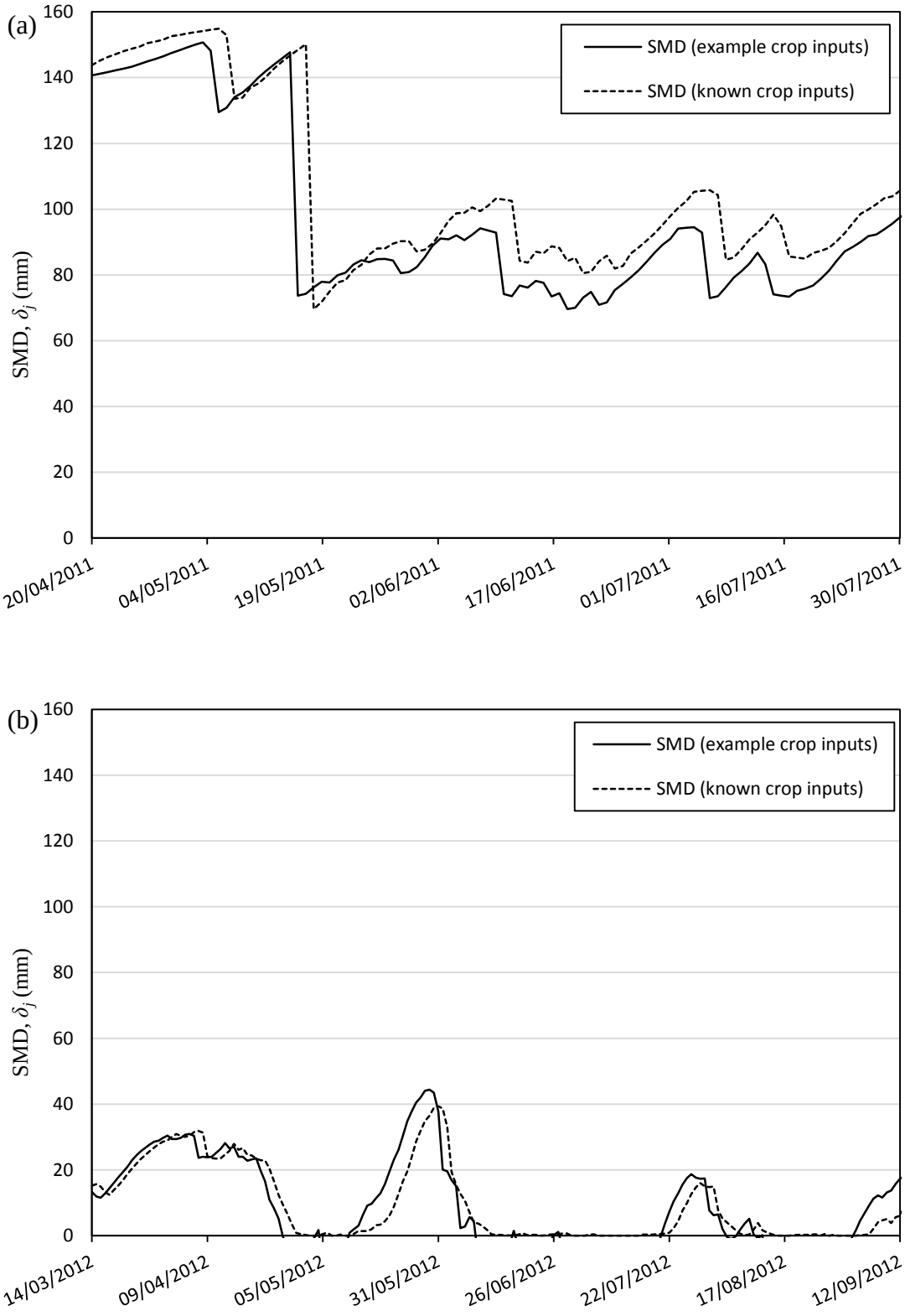

Figure 6.27 Modelling of SMD using soil database and example crop inputs.

(a) CQF 2011 (b) CQF 2012

6.8.4 Database Weather Inputs

The previous sections showed that using database soil and crop inputs gives an output SMD for CQF 2011 and CQF 2012 that reflects outputs using measured and known data with an accuracy of ±10mm (due to soil inputs) and a 2 day lag (due to crop inputs). The final replacement of measured data in the model is for weather inputs. Data from the CQF weather station has been replaced with freely available data (The Weather Channel, 2012) from a weather station approximately 8km to the west of the research location.

Precipitation, and minimum and maximum daily temperatures were obtained, although solar radiation for the calculation of evaporation was not available. An evaporation default file was created using average monthly values given in Jones and Evans (1975).

The resulting model outputs for CQF 2011 and CQF 2012 are shown in Figures 6.30(a-b) respectively. The graphs show that varying weather inputs has a much greater effect on the SMD output than soil and crop inputs. There is a general rise in SMD throughout both growing seasons, although, there are trends which can be identified. Fluctuations in SMD occur with a greater time lag than seen from using database inputs for soil and crop alone. Using database crop inputs resulted in a time lag of approximately 2 days, which is increased to 5 days with the addition of the database weather inputs.

The accumulated precipitation and evapotranspiration data for the measured and database weather have been compared in Figures 6.31(a-b). The database precipitation for both CQF 2011 and CQF 2012 is only approximately 66% and 87%, respectively, of the precipitation recorded by the onsite weather station. The evapotranspiration is 113% and 175%, respectively. The lower rainfall (water gain) and higher evapotranspiration (water losses) in the database weather is the cause of the general rise in SMD.

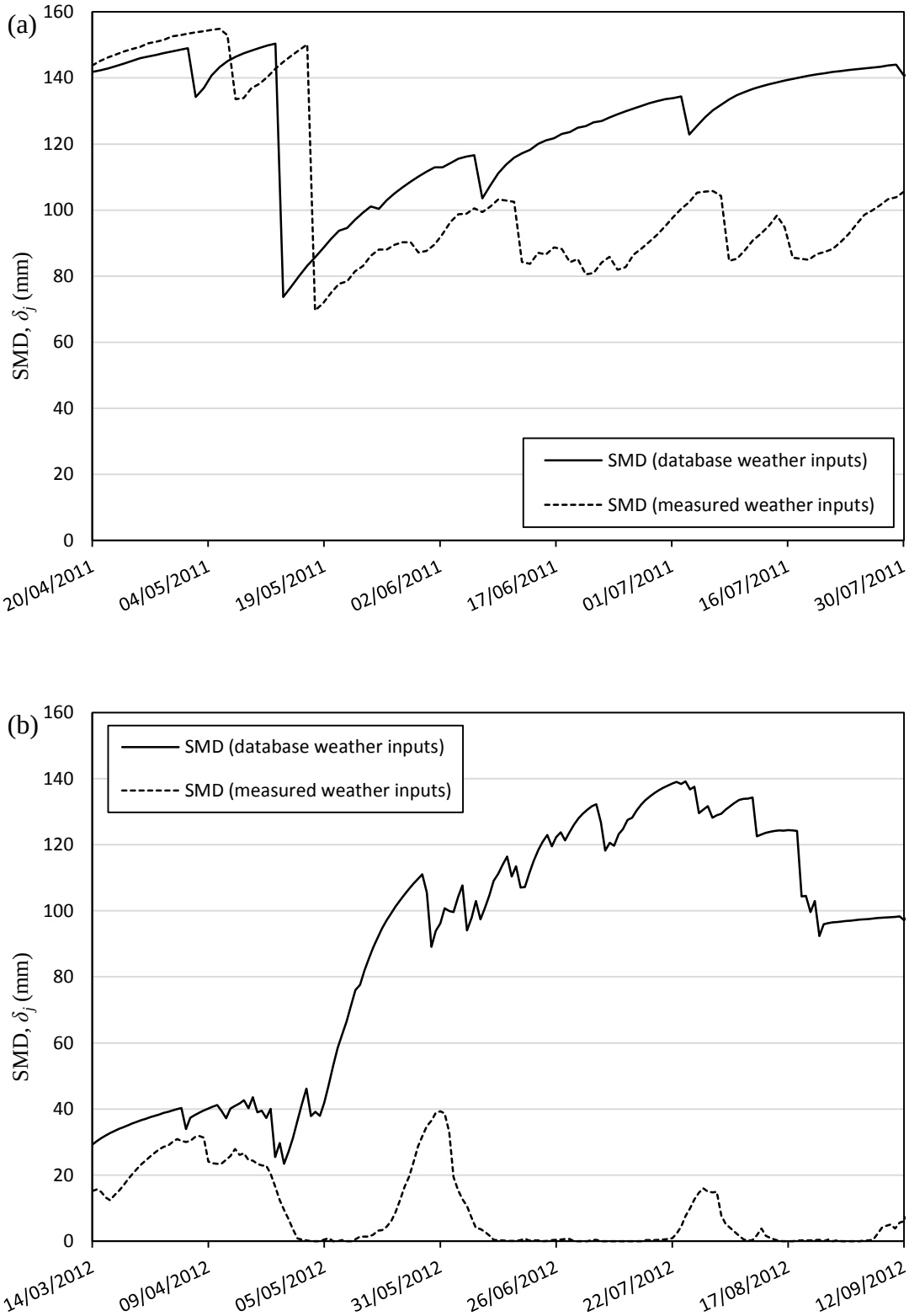

Figure 6.28 Modelling of SMD using soil database, example crop, and database weather inputs.

(a) CQF 2011 (b) CQF 2012

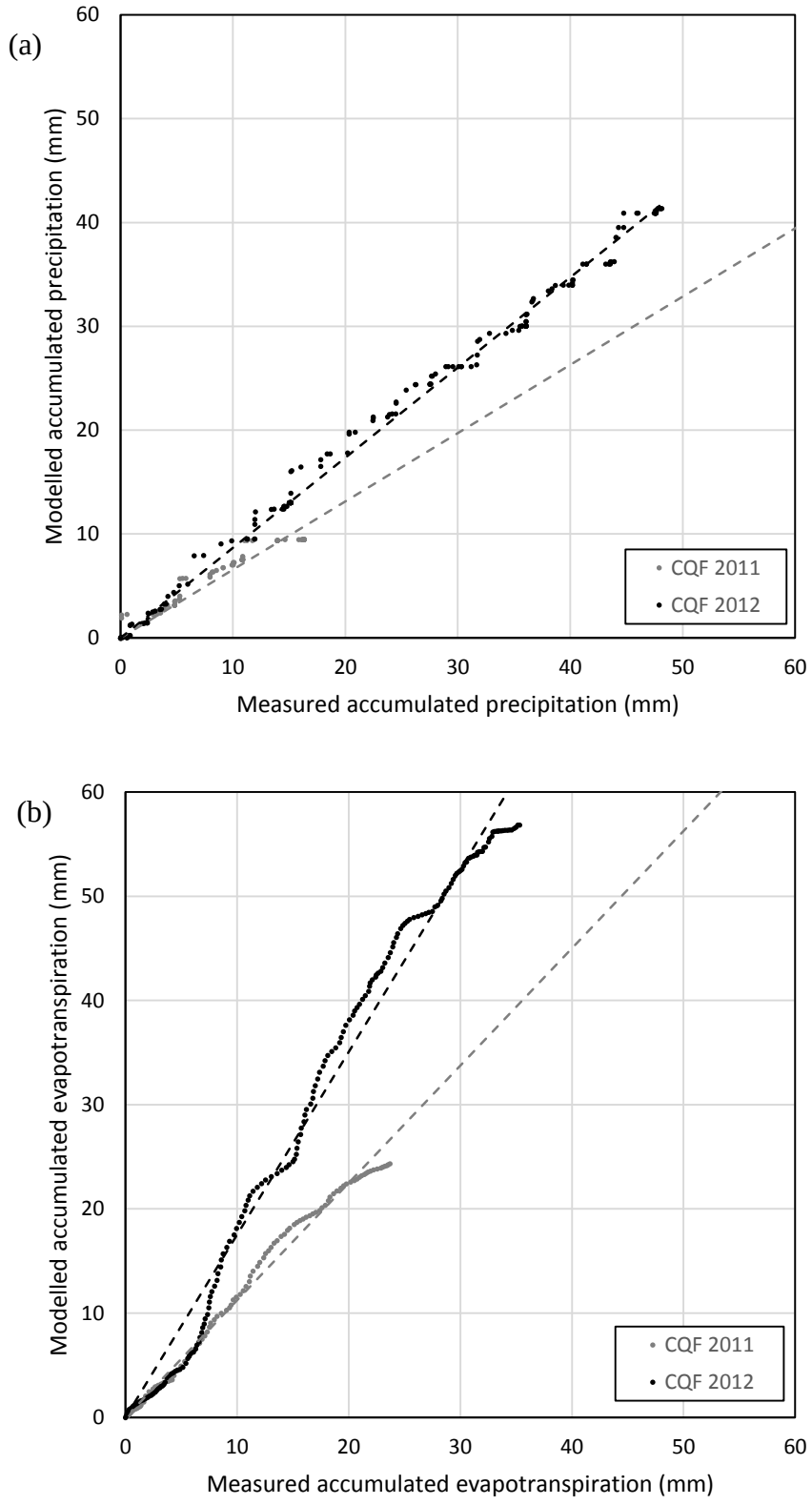

Figure 6.29 Comparisons of accumulated precipitation and evapotranspiration from measured weather data, and modelled using database weather inputs.

(a) CQF 2011 (b) CQF 2012

6.8.5 In Summary

This section assessed the effect of using soil, crop and weather inputs from database sources in place of measured and known data on the modelled SMD output. Since the correction factor, found for the tested case to compensate for model limitations, was not applicable in all cases, it was not applied in this analysis.

The sensitivity analysis (Section 6.6.2) showed that the difference in the SMD due to varying the soil parameters *C*, *S*, *R* and *OM* in the tested range was up to ±16mm, with *C* having the greatest effect. Database inputs for CQF were similar to the measured values, and were all within the tested ranges with the exception of *R* in the lower layers. In this case, results were within 10mm of the SMD modelled using measured soil data. Database values for *C* at DCF were outside the sensitivity tested range for Topsoil and Clay 1, with values of up to 0.16 higher. Using the database input values resulted in SMD being between 5-30mm higher, with systematic error evident.

Replacing known crop data with example datasets built into the model resulted in a time lag, but very little change to the values of SMD. Using weather data (precipitation and temperature) from a station 8km away, and typical monthly evaporation data in place of measured data, resulted in a significant increase in SMD in both tested cases. Some similar fluctuations were evident with a time lag of approximately 5 days, but could not be considered representative of the model output using measured weather.

6.9 CHAPTER SUMMARY

This chapter addresses four objectives of the study: the differences between the soil water characteristics of the AS and DS has been compared with the appearance of cropmarks, to determine the mechanisms of differential growth; where possible the background SMD

has been compared with the appearance of cropmarks within the same soil unit; the SPAW model with measured soil, crop and weather inputs has been assessed for use as a replacement for long-term monitoring of VWC; and the sensitivity of the SPAW model to soil input parameters has been assessed in the context of using existing soil database records in the place of measured inputs.

Long-term monitoring of the VWC using TDR in vertical sections through and adjacent to ditch features has revealed information about the mechanisms which cause differential growth. Comparisons of suctions at the level above the ditch may be affected by the natural variation of water contents in the plough soil. Cropmarks formed during both monitored growing seasons at CQF and mechanisms of their formation have been suggested through comparison of the suctions in the vertical sections, although the level of data acquired though the monitoring stations cannot confirm the suggested causes. At DCF and DPF, there was no indication of a cropmark throughout the monitoring period. Nevertheless comparisons of the suctions reveals information of the conditions in which cropmarks do not form.

The SMD of the AS at each of the research sites, calculated from TDR VWC, has been used to represent the background SMD across an area where the ground conditions are similar, within the same soil unit. Comparing this with the appearance of cropmarks over the buried features provides information on the general conditions in which cropmarks become apparent.

The results of using this analysis on the data from the research sites both confirmed and contradicted current knowledge. Near to the DPF research site, crop growing in the river terrace gravels displayed cropmarks at a high SMD of >130mm, in line with current knowledge. Aerial images taken of CQF at a background SMD of <50mm recorded both

indicative and mappable cropmarks, whereas for this clay-dominated site it was expected from the literature that a much higher SMD would be needed for a cropmark to become apparent.

The method of monitoring VWC of soils within and adjacent to buried features in the long-term has been useful both in suggesting mechanisms of cropmark appearance and comparing the background SMD with cropmark appearance. However, semi-permanent installation of monitoring stations is expensive. The chapter continues by determining whether the measured VWC from TDR can be replaced by modelled VWC whilst still giving similar results from the two analyses.

The SPAW model was chosen for application, the output tested against measured data, and a sensitivity analysis to soil input parameters carried out. For a tested case, the model was found to follow trends in both TDR VWC and TDR SMD. However, an inconsistency was found which resulted in the value of FC being greater than the saturated VWC.

Through sensitivity analysis, the cause of the inconsistency was found to be related to density inputs. The standard particle density used in model calculations did not allow for data inputs of measured matric density. This cannot be corrected within the model and reprogramming would be required to allow for high density soils (this is outside the scope of the current research).

Attempts were made to find a method of compensating for the inconsistency. For a test case, the use of SPAW model default values of density and applying a correction factor to the output of both VWC and SMD enabled the modelled output to reproduce the measured values within 0.03 for VWC and 20mm for SMD. The accuracy of the VWC was not high enough to allow reproduction of the analysis where sections are compared

to indicate the mechanisms of cropmark appearance. However, the analysis of background SMD and cropmark appearance required a lower accuracy of data, and the results were representative of TDR SMD.

The correction factor was found to vary greatly between the three growing seasons modelled, and with only three datasets it was not possible to determine the cause of the variation. Therefore, although modelled SMD can be used to indicate trends in the SMD data, without firstly reprogramming of the SPAW model to allow for high density soils and further analysis it is not possible to accurately reproduce SMD values.

Although it was not possible to find a single correction factor to correct for the inconsistencies, the model output (without correction) was compared with the output using inputs from database sources. Where possible, simulations were run using soil profiles constructed from desk study sources. It was found that the SMD output could be reproduced to within 10mm for CQF and 30mm for DCF. The greater inaccuracy at DCF was due to a larger difference between the measured soil data and the database source. The results of the sensitivity analysis showed that, for the tested ranges, SMD could be expected to be within 20mm of the TDR SMD. Therefore, should source data be representative within the tested range of a soil unit, the SMD of the unit can be determined by the SPAW model to within 20mm.

Using example crop data in the model resulted in negligible change to the SMD, but a time lag was introduced. Using database weather data had the greatest effect on the model output. Some similar fluctuations were evident that could indicate a time lag, but the simulated values could not be considered representative of those using data from the onsite weather stations.

This chapter has used measured data to indicate, where possible, mechanisms of cropmark appearance through comparison of suctions in feature and adjacent soils, and compared background SMD with cropmark appearance to determine the general conditions in which cropmarks form. The measured data has been progressively replaced by modelled data and data from desk study sources, and the effect on the results assessed. Using modelled data and data from desk study sources reduces the need for costly and destructive intrusive works.

The following chapter proposes and tests three simple models that use only existing data, and can provide further information on the conditions in which cropmarks appear.

CHAPTER 7. METHODS OF CROPMARK ANALYSIS

7.1 INTRODUCTION

The literature review showed that current practice in aerial archaeology uses a very simple model as an indicator of likely cropmark appearance. Values of >50mm SMD indicate cropmark appearance in areas of coarse grained or shallow soils, and >100mm SMD in areas of fine grained soils.

Three simple methods have been developed as part of the current research to improve the understanding of the ranges of SMD at times when cropmarks appear over differing ground conditions. Based primarily on data acquired in the desk study, the methods have been used to evaluate current practice and show the type and level of information which can be obtained from each method.

There is a wealth of existing information relating to the archaeological record, geological and soil mapping, and historical weather data that can be easily accessed and utilised. The methods presented to evaluate current practice have been designed to maximise the use of these existing datasets to obtain information without the need for expensive research methods. There is, however, inherent bias in the aerial image archive which has resulted from the need to maximise the productivity of aerial reconnaissance programmes.

Each of the methods focuses on assessing a different aspect of aerial reconnaissance. The first method, “the cropmark approach”, looks at individual sites and compares the appearance of cropmarks indicating their presence with the SMD in the lead up to, and at the time of, imaging. Although the method uses only factual data with no assumptions

made to mitigate bias, it provides a range of SMD in which a site has been positively identified as a cropmark.

The second method, "the flight productivity approach", assesses historical sorties and determines how successful they were in recording cropmarks at the SMD in which they were flown. It uses the same data sources and has a similar process as the first method, although by making assumptions, the bias in the datasets is mitigated where possible. This method results in data which can be statistically analysed to determine a productivity for each sortie.

The third method, "the ground conditions approach", assesses areas of a single background soil type and ground cover for the appearance of cropmarks at known SMDs. The definition of "background soil type" refers to the soils in the area in which a feature is located, not the soils forming the feature. The definition of "ground cover" refers to the land use, for example cereal crops or grazing. The method divides a study area into cells of a known area where both the background soil type and ground cover are unique, grading each cell with respect to the appearance of cropmarks over particular feature types across a range of SMDs.

The first two methods only require data which already exists, available from sources such as Historic England (HE), the British Geological Survey (BGS) and the Environment Agency (EA). They bring together records from the National Record of the Historic Environment (NRHE), geological and soil mapping and historical SMD data. The third method could also be carried out using only existing data, though in the example case used in this study it has been complemented with additional aerial images collected by the DART project to increase the dataset.

This chapter presents the methodologies for each of the three approaches and the results of application to the research locations. The results of the analyses provide valuable information on the appearance of cropmarks with respect to SMD, considering both the types of features and the background soil types in which they are located.

7.2 DATA SOURCES

7.2.1 Archaeological Records

The NRHE is a database of sites of historical and archaeological interest. Over 420000 records of sites can be searched via the pastscape website (Historic England, 2015b) A simple search for the keyword "cropmarks" returns over 24200 records. Each of the records provides a short description, a location as a grid reference, and the source data for the record. These source data give any reference numbers of historical aerial images which have been used create the record. It follows that these source images display cropmarks allowing the geometry of the feature to be mapped. The cropmark and flight productivity approach cross reference these data with the Historic England Archive (HEA), which can provide the image dates by the reference number.

The results used in this study are given in Tables 4.1 and 4.3. Additional data may be available from archaeological studies. For the ground conditions approach, data held by HE acquired by the NMP was requested and provided in a Geographical Information System (GIS) format which was added to the dataset.

7.2.2 Background Soil Information

The BGS holds a wealth of data which can be accessed free of charge via their website (http://www.bgs.ac.uk/). Online viewers such as the Geology of Britain Viewer and the GeoIndex Viewer allow a user to display layers relating to bedrock and superficial geology, borehole data, geochemistry, geophysics, hydrogeology and terrain, amongst

many others. Geology maps (at 1:635 000 scale) in GIS format and some parameters of the soil parent material model (at 1km scale) are also available for free download. Should additional or smaller-scale data be required, licences can be purchased for use of data.

Another source of soil data is the Land Information System (LandIS) provided by the Cranfield Soil and AgriFood Institite. LandIS provides a NATMAP vector map, which is a 1:250 000 digital soil map of England and Wales that gives written descriptions of the soil types and associated data. As with the BGS data, a simplified version is available as the soilscapes online viewer, where soils are divided into 27 categories based on properties such as texture, drainage, land cover and fertility.

7.2.3 Historical SMD

Historical SMD data are available on request from both the Met Office and the EA. The Met Office use the MORECS model, which has been described in Section 2.4.4. It is understood that the EA use SMD values which are based on the MORECS model, although adjustments are made to the data before publication. Each region has its own modifications to the MORECS data, though the details of these calculations are unavailable. A monthly situation report is published for each region, which includes some information on SMD (such as a value at the month end or a range to the nearest 10mm). More detailed information was made available free of charge on request.

7.2.4 Aerial Images

The HEA holds historical aerial images which are searchable by location and provide an image date. This database was used for cross referencing images with records in the NRHE for the first two methods.

The ground conditions approach benefits from a large dataset of aerial images. In this study, a total of 246 vertical and oblique images were obtained from the HEA and the

DART Project. In addition results of 1 NERC and 2 EA hyperspectral (though only assessing the resulting image within the visible spectrum) sorties of the study area, flown as part of the DART Project, were used. A small number of undated images in the dataset were reviewed to aid the mapping of markings, though these could not be compared with SMD, and were not included in further analysis. Images were found for 39 dates, stretching from 10/04/1946 to 06/10/2012, though not all dates cover the entire study area. Where an area has not been imaged on a particular date, no data have been recorded for analysis.

7.2.5 Mapping

The ground conditions approach requires further information which can help determine the locations of any buried features within a study area. Since modern buried features such as utilities may be present, utilities maps from sources such as the National Grid were used. Historical mapping can reveal features such as old field boundaries. Historical OS maps have been used to determine the locations of extinct features which may appear as cropmarks. The maps reviewed in for this study are listed the Desk Study in Tables 4.2 and 4.4.

The resulting information from mapping can rule out cropmarks over modern or recent buried features, though in this study they have been included to widen knowledge of the appearance of cropmarks over a variety of buried features, not just those relating to archaeology.

7.2.6 Information from the Land Owner

Land owners can provide a wealth of information relating to soils, ground cover, buried features, and known locations of cropmarks. For the Cirencester study area, the RAU provided information including: the locations of modern services; the locations of

cropmarks which appear commonly; land drainage maps; and crop data throughout the monitoring period.

7.3 DATA BIAS

7.3.1 Aerial Images

There are a number of biases related to the conditions in which an aerial image was taken and the suitability of the image for analysis of surface features, for example:

1. The clarity of the air, influenced by factors such as haze, mist, fog or cloud cover, may mask surface features.
2. The time of day when images were taken may also affect the visibility of cropmarks. A low sun angle can cause shadowing where crops above a feature are of a different height to those adjacent to it.
3. Vertical and oblique camera angles can reveal different information about the ground surface.
4. Older images may be of lower quality or lower resolution than those taken with more modern cameras, and might not reveal cropmarks which may have been present.
5. The altitude of the camera may affect the resolution.
6. Monochromatic images may reveal features that are less easily noticeable on panchromatic images, and vice versa.
7. The alignment of oblique images compared to the alignment of features can also affect the visibility. Images taken perpendicular to a linear feature may not record as striking a cropmark as where the image is aligned with the feature.

Due to these biases, the purpose of the image being taken is important. Early photographs, mostly dated between the 1940's and 1960's, were taken by the RAF for

reconnaissance and mapping, commissioned by the Ordnance Survey. These older images are all monochromatic, vertical, and taken from a greater height than those for archaeological prospection. They are also taken on sorties with predetermined flight paths at a given altitude. More recent images taken for archaeological research are commonly taken as oblique and both monochromatic and panchromatic. The flight paths are directed by the aerial archaeologist on board, allowing for circling of an area of interest. This means that images can be taken in optimised conditions, for example, aligning the aircraft with features or avoiding cloud cover.

7.3.2 SMD at the Time of Imaging

Since the 1970's, most sites have been recorded during flights in the summer months, reflecting the introduction of the RCHME annual national reconnaissance programme, where the purpose of the image was to document historic and archaeological features. Planning flights at higher SMD using the predictive model outlined in Section 2.4.3 has perpetuated this bias. This results in larger representation in the dataset of successful sorties at high and rising SMD. Figure 7.1 shows the number of sorties which recorded cropmarks grouped by the months of the year for the tested dataset. The data from near the Cirencester research location have also been divided into those images taken for mapping and archaeological prospection purposes. Unfortunately, information was not available to split the data from near the Diddington research location in this way. The results show that mapping sorties were made over all seasons without flying in climatic conditions considered optimal for archaeological prospection, whereas archaeological reconnaissance sorties were most commonly made in June and July in the "flying season".

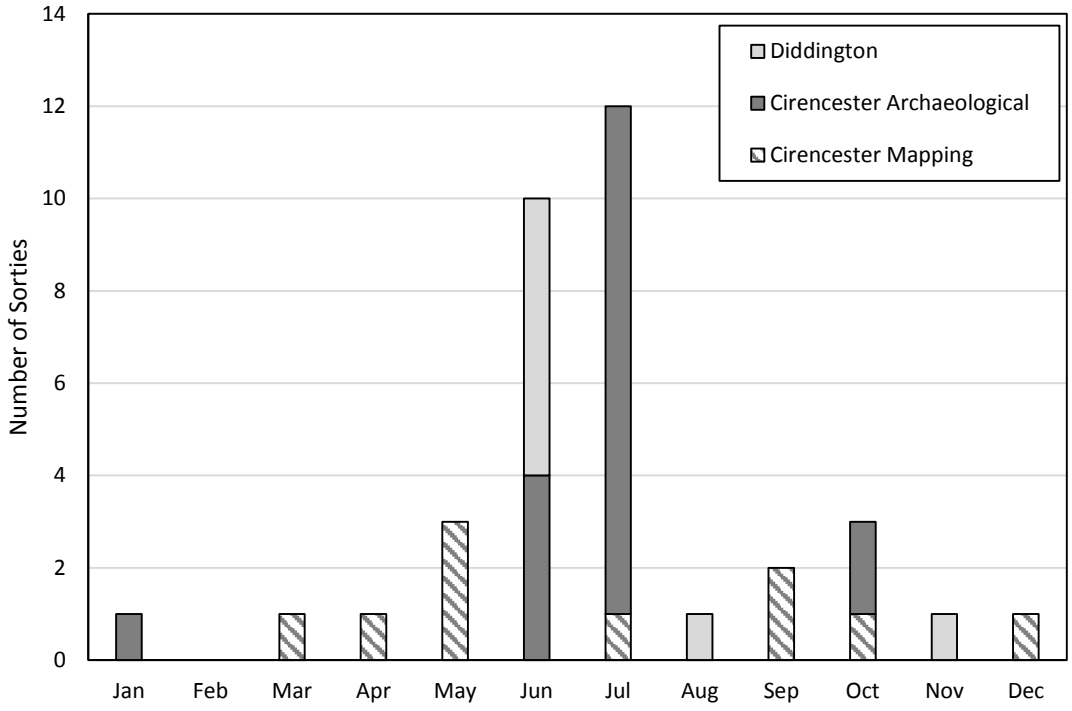

Figure 7.1 The sorties that provided images forming the archaeological record in the study areas by month of the year.

7.3.3 Negative Data

Perhaps the most important gap in the data in terms of analysis is the lack of negative data, that is, there are no records to confirm that a site was not visible as a cropmark at a given date or SMD. Images for mapping purposes may show that a cropmark was not apparent, although the image would not be listed as a data source in the NRHE. Sorties may have been made over an area at times other than the dates where images have entered the record, although if no cropmark was evident no image was taken, and a negative data point for analysis was not recorded. In order to carry out any statistical analysis of the SMD at times of cropmark appearance it is necessary to have negative data.

7.4 METHOD 1: THE CROPMARK APPROACH

7.4.1 Methodology

The cropmark approach is a simple comparison of archaeological and geological datasets reviewed in the desk study compared with historical SMD data. The methodology is summarised in Figure 7.2, which shows the four data sources, the processes and outputs of the analysis to determine the SMD in the lead up to, and at the time of, cropmark appearance at the location of a site.

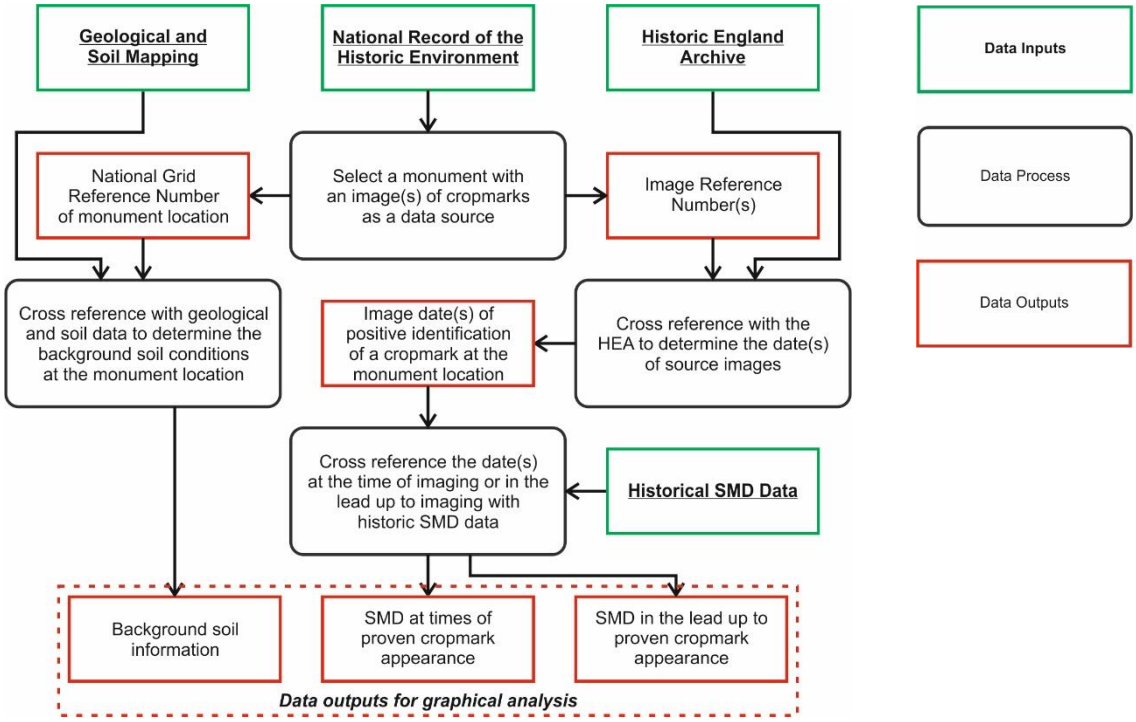

Figure 7.2 Method 1, the cropmark approach.

The metadata for a site in the NRHE gives a National Grid Reference, which is compared with geological and soil mapping to determine the background soil type (with information such as dominant particle size and soil depth) in which the buried feature lies. The site source information gives reference numbers of any images which were used in the creation of the record. These numbers are cross-referenced with the HEA to determine the dates where the source images of a site appearing as a cropmark were

taken. The dates are compared with historical SMD data for the area to determine the SMD in the lead up to, and at the time of, imaging.

7.4.2 Data

Search areas with a radii of 2km around the approximate centre of each of the two research locations were chosen for analysis. The NRHE was searched, returning 89 and 52 records at the Cirencester and Diddington research locations respectively. These records were manually filtered to determine a total of 61 and 21 sitess which were recorded with cropmarks as a source of data. Of those, 43 and 14 included source data which could be cross referenced with the HEA to determine dates of images. Those sites and source data have been summarised in the Desk Study in Tables 4.1 and 4.3.

The NRHE gives national grid references for each site using either 4, 5 or 6 figures (that is, the reference itself is accurate to between 1 and 100m). Although there is some variation in the accuracy of the location, it should be borne in mind that the cropmarks indicating these sites may cover an area and only an approximate centre is provided. The locations of each of these sites identified as cropmarks have been plotted in the desk study in Figures 4.6 and 4.14, each with an identification number.

The underlying background soil information for each site has been determined from the data arising in the geological and geotechnical setting in the desk study (see Sections 4.3.2.3 and 4.3.3.3). The four background soil types present have been classified as: alluvium; shallow Cornbrash Limestone; shallow Forest Marble Limestone; and clay of the Forest Marble Mudstone.

Historical SMD data were provided by the EA, South East Region (for the Cirencester research location) and the EA, Anglian Region (for the Diddington research location).

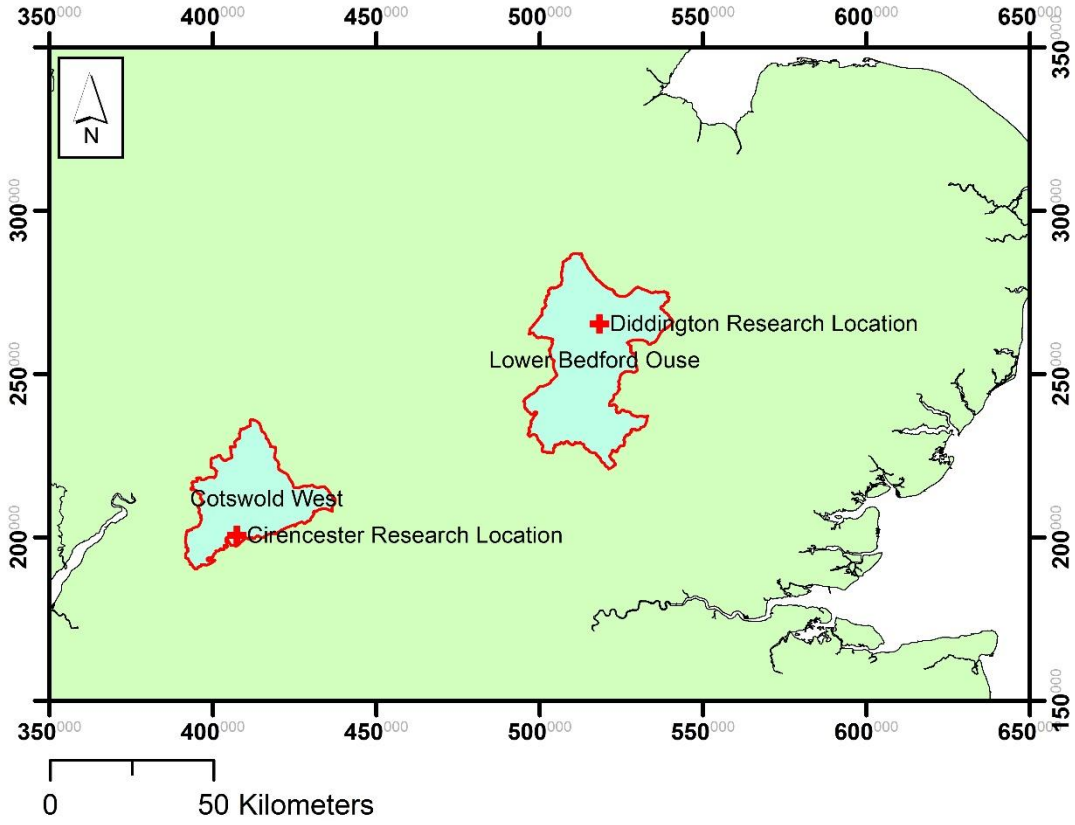

Figure 7.3 The areas covered by the EA SMD data.

The two regions calculate and disseminate data separately, so the SMD data made available for study differs for each research location. The two areas over which the historical SMD has been calculated are shown in Figure 7.3. The data for the Cirencester research location have been calculated over an area of 966km^2, defined by the EA as Cotswold West, part of the West Thames Area. The equivalent area in which the Diddington research location lies is the Lower Bedford Ouse, part of the Cambridgeshire and Bedfordshire Area, covering and area of 1575km^2. The SMD data are based on information provided by the MET Office using the MORECS (Met Office Rainfall and Evaporation Calculation System) model over 40km grid squares. The MORECS figures have been adjusted by the EA using their own models.

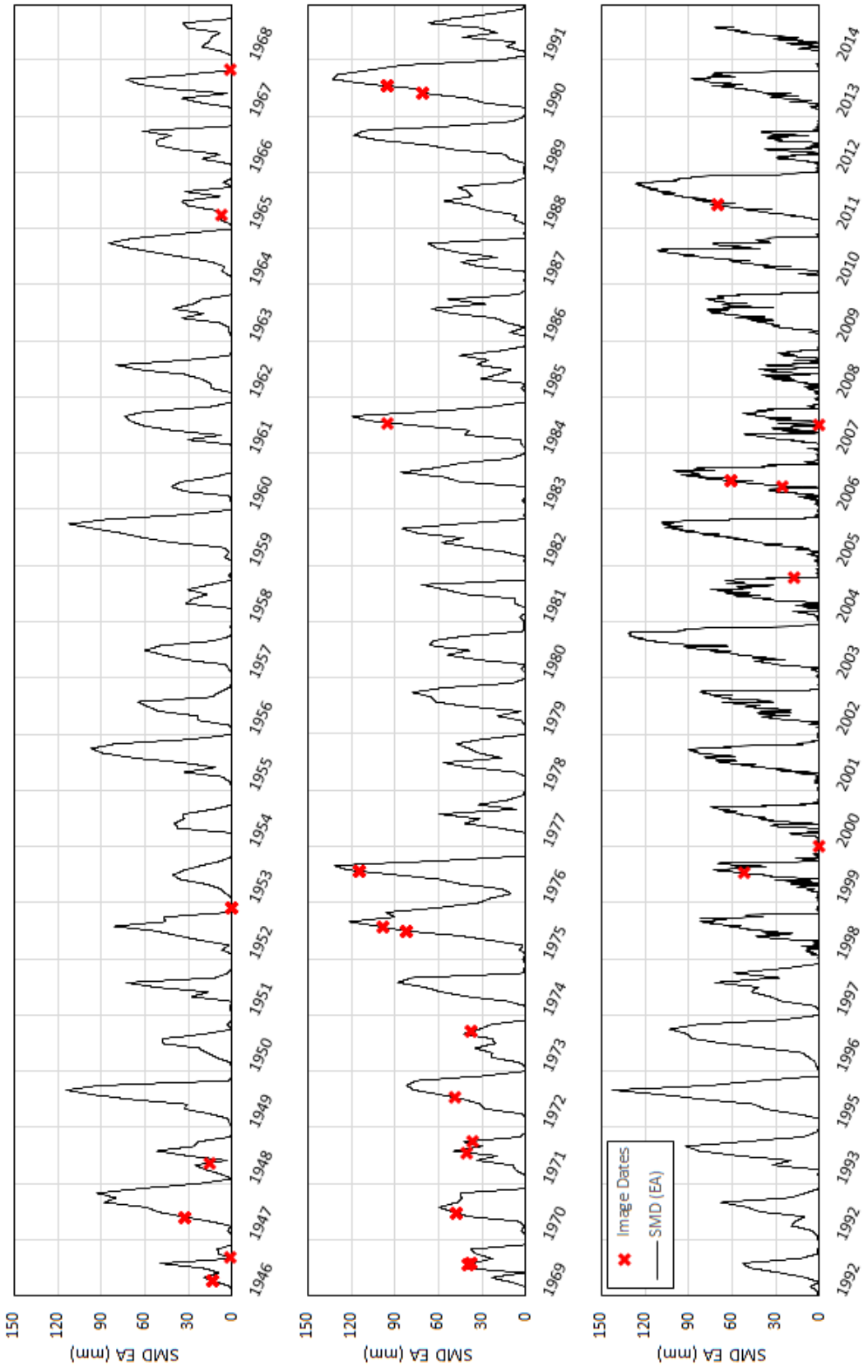

Figure 7.4 Example of the SMD data provided by the EA for the Cotswold West Area.

SMD for Cotswold West stretched back to 31st January 1946, and monthly values for the last date in each month were provided up until the end of 1997. From the 1st January 1999, daily data have been made available. For the Lower Bedford Ouse, records began on the 3rd January 1961 and weekly values were provided for the full period. In both datasets, where daily data were unavailable a linear interpolation of the values has been used to allow for comparison with the dates of any images forming the archaeological record. An example of the resulting data for Cotswold West has been plotted in Figure 7.4, along with the dates of referenced archived images. The yearly pattern of rising SMD during the summer months and falling SMD during the wet winter months is evident, with the largest summer peaks indicating the driest years.

7.4.3 Results

Figure 7.5 shows the recorded sites grouped by the underlying geology, plotted against the historical SMD at the date of images which revealed them as cropmarks. The colours of the underlying geologies are as in the geological mapping (Figures 4.4 and 4.12), and records from the area near to the Cirencester Research Location are shown in boxes and those near to the Diddington Research Location are in circles.

Only six sorties over the Diddington location recorded sites, with one very successful flight at 109mm SMD being responsible for 7 of the 14 records. Only one sortie flown at a SMD of below 80mm (5mm) was successful in adding to the record, although only one site was recorded in the till.

Figure 7.5 shows that in the Cirencester study area, cropmarks occur across a wide range of SMD in all background soil types. Although sites have been recorded over the full range of SMD, in some cases there tends to be a narrower range of SMD for which each

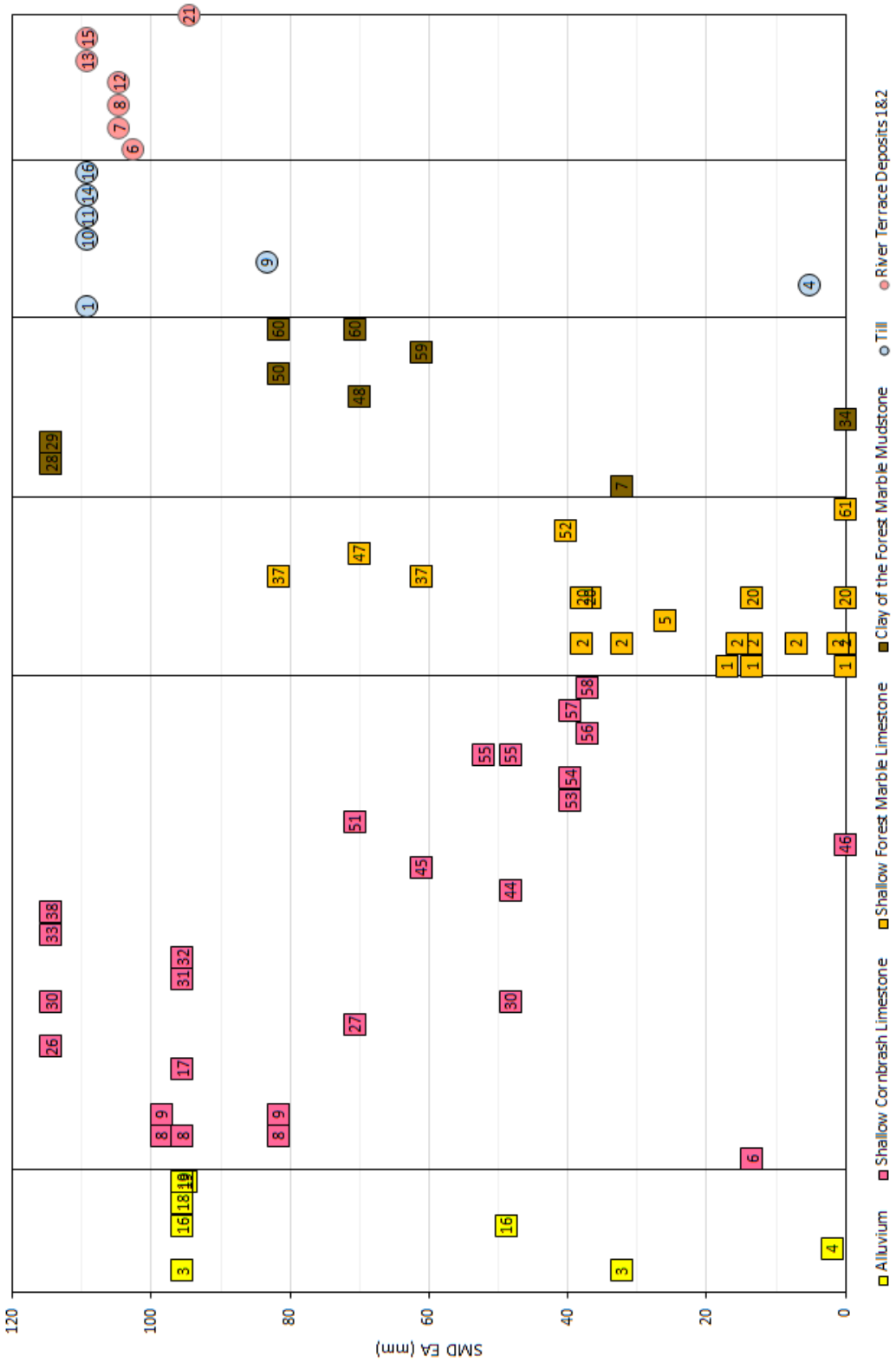

Figure 7.5 The appearance of cropmarks over sites by background soil type and SMD.

individual site will appear. For example, over shallow limestone site ID 8 was recorded on three occasions between 80-100mm SMD, but never outside this range. Similarly, sites ID 1, 2 and 20 were recorded during a number of sorties, though never above 40mm

SMD. Figure 7.6 shows the number of sites from near the Cirencester research location which were recoded only below, only above and both above and below 50mm SMD. Since a single sortie could be assumed to cover this small area, a column of the totals has been included. Only 4 of all the sites in the area were recorded as cropmarks at both high and low SMD, and more showed at >50mm SMD (22), than <50mm SMD (17). However, had the area only been flown at SMDs of >50mm, then 17 of the total 43 sites in the area would not have been recorded, mostly those over shallow rock.

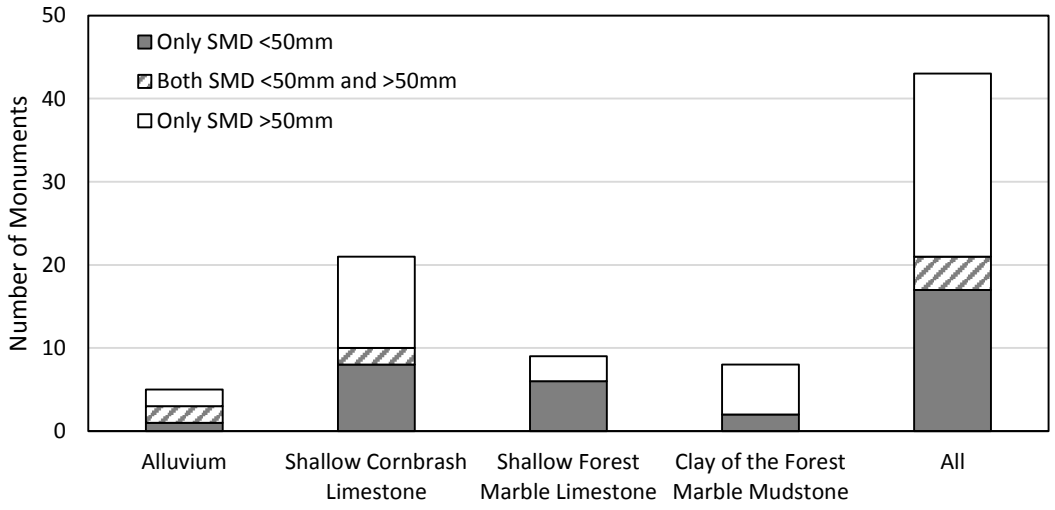

Figure 7.6 Number of sites appearing as a cropmark above and below 50mm SMD by background soil type.

Cropmarks occur due to the differential growth of a crop rooted in, or near to, a subsurface feature from the surrounding area. The onset of differential growth can occur at any time during the life of the crop from germination to maturity, although it may become more apparent and develop as a cropmark at times where the growth of the crop enters a new stage. If the rate of growth is impeded at an early stage, the crop may show differences in appearance even after the differential soil conditions have equalised and the rate of growth returns to that of the surrounding crops. Therefore, the SMD at the

date of a proven cropmark appearance alone may not be indicative of differential growth, but the conditions preceding the image date must also be of importance, possibly as far back as the drilling of the crop.

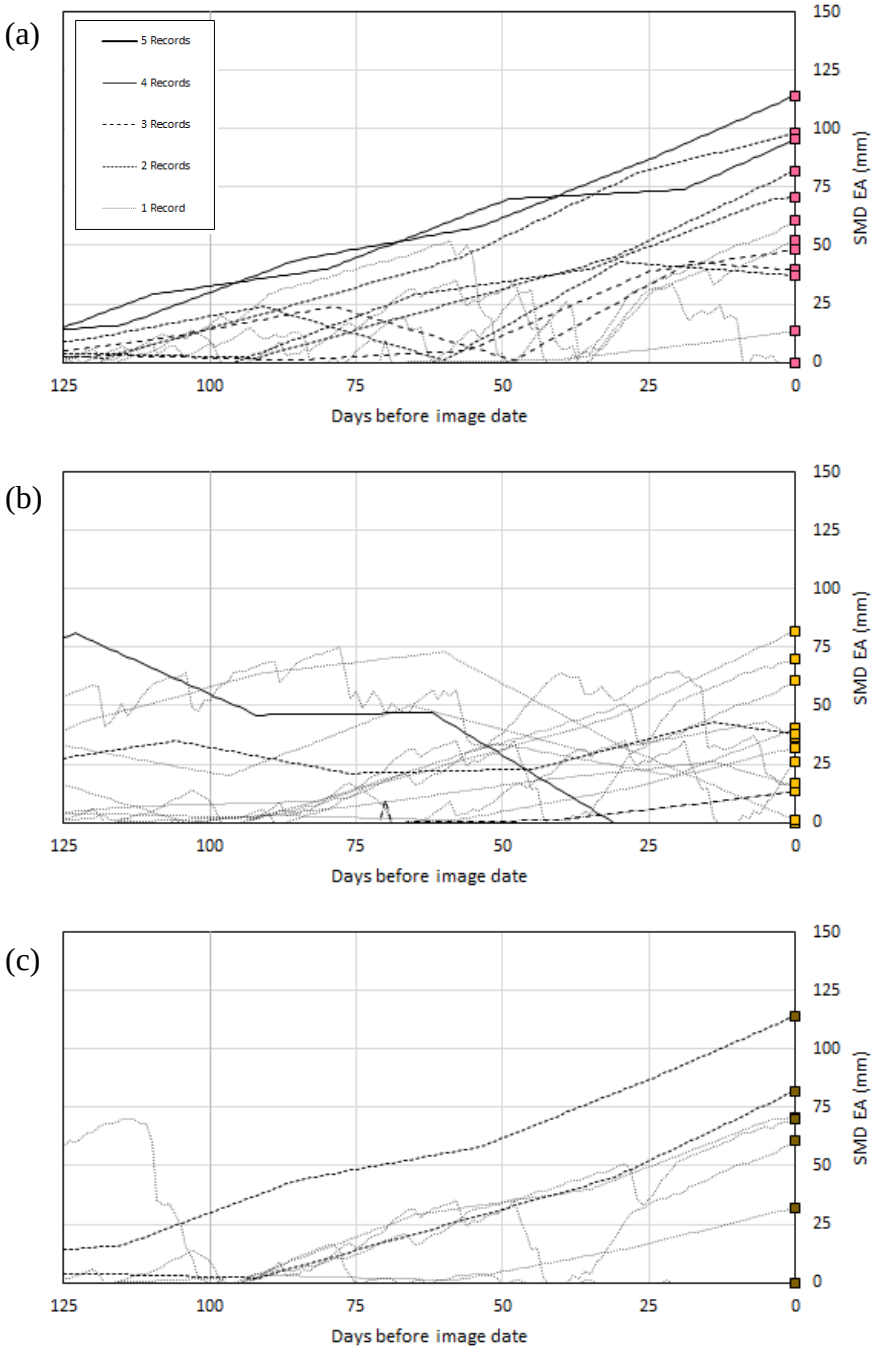

Figure 7.7 SMD in the lead up to proven cropmark appearance.

(a) Shallow Cornbrash Limestone (b) Shallow Forest Marble Limestone
(c) Clay of the Forest Marble Mudstone

Figures 7.7(a-c) show the SMD for the 125 days prior to the image dates of proven cropmark occurrence for the background soil types of shallow Cornbrash Limestone, shallow Forest Marble Limestone and the clay of the Forest Marble Mudstone. Each line represents the SMD in the lead up to a single sortie, and the format of the lines indicates the number of sites recorded for the flight.

With the exception of the shallow Forest Marble Limestone, most cropmarks were recorded at times of rising SMD, and those most successful sorties are typically flown at higher SMD. This pattern is also seen for all background soil types. However, the most successful sortie over the shallow Forest Marble Limestone, where 4 sites were recorded, was at 0mm SMD.

From these results it could be concluded that high and rising SMD is an indicator of the likely appearance of cropmarks, which does concur with the information found in the literature review. However, bias in the dataset towards flights in the summer months may undermine this conclusion. The flight productivity approach addresses this bias.

7.4.4 Discussion

There may be ranges of SMD in which individual sites become apparent as a cropmark which are not always at the higher SMD expected from the literature review. There are some features which have only been recorded at SMDs lower than the 50mm value used as an indicator of cropmark appearance in current practice. Most commonly those which show at higher SMD do not also show at low SMD. Within the Cirencester study area, should images have not been taken at lower SMD, the population of the archaeological record would be reduced by approximately 40%.

The results from applying the cropmark approach to the Cirencester study area show that, with the exception of the shallow Forest Marble Limestone, sorties made at times of

rising and high SMD are more successful in recording cropmarks. However, bias due to the purpose of the image being taken and a high representation of sorties made in the summer months may skew the results.

The highest representation of features appearing at low SMD are over shallow limestone. A mechanism of cropmark appearance is the hampering of root development due to shallow rock (see Section 2.3.5). If root development were the primary cause of differential crop growth, an even distribution of cropmark appearance over the full range SMDs would be expected. This is the case over the Cornbrash Limestone, but over the Forest Marble Limestone more features are apparent in ranges below 50mm SMD, indicating that SMD is likely to be a factor in cropmark appearance.

In current practice, very high SMD of >100mm is used as an indicator of likely appearance of cropmarks over areas of clays soils. In the cropmark approach, of the 8 sites which are located over the clay of the Forest Marble Mudstone, 6 have only been imaged below 100mm SMD. However, only one of these has been imaged more than once, and this limited dataset may be too small to draw generalised conclusions relating to ranges of SMD in which sites appear.

Assessing the SMD in the lead up to a known cropmark appearance may be of interest as onset of differential growth can occur at any time throughout the growth of a crop. The results show that times of rising SMD indicate increased cropmark appearance. However, because of the tendency of images in the historical archive to be from the summer months, this may not be a true representation. If it were possible to use a dataset without this bias, analysis of the SMD in the lead up to cropmark appearance would provide further information.

7.5 METHOD 2: THE FLIGHT PRODUCTIVITY APPROACH

7.5.1 Methodology

The flight productivity approach is a continuation of the cropmark approach which mitigates bias in the resulting data. It takes the data a step further by considering an area as opposed to single sites. The data inputs and some of the processes are the same, although the bias relating to the greater representation of data at high and rising SMD and the lack of negative data, can be addressed by assessing the productivity of sorties over the selected area.

There are many reasons, unrelated to background soil type, why a site might not be observed as a cropmark. For example, some crop cover such as grass may not respond to the differences in soil conditions as well as others, the weather conditions (e.g. haze or clouds) may hamper visibility, or the quality or resolution of older images may not be good enough for the mark to be visible. Bearing in mind that that negative data are not only dependent on soil conditions, but other unavoidable circumstances, it is possible to add negative data to the dataset should assumptions be made.

The application of the 2km radius around the two research locations in this study is assumed to be narrow enough that each of the known flights over the area would have had the opportunity to view all locations where recorded sites are present. This assumption may not be such a leap of faith. The early flights for mapping purposes were planned in such a way the whole area was imaged. In these cases, since the evidence is in the archive, this assumption is more reliant on the researcher looking back through the images checking the complete area. For later sorties, made for archaeological prospecting, where flights are directed by the on-board aerial archaeologist, cropmarks are imaged obliquely from the window as the plane is banked, circling the area. Because

all the sorties considered in the study have at least one cropmark imaged, it can be assumed that the area was well covered during circling. Therefore, where no image of the location of a site in the record has been taken, it is assumed that no cropmark was apparent.

Each flight made where at least one recorded site has entered the record is assumed to have had the opportunity to view all locations were a recorded site is present. The productivity of a flight can be analysed by assessing the number of sites recorded during the flight compared with the number of sites in the area which are known to have appeared as a cropmark. The productivity of each flight can then be defined as the

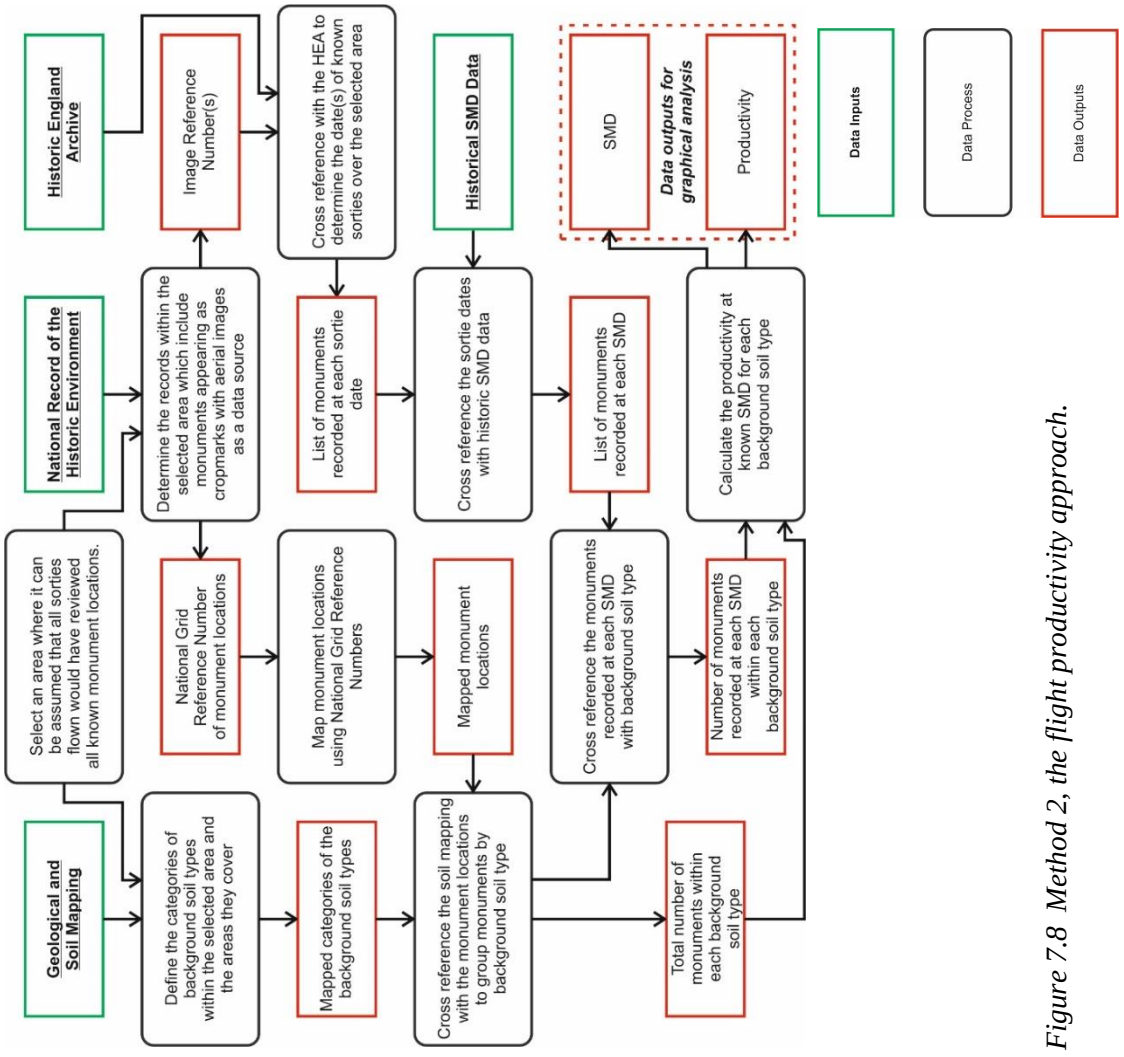

Figure 7.8 Method 2, the flight productivity approach.

number of sites recorded as cropmarks divided by the total number of recorded sites in the area.

This process is outlined in Figure 7.8 which summarises the methodology for the flight productivity approach.

7.5.2 Results

Figures 7.9 and 7.10 show the productivity of sorties made in the Cirencester and Diddington study areas, respectively, against the SMD at the time of flying in each of the background soil types.

Figure 7.9 shows that the alluvium, shallow Cornbrash Limestone and clay of the Forest Marble Mudstone have a fairly even distribution of productivity below 0.2 across the full range of SMD. The shallow alluvium and clay of the Forest Marble Mudstone both have flights which were more productive at higher SMD, with one particular flight of note at 95mm SMD recording a productivity of 0.8 in the alluvium. With the exception of the shallow Cornbrash Limestone, flights made at SMD of >70mm all have at least one flight with a productivity of 0.0. The shallow Forest Marble Limestone has the most productive flights at lower SMD (0.5 at 0mm SMD and 0.38 at 13mm SMD), and flights made at the highest SMDs had productivities of 0.

The results from the Diddington study area (Figure 7.10) show that flights at SMD of >100mm are most productive over both background soil types, although lower productivity is also seen in this range. However, in this case the dataset is small and no flights were made between 10-80mm SMD, so any conclusions may not be representative.

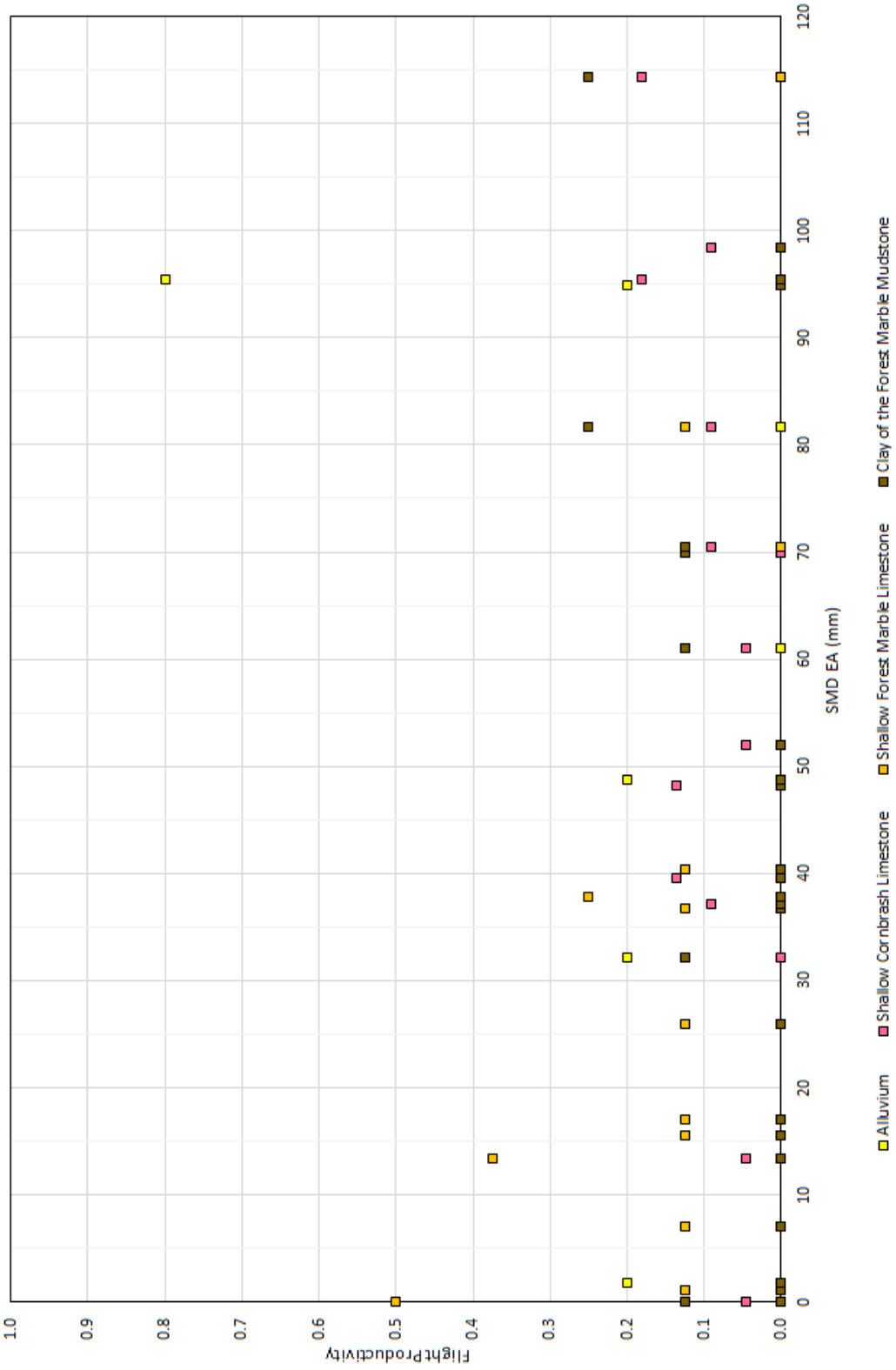

Figure 7.9 Cirencester study area flight productivity by SMD and background soil type.

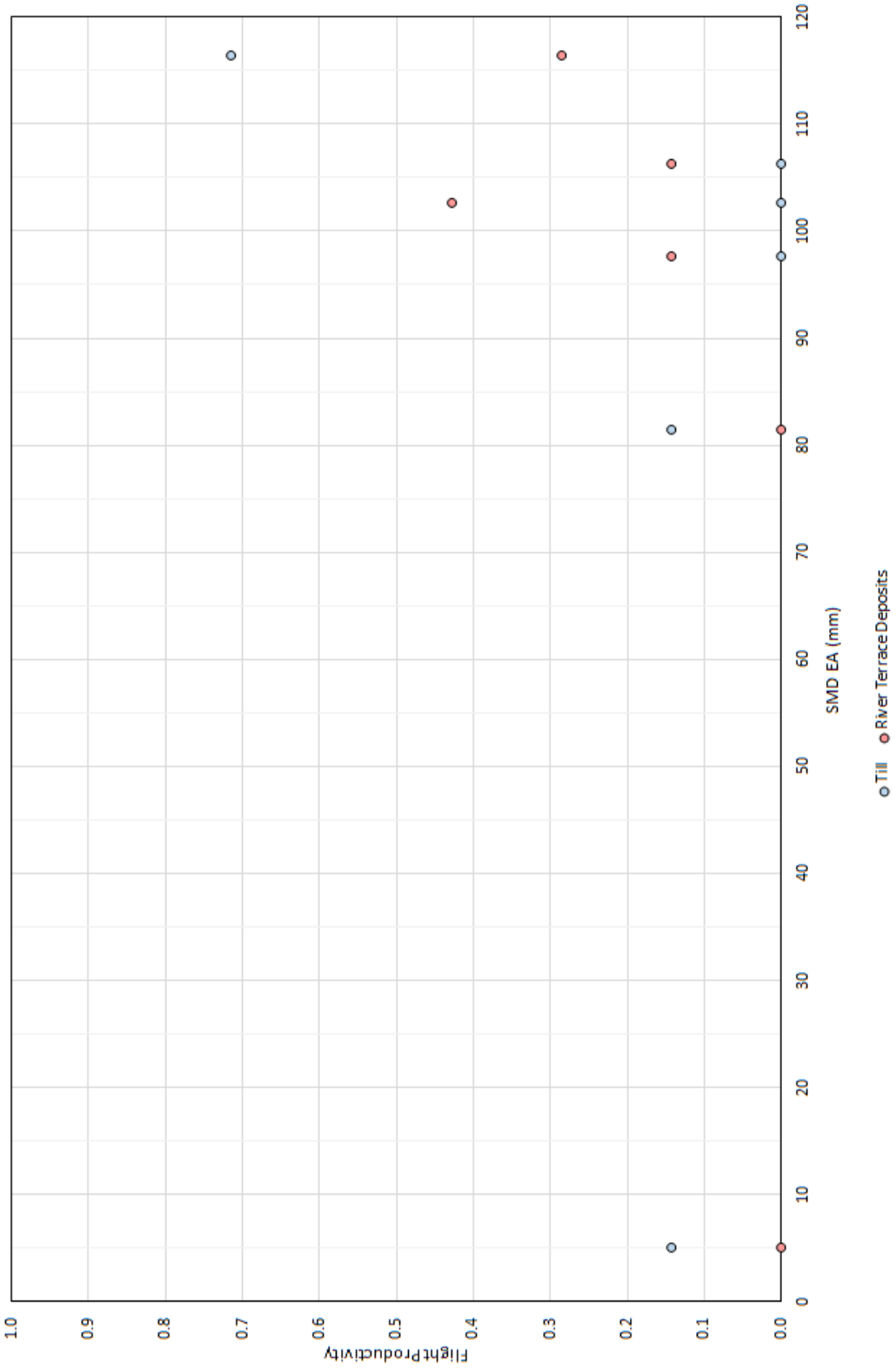

Figure 7.10 Diddington study area flight productivity by SMD and background soil type.

7.5.3 Discussion

Although no confirmed negative data are available, by assuming negative data statistical analysis is possible in the flight productivity approach.

The results show that the productivity of flights made over alluvium and clay of the Forest Marble Mudstone are more productive at high SMD. However, in these areas high SMD does not always indicate better productivity, and low SMD does not rule out positive results. In areas of the shallow Cornbrash Limestone the distribution of productivity is fairly even across the full range of SMD, though marginally higher at high SMD.

Shallow limestone of the Forest Marble formation shows the highest productivity in low SMD. As mentioned in the results of the cropmark approach it may be the presence of shallow rock impeding the development of roots that is the more dominating factor causing differential root growth. However, in this case a more even distribution of productivities over the range of SMD would be expected as the presence of the rock does not change over time. Figure 7.9 suggests that low SMD may be as likely an indicator of a productive flight over the Forest Marble Limestone as high SMD is in other background soil types near the Cirencester research location. Shallow limestone from the Cornbrash Formation is also present, though its distribution of productivity is more similar to that of the alluvium and clay of the Forest Marble Mudstone.

The dataset over the Till and River Terrace Gravels near the Diddington research location may be too small to make generalised conclusions.

Method 1 showed that some sites were only apparent as cropmarks within a limited range of SMD, resulting in a more even distribution of flight productivity across the range of SMD than would be expected from current knowledge. Where flights are of low productivity, there may be reasons other than the optimal combination of SMD and

background soil type, such as ground cover not being suitable for the formation of cropmarks.

7.6 METHOD 3: THE GROUND CONDITIONS APPROACH

7.6.1 Methodology

This method assesses the appearance of cropmarks on aerial images over areas of known background soil types and compares the results with historical SMD data. The methodology is summarised in Figure 7.11, which shows the data sources used in this study (though these can be tailored to the requirements of the analysis), the processes and outputs of the analysis. Combining all the source information into a GIS allows the source data to be plotted and locations of features can be compared with ground cover and soil mapping efficiently.

For this study, the area around the Cirencester research location was chosen, as it had the largest volume of data available for analysis. The boundary of the study area was chosen to encompass an area which was most commonly imaged to maximise the population of the aerial dataset.

The chosen study area is divided into cells where there is a single background soil type and a single type of ground cover. The ground cover most often will relate to the area of a field, where a single crop covers the area at any point in time, though in the case of this study, some larger fields required dividing as different land use rotations were used within the same field boundary.

The method comprises four processes (see Figure 7.11): defining and mapping cells; grouping and mapping of buried features; determination of SMD; and grading of cells.

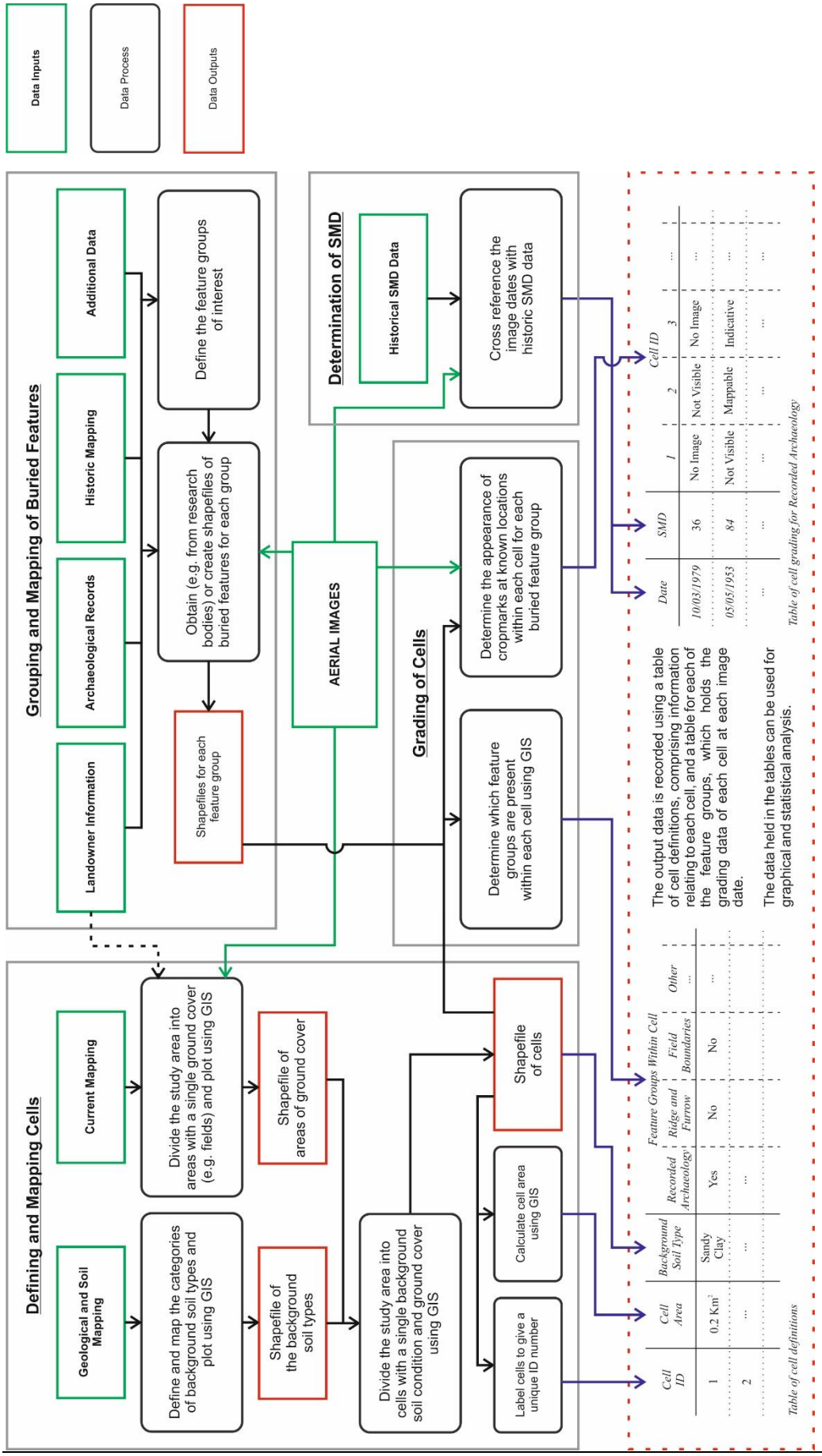

Figure 7.11 Method 3, the ground conditions approach.

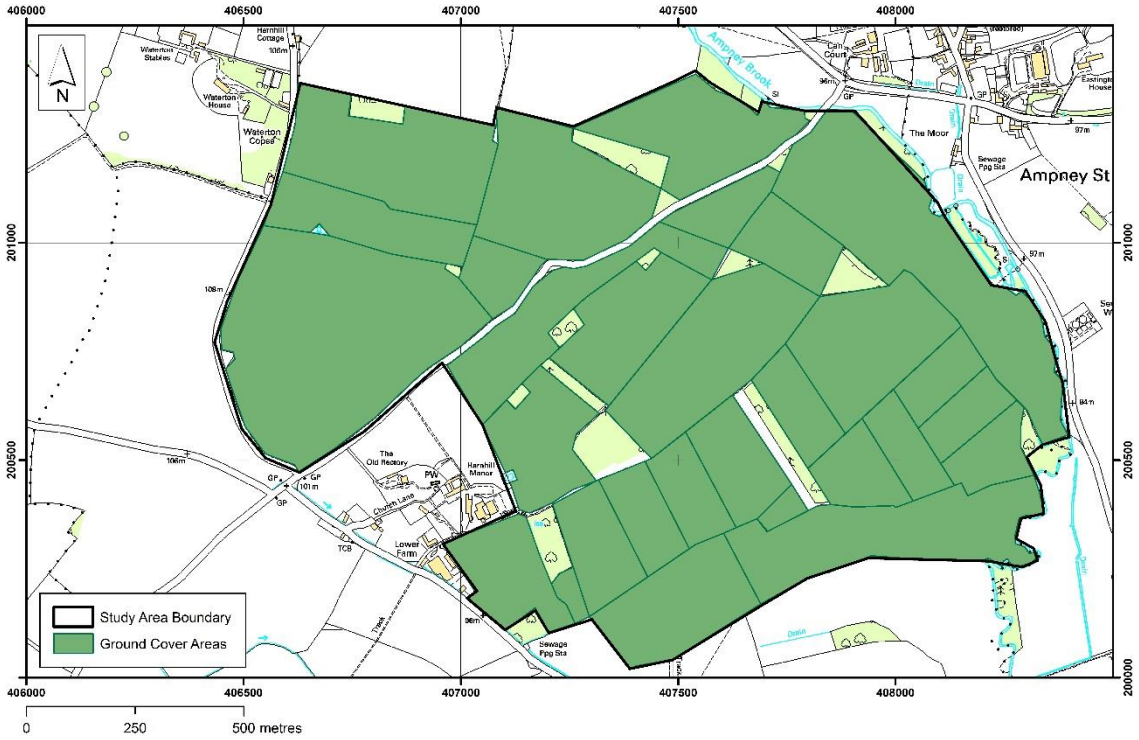

Figure 7.12 Areas of unique ground cover.

To define and map the cells, the results of soil mapping are plotted as a GIS shapefile (Figures 4.4 and 4.12). In the present research, information from aerial images, historical mapping and the landowner was combined to create a shapefile of areas of ground cover as in Figure 7.12. The cells are determined by intersections of areas of ground cover with background soil types. The GIS intersection tool is used to give a shapefile of cells where there is a single background soil type and at any one time a single ground cover as in Figure 7.13. Using GIS, each cell is given a unique ID number and the area it covers is calculated.

Mapping of buried features can be achieved using a variety of data sources (in this case, aerial images, archaeological records, utility mapping, historical mapping, and information from the land owner). All known buried features and cropmarks within the study area were plotted using GIS as shown in Figure 7.14. The cropmarks were divided into groups based on the type of underlying buried feature, should it be identifiable. The

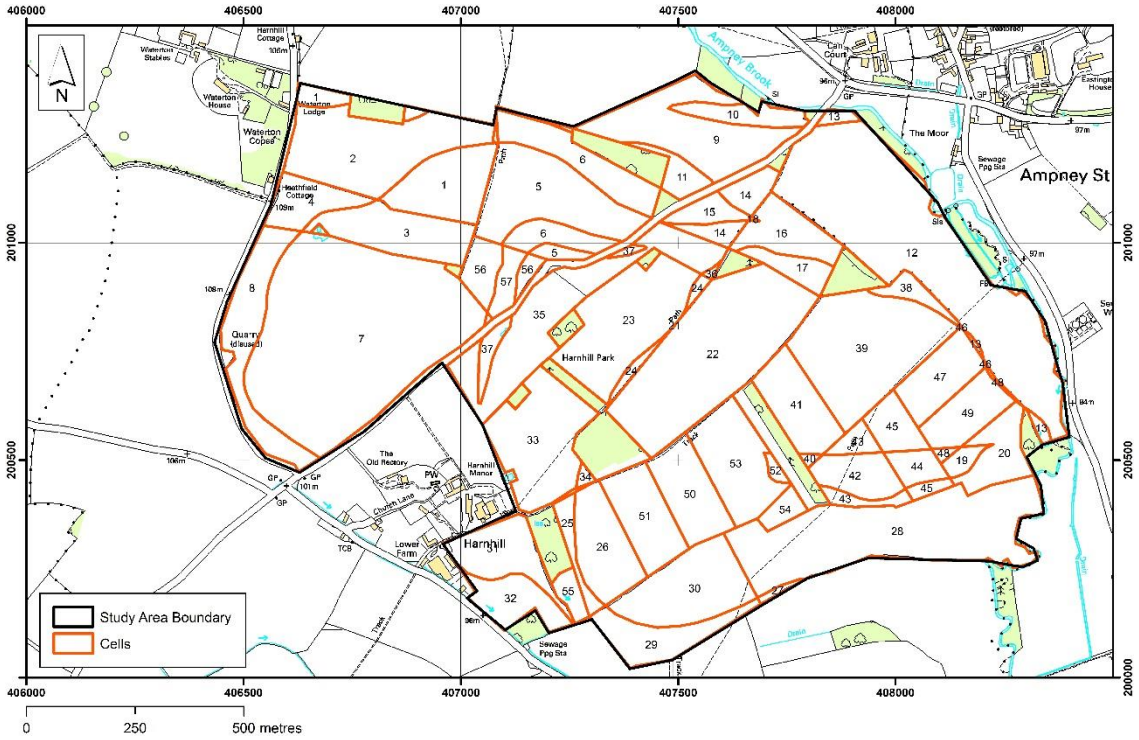

Figure 7.13 Cells with a single background soil type and single ground cover.

six groups used in this study are listed in Section 7.6.2 along with the information describing how they were categorised and the sources of data. Using GIS the feature groups which are present within each cell are determined.

Each of the image dates is cross referenced with historical data to determine the SMD at the time of imaging.

Aerial images were analysed to grade cells based on the appearance of cropmarks at the location of the features within each cell at each of the image capture dates. This process gives each cell one of three grades: "not visible"; "indicative"; or "mappable" at any image date. These grades are defined in Section 7.6.3.

The resulting tabular outputs are record the information relating to each cell (area, soil type, and features present). A further set of tables are produced for each feature group, comprising the grading of each cell. Examples of the output tables are given in Figure 7.11.

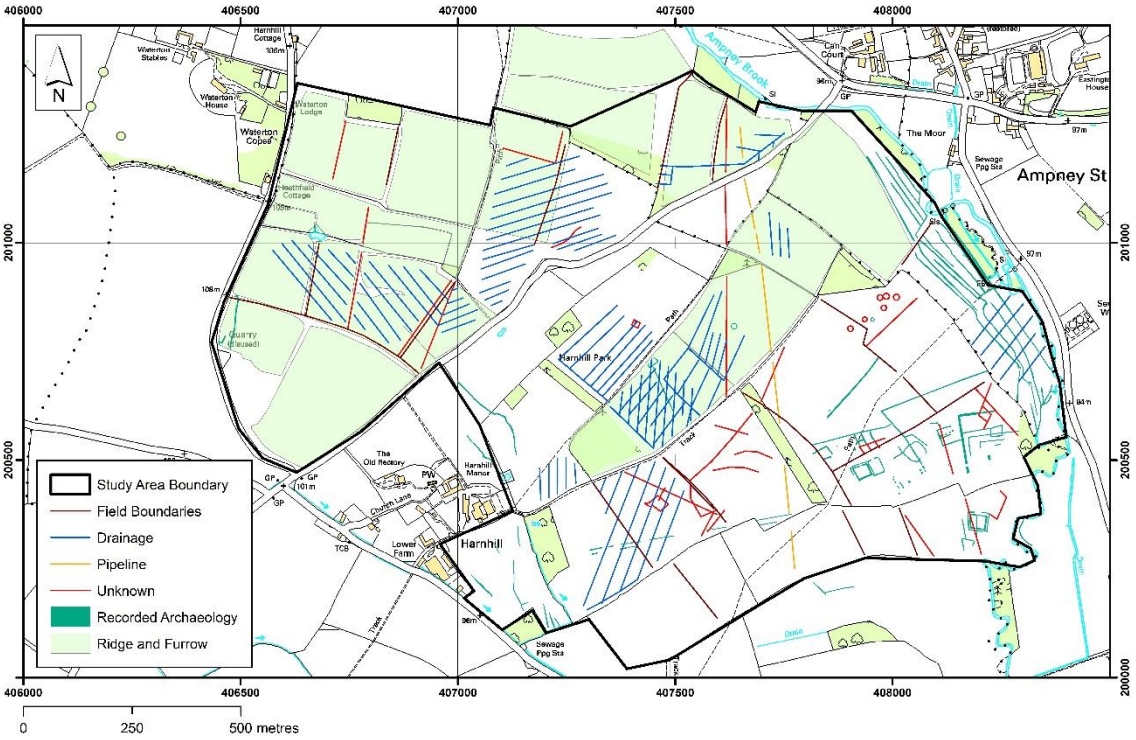

Figure 7.14 Cropmarks for each of the feature types.

The information in these tables can be plotted to statistically analyse areas based on the background soil type, the SMD and the grade of appearance. For each SMD, an area which is classed as a particular grade of appearance for a feature type is calculated as a percentage of the area in which the feature type could appear. This was done by determining the sum of the area of the cells which contain a feature type at a particular grade and dividing it by the sum of the area of cells which are known to contain the feature type.

7.6.2 Feature Groups

Figure 7.14 shows all the cropmarks identified within the study area. They have been divided into six groups (described below) based on the type of underlying buried feature.

Ridge and Furrow

Ridge and furrow is a pattern of parallel ridges and troughs which are the result of a method of ploughing common in the Middle Ages. Modern ploughing levels the

ground surface, though locations where ridge and furrow was once present can still appear as markings. Both upstanding earthworks and levelled ridge and furrow are present with the study area. For the purpose of this study, areas where ridge and furrow is still present topographically as earthworks have been discounted as not constituting a buried feature, and only levelled ridge and furrow has been considered. The ridge and furrow data forms part of the archaeological record and were provided as a GIS layer file by HE.

Archaeology

This group includes all other information which is included in the archaeological record, with the exception of upstanding sites and earthworks (again discounted as not constituting buried features). Within the study area, this includes linear and rectilinear features recorded as Roman roads and villas. The recorded archaeology data were provided as a GIS layer file by HE.

Field Boundaries

Field sizes have increased as development of farm machinery has allowed larger areas to be covered quickly. Boundaries dividing fields have been removed to reduce the time it takes to plough and harvest crops. The removed hedges, trees, walls and fences which formed the boundaries can leave soils which can differ from the surrounding farmed areas. After ploughing the surface soils homogenise but can leave soils which vary from the surrounding area beneath the plough depth.

The locations of any removed boundaries have been determined using historical mapping as part of the desk study (Sections 4.3.2.5 and 4.3.3.5). Any images which

show field boundaries before they were removed have not been included in analysis as they have been discounted as not constituting a buried feature.

Drainage

These include marks which appear above recent field drains. Within the study area, these appear as either as a parallel or herringbone pattern. Some of the images taken prior to 1973 show very distinct markings at the location of the drains. These marks may be related to excavation and installation of the drains. Therefore, marks due to drainage have only been assessed after 1975 to exclude any negative data from dates where no drains were present and to allow time for the effect of recent installation to subside. Mapping of the drainage has been carried out using aerial images and information provided by the RAU (landowner).

Pipeline

An enquiry to the National Grid did not return any services within the study area. However, from information provided by the RAU, HE and cropmarks recorded during the analysis of aerial images indicated that a pipeline or cable was located crossing the study area (see Figure 4.9).

Unknown Origin

A number of additional markings were noted during the analysis of the aerial images. From the location, and shape of the markings, they are likely to include archaeology, field boundaries and services. As none of the marks could be proven to be part of these groups, they have been analysed separately as markings of unknown origin.

7.6.3 Grading of Cells

For each date where cells were imaged (not all image dates covered the full study area), cells were graded as to the appearance of the marks within the cell boundary. The system used is similar to the one defined in Section 6.2 and shown in Figures 6.1(a-d), 6.2(a-d) and 6.3(a-d). However, since the grading is being applied to a cell where there may be more than one cropmark as opposed to a single cropmark, there are some minor changes to the definitions. For each feature group, each cell was graded as: not visible; indicative; or mappable. The definitions of these grades are given below.

Not Visible

This grading was given to cells which did not show any markings where buried features were known to be present.

Indicative

Where either some of the marks appeared over features known to be present, or where marks were partially visible, or present but indistinct, the cell was graded as indicative of the buried features.

Mappable

Where marks were highly visible and would be easily recorded, the cell was graded as mappable. In cells where a high proportion of the markings were very distinct and others are either not visible or indicative the cell was still graded as mappable, as imaging at this time would still provide data which can be mapped.

As there is some cross over between the indicative and mappable grades, this analysis is subjective. To avoid bias in this process, all the grading was carried out by a single person.

7.6.4 Mitigating Bias

7.6.4.1 Input Data

The biases described in Section 7.3 relating to the historical image archive remain unavoidable, although the bias relating to negative data has been reduced in a number of ways. Images taken for mapping purposes are not targeted at times when cropmarks are considered more likely, so include a range of SMD. Archaeological reconnaissance images of a target at one location reveal further information in the periphery, so adjacent areas can be reviewed where cropmarks may not be present. The additional images added to the dataset from the DART Project include some taken of the research locations at times when cropmarks are not present. These additional images were targeted directly at the monitoring locations, and therefore did not always cover the entire study area chosen, however, many additional cells could be assessed in the periphery of images. Although these images only span an 18 month period, with a gap during the winter months, they are valuable in determining conditions in which cropmarks do not form.

7.6.4.2 Analysis Method

To minimise bias other methods of analysis were considered in the design of this study, but were discounted due to high subjectivity.

The grading of each individual buried feature was considered. This may be easy in groups such as field boundaries, where only a single linear feature is present. However, when considering data from the archaeological record, assessing a "single" feature is impossible. For example, are two parallel linear buried ditches considered two features, or does the footprint of a Roman villa identified from a number of rectilinear cropmarks constitute a single feature or a group of features?

A method using the total length or area of features was also considered, though a similar issue is present. A double ring ditch (concentric circles) could be measured by the area or circumference of the outer ditch, or the total circumference of both ditches.

These discounted methods either imply or apply a value directly to a feature. Considering a Roman villa as a number of features as opposed to a single feature may imply greater value, and a greater weighting in analysis. The application of a number describing the area or length of a feature gives a specific value to that feature. Should a Roman road with a total length of 500m be statistically comparable with a burial mound with a 50m circumference? A single small cropmark may reveal much more information to one archaeologist than a group of features, and as such may have more research value, although another archaeologist may not agree. This implication of value is subjective and cannot be statistically assessed.

The chosen method of assessing cells avoids the need to imply or assign value directly to features. However, simply assessing the number of cells with particular attributes would result in a large cell with many markings having as much influence in the data as a small cell with a single mark.

To mitigate this bias, it is assumed that should a cell be graded as either not visible, indicative or mappable for a feature group, any similar feature within the cell would also have the same appearance. That is, the classification applies to the whole area of a cell since it has a single background soil type and ground cover. Calculations of the areas of cells allows the data to be weighted by its size. Assessing the results as a percentage of the total possible area where a feature type in a background soil type is present normalises the data for comparison.

7.6.5 Results

Three background soil types are present within the study area: shallow Cornbrash Limestone; shallow Forest Marble Limestone; and deep clay of the Forest Marble Mudstone. Each of these has been considered separately in the analysis.

The resulting data from plotting the percentage area by SMD for the feature types recorded archaeology and ridge and furrow are shown in Figures 7.15(a-c) and 7.16(a-c) and are discussed below. A summary of the resulting information is shown in Table 7.1.

Over the shallow Cornbrash Limestone (Figure 7.15(a)), recorded archaeology can be apparent over the full range of SMD. The largest percentage of areas where cropmarks are mappable are at SMDs of approximately 48mm, 70mm and >110m, though a sortie at 112mm also showed no indication of cropmarks. A number of sorties <35mm showed little or no indication of cropmarks.

Only three cells over areas of shallow Forest Marble Limestone contained recorded archaeology (Figure 7.15(b)), two of which never showed indication of cropmarks. The known data in the graph are the results of the third cell, which makes up around 60% of the area. The cell is mappable between 70-90mm SMD, and sometimes indicative between 30-60mm, but no cropmarks are evident outside this range.

Over the clay of the Forest Marble Mudstone (Figure 7.15(c)), recorded archaeology was typically only indicative or mappable below 50mm SMD, though there are also sorties in this range of SMD which did recorded all imaged cells as not visible. With the exception of a single sortie at approximately 70mm SMD which recorded just 1%, no areas were classed as mappable over 50mm SMD.

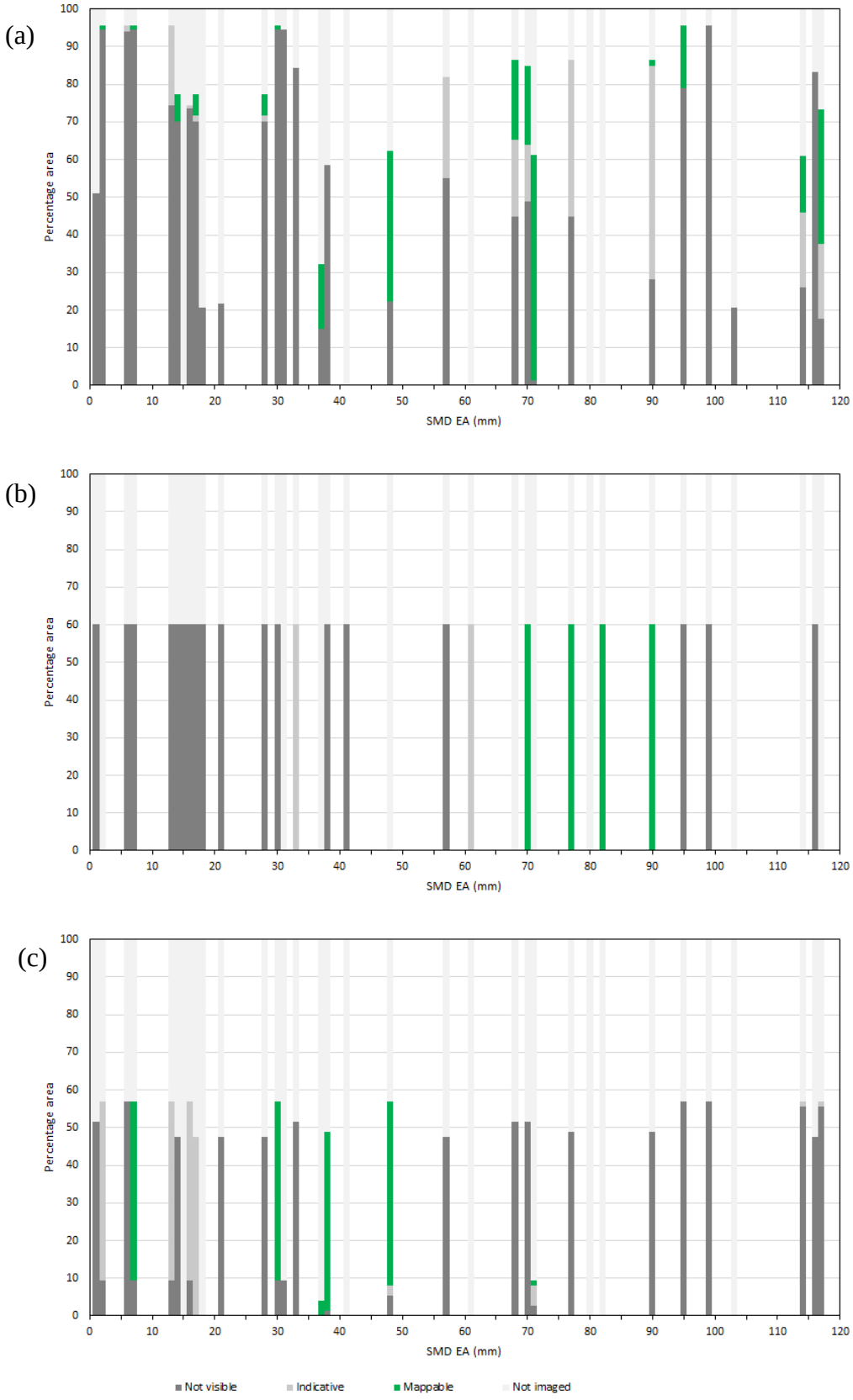

Figure 7.15 Percentage of area graded for recorded archaeology features.

(a) Shallow Cornbrash Limestone (b) Shallow Forest Marble Limestone

(c) Clay of the Forest Marble Mudstone

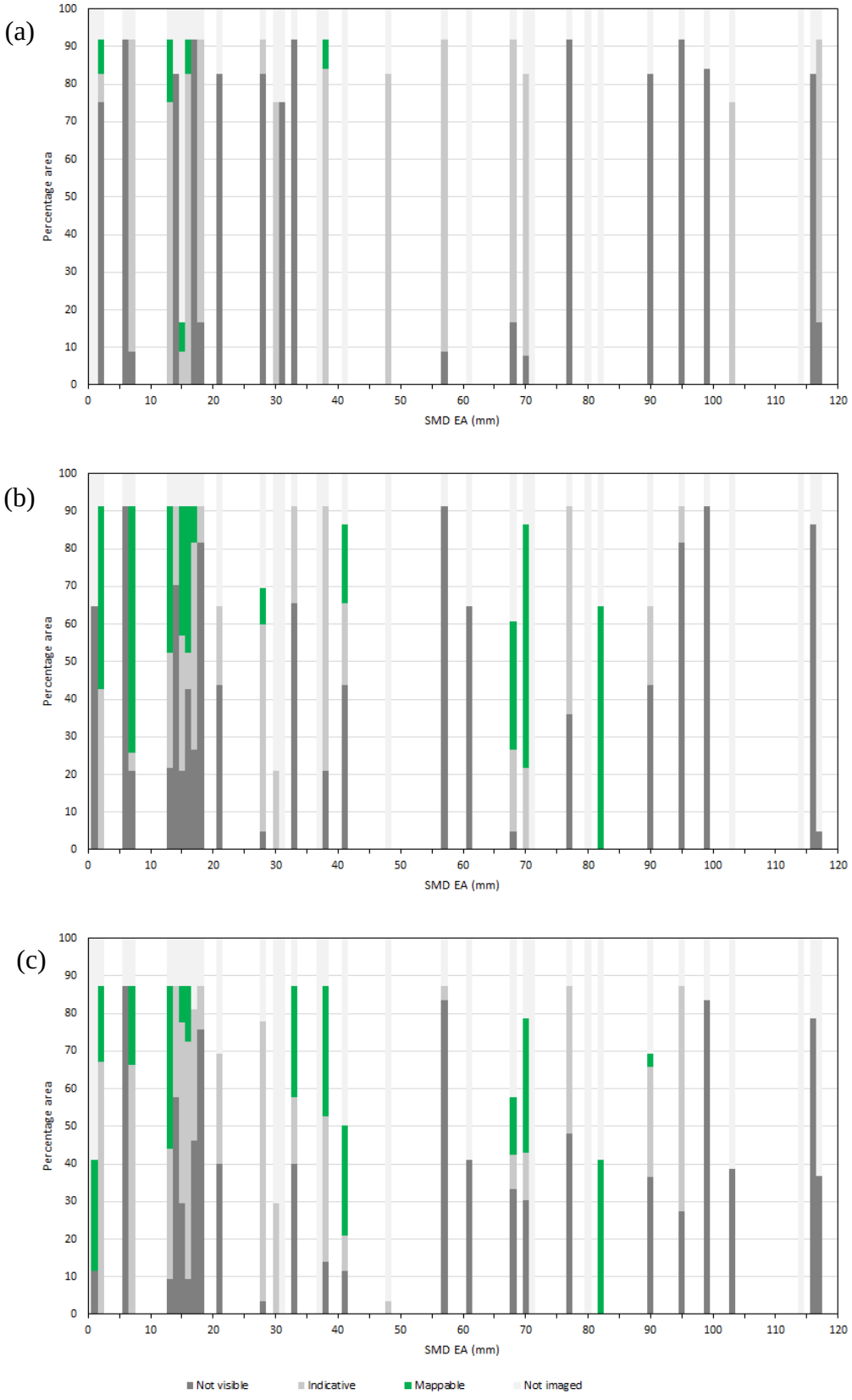

Figure 7.16 Percentage of area graded for ridge and furrow features.

(a) Shallow Cornbrash Limestone (b) Shallow Forest Marble Limestone

(c) Clay of the Forest Marble Mudstone

Table 7.1 Summary of the results of the ground conditions approach for all background soil types and feature groups.

	Shallow Cornbrash Limestone	*Shallow Forest Marble Limestone*	*Clay of the Forest Marble Mudstone*
Recorded Archaeology	Indicative 0-120mm Mappable ≈50mm, ≈70mm, >110mm	Indicative 30-65mm Mappable 70-90mm	Indicative <20mm Mappable <50mm
Ridge and Furrow	Indicative 0-120mm Mappable <40mm	Indicative <95mm Mappable <45mm, 65-85mm (particularly <20mm, ≈70mm)	Indicative <100mm Mappable <45mm, 65-85mm
Field Boundaries	Indicative 0-120mm Mappable 0-120mm (particularly ≈70mm, >110mm)	Indicative <95mm Mappable <40mm, 60-90mm (particularly ≈70mm)	Indicative <100mm Mappable <100mm (particularly <45mm, ≈70mm)
Drainage	Indicative 0-120mm Mappable >30mm, ≈70mm	Indicative <20mm Mappable ≈40mm	Indicative 0-120mm Mappable ≈40mm, ≈70mm, ≈110mm
Pipeline	Indicative 30-120mm Mappable 55-110mm	Indicative N/A (only 1 cell) Mappable ≈60mm, 90-95mm	Indicative 10-20mm Mappable 55-95mm
Unknown	Indicative 0-120mm Mappable 15-120mm (particularly ≈70mm)	Indicative 65-85mm Mappable ≈40mm	Indicative 0-120mm Mappable 30-45mm, ≈70mm, ≈105mm

Ridge and furrow was sometimes recorded as indicative over the full range of SMD areas of the shallow Cornbrash Limestone, though only mappable below 40mm SMD (Figure 7.16(a)). The Forest Marble Limestone and clay of the Forest Marble Mudstone had similar patterns of cropmark appearance (Figures 7.16 (b-c)). More often than not, areas were classed as indicative or mappable below 50mm SMD, and between 65-90mm SMD. No visible areas were recorded between 50-65mm SMD, however only two sorties were made in this range. Neither background soil type recorded visible areas of ridge and furrow above 100mm SMD.

Comparing the results of this analysis with the information in the literature review shows some discrepancy. It was expected that in the clay of the Forest Marble Mudstone, high SMD of >100mm would be required for cropmarks to become evident, however, the recoded archaeology is only indicative or mappable below 50mm SMD with only one very small area showing cropmarks above this at ≈70mm SMD. The ridge and furrow is also most evident at low SMD, though it also appears at 65-85mm SMD. Larger percentage areas of clay are also more conducive to cropmarks over other feature types at SMDs of <100mm.

The shallow Limestones of the Cornbrash and Forest Marble Formations would be expected to have the largest percentages of areas classed as mappable at SMDs >50mm. This is the case for recorded archaeology. Contrary to the literature, the ridge and furrow was most evident at low SMD (<40mm), though was also seen between 65-85mm SMD in the areas of Forest Marble Limestone.

7.6.6 Discussion

The method of grading cells showed that for recorded archaeology, the highest proportion of areas over shallow limestone were classed as mappable at SMD >50mm, as was

expected from the current knowledge. The ridge and furrow over shallow limestone had high proportions of area graded as mappable at <50mm SMD, although in the Forest Marble Formation, the range 65-85mm was also found to be optimal. This is in agreement with the cropmark approach where sites 2 and 20, referred to as ridge and furrow (Table 4.1), were commonly imaged at low SMD over the shallow Forest Marble Limestone.

For recorded archaeology and ridge and furrow, the largest proportions of area over the clay of the Forest Marble Mudstone were graded as mappable at SMDs of <50mm, with ridge and furrow also being mappable from 65-85mm. This is contrary to the current knowledge, where extreme high SMD is considered an indicator of cropmark appearance.

Comparatively high proportions of areas are noted as indicative or mappable for all feature types in all soil types at ≈70mm SMD. With the exception of recorded archaeology and field boundaries in the Cornbrash Limestone, there is a low representation of mappable features at high SMDs of >100mm, particularly over the Forest Marble Limestone which did not record a single mappable cell for any feature group in this range. However, not all negative data is due to the combination of SMD and background soil type considered in this method. Other factors must be in place, particularly the ground cover, which must be optimal at the time of flying. The sorties made at a SMD ≈70mm were between 31st May and 04th June (though in different years) and may have been before crops were harvested, whereas those at >100mm, dated between 24th July and 15th September may be afterwards, and hence no crop would have been present.

Another feature in the data is simultaneous negative and positive data. An example of this is for recorded archaeology, which is mappable in the Cornbrash Limestone at SMDs

Figure 7.17 Images of the same location at 114mm SMD and 116mm SMD.

of 114mm and 117mm, though there is a sortie at 116mm which did not return any mappable cells. This sortie was made in September, so although high SMD is present, the ground cover may not be suitable for the formation of cropmarks. Images from the

sortie at 114mm and 116mm are shown in Figure 7.17. Both these images are clear and directly target the same area but with differing ground cover. The cropmarks are visible at 114mm (denoted with a white line), but not at 116mm. In all background soil types and all feature groups, SMD ranges of mappable cells also contain sorties which did not record cells as mappable.

7.7 CHAPTER SUMMARY

In this chapter, three simple and inexpensive methods have been presented and tested to analyse existing data, improving understanding of the conditions in which cropmarks appear. This addresses Objective 8. The three methods each use a different approach to analyse existing datasets. They assess individual sites for the range of SMD in which they appear, the productivity of reconnaissance flights, and grade background soil types across a range of SMD based on the appearance of cropmarks.

Where possible, each method has been applied to the research locations. The results of Method 1, the cropmark approach, indicate that individual sites have a range of SMD in which they may appear, although this range does not always agree with current knowledge. By making assumptions to mitigate bias, Method 2, the flight productivity approach, shows that both productive and non-productive flights have been made over all the background soil types across a full range of SMD, although they may be marginally more productive at either high or low SMD depending on the background soil type. Method 3, the ground conditions approach, grades areas of background soil types based on the appearance of cropmarks (if any) over known locations of buried features and provides ranges of SMD in which certain types of features have been evident.

The following chapter gives a broad discussion of the present research.

CHAPTER 8. BROAD DISCUSSION

8.1 INTRODUCTION

This chapter discusses the combined results of the present research, bringing together the information gained throughout the study.

The literature review identified a need for increased knowledge as to the conditions in which cropmarks appear to aid aerial archaeologists in perpetuating the usefulness of aerial surveys for prospection. Historically, aerial surveys have been fundamental in archaeological research, however repeated surveying of areas where cropmarks are most commonly seen has led to a bias in the dataset. This research has proposed and tested a number of methods that can increase the knowledge on the soil related mechanisms which cause cropmarks to appear, and the conditions in which they appear.

Two research locations were selected by the DART Project for investigation, each location comprising two research sites where a buried ditch feature was present. These research locations were used to test proposed methods of analysis to assess the level of information relating to cropmark appearance that can be gained.

Initially, data were acquired for analysis. A desk study of the geographical, hydrological and topographical, geological and geotechnical, hydrogeological and historical and archaeological settings of the two research locations was carried out. This was followed by field investigations of the four research sites, where, in conjunction with the DART Project, the buried features were excavated to reveal cross sections, and to obtain soil samples for analysis. Bespoke monitoring stations (designed and constructed by D. Boddice, University of Birmingham) were installed at each research site to obtain TDR and temperature data for the soils both forming and surrounding the ditch features and weather data. Throughout a

period of monitoring, the DART Project commissioned aerial surveys, providing images of the research locations. The soil samples retrieved from site were geotechnically characterised, providing density, particle size distribution and plasticity data.

These data were applied to a number of methods, modelling the soil water characteristics, and cropmark appearance. Each of the methods is discussed addressing how each could aid archaeologists, both in the planning of aerial surveys, and improve understanding of bias in the existing dataset.

8.2 MODELLING THE SOIL WATER CHARACTERISTICS

Chapter 6 used data acquired from long-term monitoring to compare the sections to determine mechanisms of cropmark appearance and the background conditions in which they form. A grading system for cropmark appearance was defined whereby the appearance of the crop over known buried features were graded as either not visible, indicative or mappable.

Two analyses were performed on the same datasets. Firstly, soil suctions were compared in vertical profiles through and adjacent to the ditch features. Secondly, the background SMD was compared with the appearance of cropmarks. These analyses required monitoring of VWC using TDR monitoring stations, the geotechnical characterisation of the soils for empirical determination of suctions and SMD, and the grading of cropmarks from aerial imagery.

Three limitations were encountered relating to the method:

1. TDR probes cannot be used where rock is present.
2. The Saxton and Rawls equations for conversion of VWC to suctions are not valid where suctions are >1500 kPa.

3. Differences in suctions caused by buried features may be masked by high spatial variability of water content in plough soils.

Further limitations were found that were specific to this study:

1. CCC was located in an area of shallow limestone, therefore monitoring of VWC was not possible.
2. The monitoring stations had periods of failure where no data were collected. Further information on this is covered in Boddice (2014).
3. Voids within a disused pipe at the base of the ditch at CQF may have caused water to become perched in the wet year of 2012, causing differences in the hydrogeological regime of 2011 and 2012.
4. No indication of a cropmark was recorded at either DCF or DPF throughout the monitoring period.
5. Only a limited number of aerial images were available.

With these limitations, it was still possible to suggest mechanisms of cropmark appearance for both growing seasons at CQF, and quantify the differences in suctions at DCF and DPF which do not result in a cropmark, and determine the background SMD at times where cropmarks were recorded as not visible, indicative or mappable (Sections 6.4.1 and 6.4.2). Therefore, this method has merit in understanding both the mechanisms of cropmark appreance and the conditions in which they become apparent.

The monitoring of the research sites was not specifically designed for the purpose of this analysis. Other than geotechnical aspects, the methodology of data collection was designed to fulfil the needs of the DART Project. The limitations stemming from this can be addressed, which would improve the method. For example: ensuring monitoring stations

are robust for remote use would reduce the possibility of periods of failure; fully investigating features prior to installation would avoid issues relating to inappropriate ground conditions, such as the presence of horizons in which probes cannot be inserted; and scheduling of aerial surveys with a high temporal resolution would maximise the number of data for analysis.

This initial analysis used VWC data from TDR monitoring stations, which are costly and require installation and monitoring over a period of time. The subsequent method tested whether it is possible to simulate the VWC using an existing hydrogeological model (the SPAW model), negating the need for long-term monitoring of VWC. The empirical calculation to convert TDR VWC to suctions required geotechnical characterisation of soils. The SPAW model requires the same soil data for input, along with weather data from onsite weather stations and information about the crop.

Simulations were found to follow trends well in both the VWC and SMD as determined from TDR. However, an inconsistency in the model caused an error in the values. The sensitivity analyses showed that this inconsistency was likely to relate to limitations on the values of particle density inherent in the SPAW model. Particle density is fixed to a standard 2.65 Mg/m^3 in the model calculations, whereas measured values of matric density can be used. For some soils from the research sites, particle densities were higher than the standard, and matric density values were high. Using measured matric density values with the standard particle density caused a calculation error, whereby the VWC at saturation was lower than the VWC at field capacity, and conductivity calculations were invalid.

The simulation outputs followed trends in the data and could therefore be adjusted by the addition of a correction factor, to better agree with the results from TDR data. The VWC

could be corrected to within 0.04 (decimal %), however, this accuracy is not high enough to compare the differences in suctions between the sections. The SMD could be corrected to within 15mm for CQF, however no single correction factor could be applied. At CQF, where soils are the same, correction factors were required to halve the SMD in one growing season, and more than double the SMD in the next season.

This variation in the correction factor could indicate that it is not only density which causes an error in the model, however the sensitivity analysis showed that reductions in matric density can cause both increases and decreases in SMD peak magnitudes, whilst reducing the minimum SMD. At DPF, where density inputs did not cause an error, the model output was accurate to within 20mm of the SMD calculated from TDR data. It is therefore possible that correcting density values in the model could be the primary cause of the inaccuracy of the SMD. In order to confirm that errors are a result of limitations on density inputs, it would be necessary to reprogram the SPAW model to allow variation of particle density in the calculations. In a study of organic soils with a low particle density, Ros Mesa (2015) also suggested that incorporating a variable particle density would improve the SPAW model.

Allowing for the error in the SPAW model, likely due to density inputs, where possible, simulation outputs were compared with use of soil input data from database sources as opposed to laboratory measured inputs. At CQF, database soil inputs were similar to those measured, and the resulting SMD was within 10mm of the output using measured inputs. At DCF, database soils had a greater difference from the measured data, particularly in the clay fraction, which the model is known to have a high sensitivity to. In this case the SMD was up to 30mm higher than the output using measured soil inputs. These results were consistent with the differences expected from the sensitivity analysis.

This analysis has been proposed in the context of advising aerial surveyors as to the likelihood of cropmark appearance, using SMD as an indicator. Therefore, the SMD should be representative of a larger area, such as a soil unit. In this case, it is perhaps the variability of SMD within the unit which is of importance rather than the SMD at a single point. If the variability of soils within a unit can be assessed by using multiple data points from databases such as the NGPPD, the variation in SMD could be modelled. Where database sources can only provide data from a small area within a soil unit, the sensitivity analysis can be used to give information on the variability of SMD. Geographically localised data is common within the NGPPD because it comprises results from intrusive site investigations for construction purposes, such as buildings and roads. However, the database is perpetually increasing, improving coverage.

The current research was focussed on the effect of soils on the modelling of SMD, however the SPAW model also uses inputs of crop and weather. The effects of using example crop data built into the SPAW model and freely available data from nearby weather stations was assessed to give a general indication of the effects on the SMD output.

CQF was the only research site which used known dates of drilling and harvest. Varying the dates of drilling, harvest and rooting depths was found to have little effect on the trends and values of SMD, but it introduced a short time lag in the data. Although the drilling of the crop was 30 days earlier than in the example file, the lag was just 2 days.

Precipitation and temperature values were available for CQF from a station approximately 8km away. However, measured evaporation data could not be found in the nearby area. It was necessary to create an evaporation default file from the literature, which used monthly averages. The resulting SMD output was greatly affected. Although some general trends

were indicated, a general rise in SMD was seen throughout both CQF 2011 and CQF 2012, and the results could not be considered comparable. The measured precipitation was significantly higher and the evaporation was significantly lower, than was seen in the database, causing the rise in SMD.

8.3 METHODS OF CROPMARK ANALYSIS

Three methods have been proposed to determine the background conditions in which cropmarks are apparent. The methods use existing data available from sources such as the BGS, HE, and the EA, although they are fundamentally centred on aerial images. The historical aerial image archive has inherent bias relating to the practice in data collection. Flights with the purpose of archaeological reconnaissance are made in conditions considered optimal for maximising return. Although many of the flights made are during the summer months, the range of SMD achieved from the image dataset in the Cirencester study area used for analysis have a wide distribution. The Diddington study area has both fewer images and narrower ranges of SMD.

The archive includes mostly images taken for archaeological reconnaissance, and as such do not include negative data. Negative data can occur for a number of reasons, even where both the background soil types and SMD may indicate a cropmark is likely. There may not be a cropmark because ground cover may not be conducive to cropmark appearance, for example after harvest. Alternatively, there may be a cropmark present but it was not recorded, for example atmospheric conditions hampering visibility. With the current practice used in aerial reconnaissance, is not possible to quantify the causes of negative data.

Method 1, the cropmark approach, does not mitigate against the lack of negative data, however it still provides information on the ranges of SMD in which individual sites appear

as cropmarks. Methods 2 and 3 do include ways of mitigating against the lack of negative data. The flight productivity approach uses assumptions based on the area covered during a sortie, allowing negative data to be added to the dataset. The ground conditions approach uses information contained in the periphery of images targeted at a particular location. For this study, the dataset has also been expanded by using aerial images taken on behalf of the DART Project, which are not directly targeted at optimal flying conditions, including images which show the study area at times when no cropmarks are apparent.

Throughout all the methods, the uncertainty in negative data is present. Although many factors may cause negative data to occur at times where background soil types and SMD may be optimal, the suitability of ground cover at the time of imaging is fundamental. Whether negative data has been assumed (as in the flight productivity approach) or confirmed (as in the ground conditions approach), there will always be negative data in the ranges of SMD where features are evident as a result of suitability of ground cover and other factors. Focusing the analysis on the ranges of SMD with positive results still allows information to be gained, though these ranges may be interspersed with negative data.

Although information can be drawn from a study of flight productivity, increasing productivity does not necessarily increase the population of sites in the record. Since the cropmark approach shows that there are ranges of SMD in which individual sites appear, to record all sites in an area flights should be made at a variety of SMDs. Repeated flying at a smaller range of SMD would result in the rerecording of known sites. The discovery of a single new site to add to the record may be of more significance to an archaeologist than a sortie imaging a number of already known sites. It has been shown that, in general, more sites have been recorded at high SMDs, though a low SMD does not preclude the appearance of cropmarks. Should those sites recorded at low SMD also appear as cropmarks in high

SMD, then the likely productivity should dominate planning of sorties. However, if sites recorded at low SMD do not appear as a cropmark at times of high SMD, there is a need to balance the discovery of new sites with higher productivity.

The shallow limestones of the Cornbrash and Forest Marble Formations have surprisingly different results in all three analysis methods. The cropmark approach showed that sites over the Cornbrash Limestone became evident in a fairly even distribution across a wide range of SMD, although less showed at lower SMD. Those over the Forest Marble Limestone most commonly became apparent in low SMD ranges. Flight productivity was marginally better in high SMD over the Cornbrash Limestone, and significantly better in low SMD over the Forest Marble Limestone. The ground conditions approach shows that, for all buried features, the largest percentages of the Cornbrash Limestone were mappable at >65mm SMD. The Forest Marble Limestone, however, had significant areas mappable <50mm, though high proportions were also evident at 70-80mm SMD, but never >100mm, similar to the distribution seen in the Forest Marble Mudstone. Both soils are reported to be of a similar depth, have the same genesis, the same minimum, maximum and dominant grain size and the same mineralogy (British Geological Survey, 2015d). The reported difference found between the soils with the parent materials of the Cornbrash and the Forest Marble Limestone is the soil group, which is described as “Heavy to Medium” and “Medium(silty) to Light(silty) to Heavy” respectively. This implies that there is a difference in the plasticity between the two soils which may contribute to the differing patterns of cropmark appearance.

The following section presents the opportunities for further analysis based on the knowledge acquired from the present research.

8.4 OPPORTUNITIES FOR FURTHER ANALYSIS

This study used data acquired by the DART project to compare suctions between vertical profiles through and adjacent to buried ditch features. Although a very limited dataset was available, it was shown that monitoring of the VWC in the profiles using TDR provided information which could indicate mechanisms of cropmark appearance, and determine the differences between the profiles which did not result in any indication of cropmark. Should this method of analysis be applied to further buried features, it would be possible to widen knowledge on the differences between feature and adjacent soils at times of cropmark appearance and further knowledge on the mechanisms of cropmark appearance.

Monitoring of the background SMD used the same method, where again the dataset used was very limited and generalised conclusions could not be drawn. However, some results contradicted the current knowledge of the likely appearance of cropmarks on clay-dominated background soils. Applying this method over a wider area would investigate this discrepancy, and provide further information on the conditions in which cropmarks form.

These two analyses both use data from monitoring stations which are costly and require installation and monitoring in the long term. This study tested the use of an existing hydrogeological model, to replace this data. The SPAW model was found to follow trends in the VWC well. Post processing of the data to SMD also followed trends. However, an inconsistency in the model resulting from limitations on density parameters caused values to be inaccurate. Reprogramming of the model to allow for variable particle density is expected to resolve these issues. Where soil densities are high, to carry out the same two analyses of the comparison of the sections and background SMD without the need for installation of monitoring stations, reprogramming of the SPAW model is necessary.

Although it was not possible to accurately reproduce values of SMD with the SPAW model, because trends were followed well the output was tested using database soil inputs, example crop data and database weather inputs. The variability of SMD over a soil unit is directly due to the variability of soil parameters, therefore for soil units where data are available the model, used in conjunction with the sensitivity analysis, can indicate a range of SMD. Using example crop data introduces a time lag, however the change in the SMD trends are negligible. The SMD was found to be highly dependent on the weather.

If reprogramming of the SPAW model to allow variable particle density resolved inconsistencies in the output, the SMD over a soil unit could be determined using only database and example data, although the weather data should be sought from as near to the unit as possible. Data from the personal weather station network across the UK are available for hundreds of locations from sources such as wunderground (The Weather Channel, 2012), although the data are not verified.

Three methods of analysis of cropmark appearance have been presented and tested at the research locations. The areas to which the presented methods have been applied are limited in terms of the range of background soil types, and geographical extent. However, the results of this study provide some previously unreported information relating to the appearance of cropmarks. There is an indication that the ranges of SMD over which cropmarks appear in certain background soil types may be more complex than the simple predictive model used in current practice. Although the dataset on which these analyses are based may be too small to make more generalised conclusions, further analysis would aid in refining the model used.

The three methods are all based on data which exist in the records of bodies such as HE, the BGS and the EA. Applying these methods to a wider area and over a wider range of soil

types, would be simple and of low cost, possibly increasing flight productivity and the rate of discovery of new sites.

The complexity and difficulty in analysis resulting from the lack of negative data in the historical aerial image archive could be addressed by simple changes to the methods of data collection. Imaging of areas where buried sites are known to be present at times when no cropmarks are apparent would add confirmed negative data to the dataset allowing for a more robust analysis. It is proposed that should an area be selected for analysis using the methods presented here, a more consistent approach to imaging could be applied. For instance, if the selected area were near an airfield used for aerial reconnaissance, or under a flightpath commonly flown, taking additional images would not incur any significant research cost. Alternatively, with relatively low cost drone technology, a selected area could be imaged on a regular and methodical basis.

Should the landowner at a selected location be forthcoming, information on ground cover, crop rotations and crop management (such as irrigation) could also be considered, and an additional step in the analysis could be created to improve understanding of the growth stages of crops in which differential crop growth becomes apparent.

Cross-referencing the results of the analysis with databases of soil properties such as the BGS PMM or the NGPPD, could improve the understanding of how factors such as the mineralogy or plasticity of clayey soils may affect the appearance of cropmarks. Since these data can be supplied in GIS format, this would be a quick and simple analysis.

The three methods require historical SMD data. In this research, data from the EA, based on MORECS, has been used in the analyses, which provides an average SMD over a wide area and a number of soil types. The Met Office uses data from around 200 automated

weather stations across the UK, located approximately 40km apart. The resulting data are used in MORECS to provide single values of SMD for 40km squares. Current practice in aerial archaeology uses these data to indicate areas where cropmarks are more likely to appear. This study has shown that SMD is highly dependent on weather data. Although the MORECS data can be used successfully for planning of surveys, it would be of benefit to obtain SMD with a higher spatial resolution for analysis of the conditions in which cropmarks form.

This research has shown that simple analysis methods using existing data can be applied to increase the understanding of the appearance of cropmarks based on the background soil unit. If inconsistencies in the SPAW model can be resolved by reprogramming, SMD for a single soil unit can be used in the analyses, significantly increasing the spatial resolution of the data over those used in current practice.

Although methods have been presented which mitigate for bias in the existing dataset, they require a number of assumptions. Methods in data collection could be improved to address this bias directly, by imaging locations where it is known that buried features are present at times when no cropmark is evident.

If applied to a wider area, the proposed methods could aid archaeologists, both in the planning of aerial surveys, and improve understanding of bias in the existing dataset, this fulfils Objective 8 of this study.

The following chapter presents the conclusions of the present study.

CHAPTER 9. CONCLUSIONS AND RECOMMEDATIONS FOR FURTHER WORK

9.1 INTRODUCTION

The hypothesis of this study is that in order to perpetuate the usefulness of traditional aerial surveying, there is a need to calibrate the results of aerial surveys against ground conditions, to improve the understanding of the conditions in which they appear. This thesis has proposed cost effective, soil based methods of analysis that can be applied to improve the understanding of cropmark appearance and optimise the use of aerial surveys for the detection of buried archaeological features, fulfilling the aim of the study. Applying these methods to an area has shown that further knowledge of the influence of soils on why, and in what conditions, cropmarks become apparent would increase the understanding of the bias in the existing dataset, and aid archaeologists in reducing future bias.

9.2 CONCLUSIONS

Methods of analysing cropmark appearance have been proposed, and tested, using two research locations as case studies. A number of conclusions specific to the case studies can be drawn from the results of the tests:

1. Monitoring of the VWC in sections through and adjacent to buried features and empirically converting the data to suctions provided information which could indicate the mechanisms of cropmark appearance. For example, in the CQF 2012 growing season, a positive cropmark was recorded at a time when suctions were lower at a level below the ditch feature than they were in the adjacent soils, indicating that enhanced plant growth over the feature may be due to soil water being more easily available.

Quantitative information can also be gained where no cropmark becomes apparent. For example, at DPF, high log suction differences of >0.4 at the ditch level, sustained for over 2 months, did not result in any indication of a cropmark in pasture.

2. Comparing the background SMD with cropmark appearance provides information relating to the conditions in which cropmarks form. The case studies were found to both confirm and contradict current knowledge. Crops growing in the river terrace gravels displayed cropmarks at a high SMD of >130mm, in line with current knowledge. Unexpectedly, with a background SMD of <50mm, both indicative and mappable cropmarks were recorded at CQF, whereas for this clay-dominated site it was expected from the literature that a much higher SMD would be needed for a cropmark to become apparent. This area would not have been selected for survey at this low SMD using current practice in aerial survey. This shows that there are cases of cropmarks in clay-dominated areas at low SMD and a review of methods would be necessary to include these in the dataset. This is an important finding which may impact on future methods of survey.

3. The cropmark approach of analysis found that individual sites may have a range of SMD in which they appear. This range does not always agree with current understanding from the literature. For example, a very high SMD of >150mm is used as an indicator of cropmark appearance on clay-dominated background soils, however six of eight sites appeared as cropmarks below 100mm SMD over the clay of the Forest Marble Mudstone. This finding further confirms the importance of the previous conclusion as this area would not have been selected for survey at this this range of SMD using current practice in aerial survey.

4. The flight productivity approach of analysis showed that both productive and non-productive flights have been made over all the background soil types across a full range of SMD, although they may be marginally more productive at either high or low SMD depending on the background soil type. For example, flights were more productive at low SMD over the Forest Marble Limestone. In this case, the depth of soil may contribute to cropmark appearance, although flights over the shallow Cornbrash Limestone were more productive at higher SMD.
5. The ground conditions approach of analysis showed that grading areas of background soil types based on the appearance of cropmarks (if any) over known locations of buried features can provide ranges of SMD in which certain types of features were evident. Contrary to expectation, the largest proportions of area over the clay of the Forest Marble Mudstone were graded as mappable for recorded archaeology at SMDs of <50mm.
6. There are soil properties not considered in the SPAW model such as the plasticity and mineralogy of clay soils that would have a bearing on both the mechanisms of cropmark appearance and analyses on background SMD. For example, CQF displayed cropmarks throughout two growing seasons. At this research site, the PSD and density of the ditchfills and adjacent soils were similar, although the plasticity was much lower in the upper levels of the ditch soils than the soil at the same depth adjacent to it, and much higher in the lower levels of the ditch soils than those adjacent to it. These behavioural properties would also affect the range of SMD in which cropmarks become apparent. For example, the soils with parent materials of the Cornbrash and the Forest Marble Limestones had different patterns of cropmark appearance. Database information indicated a difference in the plasticity between the two soils.

This conclusion shows that hydrogeological modelling would benefit from including properties affecting the behaviour of clay soils in the empirical determination of the SWCC.

Although these conclusions cannot be generalised because of the limited datasets used, they give results which do not always agree with the current knowledge of the likely appearance of cropmarks. Further study would be of benefit in refining current knowledge to aid aerial archaeologists in improving methods of survey to reduce methodological bias, and further understanding of the geographical bias in the existing aerial image dataset.

Further conclusions from this study relate to the generalised use of these methods:

1. The three proposed methods all require knowledge of the SMD. Currently sources of data such as MORECS and the EA give values with a low spatial resolution. In the context of understanding the influence of soils, values should be sought for areas where ground conditions are laterally homogeneous, such as a soil unit.
2. This study determined SMD by insitu monitoring of water content using time domain reflectometry, and assessed the possibility of modelling SMD using an existing model (SPAW) with measured soil, crop and weather data inputs to reduce costs. The model was found to reproduce trends in the SMD determined from monitoring data, but an inconsistency was found relating to limitations on soil density inputs which caused inaccuracy in the absolute values. It is expected that reprogramming of the model would correct the inaccuracy in the SMD, making the model applicable for use in determining SMD over an area where soils are laterally homogeneous.
3. To further reduce the cost of obtaining SMD with a high spatial resolution, the SPAW model output using database inputs were tested against the output from measured

inputs. It was found that the sensitivity analysis could be used to assess the variation of SMD with the variation of soil parameters, although the methods used to characterise the soils in the database, such as laser diffraction methods for clay content, may affect the results. Varying the crop inputs to example crop data built into the SPAW model caused only a short time lag, but negligible change to the SMD. The SMD is sensitive to weather inputs, and weather has a high spatial variability, therefore it is necessary to seek weather data from as close to the area of study as possible.

4. The three methods presented can all be carried out over wider areas using already existing data, without the need for expensive additional data collection. However, assumptions must be made to include negative data, which is lacking in the aerial image archive, if any statistical analysis is required. If Method 2, the flight productivity approach, and Method 3, the ground conditions approach, were to be applied to a larger area than in the present research, the existing dataset could be increased and improved (reducing bias) with only small changes to methods in aerial reconnaissance, or inexpensive additional study.

9.3 RECOMMENDATIONS FOR FURTHER WORK

The conclusions indicate that further work would increase the understanding of the appearance of cropmarks and aid archaeologists in both understanding bias in the data, and the planning of aerial surveys. These recommendations are outlined below.

1. Reprogramming of the SPAW model to allow for variation of soil particle density is expected to resolve inconsistencies in the calculations and error in the results.
2. Reprogramming of the SPAW model to allow for the use of empirical methods of determining the SWCC that take into account the behavioural properties of clay soils.

3. Implementation of the reprogrammed SPAW model using data from database sources to give a higher spatial resolution of SMD data for analysis.
4. Recording negative data over known buried features during survey would improve the understanding of the range of SMD in which cropmarks do not form and reduce bias in the dataset.
5. Applying the three proposed methods, using SMD data with a high resolution, and datasets that include proven negative data, to a wider area would provide knowledge on the appearance of cropmarks with respect to SMD.
6. Future analysis of cropmark appearance should include a higher temporal resolution of aerial data that includes negative data, which could be achieved by selecting an area near commonly used flight paths near an airfield or drone technology.

9.4 IN SUMMARY

Through a critical review of the literature, six gaps in knowledge relating to the appearance of cropmarks were identified. These gaps were addressed by desk and site investigations, geotechnical characterisation, hydrogeological modelling, and the proposal of cropmark appearance analysis methods. At three research sites both the differences in the geotechnical properties, and soil water characteristics, between archaeological features and the adjacent soils were quantified and related to cropmark appearance (knowledge gaps 1 and 2). Three methods of cropmark appearance have been proposed and tested, to assess the predictive model currently used to predict the likely appearance of cropmarks (knowledge gap 3). Applying these models to a wider area would aid archaeologists in understanding of distributional and methodological bias in the existing dataset (knowledge gaps 4 and 5). The three proposed methods compare data from aerial surveys with soil information (knowledge gap 6).

This study has proposed and tested methods which compare the results of aerial surveys with ground conditions. The methods use existing data wherever possible to determine the soil and soil water conditions in which cropmarks are, or are not, apparent. Applying these methods to a wider area, would increase knowledge of the conditions in which cropmarks are likely to form. This knowledge could be applied to planning of future surveys, improving rates of discovery of buried archaeological features or the productivity of flights in areas of clay-dominated soils, termed "difficult" by archaeologists. Improving survey methods would reduce both the methodological and geographical bias in future surveys, and further knowledge of why and in what conditions cropmarks form would increase understanding of the biases in the existing dataset.

REFERENCES

Ahangar-Asr, A., Johari, A. and Javadi, A. (2012) An evolutionary approach to modelling the soil–water characteristic curve in unsaturated soils. **Computers & Geosciences** [online], 43: 25–33. Available from: http://dx.doi.org/10.1016/j.cageo.2012.02.021

American Society for the Testing of Materials (2000) **ASTM D5550 - 06 Standard Test Method for Specific Gravity of Soil Solids by Gas Pycnometer**

Barber, M. (2005) Stonehenge from the air in 1900: The ballooning adventures of the Reverand John Mckenzie Bacon. **AARGNEWS 30**, pp. 9–16

BBC (2014) **Stonehenge "complete circle" evidence found** [online]. Available from: http://www.bbc.co.uk/news/uk-england-wiltshire-28967538 [Accessed 11 September 2014]

Beazeley, A.G.A. (1919) Air Photography in Archæology. **Geographical Journal**, 55: 330–335

Beck, A. (2011) Archaeological applications of multi/hyper-spectral data - challenges and potential. **Remote Sensing for Archaeological Heritage Management, EAC Occasional Paper No. 5**, pp. 87 – 97

Beck, A. and Neylon, C. (2012) A vision for Open Archaeology. **World Archaeology**, 44 (4): 479–497

Bewley, B. (2001) Understanding historic landscapes in Britain and Europe: an aerial perspective. In **IScanning the Present and Resolving the Future. Proceedings. IEEE 2001 International Geoscience and Remote Sensing Symposium**. **2001**. IEEE. pp. 57–60

Bewley, R.H. and Rączkowski, W. (2002) "Past Achievements and prospects for the future development of aerial archaeology: an introduction." In Bewley, R.H. and Rączkowski, W. (eds.) **Aerial Archaeology, Developing Future Practice**.

IOS Press. pp. 1–8

Boddice, D. (2014) **Changing Geophysical Contrast between Archaeological Features and Surrounding Soil**. University of Birmingham

British Geological Survey (2009a) **Digital Geological Bedrock Map of Great Britain. 1:25 000 scale. (DiGMap-50) [Digital].**

British Geological Survey (2009b) **Digital Geological Superficial Deposits Map of Great Britain. 1:25 000 scale. (DiGMap-50) [Digital].**

British Geological Survey (2012) **Lexicon of Named Rock Units.** [online]. Available from: http://www.bgs.ac.uk/lexicon/ [Accessed 1 January 2015]

British Geological Survey (2015a) **Digital Hydrogeological Map of Great Britain 1:625 000 scale.** [online]. Available from: http://www.bgs.ac.uk/products/hydrogeology/maps.html [Accessed 1 January 2015]

British Geological Survey (2015b) **National Geotechnical Physical Properties Database. [Digital Download].**

British Geological Survey (2015c) **Scans of Borehole Records.** [online]. Available from: http://www.bgs.ac.uk/data/boreholescans/home.html [Accessed 1 January 2015]

British Geological Survey (2015d) **Soil Parent Material Model**

British Standards Institute (1990) **BS1377-2:1990 Methods of test for soils for civil engineering purposes — Part 2: Classification tests**

Brooks, R. and Corey, A. (1964) Hydraulic properties of porous media. **Hydrology Papers, Colorado State University** [online], 3. Available from: http://www.citeulike.org/group/1336/article/711012

Campbell, J.R. (2003) **Limitations in the Laser Particle Sizing of Soils**., pp. 38–42

Chappell, A. (1998) Dispersing sandy soil for the measurement of particle size distributions using optical laser diffraction. **CATENA** [online], 31 (4): 271–281. Available from: http://linkinghub.elsevier.com/retrieve/pii/S0341816297000490

Coles, J.M. (1972) **Field Archaeology in Britain**. 1st ed. Methuen & Co. Ltd., London

Cowley, D.C. (2002) A case study in the analysis of patterns of aerial reconnaissance in a lowland area of southwest Scotland. **Archaeological Prospection** [online], 9 (4): 255–265. Available from: http://doi.wiley.com/10.1002/arp.199 [Accessed 10 October 2013]

Cowley, D.C. (2007) Clays and difficult soils in eastern and southern Scotland: dealing with the gaps. In Mills, J. and Palmer, R. (eds) (eds.) **Populating Clay Landscapes**. Tempus Stroud. pp. 43–54

Cowley, D.C. (2012) **Personal Communication**

Cowley, D.C. and Brophy, K. (2001) The impact of aerial photography across the lowlands of south-west Scotland. **Transactions of the Dumfries and Galloway Natural History and Antiquarian Society**, 75: 47–72

Daniel, G.E. (1967) **The Origins and Growth of Archaeology**. Penguin Books, Harmondsworth

DART (2013) **DART CKAN Portal** [online]. Available from: dartportal.leeds.ac.uk

Davis Instruments (2001) **Vantage Pro Technical Reference**

Drewett, P. (2012) **Field Archaeology: An Introduction**. Routlege

Environment Agency (2010) **Great Ouse Catchment Flood Management Plan**. Peterborough: Environment Agency

Evans, R. (1990) Crop patterns recorded on aerial photographs of England and Wales : their type , extent and agricultural implications. **Journal of Agricultural Science**, 115 (3): 369–382

Evans, R. (2007) The weather and other factors controlling the appearance of crop marks on clay and other "difficult" soils. In Mills, J. and Palmer, R. (eds.) **Populating Clay Landscapes**. Tempus Stroud. pp. 16–47

Evans, R. and Catt, J.A. (1987) Causes of Crop Patterns in Eastern England. **Journal of Soil Science**, 38: 309–324

Evans, R. and Jones, R.J.A. (1977) Crop Marks and Soils at Two Archaeological Sites in Britain. **Journal of Archaeological Science**, (4): 63–76

Featherstone, R. and Bewley, R. (2000) Recent aerial reconnaissance in North Oxfordshire. **Oxoniesia**, 65: 13–26

Fredlund, D.G. and Xing, A. (1994) Equations for the soil-water characteristic curve. **Canadian Geotechnical Journal** [online], 31 (4): 521–532. Available from: http://www.nrcresearchpress.com/doi/abs/10.1139/t94-061 [Accessed 3 December 2014]

Friends of Paxton Pits (2014) **Paxton Pits** [online]. Available from: paxton-pits.org.uk [Accessed 14 January 2014]

Fry, R. (2011) **Land at Harnhill, The Royal Agricultural College, Cirencester: Geophysical report on preliminary fluxgate gradiometer survey.**

Fry, R. (2014) **Time-lapse geophysical investigations over known archaeological features using electrical resistivity imaging and earth resistance**. University of Bradford

Gardner, W. (1956) Mathematics of Isothermal Water Conduction in Unsaturated Soils. **Highways Research Board Special Report 40, International Symposium on Physico-Chemical Phenomenon in Soils**, pp. 78–87

Gatliff, R.W. (1981) Mineral Assessment Report 54. The sand and gravel resources of the country around Huntingdon and St Ives, Cambridgeshire. **Institute of Geological Sciences. Natural Environment Research Council.**

van Genuchten, M.T. (1980) A Closed-form Equation for Predicting the Hydraulic Conductivity of Unsaturated Soils. **Soil Science Society of America Journal**, 44 (5): 892

Grady, D. (2007) "Cropmarks on Clay - Getting the Timing Right." In Mills, J. and Palmer, R. (eds) (eds.) **Populating Clay Landscapes**. Tempus Stroud. pp. 34–42

Grady, D. (2014) **Personal Communication**

Head, K.H. (1992) **Manual of Soil Laboratory Testing Volume 1: Soil Classification and Compaction Tests**. 2nd ed. Pentech Press, London

Historic England (2011) **National Heritage List for England, Schedule list entry 1021448, Roman villa and earlier settlement 1120m east of Harnhill Manor.** [online]. Available from: list.english-heritage.org.uk/resultsingle.aspx?uid=1021448 (05/02/2014)

Historic England (2015a) **Aerial Investigation and Mapping** [online]. Available from: https://historicengland.org.uk/research/approaches/research-methods/airborne-remote-sensing/aerial-investigation/ [Accessed 24 March 2015]

Historic England (2015b) **Pastscape** [online]. Available from: http://www.pastscape.org.uk/ [Accessed 24 March 2015]

Historic England (2015c) **Satellite Imagery, Multi and Hyper-Spectral Data** [online]. Available from: https://historicengland.org.uk/research/approaches/research-methods/airborne-remote-sensing/satellite-and-ms-imagery/

Historic England (2015d) **Stonehenge World Heritage Site NMP** [online]. Available from: https://historicengland.org.uk/research/research-results/recent-research-results/south-west/stonehenge-whs-nmp/

Hough, M. and Hood, M. (2003) An historical comparison between the Met Office Surface Exchange Scheme-Probability Distributed Model (MOSES-PDM) and the Met Office Rainfall and Evaporation Calculation System (MORECS). **Manager**

[online]. Available from: http://bfw.ac.at/crue_documents/pjr_142_411.pdf

Hough, M.N. and Jones, R.J.A. (1997) The United Kingdom Meteorological Office rainfall and evaporation calculation system: MORECS version 2.0-an overview. **Hydrology and Earth System Sciences** [online], 1 (2): 227–239. Available from: http://www.hydrol-earth-syst-sci.net/1/227/1997/

Johari, A., Habibagahi, G. and Ghahramani, A. (2006) Prediction of Soil–Water Characteristic Curve Using Genetic Programming. **Journal of Geotechnical and Geoenvironmental Engineering** [online], 132 (5): 661–665. Available from: http://ascelibrary.org/doi/abs/10.1061/%28ASCE%291090-0241%282006%29132%3A5%28661%29 [Accessed 3 December 2014]

Jones, R.J.A. and Evans, R. (1975) Soil and Crop Marks in the recognition of Archaeological sites by Air Photography. **Council for British Archaeology: Aerial Reconnaisance for Archaeology**, Research R: 1 – 9

Jordan, D. (2013) A Geoarchaeologists view of Aerial Archaeology. **AARGNEWS 46**, pp. 29–36

Kerry, R., Rawlins, B.G., Oliver, M. a., et al. (2009) Problems with determining the particle size distribution of chalk soil and some of their implications. **Geoderma** [online], 152 (3-4): 324–337. Available from: http://linkinghub.elsevier.com/retrieve/pii/S0016706109002067 [Accessed 23 March 2013]

Lamara, M. and Derriche, Z. (2008) Prediction of unsaturated hydraulic properties of dune sand on drying and wetting paths. **Electronic Journal of Geotechnical Engineering**, 13 B

Large, E.C. (1954) Growth Stages in Cereals, Illustration of the Feekes Scale. **Plant Pathology** [online], 3 (4): 128–129. Available from: http://doi.wiley.com/10.1111/j.1365-3059.1954.tb00716.x

Leong, E.C. and Rahardjo, H. (1997) Review of Soil-Water Characteristic Curve Equations. **Journal of Geotechnical and Geoenvironmental Engineering**

[online]. 123 (12) pp. 1106–1117. Available from: http://ascelibrary.org/doi/abs/10.1061/%28ASCE%291090-0241%281997%29123%3A12%281106%29 [Accessed 3 December 2014]

MacLeod, D. (2011) **Aerial Archaeology** [online]. Available from: http://www.bbc.co.uk/history/ancient/archaeology/time_flyers_01.shtml

Malaya, C. and Sreedeep, S. (2012) Critical Review on the Parameters Influencing Soil-Water Characteristic Curve. **Journal of Irrigation and Drainage Engineering** [online], 138 (1): 55–62. Available from: http://ascelibrary.org/doi/abs/10.1061/%28ASCE%29IR.1943-4774.0000371 [Accessed 3 December 2014]

McBurney, C.B.M. (1963) "Archaeology and Dating." In Brothwell, D. and Higgs, E. (eds.) **Science in Archaeology, A comprehensive Survey of Progress and Research**. 1st ed. Thames and Hudson. pp. 21–23

Mills, J. and Palmer, R. (eds) (2007) **Populating Clay Landscapes**. Tempus Stroud

Monteith, J.L. and Unsworth, M.H. (1990) **Principles of Environmental Physics**. Butterworth-Heinemann

Nachabe, M.H. (1998) Refining the Definition of Field Capacity in the Literature. **Journal of Irrigation and Drainage Engineering** [online], 124 (4): 230–232. Available from: http://ascelibrary.org/doi/10.1061/(ASCE)0733-9437(1998)124:4(230)

Nyambayo, V.P. and Potts, D.M. (2010) Numerical simulation of evapotranspiration using a root water uptake model. **Computers and Geotechnics** [online], 37 (1-2): 175–186. Available from: http://dx.doi.org/10.1016/j.compgeo.2009.08.008

Ordnance Survey (1884) **County Series 1st Edition [TIFF geospatial data], 1:2500, Cirencester (sp0600, sp0700, sp0800), published 1884.** [online]. Available from: digimap.edina.ac.uk (14/01/12)

Ordnance Survey (1888) **County Series 1st Edition [TIFF geospatial data], 1:2500,**

Diddington (tl1765, tl1865, tl1965), published 1888. [online]. Available from: digimap.edina.ac.uk (14/01/12)

Ordnance Survey (1921) **County Series 2nd Revision [TIFF geospatial data], 1:2500, Cirencester (sp0600, sp0700, sp0800), published 1921.** [online]. Available from: digimap.edina.ac.uk (14/01/12)

Ordnance Survey (1960) **National Survey 1st Imperial Edition [TIFF geospatial data], 1:10560, Cirencester (sp00se), published 1960.** [online]. Available from: digimap.edina.ac.uk (14/01/12)

Ordnance Survey (1970) **National Survey 1st Revision [TIFF geospatial data], 1:10560, Diddington (tl16ne), published 1970.** [online]. Available from: digimap.edina.ac.uk (14/01/12)

Ordnance Survey (1982) **National Survey Latest Metric Edition [TIFF geospatial data], 1:10000, Cirencester (sp00se), published 1982.**

Ordnance Survey (1984) **National Survey Latest Metric Edition [TIFF geospatial data], 1:10000, Diddington (tl16ne), published 1984.** [online]. Available from: digimap.edina.ac.uk (14/01/12)

Ordnance Survey (2005) **GB National Outlines [SHAPE geospatial data], 1:250000, GB, Updated 2005.** [online]. Available from: digimap.edina.ac.uk (12/02/2014)

Ordnance Survey (2013a) **1:25k Raster [TIFF geospatial data], 1:25000, Cirencester (sp00, sp10, su09, su19), April 2013 version.** [online]. Available from: digimap.edina.ac.uk (27/02/2014)

Ordnance Survey (2013b) **1:25k Raster [TIFF geospatial data], 1:25000, Diddington (tl16, tl26), April 2013 version.** [online]. Available from: digimap.edina.ac.uk (27/02/2014)

Ordnance Survey (2013c) **Mastermap [TIFF geospatial data], 1:2000, Cirencester (su09, su19, sp00, sp10), Updated 2013.** [online]. Available from:

digimap.edina.ac.uk (29/01/2014)

Ordnance Survey (2013d) **Mastermap [TIFF geospatial data], 1:2000, Diddington (tl16, tl26, tl36), Updated 2013.** [online]. Available from: digimap.edina.ac.uk (16/01/2014)

Ordnance Survey (2013e) **Terrain-50 Contours [SHAPE geospatial data], 1:50000, Cirencester (su09, su19, sp00, sp10), Updated 2013.** [online]. Available from: digimap.edina.ac.uk (29/01/2014)

Ordnance Survey (2013f) **Terrain-50 Contours [SHAPE geospatial data], 1:50000, Diddington (tl16, tl26, tl36), Updated 2013.** [online]. Available from: digimap.edina.ac.uk (16/01/2014)

Ordnance Survey (2013g) **Terrain-50 DTM [ASC geospatial data], 1:50000, Cirencester (su09, su19, sp00, sp10), Updated 2013.** [online]. Available from: digimap.edina.ac.uk (29/01/2014)

Ordnance Survey (2013h) **Terrain-50 DTM [ASC geospatial data], 1:50000, Diddington (tl16, tl26, tl36), Updated 2013.** [online]. Available from: digimap.edina.ac.uk (16/01/2014)

Ordnance Survey (2014) **Miniscale [TIFF geospatial data], 1:100000, GB, Updated 2014.** [online]. Available from: digimap.edina.ac.uk (12/02/14)

Owen, J. (2009) **Huge pre-Stonehenge complex found via "crop circles"** [online]. Available from: http://news.nationalgeographic.com/news/2009/06/090615-stonehenge-tombs-crop-circles.html [Accessed 11 September 2014]

Pallottino, M. (1968) **The Meaning of Archaeology**. H. N. Abrams, New York

Parrington, M. (1983) Remote Sensing. **Annual Review of Anthropology**, 12: 105–124

Pedroso, D.M. and Williams, D.J. (2010) A novel approach for modelling soil-water characteristic curves with hysteresis. **Computers and Geotechnics** [online], 37 (3): 374–380. Available from:

http://linkinghub.elsevier.com/retrieve/pii/S0266352X09001839 [Accessed 3 December 2014]

Perera, Y., Zapata, C., Houston, W., et al. (2005) Prediction of the Soil-Water Characteristic Curve Based on Grain-Size-Distribution and Index Properties. **Geotechnical Special Publication** [online], 130: 1–12. Available from: http://ascelibrary.org/doi/abs/10.1061/40776(155)4 [Accessed 3 December 2014]

Pham, H.Q. and Fredlund, D.G. (2008) Equations for the entire soil-water characteristic curve of a volume change soil. **Canadian Geotechnical Journal** [online], 45 (4): 443–453. Available from: http://www.nrcresearchpress.com/doi/abs/10.1139/T07-117 [Accessed 3 December 2014]

Piggott, S. (1959) **Approach to Archaeology**. Harvard University Press, Cambridge

Rapp, G.R. and Hill, C.L. (1998) **Geoarchaeology: The Earth-science Approach to Archaeological Interpretation**. Yale University Press

Rawlins, B.G. (2014) **Personal Communication**

Rawls, W.J., Ahuja, L.R., Brakensiek, D.L., et al. (1992) "Infiltration and Soil Water Movement." In Maidment, D.R. (ed.) **Handbook of Hydrology**. New York: McGraw-Hill Inc. pp. 5.1–5.51

Reeves, D.M. (1936) Aerial Photography and Archaeology. **American Antiquity**, 2: 102 – 107

Riley, D.N. (1996) **Aerial Archaeology in Britain**. Ltd., S.P. (ed.). Aylesbury: Shire Publications Ltd.

Riley, D.N. (1982) **Air Photography and Archaeology**. London.

Ros Mesa, I. (2015) **Stochastic modelling of soil carbon stocks under different land uses : a case study in South Africa**. Stellenbosch University

Röver, M. and Kaiser, E.A. (1999) Spatial heterogeneity within the plough layer: Low and moderate variability of soil properties. **Soil Biology and Biochemistry**, 31 (2): 175–187

Rubey, W.W. (1933) Settling velocities of gravel, sand, and silt particles. **American Journal of Science**, 25: 325–328

Ryżak, M. and Bieganowski, A. (2011) Methodological aspects of determining soil particle-size distribution using the laser diffraction method. **Journal of Plant Nutrition and Soil Science** [online], 174 (4): 624–633. Available from: http://doi.wiley.com/10.1002/jpln.201000255

Saxton, K. and Willey, P. (2005) "The SPAW Model for Agricultural Field and Pond Hydrologic Simulation." In Frevert, D. and Singh, V. (eds.) **Watershed Models** [online]. CRC Press. pp. 400–435. Available from: http://books.google.com/books?hl=en&lr=&id=mn8Foj3rAwQC&oi=fnd&pg=PA401&dq=THE+SPAW+MODEL+FOR+AGRICULTURAL+FIELD+AND+POND+HYDROLOGIC+SIMULATION&ots=o8VENZHHnD&sig=FKYmSyBRZX3w7KnLRlQmnMuDAZM

Saxton, K.E. and Rawls, W.J. (2006) Soil Water Characteristic Estimates by Texture and Organic Matter for Hydrologic Solutions. **Soil Science Society of America Journal** [online], 70 (5): 1569. Available from: https://www.soils.org/publications/sssaj/abstracts/70/5/1569 [Accessed 13 July 2014]

Saxton, K.E., Willey, P.H. and Rawls, W.J. (2006) "Field and Pond Hydrologic Analyses with the SPAW Model." In **American Society of Agricultural and Biological Engineers**. **2006**

Scollar, I., Tabbagh, A., Hesse, A., et al. (1990) **Topics in Remote Sensing 2: Archaeological Prospecting and Remote Sensing**. Cambridge University Press

Sheng, D., Zhou, A.-N. and Carter, J.P. (2012) Modelling the effect of initial density on

soil-water characteristic curves. **Géotechnique** [online], 62 (8): 669–680. Available from: http://www.icevirtuallibrary.com/content/article/10.1680/geot.10.P.120 [Accessed 3 December 2014]

Smith, R. and Cox, P. (1986) **The Past In The Pipeline**. Cox, P. (ed.). Trust for Wssex Archaeology

St Joseph, J.K.S. (1977) "Air Photography and Archaeology." In St Jospeh, J.K.S. (ed.) **The Uses of Air Photography**. London: John Baker Publishers Ltd. pp. 165–153

Di Stefano, C., Ferro, V. and Mirabile, S. (2010) Comparison between grain-size analyses using laser diffraction and sedimentation methods. **Biosystems Engineering** [online], 106 (2): 205–215. Available from: http://linkinghub.elsevier.com/retrieve/pii/S1537511010000656 [Accessed 9 April 2013]

Stott, D. (2014) **Understanding Contrast Formation in Archaeological Features in Optical RemoteSensing Data.** University of Leeds

Sumbler, M.G., Barron, A.J.M. and Morigi, A.N. (2000) **Geology of the Cirencester District, Memoir of the British Geological Survey, sheet 235**. London: The Stationary Office

The Weather Channel (2012) **Weather Underground** [online]. Available from: http://www.wunderground.com/

Topp, G.C., Davis, J.L. and Annan, A.P. (1980) Electromagnetic determination of soil water content: Measurements in coaxial transmission lines. **Water Resources Research** [online], 16 (3): 574–582. Available from: http://doi.wiley.com/10.1029/WR016i003p00574 [Accessed 15 December 2014]

Torres-Hernandez, G. (2011) **Estimating the Soil–Water Characteristic Curve Using Grain Size Analysis and Plasticity Index** [online]. Arizona State University.

Available from: http://medcontent.metapress.com/index/A65RM03P4874243N.pdf\nhttp://repository.asu.edu/attachments/56747/content/TorresHernandez_asu_0010N_10702.pdf

Wilkinson, K. (2013) **DART Excavation Data** [online]. Available from: dartportal.leeds.ac.uk/dataset/dart_excavation_data [Accessed 26 February 2014]

Wilson, D.R. (2000) **Air Photo Interpretation for Archaeologists**. 2nd Ed. Tempus Stroud

Worssam, B.C. and Taylor, J.H. (1969) **Geology of the Country around Cambridge, Memoirs of the Geological Survey of Great Britiain**. London: Her Majesty's Stationary Office

Yang, H., Rahardjo, H., Leong, E.-C., et al. (2004) Factors affecting drying and wetting soil-water characteristic curves of sandy soils. **Canadian Geotechnical Journal**, 41 (5): 908–920

Zapata, C.E., Houston, W.N., Houston, S.L., et al. (2000) "Soil Water Characteristic Curve Variability." In **Geo-Denver 2000: Advances in Unsaturated Geotechnics**. **2000**. pp. 84–124

Zhai, Q. and Rahardjo, H. (2012) Determination of soil-water characteristic curve variables. **Computers and Geotechnics** [online], 42: 37–43. Available from: http://linkinghub.elsevier.com/retrieve/pii/S0266352X1100187X [Accessed 3 December 2014]

APPENDIX A – GEOTECHNICAL CHARATERISATION ADDITIONAL DATA

A.1 DRY DENSITY BY THE WATER DISPLACEMENT METHOD

The water displacement method used for dry density determination presented in BS1377:2 (British Standards Institute, 1990) was followed as far as was possible, however, some deviation in the sampling method was necessary. The standard states that samples should be cylindrical or cubical in shape with each dimension approximately equal to 100mm. Though the sampling method (using monolith tins 100mm x 100mm x 500mm) should have allowed specimens to be recovered in the appropriate size range, significant disturbance of the samples was encountered during extraction from the tin, sometimes due to a lack of cohesion of the soils themselves. Therefore, in general, only smaller specimens could be obtained as undisturbed, and in some cases no suitable specimen was recoverable from UD samples (CCC Ditchfills 1 and 2).

In order to reduce possible uncertainty of the data caused by small specimen sizes, where possible, between two and four of the largest recoverable undisturbed specimens were selected for analysis from each soil type in the UD samples. Initial sample masses were in the range of approximately 100-1000g. This may have introduced methodical error into the results.

Firstly, the small specimen sizes are less likely to be representative of the sample as a whole, especially where larger particles were present. Secondly, the small sample size caused methodological issues during water displacement for determination of the volume. The apparatus used requires an initial upward flow in order to drain the displaced water. Where a specimen was small and did not displace enough water to begin the flow, it was started

manually by agitating the water to begin the siphon process. However, disturbance of the water sometimes caused more or less than the equivalent sample volume of water to be displaced, due to lapping of the water surface against the siphon tube. Two specimen results (from DCF Clay 2 AS and DCF Clay 2 DS) were discounted due to significant difficulty in displacing the equivalent volume of water. In both cases two further specimen results were still available for analysis.

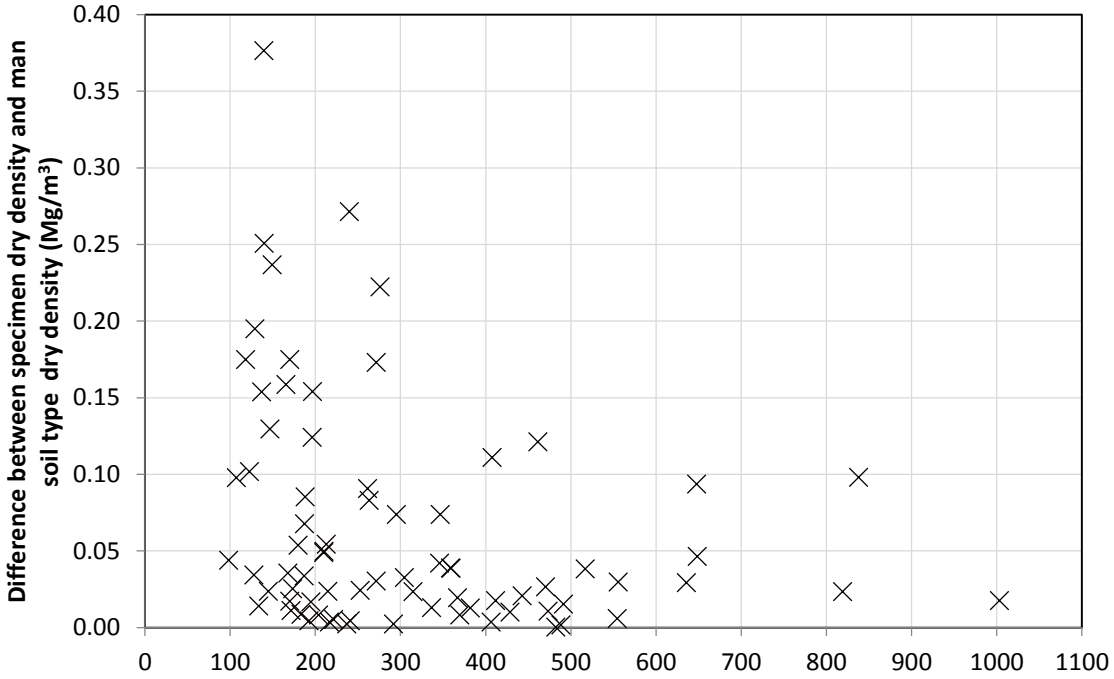

Figure A.1 Graph to show the dependence of the precision of dry density on initial sample size.

Analysis was carried out to assess the effect of the sample size on the dry density results. Since the volume of a specimen is a calculated result, the initial specimen mass has been used as an indicator of the sample size. Figure A.1 shows the initial mass of each specimen tested plotted against the difference between the specimen dry density and the mean soil type dry density. The graph shows that the results for specimens with an initial mass >500g fell within 0.10 Mg/m^3 of the sample average dry density, those with initial masses between 300-500g were within 0.20 Mg/m^3, and those >300g were within 0.40 Mg/m^3. This

correlation of specimen mass with precision indicates that the ranges in results may stem from methodical error than sample variation.

A.2 PARTICLE DENSITY BY THE SMALL PYCNOMETER METHOD

The small pycnometer method used for particle density determination presented in BS1377:2 (British Standards Institute, 1990), was followed as far as was possible, however, some difficulty was encountered in obtaining a known pressure in the vacuum desiccator. Initially, there was no equipment available to monitor or vary the strength of the vacuum pump applied to the desiccator, which was known to apply a pressure much higher than the 20mm mercury stated in the standard, this resulted in excessive bubbling of some of the samples and a loss of a small amount of sample through the neck of the pycnometer, causing error in the results of some tests. The resulting data were discounted and the tests repeated with the following modification. Two diversions were installed to the vacuum tubing linked to the desiccator, one with a valve to allow a reduction in the pressure, and another with a pressure gauge attached, so the pressure required by the standard could be achieved.

A.3 PARTICLE DENSITY BY THE GAS PYCNOMETER METHOD

In order to compare traditional and modern instrumentation methods, an AccuPyc II 1340 Gas Displacement Density Analyser (Micrometrics Instruments Corporation) at the Advanced Materials Laboratory 2, Chemical Engineering, University of Birmingham, was also used to determine the particle density of the soils. It uses the same principle of displacement as the small pycnometer method, but with a displacement medium of helium as opposed to water. The instrument was controlled, and the results collated using software provided by the manufacturer.

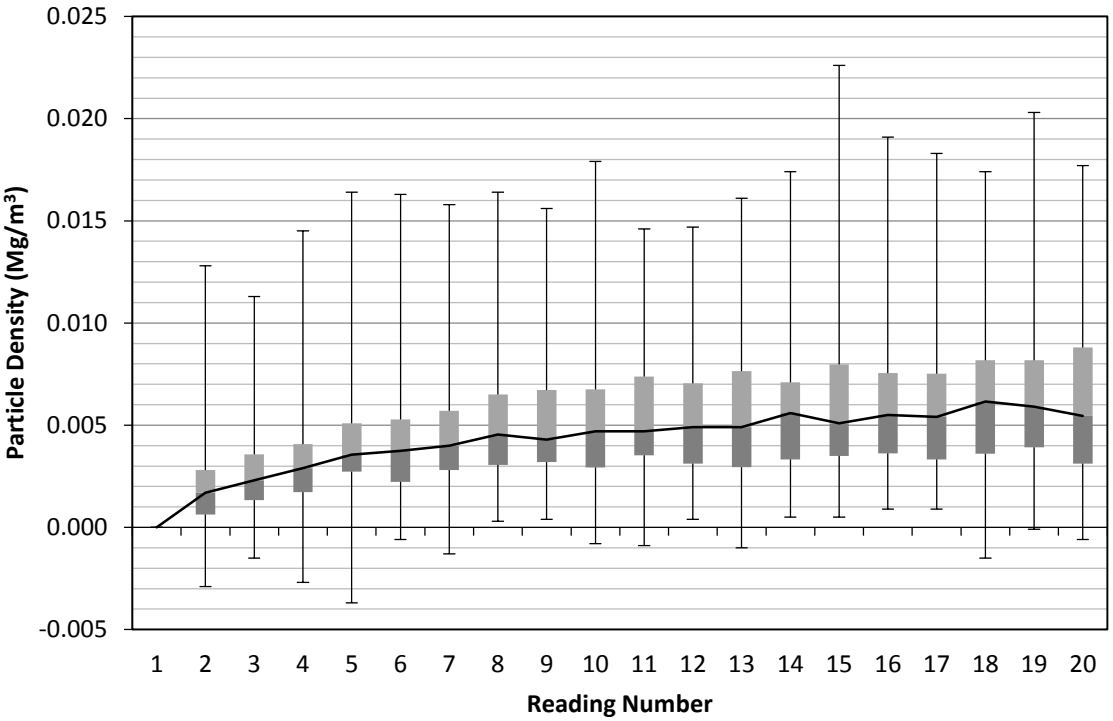

Figure A.2 Box and whisker plot of the difference of successive gas pycnometer readings from the initial reading.

The mass of approximately 0.6 – 1.0g of oven dried soil was determined by weighing to an accuracy of ±0.00005g. The specimen was then placed in a 1.0000 cm^3 sample chamber and sealed inside the instrument. The chamber is purged with helium 100 times to a maximum pressure of 19.5 psid to remove any air. The instrument determines the volume of the solid phase of the specimen by filling the chamber to a known pressure and discharging the gas into a separate measurement chamber. The instrument was set to take 20 readings of the specimen volume.

The raw data showed a tendency for the value of particle density to rise throughout the 20 readings. In order to assess the general increase throughout the successive readings, all the values of particle density were recalculated as a difference from the initial reading. A box and whisker plot of the results with quartile data are shown in Figure A.2. A possible explanation for this phenomena is that, although the pressure reached during purging is the

same as that during readings (19.5 psid), the length of time the pressure is held is shorter. It is therefore possible that the air-helium exchange is not fully complete after 100 purges.

The median value stabilises to within ±0.001 Mg/m^3 of the mean average value (0.0052 Mg/m^3) for the last 13 readings. Therefore, the first 7 readings of all the tests carried out have been discounted and an average of the final 13 readings taken as the particle density of the specimen being tested. The average increase in the sample mean particle density calculated for the final 13 readings from that of the mean of the complete dataset is 0.001 Mg/m^3, and the maximum increase in the sample mean due to the discounting of the initial 7 results is 0.004 Mg/m^3.

Using data provided by the manufacturer, a quantification of the expected error can be made. Determination of the experimental errors allows a clear assessment of the range of data due to sample variation. Particle density is a calculated result based on two separately determined parameters, the specimen mass and the specimen volume. The expected error in the density, E_D, arises from a combination of the expected error in mass, E_M, and the expected error in volume, E_V, and is represented by Equation A.1.

$$E_D = \frac{E_M}{M} + \frac{E_V}{V} \qquad [\text{ A.1 }]$$

where M is the measured mass of the specimen (g)
and V is the measured volume of the specimen (cm^3).

Since masses were determined to the fourth decimal place, the expected error in mass, E_M , is a maximum of 0.0001g.

Documentation provided by the manufacturer states that the accuracy of the volume readings are with 0.03% of the reading plus 0.03% of the sample capacity. In this case the sample

capacity is 1.0cm^3, therefore the maximum expected volume error for a reading can be expressed by Equation A.2.

$$E_V = 0.0003 \times (V + 1) \qquad [\text{ A.2 }]$$

The average expected error calculated for all 86 samples tested was 0.2%, with a minimum of 0.1% and a maximum of 0.5%.

Where two results for a soil type were available (a total of nine soil types), the difference between results were all within the average expected error with the exception of CCC Ditchfill 1, which had a difference of 0.21 Mg/m^3. The sum of the individual expected errors for these two results was 0.005 Mg/m^3 indicating that sample variation is the likely cause of the wide range.

A.4 PSD BY THE SIEVE METHOD

Two deviations from the standard were necessary for some of the Sv tests. Initially, a full set of sieves with apertures required by BS1377:2 (British Standards Institute, 1990) was not available, and the sieves used did not stack adequately. Early tests (samples from DCF and DPF) were therefore carried out in stages, as was allowed by stacking, and using apertures available (either complying with American Society for the Testing of Materials (2009), or old imperial sieves). This method only required changes to the calculation method and was not considered to affect the final results. Later tests (samples from CQF and CCC) were unaffected.

The Sv method was assessed for repeatability (precision), using identical specimens from the same sample preparation, and sample variation (range), using duplicate samples prepared separately, of results. Though sample sizes were small and multiple tests could not be carried out on all soil types, assessments have been made where more than one dataset was available.

For the three soil types where two separate samples were retrieved (DCF Subsoil ditch section, DCF Ditchfill 1 and CCC Ditchfill 1) and where sample volumes allowed two specimens from the same sample preparation to be tested (DCF Topsoil ditch section, DPF Topsoil adjacent section, DPF Subsoil adjacent section, and DPF sand), the results have been compared.

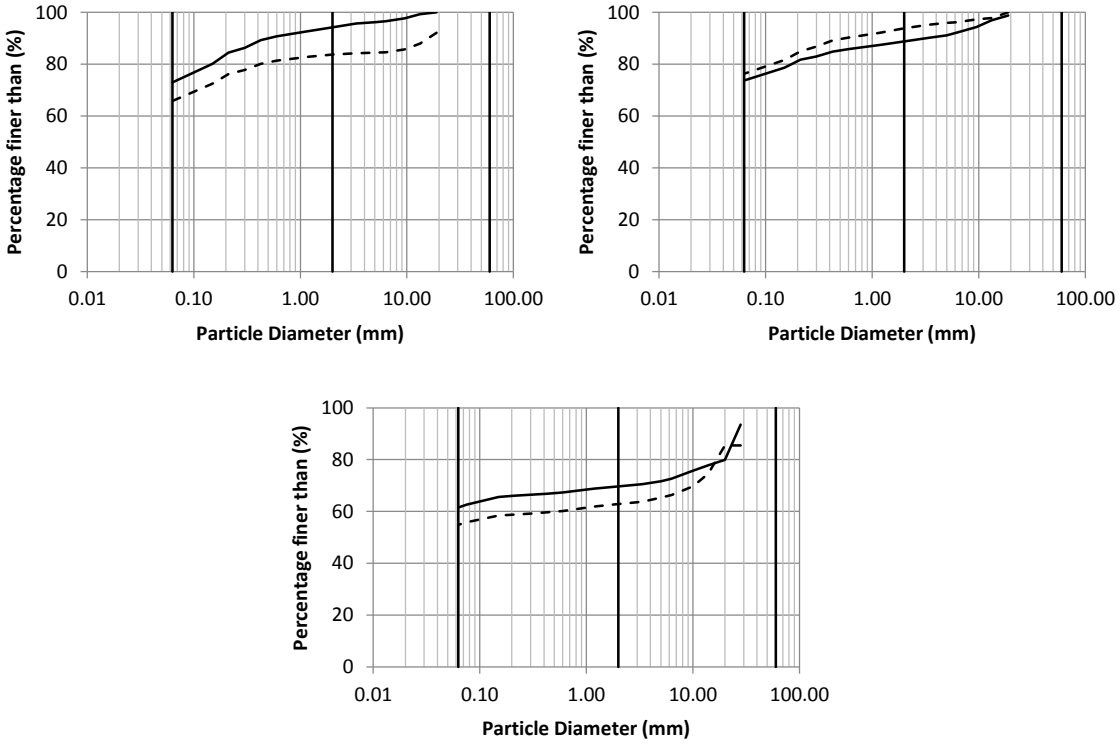

Figure A.3 Comparison of sieve results for two samples of a soil type.

(a) DCF Subsoil (DS) (b) DCF Ditchfill 1 (c) CCC Ditchfill 1

Figures A.3(a-d) show a comparison of the calculated percentages in the gravel and sand fractions where two separate samples of the same soil type were tested. The gravel fraction shows differences of up to 10% between the two samples whereas the sand fraction percentages were always within 3%. This shows that sample variation in the gravel fraction is higher than that of the sand fraction. The requirement to sample on a small scale, and the

resulting limitations on sample sizes, may have affected the representativeness of the soil type within the gravel fraction. Sample sizes tested were typically in the range 600-750g. In order to provide representative results, BS1377:2 (British Standards Institute, 1990) requires sample sizes to be >600g where the largest significant particle size is 10mm, rising to >2000g where the largest significant particle size is <20mm, possibly explaining the lack of consistent data sometimes shown in this range.

Figure A.4(a-d) show a comparison of the calculated percentages in the gravel and sand fractions where two specimens of the same sample preparation were tested. All results were within 2% with one exception in the sand fraction of DPF Topsoil AS which had a difference of 5% in the sand fraction.

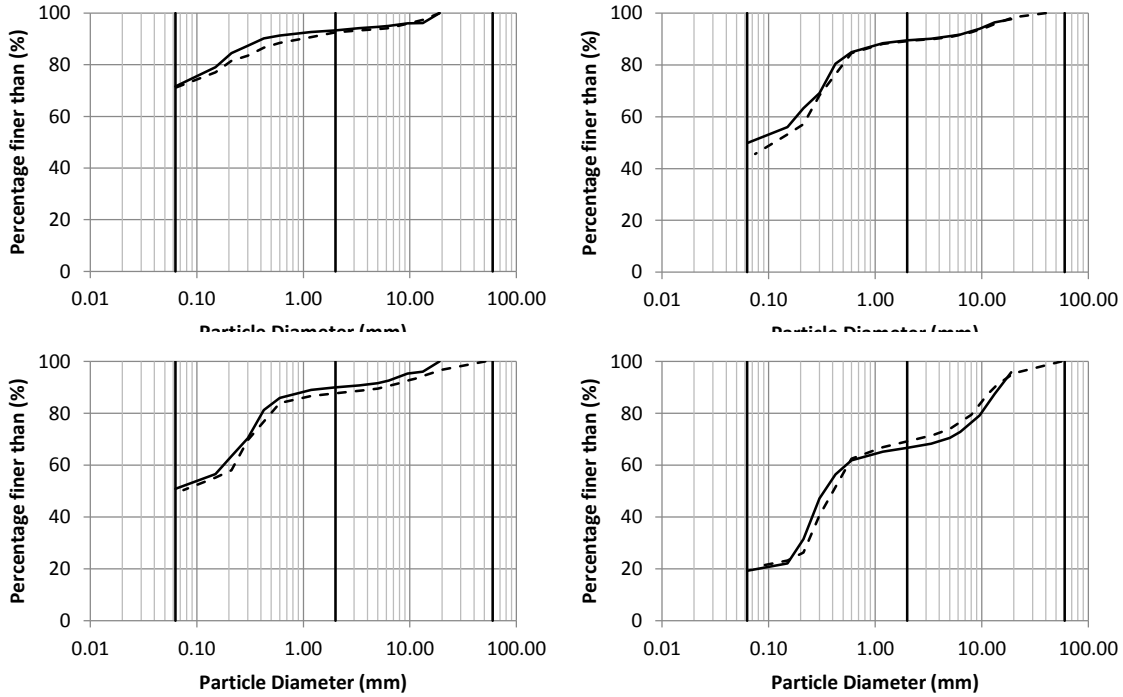

Figure A.4 Comparison of sieve results for two specimens of a sample.

(a) DCF Topsoil (DS) (b) DPF Topsoil (AS)

(c) DPF Subsoil (AS) (d) DPF Sand (AS)

A.5 PSD BY THE SEDIMENTATION BY HYDROMETER METHOD

Calibrations were carried out for the volume and scale of the hydrometer, and correction coefficients calculated for meniscus (allowing readings to be taken at the top of the meniscus), water viscosity (with respect to temperature) and inconsistencies in the factory calibration of the hydrometer (see Head, 1992). The calibration of temperature using a blank column containing dispersant solution was conducted separately prior to testing. The hydrometer readings of a sedimentation column containing 100ml dispersant solution and 900ml deionised water were taken at a range of temperatures from 18-25˚C. The equation of the linear regression line was used to calculate the expected reading of the blank column at each reading. Since the water bath has space for three columns, this increased efficiency, allowing three tests to be carried out concurrently, as opposed to two test columns and a calibration column.

BS1377:2 (British Standards Institute, 1990) states that readings should be taken at specific time intervals after the test has begun. However, reading of the scale of the hydrometer was awkward, and more accurate readings could be taken by recording the time at a graduation mark on the scale. The readings were therefore taken at non-specific particle diameters, due to the dependency of this calculation on time. This did not affect the accuracy of the resulting PSD curves, but further calculations were necessary to compare results between specimens.

Readings were taken at graduation marks on the hydrometer as opposed to given time intervals, therefore further calculation was necessary to compare the percentage passing specific diameters. In order to assess the percentages within fractions (coarse silt, fine silt, medium silt and clay), the percentage passing 63µm (sand-silt boundary), 20µm (coarse-medium silt boundary), 6µm (medium-fine silt boundary) and 2µm (silt-clay boundary) have

been approximated by using the equation of the line passing through the known points either side.

To assess precision, three separately prepared specimens of a sample (CQF Ditchfill 1) were tested and results calculated using data from a single SH test. Again the maximum difference between the percentages in both the clay and silt fractions was 1%. Figures A.5(a-d) show a comparison of the calculated percentages in the silt and clay fractions where two specimens of the same sample preparation were tested. In these cases, values were calculated using Sv results specific to the specimen. All results were within 2% with one exception in the silt fraction of DPF Topsoil AS which had a difference of 5%.

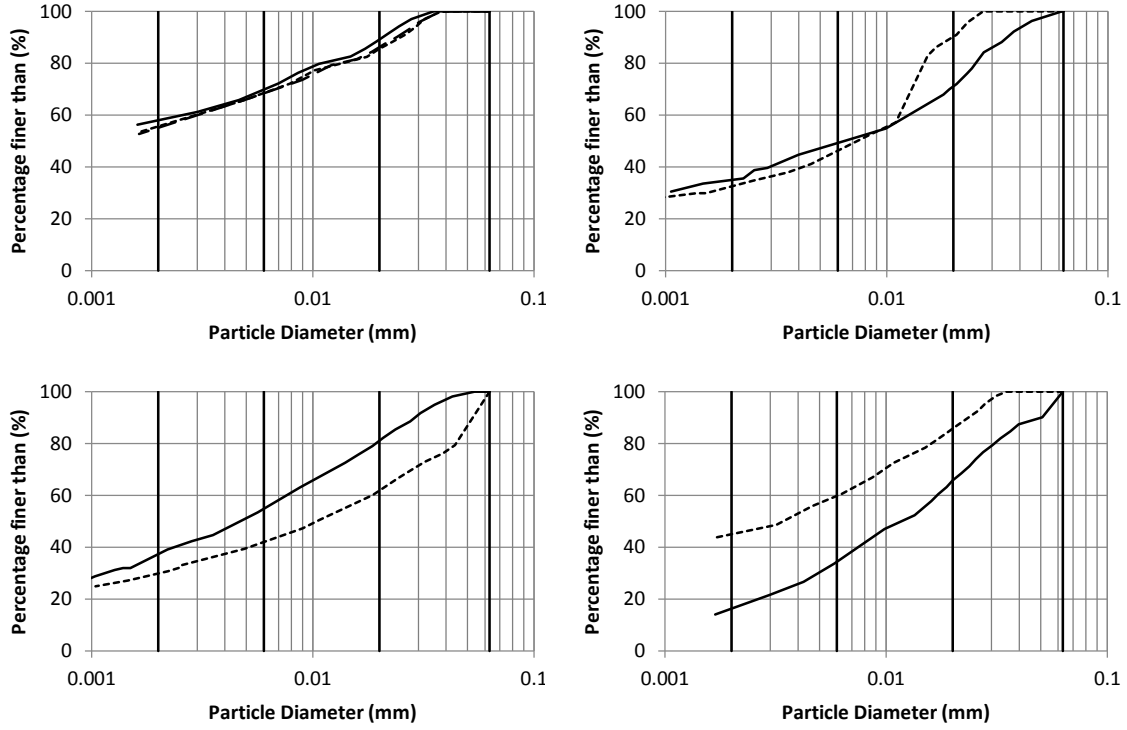

Figure A.5 Sedimentation by hydrometer results, tests on the multiple specimens of the same soil type.

(a) CQF Ditchfill 1 (b) DCF Subsoil (DS)

(c) DCF Ditchfill 1 (d) CCC Ditchfill 1

A.6 PSD BY THE LASER DIFFRACTION METHOD

As there is no standard for testing of soils using the LD method, a review of literature and initial tests were carried out to determine the appropriate method of analysis on the site soils.

The LD analysis was carried out using a wet dispersion, with the dispersant medium being ultrasonically deaired. A background reading was taken prior to each specimen being added to the instrument. The dispersant was stirred at a maximum of 2500rpm to avoid air bubbles forming. The refractive index was set to 1.54 (the approximate refractive index of quartz). Based on manufacturer advice, specimens were tested at a light obscuration of approximately 10%.

The optimal measurement time for a specimen was found to be 1 minute by Ryżak and Bieganowski (2011) using the same instrument. For this analysis, two 1 minute measurements were taken on each specimen to ensure the results were concurrent. For all specimens tested, the average difference between the results of the two measurements, at any recorded particle diameter, was found to be 3.9% with an average of 0.3%.

Adequate dispersion of the particles is fundamental to ensure light scattering gives representative results. Specimens can be deflocculated using two methods; using a solution of sodium hexametaphosphate; and ultrasound, which is built into the instrument. Ryżak and Bieganowski (2011) found that the use of both ultrasonic and chemical dispersion methods on a specimen caused an increase in the median particle size and suggests that they should not be used simultaneously. Chappell (1998) found that between 1-3 minutes of ultrasound was adequate for dispersion of soil samples. However, once clay coatings have been removed, quartz grains can be broken up (Di Stefano et al., 2010). Dispersion in deionised water using ultrasound for 2 minutes was tested against dispersion using sodium

hexametaphosphate solution, prepared to the same concentration as used for dispersion in sedimentation methods. FigureA.6 shows the results of a comparison of these two methods using identical specimens. The results and were found to be approximately equivalent with marginally better dispersion by chemical methods, evident by the slightly steeper gradient of the curve.

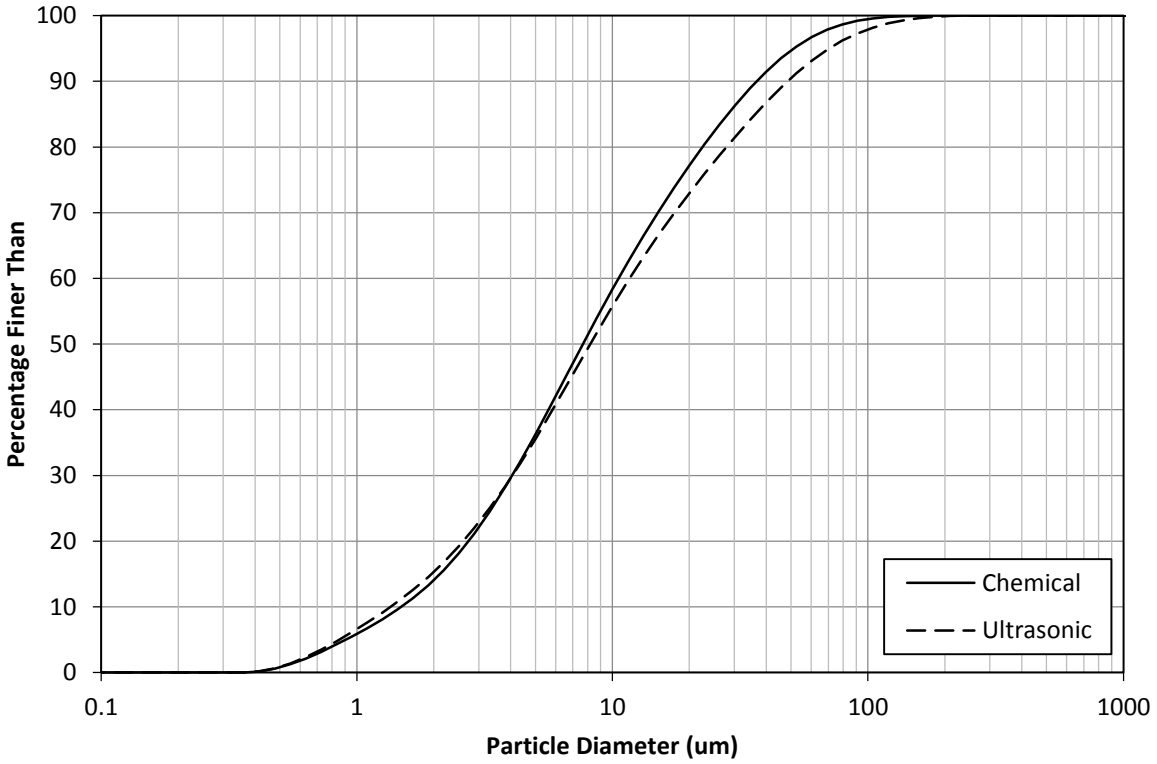

Figure A.6 Comparison of chemical and ultrasonic dispersant methods for determination of particle size distribution using laser diffraction.

The stirring time allowed before measurement is also of importance in ensuring adequate dispersion. Figure A.7 shows the results of three measurements taken on the same specimen, the first after 2 minutes of stirring and the subsequent readings at 5 minute intervals after the initial measurement. The results are equivalent for each of the three readings, indicating that no significant deflocculation of the specimen occurred after the first measurement.

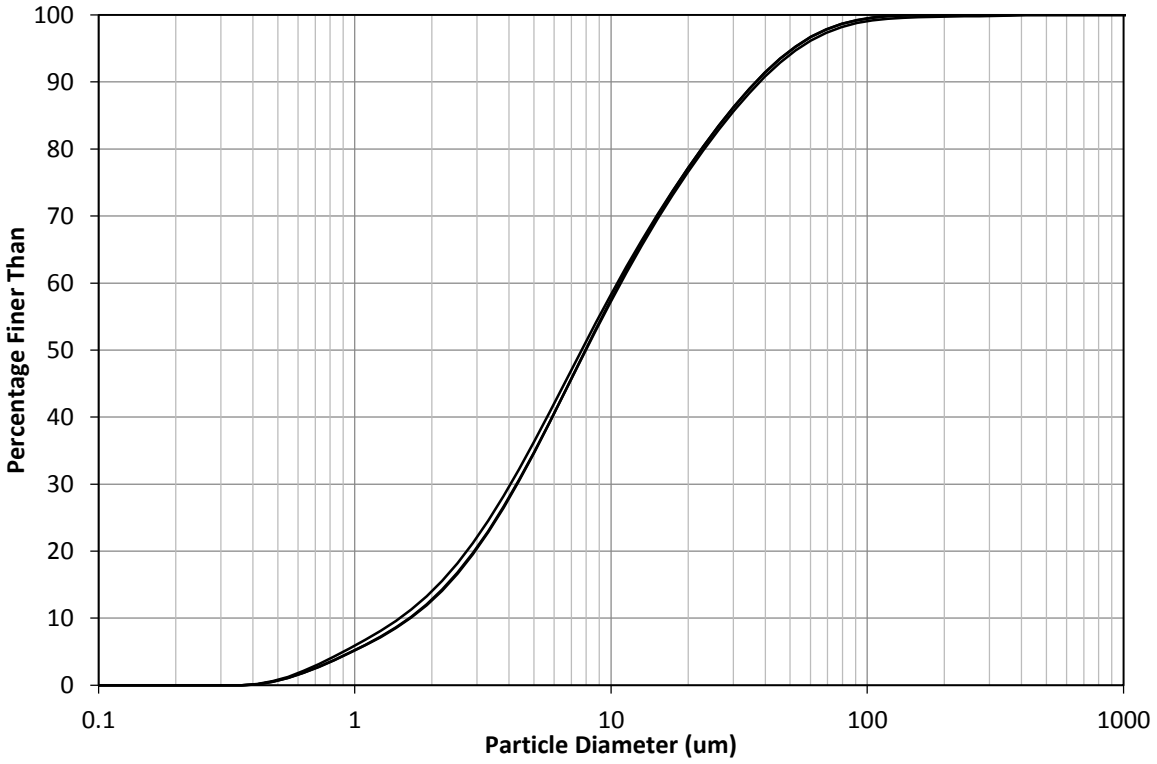

Figure A.7 Results of successive laser diffraction readings taken at 5 minute intervals.

On the basis of this test, the method of 2 minutes of ultrasonic dispersion followed by two 1 minute measurements was used for testing each specimen. The results of the two measurements at each recorded particle diameter was averaged to provide a single PSD for each specimen.

The results of LD analysis were produced using software provided by the manufacturer, which calculates the results using Mie theory. The data was calculated as a percentage by volume, which, assuming a single particle density, is equivalent to the percentage by mass recorded by Sv and SH techniques.

As with the SH method, the percentages within fractions have been approximated by using the equation of the line passing through the known points either side of the boundary diameters.

APPENDIX B – MODELLING SOIL WATER CHARATERISTICS ADDITIONAL DATA

B 1 THE SOIL WATER CHARACTERISTIC CURVE

The SWCC is fundamental in understanding the mechanics of water in soils. Empirical relationships between the SWCC and the geotechnical properties of the soil, such as PSD, plasticity, void ratio and density have been established, and their general influence on the SWCC is discussed in Malaya and Sreedeep (2012).

The most common approach to determination of the SWCC is using a fitting equation, mathematically representing the shape of the SWCC, with a number of fitting parameters which can be correlated to geotechnical properties using regression analysis. Fitting equations have been proposed by Gardner (1956), Brooks and Corey (1964), van Genuchten (1980), Pham and Fredlund (2008) and Sheng et al. (2012) amongst others, though Leong and Rahardjo (1997) concluded that the commonly used, four parameter, sigmoidal equation presented by Fredlund and Xing (1994) performed the best. Fitting parameters for the Fredlund and Xing equation, correlated with PSD and plasticity, have been proposed by Zapata et al. (2000), Perera et al. (2005) and Torres-Hernandez (2011).

Functions which give SWCCs directly from soil parameters have also been proposed, such as those by Johari et al. (2006) and Ahangar-Asr et al. (2012). These methods require inputs of void ratio, therefore determination of dry and particle density are required.

Saxton and Rawls (2006) give functions based on the PSD and organic matter to predict the water content at given suctions. To calculate the full curve, equations are presented for each part of the curve between these values.

The Fredlund and Xing (FX) method, along with equations for the fitting parameters, and the Saxton and Rawls (SR) method are outlined below.

B 2 THE FREDLUND AND XING (FX) METHOD

B 2.1 Sigmoidal Equation

Fredlund and Xing (1994) presented an equation representing the SWCC in terms of the Degree of Saturation, θ_{SAT} using four fitting parameters, *a*, *b*, *c* and Ψ_r (Equation A.3).

$$\theta_{SAT} = \left[1 - \frac{\ln\left(1 + {}^{\psi}/_{\psi_r}\right)}{\ln\left(1 + {}^{10^6}/_{\psi_r}\right)}\right] \times \left[\frac{1}{\left[\ln\left(e + \left({}^{\psi}/_{a}\right)^{b}\right)\right]^{c}}\right] \qquad [\text{ A.3 }]$$

where Ψ is the suction (kPa).

Sensitivity analyses of the SWCC to each of the fitting parameters is presented in Leong and Rahardjo (1997) and Torres-Hernandez (2011), where the resulting change in the shape of the SWCC as each of the fitting parameters is varied has been assessed.

Fitting parameters for the FX method have been determined by Zapata et al. (2000), Perera et al. (2005), Torres-Hernandez (2011), from here onwards these sets of fitting parameters are called ZA, PA, and TH respectively . Each of these has used a similar approach, classifying soils from a database as non-plastic or plastic and carrying out a regression analysis, to determine a set of equations for the parameters *a*, *b*, *c*, and Ψ_r for Equation A.3 for each classification. Differences in the resulting equations stem from the database of soils used, and the geotechnical parameters chosen for regression.

B 2.2 Zapata (ZA) Fitting Parameter Equations

Zapata et al. (2000) classifies soils which are non-plastic as those with a $PI = 0$, and those which are plastic as those with a $PI > 0$. The equations for non-plastic soils are calculated

from the PSD, using D_{60}. The equations for plastic soils are related to the *wPI*. The two sets of fitting parameters are given below.

Non-Plastic (PI = 0)

$$a = 0.8627(D_{60})^{-0.751}$$

$$b = 7.5$$

$$c = 0.1172 \times ln(D_{60}) + 0.7734$$

$$\psi_r/_a = \frac{1}{D_{60} + 9.7e^{-4}}$$

Plastic (PI > 0)

$$a = 0.00364(wPI)^{3.35} + 4(wPI) + 11$$

$$b/_c = -2.313(wPI)^{0.14} + 5$$

$$c = 0.0514(wPI)^{0.465} + 0.5$$

$$\psi_r/_a = 32.44e^{0.00186(wPI)}$$

B 2.3 Perera (PA) Fitting Parameter Equations

Perera et al. (2005) classifies soils which are non-plastic as those with a *wPI* < 1, and those which are plastic as those with a *wPI* > 1. The equations for non-plastic soils are calculated from the PSD, using D_{90}, D_{60}, D_{30}, D_{20} and D_{10}. The equations for plastic soils are related to the *wPI*. The two sets of fitting parameters are given below.

Non-Plastic (wPI < 1)

Initially calculations are made to estimate D_{100} and D_0.

$$D_{100} = 10^{\left[\frac{40}{[log(D_{90}) - log(D_{60})]} + log(D_{60})\right]}$$

$$D_0 = 10^{\left[\frac{30}{20/[log(D_{30})-log(D_{10})]}+log(D_{30})\right]}$$

$$a = 1.14[-2.79 - 14.1log(D_{20}) - 1.9 \times 10^{-6} \times P_{200}^{4.34} + 7log(D_{30}) + 0.055(D_{100})]$$

$$b = 0.936\left\{5.39 - 0.29ln\left[P_{200}\left(\frac{D_{90}}{D_{10}}\right)\right] + 3(D_0)^{0.57} + 0.021P_{200}^{1.19}\right\} \times \left\{\frac{30}{[log(D_{90}) - log(D_{60})]}\right\}^{0.1}$$

$$c = 0.26e^{\left\{0.758\left[log\left(\frac{20}{[log(D_{30})-log(D_{10})]}\right)^{1.15}-\left(1-\frac{1}{b}\right)\right]\right\}} + 1.4(D_{10})$$

$$\psi_r = 500$$

Plastic (wPI > 1)

$$a = 32.835[ln(wPI)] + 32.438$$

$$b = 1.421(wPI)^{-0.3185}$$

$$c = 0.2154[ln(wPI)] + 0.7145$$

$$\psi_r = 500$$

B 2.4 Torres-Hernandez (TH) Fitting Parameter Equations

Torres-Hernandez (2011) classifies soils which are non-plastic as those with a *wPI* < 1, and those which are plastic as those with a *wPI* > 1. The equations for non-plastic soils are calculated from the PSD, using D_{10}. The equations for plastic soils are related to the *GI*. The two sets of fitting parameters are given below.

Non-Plastic (wPI < 1)

If $D_{10} < 0.020$

$$a = 1.28$$

If $D_{10} > 0.020$

$$a = -967.21(D_{10})^2 + 218.37(D_{10}) - 2.7$$

$$b = 10^{(-00075a^3+0.1133a^2-0.3577a+0.3061)}$$

$$c = 0.0058a^3 - 0.933a^2 + 0.4069a + 0.3481$$

$$\psi_r = 100$$

Plastic (wPI > 1)

$$a = 10^{\left[0.69\left(2.7/1+e^{4-0.14GI}\right)\right]}$$

$$b = 10^{\left[0.78/1+e^{6.75-0.19GI}\right]}$$

$$c = 0.03 + 0.62e^{[-0.82(log(a)-0.57)^2]}$$

$$\psi_r = 494 + \frac{660}{1 + e^{4-0.19GI}}$$

B 3 THE SAXTON AND RAWLS (SR) METHOD

Saxton and Rawls (2006) present a number of equations to predict the VWC for three given suctions; 1500 kPa, known as the permanent wilting point, θ_{1500}; 33 kPa, field capacity, θ_{33}; and 0 - 33 kPa, from saturation to field capacity, $\theta_{(s\text{-}33)}$. The VWC at saturation, θ_s, and the suction at air entry, Ψ_e, are also defined. The method provides an adjustment for density whereby the value of matric density, ρ_m, is used to give alternative values of θ_{33} ($\theta_{(33)DF}$), $\theta_{(s\text{-}33)}$ ($\theta_{(s\text{-}33)DF}$) and θ_s ($\theta_{(s)DF}$). For all calculations in this study this density adjustment has been applied, use of these adjusted parameters is represented in equations where appropriate, though for simplicity the notation in text has not been changed.

Using these parameters, the full curve is then calculated in three segments via coefficients *A* and *B*; from the permanent wilting point to field capacity, $\Psi_{(1500\text{-}33)}$; from field capacity to air entry, $\Psi_{(33\text{-}\Psi e)}$; and from air entry to $\theta = 0$, $\theta_{(\Psi e\text{-}0)}$).

In addition to ρ_m, input parameters are the percentage by mass of sand, *S*, clay, *C* and organic matter, *OM*. Though it should be borne in mind that the method has its roots in soil science, therefore, the sand silt and clay fraction (from hereon called the matric fraction) are assumed to comprise 100% of the soil. To directly compare SWCCs using this method with the FX method, adjustments to the values of *S* and *C*, based on the percentage in the gravel fraction must be made.

VWC at given suctions

$$\theta_{1500} = \theta_{1500t} + (0.14\theta_{1500t} - 0.02)$$

$$\theta_{1500t} = -0.024S + 0.487C + 0.006OM + 0.005(S \times OM) - 0.013(C \times OM) + 0.068(S \times C) + 0.031$$

$$\theta_{(33)DF} = \theta_{33} - 0.2\left(\theta_s - \theta_{(s)DF}\right)$$

$$\theta_{33} = \theta_{33t} + [1.283(\theta_{33t})^2 - 0.374(\theta_{33t}) - 0.015]$$

$$\theta_{33t} = -0.251S + 0.195C + 0.011OM + 0.006(S \times OM) - 0027(C \times OM) + 0.452(S \times C) + 0.299$$

$$\theta_{(s-33)DF} = \theta_{(s)DF} - \theta_{(33)DF}$$

$$\theta_{(s-33)} = \theta_{(s-33)t} + \left(0.363\theta_{(s-33)t} - 0.107\right)$$

$$\theta_{(s-33)t} = 0.278S + 0.034C + 0.022OM - 0.018(S \times OM) - 0.027(C \times OM) - 0.584(S \times C) + 0.078$$

VWC at Saturation

$$\theta_{(s)DF} = 1 - \left(\rho_m / 2.65\right)$$

$$\theta_s = \theta_{33} + \theta_{(s-33)} - 0.097S + 0.043$$

Suction at Air Entry

$$\psi_e = \psi_{et} + (0.02\psi_{et}^2 - 0.113\psi_{et} - 0.70)$$

$$\psi_{et} = -21.67S - 27.93C - 81.97\theta_{(s-33)DF} + 71.12\left(S \times \theta_{(s-33)DF}\right) + 8.29\left(C \times \theta_{(s-33)DF}\right) + 14.05(S \times C) + 27.16$$

SWCC Segment Equations

$\psi_{(1500-33)}$ $\quad \psi_\theta = A(\theta)^{-B}$

$\psi_{(33-\psi_e)}$ $\quad \psi_\theta = 33.0 - \left[\dfrac{\left(\theta - \theta_{(33)DF}\right)(33.0 - \psi_e)}{\left(\theta_{(s)DF} - \theta_{(33)DF}\right)}\right]$

$\theta_{(\psi_e-0)}$ $\quad \theta = \theta_{s(DF)}$

$$A = \exp\left(ln33 + Bln\theta_{(33)DF}\right)$$

$$B = \frac{[ln(1500) - ln(33)]}{\left[ln\left(\theta_{(33)DF}\right) - ln(\theta_{1500})\right]}$$

B 4 INFLUENCES ON THE SWCC

B 4.1 Hysteresis

There are numerous influences on the SWCC and although it is not considered in models discussed in this study, hysteresis can have a significant effect. The empirical methods of SWCC calculation present a unique relationship between Ψ and θ, however, there can be differences in Ψ for a single value of θ. Hysteresis causes the relationship to differ depending

on whether the soil is undergoing wetting or drying. Hysteretic behaviour occurs because the movement of soil water is not strictly inverse between the wetting and drying process, and drying curves exhibit higher Ψ at the same θ than wetting curves, illustrated in Figure A.8.

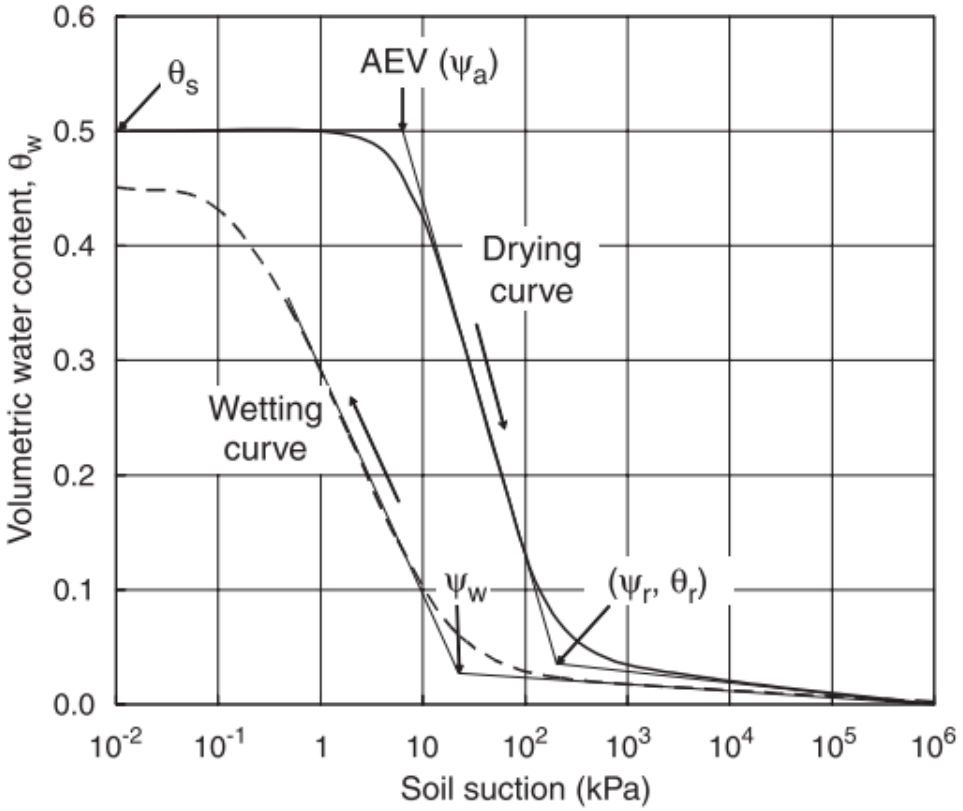

Figure A.8 Example of hysteresis in the SWCC. After Yang et al. (2004).

Though models of the SWCC taking into account hysteresis in sands, for example Yang et al. (2004), Lamara and Derriche (2008) and Pedroso and Williams (2010), there are few studies that deal with the experimental quantification of hysteresis for different types of soils and its influence on unsaturated behaviour modelling. Malaya and Sreedeep (2012) attribute this to the difficulty in obtaining wetting curves. Torres-Hernandez (2011) suggests that the database of soils (with over 36000 entries) used for his regression analysis have SWCCs

obtained upon drying. It is therefore considered likely that the equations presented are typically based on regression of data obtained from drying curves.

The lack of studies modelling hysteretic behaviour of differing soil types means that the effects of hysteresis cannot be taken into account in this study, and the models used are the best available.

B 4.2 Porosity

The porosity of a soil is equal to the saturated water content, θ_s. Although this does not have an effect on the shape of the curve, it defines the maximum water content and can affect the appearance of the SWCC depending on the way it is plotted. The SWCC can be plotted as the relationship between suction, and either the degree of saturation, θ_{SAT}, or the VWC, θ. θ_{SAT} is related to θ by the relationship shown in Equation A.4. When the SWCC is plotted in terms of θ, the curve is directly proportional to the θ_s, which is the intercept on the y axis.

$$\theta_{SAT} = \theta \times \theta_s \qquad [\text{ A.4 }]$$

B 4.3 Correlated Parameters

The equations for the fitting parameters for the FX method are divided based on plasticity. The PSD is only used in those which are classified as non-plastic (either those with a $PI = 0$ or a $wPI < 1$ depending on the method used). The SR method does not take into account the plasticity of the soil and uses input of proportions of sand and clay for all soil types.

Zapata et al. (2000) gives a family of curves which result from her equations (Figure A.9). This shows that for soils classified as non-plastic, higher Ψ is present at the same θ as D_{60} is reduced. Therefore, the general influence of PSD on the SWCC is the finer the soil, the greater the suction. The steepness of the curve between 1 and 10 kPa suction indicates that the soils have similar Ψ over a wide range of θ.

Though the plasticity of soils is not correlated with the SWCC in the SR method, the equations for the FX method use the parameters, *wPI* (ZA and PA), and *GI* (TH) to calculate the SWCC, when soils are classified as plastic. These parameters are plasticity dependant, though they also make use of the proportion of fine soil <0.075mm.

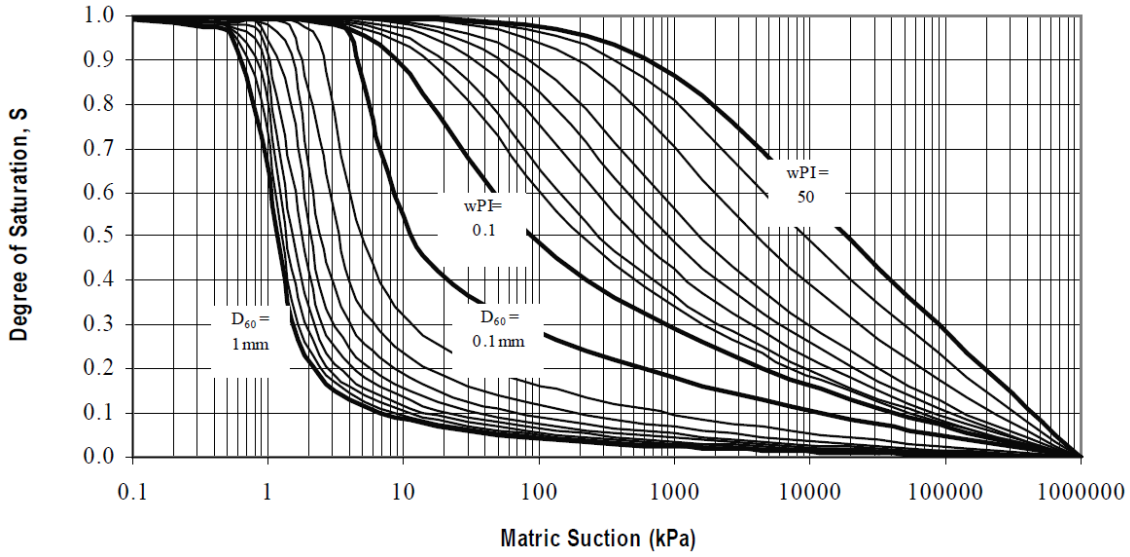

Figure A.9 Family of SWCC for non-plastic and plastic soils. After Torres-Hernandez (2011).

Figure A.9 also shows a family of curves for varying *wPI*. The shape of the curves are smoother than those calculated using PSD alone, and Ψ varies more greatly with θ than in non-plastic soils. As *wPI* increases, higher Ψ is present at the same θ, therefore the more plastic the soil, the higher the suction.

B 5 METHODS OF CALCULATION

B 5.1 Example data

To evaluate the differences between the FX method (with ZA, PA and TH fitting parameters) and the SR method, the resulting SWCC for example soils were compared using synthetic parameters. A sand and gravel, and a fine sand, with parameters such that it is borderline between plastic and non-plastic, and a clay soil were used as examples. The PSD curves are

given in Figure A.10 and calculation parameters in Table A.1. Marginally different PI inputs were used for the ZA method for fine sand so as to fit with the method requirements, keeping the parameters borderline between plastic and non-plastic.

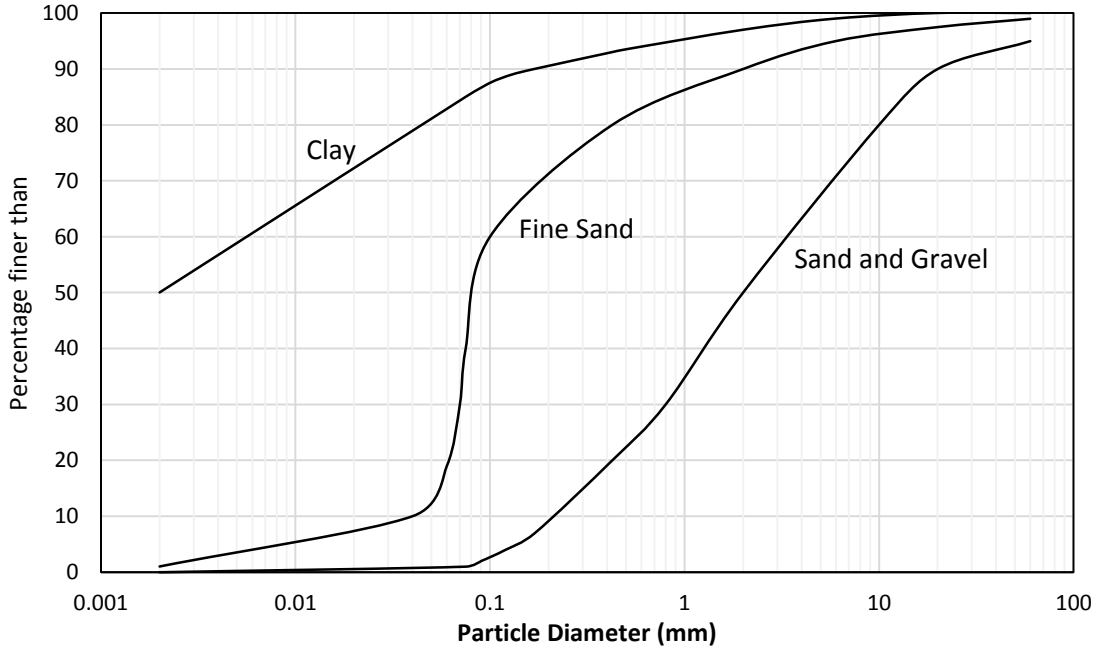

Figure A.10 PSD curves for the three example soils.

The FX model gives the SWCC as a relationship between the θ_{SAT} and Ψ, whereas the SR model uses the relationship between θ and Ψ. To convert θ_{SAT} to θ for comparison using Equation A.4, a value must be assigned for θ_s. Both Zapata et al. (2000) and Torres-Hernandez (2011) give equations to estimate θ_s, from the *wPI*. However, to avoid additional dependency, the SR method has been used for all comparison calculations.

B 5.2 Method Comparison

The SWCCs for the example sand and gravel and fine sand calculated using the SR method and the non-plastic (PSD correlated) fitting parameters for the FX method are shown in Figures A.11(a-b), and the fine sand and clay calculated using the SR method and the plastic (*wPI* correlated) fitting parameters for the FX method are shown in Figures A.11(c-d).

Table A.1 Empirical SWCC calculation input parameters for example soils.

	Sand and Gravel	*Fine Sand*	*Clay*
PSD Data			
D_{90}	20.000	2.000	0.170
D_{60}	3.350	0.100	0.006
D_{30}	0.800	0.070	
D_{20}	0.425	0.063	
D_{10}	0.200	0.040	
% finer than 2mm	50.0	90.0	97.0
% finer than 0.425mm	20.0	80.0	93.0
% finer than 0.075mm	1.0	31.0	85.0
% finer than 0.063mm	0.8	20.0	83.0
% finer than 0.002mm	0.0	1.0	50.0
Plasticity (FX methods only)			
PI	0	2 (ZA) 1.5 (PA and TH)	30
LL (TH only)	0	20	50
Organics (SR method only)			
OM	0	2	4

Unless there are large rainfalls or extreme dry weather occurs, typically the VWCs will naturally sit between field capacity, Ψ_{33}, and the permanent wilting point Ψ_{1500}. In this range for the sand and gravel, the SR model gives a similar curve to that with ZA fitting parameters (Figure A.11(a)).

Using the inputs for fine sand, the FX methods with non-plastic fitting parameters (Figure A.11(b)) all have lower VWC than those produced using the plastic fitting parameters (Figure A.11(c)). The SR method for fine sand sits between those of the non-plastic and plastic FX SWCCs.

There is a larger variation between the models for the clay soil (Figure A.11(d)), with a VWC range of approximately 0.2 across the fitting parameters for the FX model. The SWCC for the SR model sits approximately in the centre of the range.

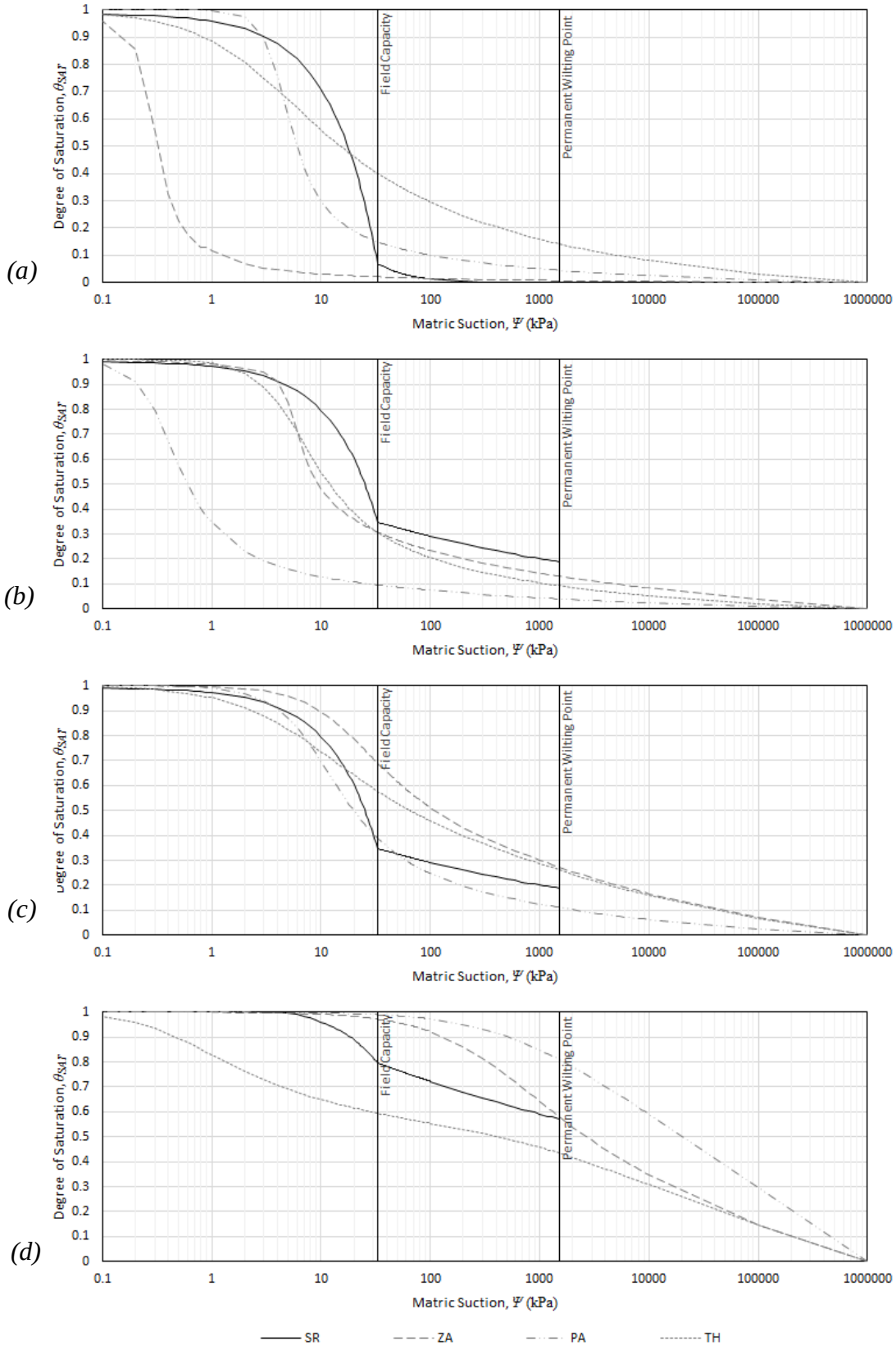

Figure A.11 SWCCs for example soils.
(a) Sand and Gravel (b) Fine Sand (non-plastic FX fitting parameters)
(c) Fine Sand (plastic FX fitting parameters) (d) Clay

The reasons for the differences between the models stem from the use of different parameters and the database of soils used for the regression analysis. Though the FX fitting parameters for non-plastic soils all use data from the PSD, different parts of the curve are used. For example, ZA uses only D_{60}, whereas TH uses only D_{10}. The SR method does not differentiate between non-plastic and plastic soils, using PSD and organic matter for all soil types. The size of the datasets used were also significantly different, ranging from under 200 soils (ZA) to over 36000 (TH). The same U.S. Department of Agriculture, National Soil Characterisation Database (USDS/NRCS) database of soils was used by both TH and SR, however, the SR model uses a subset of data (≈1700) which only includes near surface, typically organic soils.

In comparison of the range of SWCCs attained from the fitting parameters for the FX method, the SR method is considered representative for use in this study.

B 6 COMPUTATIONAL METHODS IN THE SPAW MODEL

B 6.1 Soil Water Characteristics Module

Saxton and Rawls (2006) provide a number of additional equations for hydraulic conductivity, and adjustments for density, gravel and salinity, which are used in the Soil Water Characteristics Module.

The saturated, K_s, and unsaturated, K_θ, hydraulic conductivity can be estimated using the following equations (Saxton and Rawls, 2006).

$$K_s = 1930\left(\theta_{(s)DF} - \theta_{(33)DF}\right)^{\left[3-\left(1/B\right)\right]}$$

$$K_\theta = K_s\left(\frac{\theta}{\theta_{(s)DF}}\right)^{\left[3+\left(2/(1/B)\right)\right]}$$

Salinity in soils can introduce an additional osmotic suction, which can be added to the matric suction, increasing the total suction. Though the soil water characteristic module allows assessment of osmotic SWCC with electrical conductivity inputs, these adjustments cannot be used in the simulator. Therefore this parameter has not been included for simulations and salinity of 0.0μS/cm has been applied to the soil for analysis.

Saxton and Rawls (2006) also give adjustments for gravel content, *R*, although the SWCC is not dependent on this parameter. The effect of *R* is only taken into account in calculations of saturated hydraulic conductivity, so that the K_s is replaced by a bulk saturated hydraulic conductivity, K_b.

$$\frac{K_b}{K_s} = \frac{1 - R}{\left[1 - R\left(1 - \frac{3\left(\rho_m / \rho_R\right)}{2}\right)\right]}$$

B 6.2 Simulator Module

A summary of the relevant calculation methods of the SPAW model are presented here. Additional information and calculations can be found in Saxton and Willey (2005).

Water exchange at the surface is calculated from the weather data, taking into account additional adjustments for runoff, canopy cover and interception. The rooting depths determine the water exchange from deeper soil layers to plants for transpiration.

The daily water redistribution between soil layers is calculated using a simplified finite difference form of the Darcy Equation.

$$q = K_\theta(\theta)\frac{[h(\theta) + D]}{D}(t)$$

Deep drainage parameters determine the exchange at the base of the section. When the base layer, known as the image layer achieves a specified percentage of θ_{33}, water is lost via percolation. Water can also be redistributed upwards from the image layer if it becomes drier than the overlying soil.